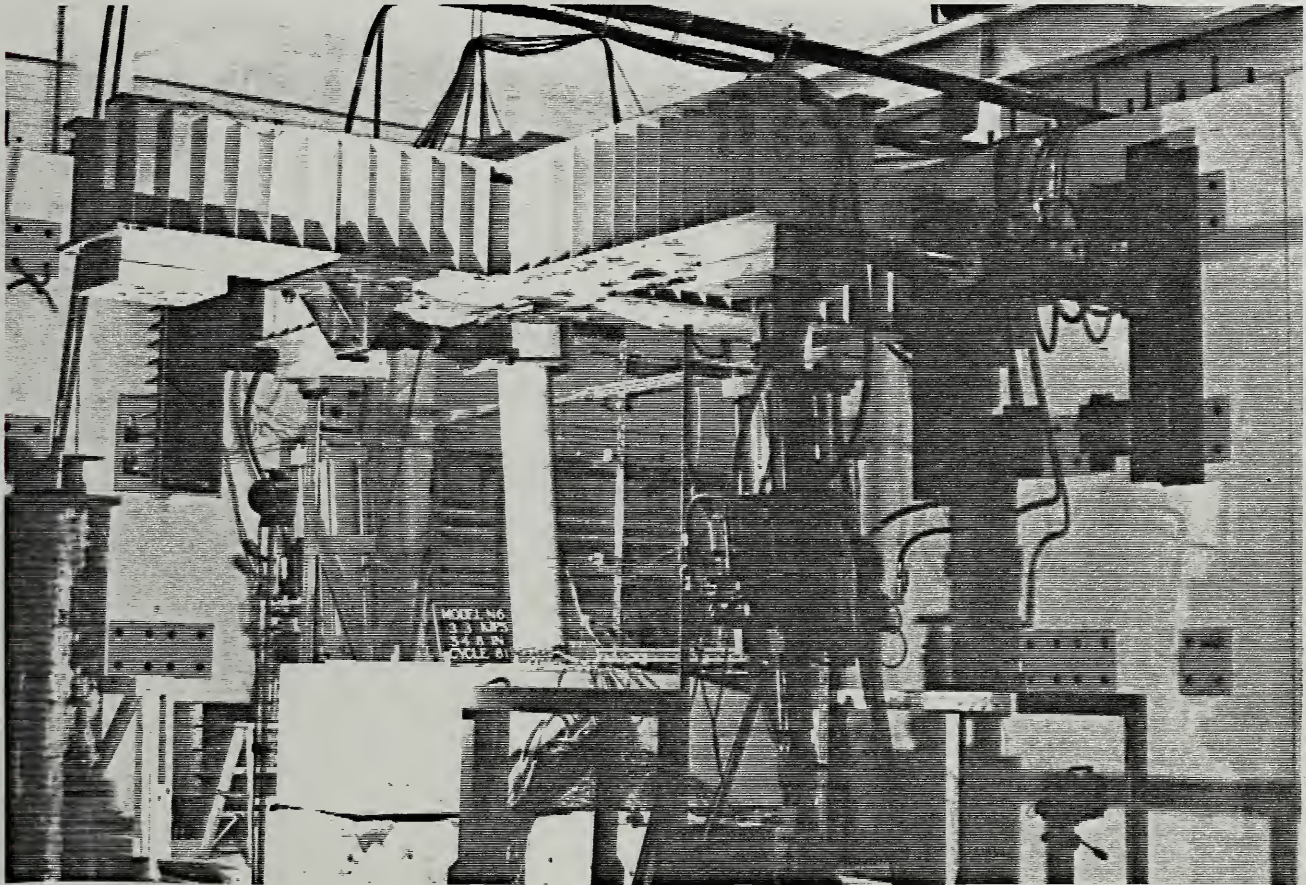




NBSIR 86-3494

Behavior of 1/6-Scale Model Bridge Columns Subjected to Cyclic Inelastic Loading



U.S. DEPARTMENT OF COMMERCE
National Bureau of Standards
National Engineering Laboratory
Center for Building Technology
Gaithersburg, MD 20899

November 1986



QC

100

.U56

86-3494

1986

DEPARTMENT OF COMMERCE

NATIONAL BUREAU OF STANDARDS

NBS

0-100

U.S.

N. 50-2

1986

NBSIR 86-3494

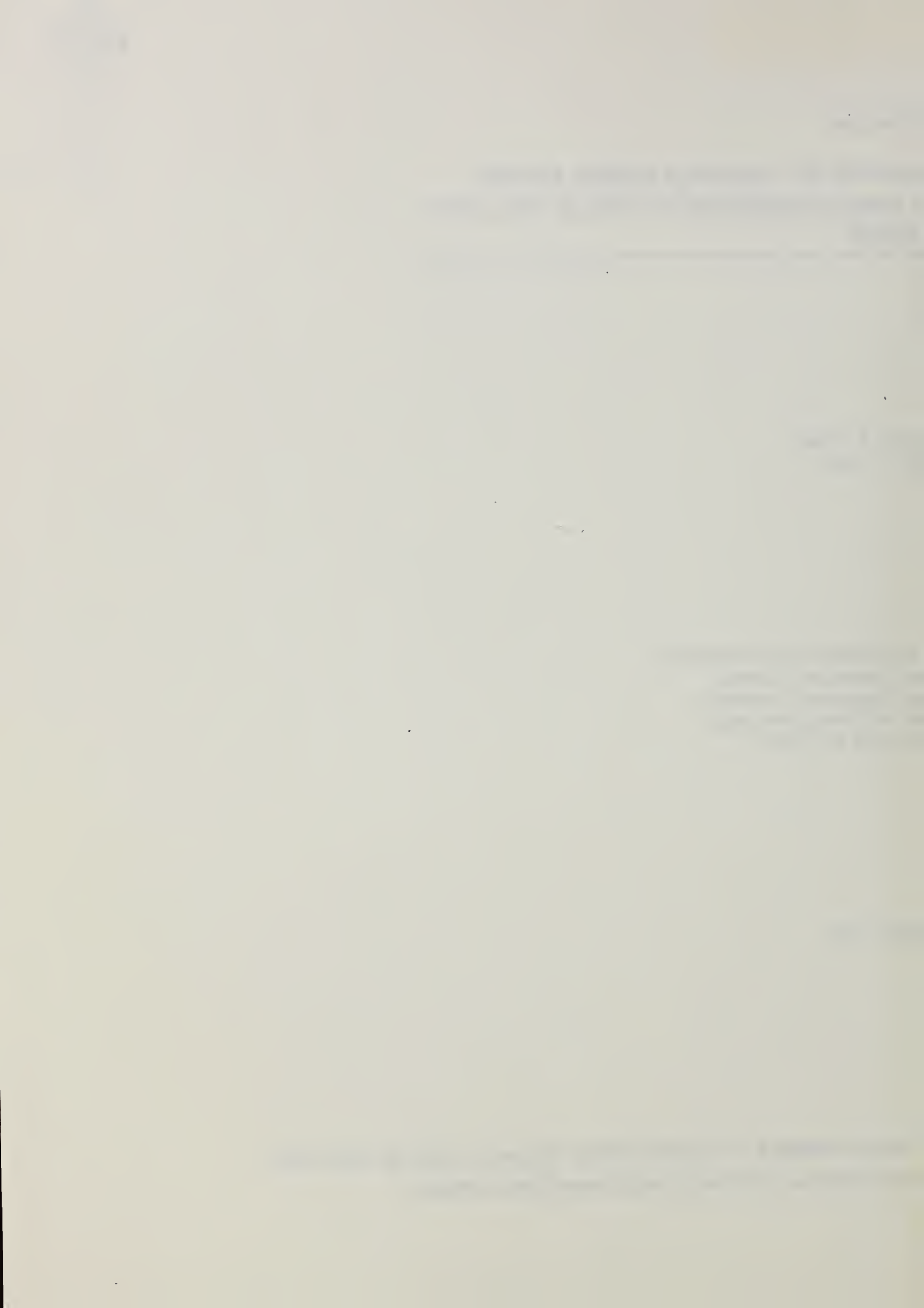
**BEHAVIOR OF 1/6-SCALE MODEL BRIDGE
COLUMNS SUBJECTED TO CYCLIC INELASTIC
LOADING**

Geraldine S. Cheek
William C. Stone

U.S. DEPARTMENT OF COMMERCE
National Bureau of Standards
National Engineering Laboratory
Center for Building Technology
Gaithersburg, MD 20899

November 1986

U.S. DEPARTMENT OF COMMERCE, Malcolm Baldrige, *Secretary*
NATIONAL BUREAU OF STANDARDS, Ernest Ambler, *Director*



ABSTRACT

Circular, spirally reinforced concrete bridge columns were subjected to cyclic inelastic loading in the laboratory. The bridge columns were one-sixth scale models of prototype columns designed in accordance with current California Department of Transportation (CALTRANS) specifications.

A total of six models were tested. Three of the models were constructed with microconcrete, and three were constructed with ready-mix concrete using pea gravel. Variables included the aspect ratio (height/width), magnitude of axial load and the use of microconcrete vs. the use of a ready-mix pea gravel concrete. The models were subjected to slow reversed cyclic loading with the axial load held constant.

Results from the tests are presented in the form of energy absorption, load-displacement hysteresis curves, longitudinal steel strains along the bar, and displacement profiles. Comparisons of the ultimate moment capacities, measured displacement ductilities, plastic hinge lengths, and the failure modes for the six models are discussed. Comparisons with previous studies are presented along with a discussion of design codes in the U.S., New Zealand, and Japan.

A series of graphics-based computer programs were developed to speed the analysis and interpretation of experimental data. Source code is presented for subroutines which integrate the area bounded by the load-deflection hysteresis curves; animate test specimen motion synchronized to position on load-deflection curve; plot individual cyclic strain energy and total strain energy for a given specimen; and which permit comparison of energy absorption performance between 2-6 specimens.

Keywords: Axial Load; Behavior; Bridges; Columns; Computer Graphics; Concrete; Confinement; Ductility; Energy Absorption; Failure; Lateral Load; Microconcrete; Modelling; Plastic Hinge; Scale Effects.

PREFACE

The majority of highway and mass transit bridges in the United States with reinforced concrete columns have been in place for many years and either were not specifically designed for earthquake loading or were designed with minimum criteria. The adequacy of these columns to withstand heavy seismic excitation is suspect, as many have failed in previous earthquakes. Dynamic analyses of structures responding elastically to ground motions recorded during severe earthquakes have shown that the theoretical response inertia loads are generally significantly greater than the static design lateral loads recommended by previous codes. However, these structures can survive severe earthquakes provided they are able to absorb and dissipate seismic energy by ductile behavior in the inelastic regime. This point was graphically demonstrated in the September 1985 Mexico Earthquake where proper detailing often meant the difference between survival and collapse of building structures.

Energy dissipation provided by the development of ductile plastic hinges in columns is essential to the satisfactory response under seismic loading of many structures. In particular, a large portion of modern bridge structures constructed in zones of high seismic activity are supported by piers consisting of one or more columns. Inelastic response of these bridge structures under seismic attack will invariably involve plastic hinging of the columns, unless mechanical energy dissipators are incorporated in the design. Bridge column behavior is consequently fundamentally different from that of building frames, where a capacity design approach is adopted to ensure beam hinging by specifying column flexural and shear strengths to be higher than the maximum column loads associated with beam hinges forming at maximum feasible beam strength.

This basic difference in philosophy between building frames and bridge frames has meant that much of the research on building frames is not directly applicable to bridge seismic design. Only two countries to this date, New Zealand and Japan, have specifically pursued extensive testing of bridge columns to augment highway construction codes. There is still a paucity of such research in the U.S., despite the obvious evidence of problems in bridge design philosophy. These problems are typified by the response of lifeline structures to the 1971 San Fernando earthquake, where 42 highway bridges received significant damage, and five structures collapsed (see figure I). Much of the damage was a consequence of inadequate detailing of the bridge columns resulting in:

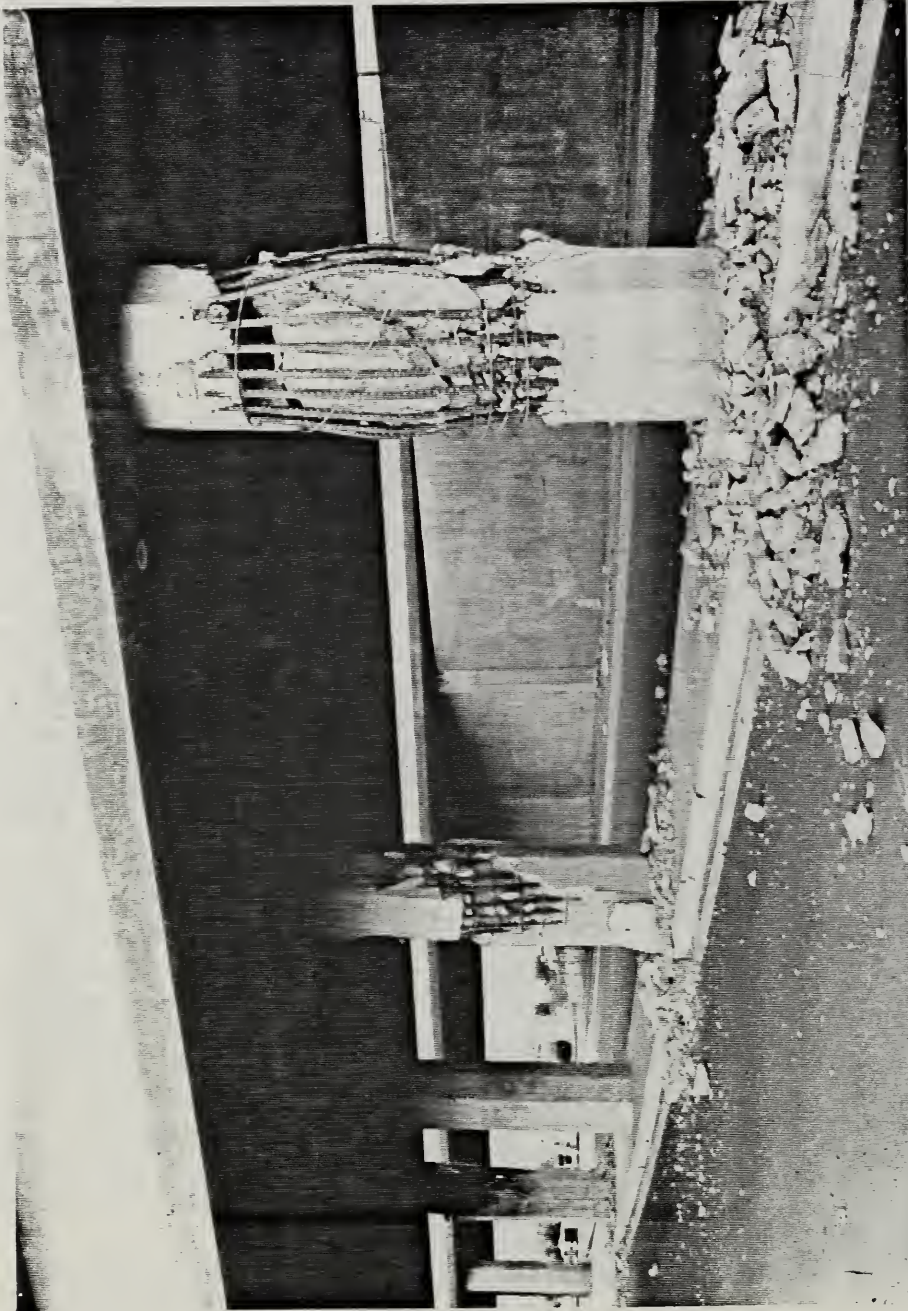
- a) insufficient ductility capacity to withstand the inelastic displacements imposed.
- b) shear failure in shorter columns
- c) anchorage failure of longitudinal reinforcement in plastic hinges forming at the column bases.

Damage to bridge piers in the San Fernando earthquake highlighted the need for reassessment of existing seismic design practice for bridges in the U.S. Since 1971, column design requirements have been changed and now require additional confinement steel to avoid "birdcaging" (compression



Collapsed bridge in the San Fernando earthquake

Fig. I



Longitudinal bar buckling - "Bird caging effect"

Fig. II

at the footings and pier cap to avoid the pull-out problem (see figure III). Until the initiation of the testing program described in this report, these new designs had not been verified through experiment.

It is now widely accepted that adequate ductility of column plastic hinges can only be obtained if sufficient transverse confining reinforcement is provided to confine the concrete core of the column, to prevent lateral buckling of the longitudinal flexural reinforcement, and to provide adequate shear reinforcement. During the San Fernando earthquake, failure of columns of several bridges and buildings could be directly attributed to inadequate confinement of the plastic hinge regions. Nevertheless, the amount and distribution of confining reinforcement necessary to insure adequate ductility without significant strength degradation is still a matter of controversy.

It is important to note that nearly all present design codes for bridge column seismic details (with the previously noted exceptions of New Zealand and Japan) have had their basis in the extensive research done on building columns. Building columns are generally much smaller in cross section (12-15 in) than the typical bridge column which can easily run 48-60 inches and larger. The reinforcement ratios differ greatly as well. These differences and others, which are elaborated in greater detail in Chapter 1, may lead to substantially different performance of the column in a seismic event.

In a workshop on earthquake resistance of highway bridges in 1979, the Applied Technology Council stated that, "There is a pressing need for experimental studies to determine the reserve capacities of various bridge components. Much of the considerable research work on column behavior has been done on relatively small specimens and has been extrapolated for bridges from tests of columns typically used in buildings. Bridge columns are larger and (usually) lower stressed axially than building columns and this does not permit easy extrapolation from the present wealth of building column data. Therefore work is (urgently) needed to determine whether the behavior of small sections can be extrapolated to larger cross sections."

Furthermore, the ASCE-TCLEE Task Committee on research needs stated in March of 1979 that, "experimental testing of selected reinforced concrete (bridge) columns should be performed to determine the lateral resistance and adequacy of reinforcement. Particular emphasis should be placed on those columns designed using pre-1971 California criteria."

Based on these recommendations the National Bureau of Standards proposed, in the fall of 1980, a test program to be known as the "Large Scale Bridge Column Project." Due to the large costs associated with the conduct of such full scale tests, sufficient funding did not become available until mid-1983 at which time design work began on the specimens -- full scale, 60-inch diameter columns -- as well as the necessary laboratory test fixtures. Sponsors for the project included the National Science Foundation (NSF), the National Bureau of Standards (NBS), the Federal Highway Administration (FHWA) and the California Department of Transportation (CALTRANS). The objectives of the project were to address the following topics:



Pullout of the longitudinal bars from the foundation

Fig. III

- a) The effect of scale factor on bridge column design (i.e. could models be effectively used to predict full-scale behavior)
- b) The effectiveness of current design details (i.e. would they achieve the desired ductility).
- c) Identification of symptomatic problems in present detailing practices.

The project was initially divided into three phases. The first phase consisted of the construction and testing of two highly instrumented full scale 60-inch (1.52 m) diameter, spirally confined bridge columns, designed to recent CALTRANS specifications to serve as benchmark data for subsequent model tests and to verify at full scale the performance of the post-1971 design requirements. The prototype specimens were to replicate to the maximum extent possible, actual bridge piers and the boundary conditions and loading conditions that would be experienced in the field. A minimum of two benchmark prototype tests will be performed to investigate two general classes of bridge columns currently in use in seismically active regions of the U.S. These included a short column measuring 15 feet (4.6 m) high (susceptible to shear type failures) and a tall column measuring 30 feet (9.2 m) high which would be used to investigate the performance of a predominately flexure-type column with continuous longitudinal reinforcement through the plastic hinge region. A special computer controlled testing laboratory, known as the NBS Large Scale Structural Research Facility, was designed and constructed to handle column axial loads of 12,000 kips (53.4 MN) to simulate the dead weight of the bridge superstructure, and lateral loads of up to 1,200 kips (5.34 MN) with associated column moments of up to 54,000 kip-feet (73.3 MN-m). Specimens weighing up to 4800 kips (21.36 MN) with heights of up to 60 feet (18.5 m) and column diameters of up to 8 feet (2.44 m) could be accomodated in the facility with access from a casting yard by means of a rail transport system (see Figure IV).

Phase II, which was conducted in parallel with Phase I, involved the construction and testing of precise 1/6-scale structural model replicas of the full scale prototypes under identical load histories and boundry conditions. Data gathering and sensor layout for the model specimens were designed to be identical to those of the prototype so that direct behavioral comparisons could be made between the two. A further variable studied in this phase was the effect of using microconcrete -- the current recommended structural modelling practice -- versus the use of a small nominal maximum size aggregate ready-mix concrete. The chief advantage of the latter was one of cost effectiveness.

The third and final phase of the project will involve the conduct of detailed comparisons between the model and prototype specimens. Such comparisons will be based on ductility factor, energy absorption capacity, ultimate moment capacity, plastic hinge length, and extent of yield penetration in the longitudinal reinforcement.

This report is the first in a series detailing the results of the NBS Large Scale Bridge Column Project and deals with the design, fabrication, testing, and evaluation of the model column specimens. An extensive literature review of previous bridge column research is presented in Chapter two. Chapters three and four detail the design requirements for similitude and the construction of the model specimens. Test results are presented in Chapter five and a detailed discussion and evaluation of the data is contained in Chapter six. Chapter seven provides a summary and the conclusions.

TABLE OF CONTENTS

	<u>PAGE</u>
Abstract	i
Preface	ii
Table of Contents	ix
List of Tables	xiii
List of Figures	xiv
1.0 Introduction	1
1.1 General	1
1.2 Object and Scope of Experiment	2
1.3 Test Outline	3
2.0 Literature Review	8
2.1 General	8
2.2 Previous Research	8
2.2.1 Studies done in New Zealand	8
2.2.2 Studies done in Japan	18
2.2.3 Tests Performed in Yugoslavia	29
2.3 Confining Reinforcement in the Plastic Hinge Region	37
2.3.1 ACI 318-77	38
2.3.2 CALTRANS	38
2.3.3 New Zealand Code	46
3.0 Similitude	48
3.1 General	48
3.2 Material	50
3.2.1 Reinforcement	50
3.2.2 Concrete	51
3.2.2.1 Microconcrete	51

3.2.2.2	Pea Gravel	54
4.0	Specimen Design and Construction	57
4.1	Design	57
4.2	Construction Process	60
4.3	Model Casting	62
4.4	Instrumentation	62
5.0	Test Results and Observations	76
5.1	Introduction	76
5.2	Model N1	79
5.2.1	Model Properties	79
5.2.2	DUCTILITY FACTOR = 1, Cycle 1	79
5.2.3	DUCTILITY FACTOR = 2, Cycles 2 & 3	79
5.2.4	DUCTILITY FACTOR = 4, Cycles 4 & 5	79
5.2.5	DUCTILITY FACTOR = 6, Cycles 6 & 7	79
5.2.6	DUCTILITY FACTOR = 8, Cycles 8, 9 & 10	85
5.2.7	DUCTILITY FACTOR = 10, Cycle 11	85
5.3	Model N2	85
5.3.1	Model Properties	85
5.3.2	DUCTILITY FACTOR = 1, Cycle 1	85
5.3.3	DUCTILITY FACTOR = 2, Cycles 2 & 3	89
5.3.4	DUCTILITY FACTOR = 4, Cycles 4 & 5	89
5.3.5	DUCTILITY FACTOR = 6, Cycles 6 & 7	89
5.3.6	DUCTILITY FACTOR = 8, Cycles 8 & 9	89
5.3.7	DUCTILITY FACTOR = 10, Cycles 10, 11, & 12 ..	89
5.3.8	DUCTILITY FACTOR = 12, Cycle 13	94
5.4	Model N3	94
5.4.1	Model Properties	94

5.4.2	DUCTILITY FACTOR = 1, Cycle 1	94
5.4.3	DUCTILITY FACTOR = 2, Cycles 2 & 3	94
5.4.4	DUCTILITY FACTOR = 3, Cycles 4 & 5	94
5.4.5	DUCTILITY FACTOR = 4, Cycles 6 - 15	100
5.4.6	DUCTILITY FACTOR = 5, Cycle 16	100
5.5	Model N4	100
5.5.1	Model Properties	100
5.5.2	DUCTILITY FACTOR = 1, Cycle 1	100
5.5.3	DUCTILITY FACTOR = 2, Cycles 2 & 3	100
5.5.4	DUCTILITY FACTOR = 4, Cycles 4 & 5	108
5.5.5	DUCTILITY FACTOR = 6, Cycles 6 & 7	108
5.5.6	DUCTILITY FACTOR = 8, Cycles 8, 9, & 10	108
5.5.7	DUCTILITY FACTOR = 10, Cycles 11, 12, & 13 ..	108
5.5.8	DUCTILITY FACTOR = 12, Cycles 14 & 15	108
5.6	Model N5	112
5.6.1	Model Properties	112
5.6.2	DUCTILITY FACTOR = 1, Cycle 1	112
5.6.3	DUCTILITY FACTOR = 2, Cycles 2 & 3	112
5.6.4	DUCTILITY FACTOR = 4, Cycles 4 & 5	112
5.6.5	DUCTILITY FACTOR = 6, Cycles 6 & 7	112
5.6.6	DUCTILITY FACTOR = 8, Cycles 8 & 9	112
5.6.7	DUCTILITY FACTOR = 10, Cycles 10, 11 & 12 ...	116
5.6.8	DUCTILITY FACTOR = 12, Cycles 13 & 14	116
5.7	Model N6	116
5.7.1	Model Properties	116
5.7.2	DUCTILITY FACTOR = 1, Cycle 1	121
5.7.3	DUCTILITY FACTOR = 2, Cycles 2 & 3	121
5.7.4	DUCTILITY FACTOR = 3, Cycles 4 & 5	121

5.7.5	DUCTILITY FACTOR = 4, Cycles 6 - 15	121
5.7.6	DUCTILITY FACTOR = 5, Cycles 16 - 18	125
5.7.7	DUCTILITY FACTOR = 6, Cycles 19 & 20	125
5.7.8	DUCTILITY FACTOR = 7, Cycles 21 & 22	125
5.7.9	DUCTILITY FACTOR = 8, Cycle 23	125
6.0	Discussion of Test Results	131
6.1	Column Deflection	131
6.2	Energy Absorption	145
6.3	Plastic Hinge Lengths	161
6.4	Confining Steel Strains	165
6.5	Ultimate Moments	166
6.6	Adequacy of Transverse Confinement	174
6.7	Failure Modes	175
6.8	Comparisons of Results With Previous Studies	176
7.0	Conclusions and Future Research Needs	178
7.1	Conclusions	178
7.2	Practical Applications	179
7.3	Areas of Future Research	180
	References	181
	Appendix A	185
	Appendix B	196
	Appendix C	270

LIST OF TABLES

		<u>PAGE</u>
1.1	Column Dimensions	7
2.1	Kuribayashi's Test Conditions	25
2.2	Comparison of AASHTO and CALTRANS Current Specifications Versus Those Prior to 1971	39
3.1	Similitude Requirements for Reinforced Concrete Models	49
3.2	Microconcrete Mix Design	53
3.3	Cylinder Test Data (compressive strength in psi) for Model Specimens	54
3.4	Pea Gravel Mix Design	56
4.1	Model Properties	61
6.1	Experimental Yield Displacements	138
6.2	Load and Moments for Model N1	153
6.3	Load and Moments for Model N2	154
6.4	Load and Moments for Model N3	155
6.5	Load and Moments for Model N4	156
6.6	Load and Moments for Model N5	157
6.7	Load and Moments for Model N6	158
6.8	Ultimate Moment Capacities	162
6.9	Plastic Hinge Lengths	163

LIST OF FIGURES

		<u>PAGE</u>
I	Collapsed Bridge in the San Fernando Earthquake	iii
II	Longitudinal Bar Buckling - "Birdcaging Effect"	iv
II	Longitudinal Bar Pullout from the Foundation	vi
1.1	Prototype and Model Dimensions	4
1.2	Column Cross Section	5
2.1	Munro's Model	10
2.2	Gill's Model Dimensions	12
2.3	Gill's Tie Arrangement	13
2.4	Ang's Model Dimensions	15
2.5	Confinement Steel Comparision	17
2.6	Ohta's Model Dimensions and Test Set-Up	19
2.7	Kuribayashi 1/4 Scale Model Dimensions	21
2.8	Kuribayashi 1/4 $\sqrt{2}$ Scale Model Dimensions	22
2.9	Kuribayashi's Column Nos. 1 & 3	23
2.10	Kuribayashi's Column No. 2	23
2.11	Kuribayashi's Column No. 4	23
2.12	Kuribayashi's Column No. 5 & 6	24
2.13	Kuribayashi's Column No. 7	24
2.14	Ohno's Model Dimension and Test Set-Up	27
2.15	Ohno's Loading Sequence	28
2.16	Petrovski's Flexure Model Dimensions and Steel Arrangement	31
2.17	Petrovski's Shear Model Dimensions and Steel Arrangement	32
2.18	Load History for Flexure Model Under Low Axial Load	33

2.19	Load History for Flexure Model Under High Axial Load	34
2.20	Load History for Shear Model Under Low Axial Load	35
2.21	Load History for Shear Model Under High Axial Load	36
2.22	Lap Splices in Vertical Column Reinforcement	45
3.1	Microconcrete Vs. Prototype Gradation	52
3.2	Pea Gravel Gradation	55
4.1	Prototype Steel Arrangement-Side View	58
4.2	Prototype Steel Arrangement-End View and Plan	59
4.3	Tying of Spiral Cage	63
4.4	Instrumented Cage	64
4.5	Tying Column Cage to Base Cage	65
4.6	Column Dimension and Steel Layout	66
4.7	Casting of Microconcrete Bases	67
4.8	Flexure Column Axial Strain Gage Location and Reinforcement Schedule	68
4.9	Shear Column Axial Strain Gage Location and Reinforcement Schedule	69
4.10	Flexure and Shear Spiral Gage Location	70
4.11	Strain Gage Locations (Top View)	71
4.12	Embedment Gage	72
4.13	LVDT Locations for Shear Columns	74
4.14	LVDT Locations for Flexure Columns	75
5.1	Experimental Definition of Yield Displacement	77
5.2	TIF Test Set-Up	78
5.3	Loading History for Model N1	80
5.4	Model N1, DF = 1, Cycle 1	81
5.5	Model N1, DF = 4, Cycle 4	82
5.6	Model N1, DF = 4, Cycle 5	83

5.7	Model N1, DF = 6, Cycle 6	84
5.8	Model N1, DF = 10, Cycle 11	86
5.9	Model N1, DF = 10, Cycle 11	87
5.10	Loading History for Model N2	88
5.11	Model N2, DF = 1, Cycle 1	90
5.12	Model N2, DF = 2, Cycle 2	91
5.13	Model N2, DF = 6, Cycle 6	92
5.14	Model N2, DF = 8, Cycle 9	93
5.15	Model N2, DF = 12, Cycle 13	95
5.16	Model N2, DF = 12, Cycle 13	96
5.17	Loading History for Model N3	97
5.18	Model N3, DF = 1, Cycle 1	98
5.19	Model N3, DF = 3, Cycle 3	99
5.20	Model N3, DF = 4, Cycle 6	101
5.21	Model N3, DF = 4, Cycle 7	102
5.22	Model N3, DF = 4, Cycle 10	103
5.23	Model N3, DF = 5, Cycle 16	104
5.24	Loading History for Model N4	105
5.25	Model N4, DF = 1, Cycle 1	106
5.26	Model N4, DF = 2, Cycle 2	107
5.27	Model N4, DF = 4, Cycle 4	109
5.28	Model N4, DF = 10, Cycle 12	110
5.29	Model N4, DF = 12, Cycle 15	111
5.30	Loading History for Model N5	113
5.31	Model N5, DF = 1, Cycle 1	114
5.32	Model N5, DF = 4, Cycle 4	115
5.33	Model N5, DF = 10, Cycle 11	117

5.34	Model N5, DF = 10, Cycle 12	118
5.35	Model N5, DF = 12, Cycle 13	119
5.36	Loading History for Model N6	120
5.37	Model N6, DF = 1, Cycle 1	122
5.38	Model N6, DF = 2, Cycle 2	123
5.39	Model N6, DF = 4, Cycle 6	124
5.40	Model N6, DF = 4, Cycle 14	126
5.41	Model N6, DF = 5, Cycle 18	127
5.42	Model N6, DF = 6, Cycle 20	128
5.43	Model N6, DF = 8, Cycle 23	129
5.44	Model N6, DF = 8, Cycle 23	130
6.1	Load Cycles for Model N1	132
6.2	Load Cycles for Model N2	133
6.3	Load Cycles for Model N3	134
6.4	Load Cycles for Model N4	135
6.5	Load Cycles for Model N5	136
6.6	Load Cycles for Model N6	137
6.7	Column Displacements for Model N1	139
6.8	Column Displacements for Model N2	140
6.9	Column Displacements for Model N3	141
6.10	Column Displacements for Model N4	142
6.11	Column Displacements for Model N5	143
6.12	Column Displacements for Model N6	144
6.13	Individual Cycle Energy for Model N1	146
6.14	Individual Cycle Energy for Model N2	147
6.15	Individual Cycle Energy for Model N3	148
6.16	Individual Cycle Energy for Model N4	149
6.17	Individual Cycle Energy for Model N5	150

6.18	Individual Cycle Energy for Model N6	151
6.19	Energy Absorbed up to Ultimate State as Defined by Zahn	152
6.20	Peak Strain Along Longitudinal Bar (Model N1)	166
6.21	Peak Strain Along Longitudinal Bar (Model N2)	167
6.22	Peak Strain Along Longitudinal Bar (Model N3)	168
6.23	Peak Strain Along Longitudinal Bar (Model N4)	169
6.24	Peak Strain Along Longitudinal Bar (Model N5)	170
6.25	Peak Strain Along Longitudinal Bar (Model N6)	171
6.26	P-M Diagram for the Flexure Models	172
6.27	P-M Diagram for the Shear Models	173
C1	Schematic of TTF	269
C2	Flexure Model in the TTF	270

1.0 INTRODUCTION

1.1 General

Many modern bridge structures in zones of high seismic activity are supported by bents consisting of one or more columns. In the United States, seismic design of bridge columns has often been based on data obtained from research performed on building columns. The basis for doing so may not be valid due to several important differences which exist between bridge and building columns. These differences are as follows:

1. Building columns typically have significantly smaller cross sections than bridge columns: 12-15 in. (304.8-381 mm) are common dimensions for buildings while 48-60 in. (1219.2-1524 mm) are common dimensions for highway bridges.
2. Because building columns have smaller dimensions and require more complex detailing at beam-column joints than bridge columns, the use of reinforcing bars greater than a # 11 (1.41-in, 3.6 cm) is not common practice. By contrast, #14 and #18 [1.69-in and 2.26-in (4.3 cm and 5.7 cm) respectively] reinforcing bars are commonly used in bridge columns. Differences in bond characteristics between small and large bars may also contribute to performance differences.
3. Building columns, in general, carry higher axial stresses than do bridge columns.
4. The design approach to building frames has been based on plastic hinges occurring in beams prior to columns. However, the development of plastic hinges in bridge columns is necessary for energy dissipation under seismic loading.
5. Bridge columns have smaller reinforcement ratios than building columns, typically less than 2%.

The San Fernando earthquake of Feb. 9, 1971 provided a focal point for the reassessment of seismic design practice in the United States. During that seismic event, five highway bridges collapsed and 42 others sustained significant damage [12]. The principal causes of damage were identified as:

1. Insufficient ductility capacity of columns to withstand the inelastic displacements experienced.
2. Shear failure in shorter columns.
3. Anchorage failure of longitudinal reinforcement in plastic hinges forming at the column bases.

Since the San Fernando earthquake, modifications to the seismic design code for the state of California and the AASHTO seismic design guidelines have been implemented. Some of these modifications in CALTRANS specifications include:

- o Increased minimum requirement for the volumetric reinforcement ratio.
- o Decreased spiral spacing.
- o Lapped splices in longitudinal bars not permitted in plastic hinge region.
- o Extension of spiral into the footing.
- o Inclusion of the axial load in the calculation of the required volumetric reinforcement ratio.

In 1979, the Applied Technology Council Workshop on Earthquake Resistance of Highway Bridges [24] identified the need for verification of these changes by means of full scale tests as being of national importance. Specifically, the recommendations from the workshop called for investigations to determine the ductile capacity of concrete bridge columns and to determine the validity of extrapolating the behavior of structures with large cross sections from the behavior of structures with small cross sections.

To meet these research needs, the National Bureau of Standards began an experimental program to investigate the performance of bridge columns subjected to inelastic reverse cyclic loading. Sponsorship of this project was jointly provided for by the National Science Foundation (NSF), the California Department of Transportation (CALTRANS), the Federal Highway Administration (FHWA), and the National Bureau of Standards (NBS). The physical test program was conducted at NBS. This report details the results of the model test program.

1.2 Object and Scope of Experiment

The overall experimental test program involves the construction and testing of full and 1/6 scale model specimens. The objectives of the research program were as follows :

1. To determine the ductile capacity of bridge columns designed to CALTRANS standards.
2. To determine the effects of scale on column behavior.
3. To study the effects of different aspect ratios on the behavior of the column.
4. To study the effect of axial load on the behavior of the column.
5. To determine the differences between the use of microconcrete and ready-mix pea gravel.

The importance of the first two objectives has already been discussed. The third and fourth objectives will help designers better understand column behavior with respect to important design variables, thereby leading to better design practices. The importance of the fifth objective is in the amount of time and research funds that could be saved if the use of ready-mix pea gravel could be substituted for the use of microconcrete.

Two types of cantilevered bridge columns were designed and constructed in accordance with recent CALTRANS specifications; both full scale and 1/6 scale columns were constructed. These specifications meet or exceed the "Seismic Design Guidelines for Highway Bridges" [26]. One column design had a relatively high moment to shear ratio, approximately 40 ft. (12.19 m); thus the failure mode was expected to be dominated by flexural effects. The second column type was designed to investigate performance in the regime dominated by shear effects. These columns had a moment to shear ratio of approximately 20 ft. (6.10 m). A total of two full scale specimens are to be tested. As of this writing the first test (a column with high moment to shear ratio) has been completed. Construction of the other test specimen is underway. Two sets of three 1/6 scale specimens were also built. One column in each set was designed to have a high moment to shear ratio; the other models were designed to investigate shear effects. Microconcrete was used for one set and ready-mix concrete with pea gravel was used for the other.

The columns were evaluated based on the following criteria:

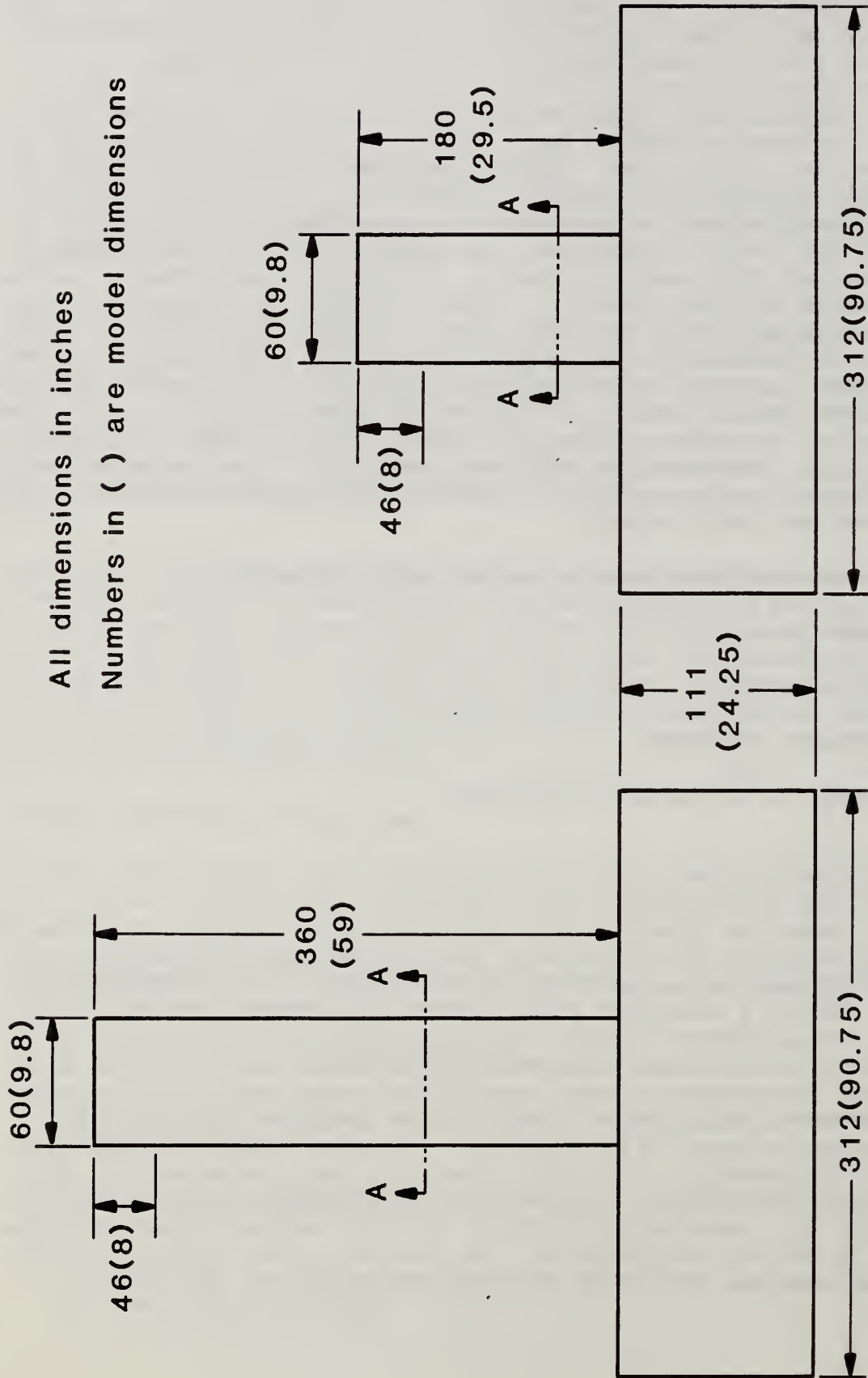
1. Energy absorption
2. Ductility capacity
3. Ultimate moment capacity
4. Effectiveness of the column confinement

1.3 Test Outline

As mentioned above two types of full scale and model bridge columns were designed for testing in the laboratory. The designs were representative of recent design practice in the state of California and are shown in Figs. 1.1 and 1.2. The tall (flexure) type specimen measured 30 ft. (9.14 m) in height while the shorter (shear) type specimen was 15 ft. (4.57 m) in height from the column base to the point of application of lateral load. These heights were chosen so that both flexure and shear failure modes could be examined. Both types of full scale specimens were circular in cross section and measured 5 ft. (1.52 m) in diameter. Axial reinforcement consisted of 25 grade 60 - #14 bars (1.69-in, 4.3cm) spaced evenly about the perimeter of the column. Transverse reinforcement consisted of grade 60 - # 5 (.625-in, 1.6cm) spirals at 3.5 in. (88.9 mm) on centers for the 30 ft. (9.14 m) column and grade 60 - #6 (.75-in, 1.9cm) spirals at 2.125 in. (53.97 mm) spacing for the 15 ft. (4.57 m) column.

PROTOTYPE AND MODEL DIMENSIONS

All dimensions in inches
 Numbers in () are model dimensions

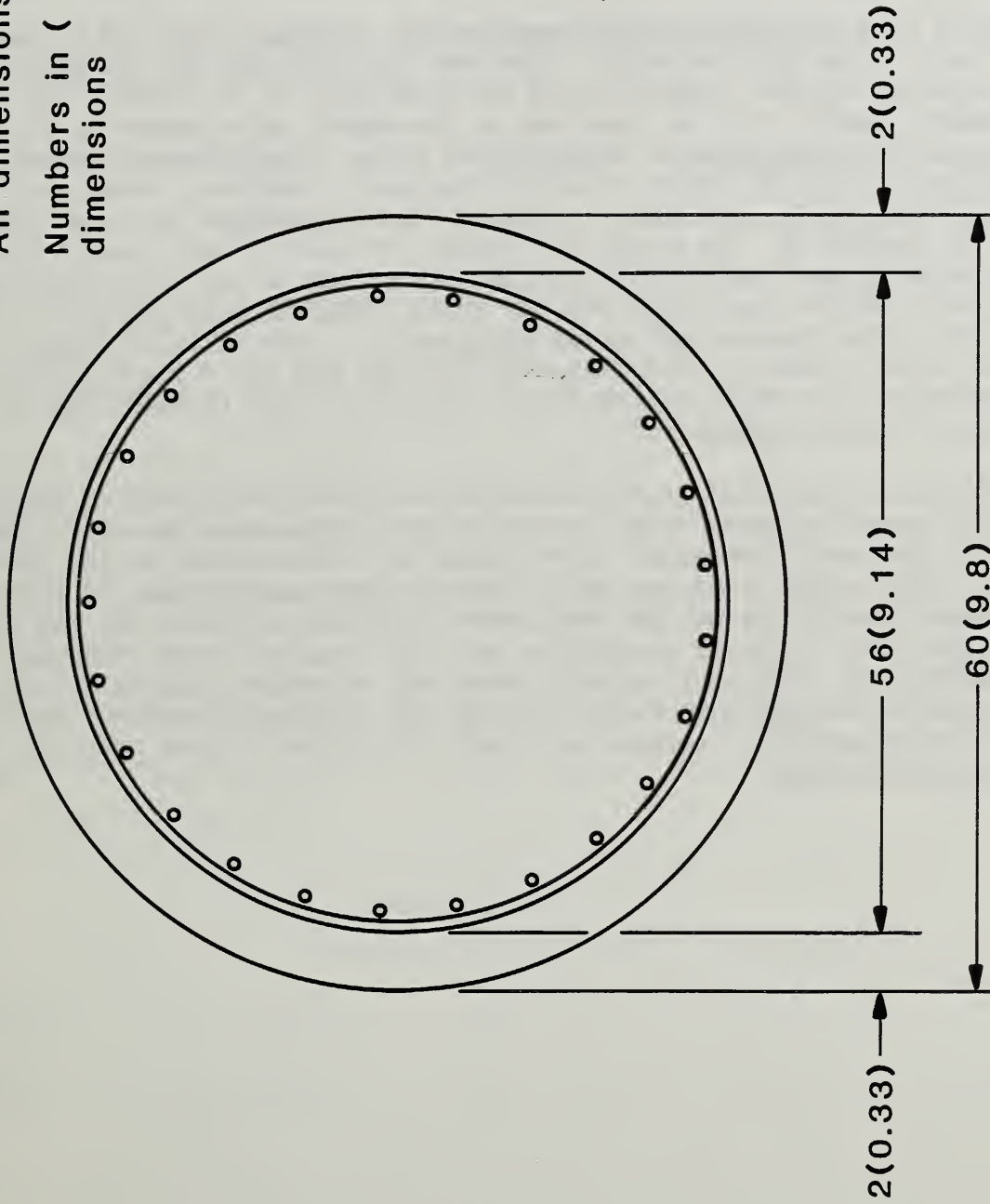


NOTE: Base width is 96 (28.375)

Fig. 1.1

Column Cross Section

All dimensions in inches
Numbers in () are model
dimensions



Section A-A

Fig. 1.2

Based on available modelling materials and testing apparatus, a scale of 1/6.1 was chosen for the model specimens. Three specimens, N1, N2, and N3, were constructed using microconcrete and three specimens N4, N5 and N6 were constructed using ready-mix concrete with pea gravel. N3 and N6 were expected to exhibit a failure mode dominated by flexure while the remaining models were designed to investigate the effectiveness of spiral reinforcement in short columns to resist shear failure. The dimensions of the models and prototype are also given in Table 1.1.

The models were subjected to reverse cyclic lateral loads and a constant axial load. The applied axial load was to simulate the weight of the bridge superstructure. Lateral load was then applied to achieve the yield displacement (which will be referred to throughout this report as 1-delta-y); thereafter the models were loaded under displacement control to achieve multiples of delta-y (e.g. 2-delta-y, 4-delta-y, 6-delta-y etc.) until failure of the specimen. Lateral load histories are described in detail in Chapter 5. To study the effect of axial load, one of the two shear models in each set had an applied axial load of $0.1 f'_c A_g$ [26.87 kips (119.52 kN)] while the other had an axial load of $0.2 f'_c A_g$ [53.75 kips (239.09 kN)]. The flexure models both had axial loads of 26.87 kips (119.52 kN). The axial load of 26.87 kips (119.52 kN) and 53.75 kips (239.09 kN) correspond to 1000 kips (4,448.22 kN) and 2000 kips (8,896.4 kN) in the prototype columns, respectively.

The tests were conducted using the NBS Tri-Directional Testing Facility (TTF) [29] operating under displacement control. The columns were initially loaded to the specified axial force prior to commencement of the lateral loading. This axial load was held constant for the duration of the test. The boundary conditions of the tests were a hinged condition at the top of the column and a fixed condition at the column base (foundation). Instrumentation included strain gages at selected points along the longitudinal reinforcing bars, and on the confining spiral bar, and external displacement transducers used to monitor column rotation and lateral displacements.

TABLE 1.1 COLUMN DIMENSIONS

SPECIMEN	TYPE OF CONCRETE	HEIGHT	DIAMETER (INCHES)	AXIAL LOAD (KIPS)
MODEL				
N1	Microconcrete	2' - 5.5"	9.8	26.87
N2	Microconcrete	2' - 5.5"	9.8	53.75
N3	Microconcrete	4' - 11"	9.8	26.87
N4	Pea Gravel	2' - 5.5"	9.8	26.87
N5	Pea Gravel	2' - 5.5"	9.8	53.75
N6	Pea Gravel	4' - 11"	9.8	26.87
PROTOTYPE				
Flexure	3/4" Gravel	30' - 0"	60	1000
Shear	3/4" Gravel	15' - 0"	60	2000

2.0 LITERATURE REVIEW

2.1 General

Although many papers have been written concerning seismic design of building columns, few papers have considered the design of bridge columns for seismic loading. Research that has dealt with seismic performance of bridge piers has been carried out principally in New Zealand and in Japan. These projects involved the testing of small to medium size columns. A discussion of the projects relevant to this study is presented in the following sections.

2.2 Previous Research

2.2.1 Tests Performed in New Zealand

The tests conducted in New Zealand were supervised by Park and Priestley at the University of Canterbury. These tests have been on-going over the last decade. Test variables included the level of axial load (P_g), volumetric reinforcement ratio (ρ_g), aspect ratio (L/D) where L = column height and D = column diameter, and the effects of differences in cross section shape. The loading sequence for these specimens was as follows:

- 1) Apply increasing lateral load until 75% of the calculated ACI ultimate moment has been induced at the column base.
- 2) Measure (experimentally) the column deflection at this load. Remove the lateral load (return to starting position) then apply lateral load in the direction 180 degrees opposite the direction of the first load application. Measure the column deflection when 75% of the calculated ACI ultimate moment has been induced at the column base.
- 3) Take the average of the displacements obtained in steps 1 & 2 and divide by 0.75. Call the result of this calculation "one-delta-y" ($1\Delta_y$), the reference yield deflection.
- 4) Continue to apply cyclic lateral loading to the column with two cycles each at multiples of one-delta-y ($+2, +4, +6, \dots$ etc.) until ultimate failure of the column.

Chapter 5.1 provides a detailed description of the implementation of this testing procedure. The displacement ductility, u , is defined as the ratio of the maximum column displacement at the point of application of the lateral load (in any cycle) to the yield displacement (measured at the same location). The discussion presented below begins with Munro's work in 1976.

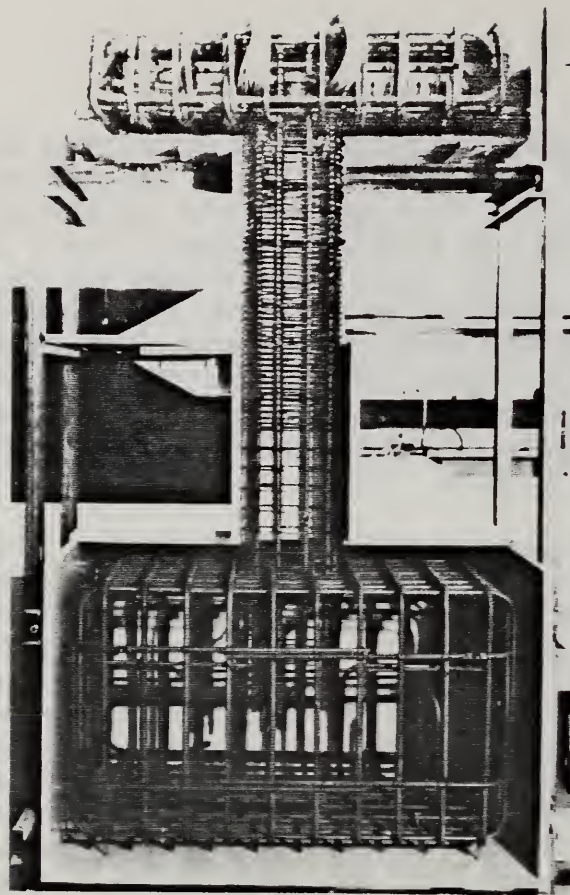
One of the objectives of Munro's study [13] was to test a 1/3 scale model of a 59 in. (1500 mm) nominal diameter bridge pier. The model specimen had an octagonal cross section with spiral reinforcement having a 19.68 in. (500 mm) diameter. The column had a clear height of 78.74 in. (2000 mm). The aspect ratio of this model was therefore 4. The longitudinal reinforcement consisted of twenty pairs of 0.51 in. (13 mm) diameter

deformed bars. The spiral reinforcement consisted of a 0.31 in. (8 mm) diameter round bar with a spacing of 1.34 in. (34 mm) on center. The steel layout is shown in Fig. 2.1. The specimen was subjected to cyclic loading and a low axial load (12 % of balanced ultimate load). The axial load was supplied by a concrete block, which represented the superstructure weight of the bridge, cast monolithically on top of the column. This was done to provide an inertial mass for shake-table tests which were planned following the static load tests. During the static tests the lateral load was applied at the center of the block. The column was designed in accordance with the Ministry of Works and Development (MWD) " Highway Bridge Design Brief" [9].

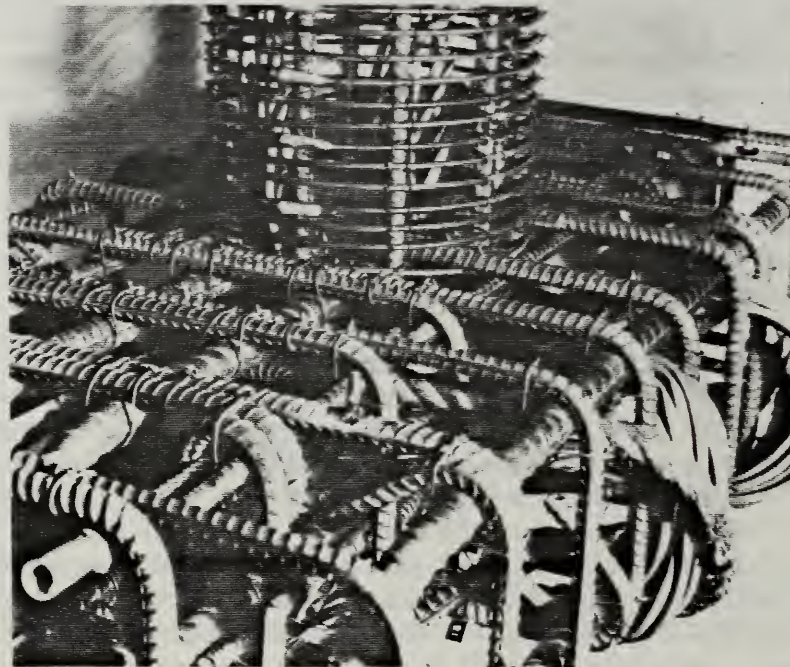
The measured yield displacement of the column was 0.75 in. (19 mm). The yield displacement was obtained by loading to an approximate displacement ductility of 0.6 and by extrapolation of the moment-displacement plot to the theoretical ultimate moment. Data from the test showed that the strain in the spiral reinforcement reached only 70% of its yield capacity at $\mu = 6$, indicating a significant reserve ductility. The calculated plastic hinge length was 0.66 H where H was defined as the overall column diameter. When compared with data from a previous study which tested columns built to ACI 318-71 [1] requirements, it was found that the MWD specifications provided adequate confinement whereas the ACI 318-71 [1] requirements were not adequate to prevent the longitudinal bars from buckling for displacement ductilities greater than 5 [21]. The lateral load vs maximum column lateral displacement hysteresis curves for the model showed little decrease in the energy absorbed per cycle (the area within a single loop) nor a marked decrease in ultimate moment up to a displacement ductility factor of 8. Higher ductility for the column was felt possible as no spiral yielding or longitudinal bar buckling was observed. However, verification was not possible due to the limited stroke of the hydraulic actuator. An average drop of 9 % in moment capacity from the first cycle at each ductility level was noted in the repeat cycle. Munro also constructed a 1/6 scale model to be tested dynamically. However, the test was halted while the column was still in the elastic range due to failure of the bearing support system of the shaking table.

Ng [16] tested Munro's 1/6 scale column specimen under cyclic static loading. The axial stress due to the concrete block cast monolithically on top of the column equalled 58 psi (0.4 MPa). The specimen was 9.8 in. (250 mm) in diameter and had a height of 39 in. (1000 mm). The aspect ratio of the model was 4. Ten deformed bars of 0.51 in. (13 mm) diameter constituted the longitudinal reinforcement. The lateral confinement was provided by smooth, round bars of 0.17 in. (4.4 mm) diameter at 0.55 in. (14 mm) spacing on center. The transverse steel reinforcement ratio was $\rho_s = 0.015$. The longitudinal steel reinforcement ratio was 0.02568.

A displacement ductility of 14 was reached without any visible sign of longitudinal bar buckling or spiral yielding even though the column had been previously subjected to vigorous dynamic testing. The yield displacement measured was 0.5 in. (11.86 mm). It was also noted that the plastic hinge length did not increase as the ductility factor increased. A drop in maximum lateral load of approximately 8 % was observed to exist between the first and second cycles at a given displacement ductility.



(a) cage in mould



(b) pier base and strain gauges

Munro's Model [13]

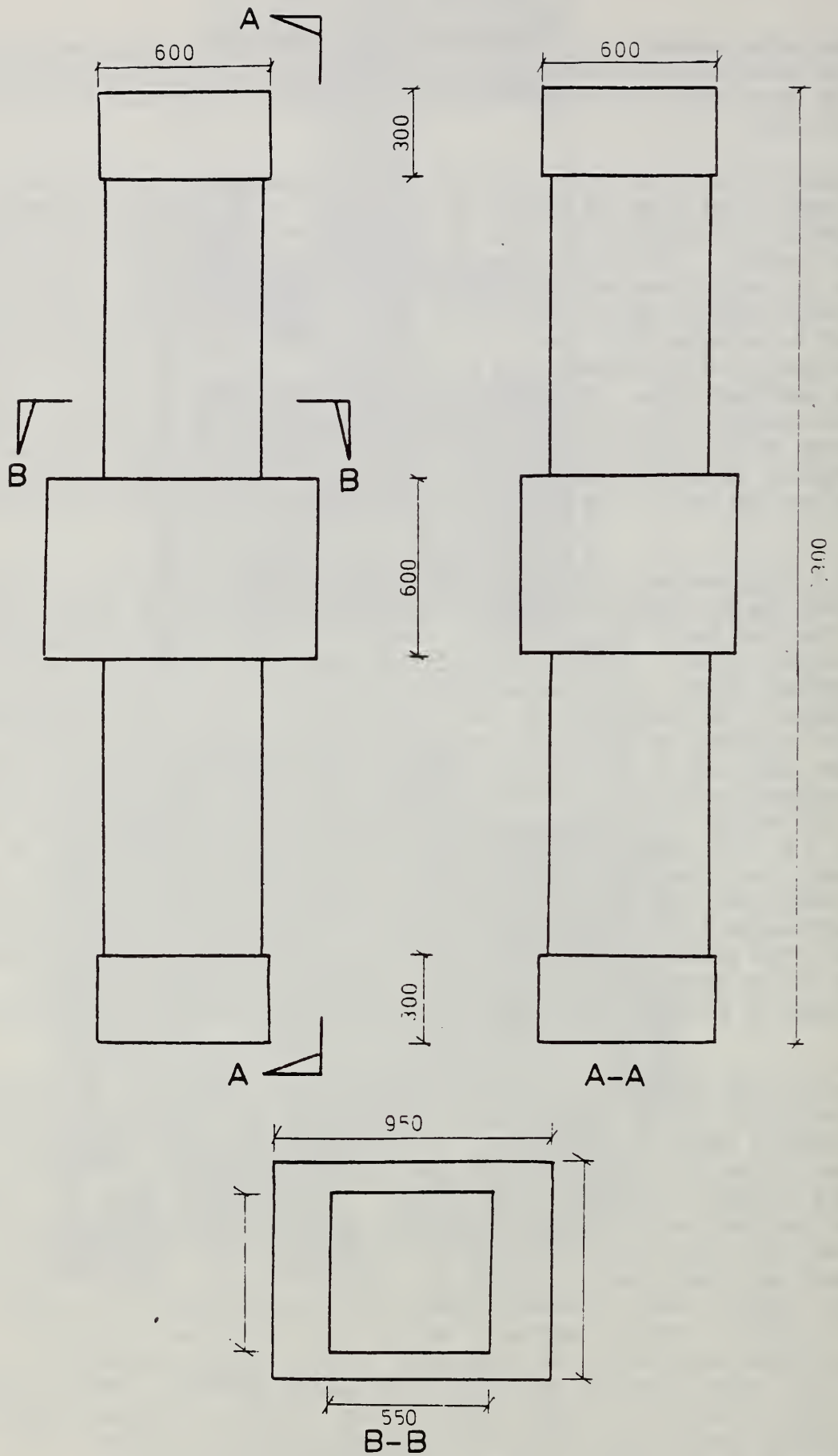
FIGURE 2.1

The moment-displacement curve from the dynamic test [13] compared very well with that obtained from this static test which indicated the acceptability of using statically obtained hysteresis loops for predicting seismic response [21].

All previous tests had been conducted with the specimens subjected to low axial loads, $0.08 f'_c A_g$ or less. In an effort to gain more information on the behavior of columns with high axial loads, Ng built and tested another 1/6 scale model. An axial stress of $0.5 f'_c$ was chosen for the model. A 1.38 in. (35 mm) diameter prestressing bar located in the center of the column was used to apply the axial load. Final load in this rod was adjusted to account for loss due to creep prior to testing the column. Longitudinal reinforcement was provided for with 10 - 0.47 in. (12 mm) diameter deformed bars. Spiral reinforcement consisted of 0.17 in. (12 mm) diameter smooth, round bars spaced at 0.39 in. (10 mm) on center. Design provisions of the draft New Zealand concrete code [15] were followed with the exception that the volumetric reinforcement ratio which was twice that required by the code. The provided volumetric reinforcement was 0.0244.

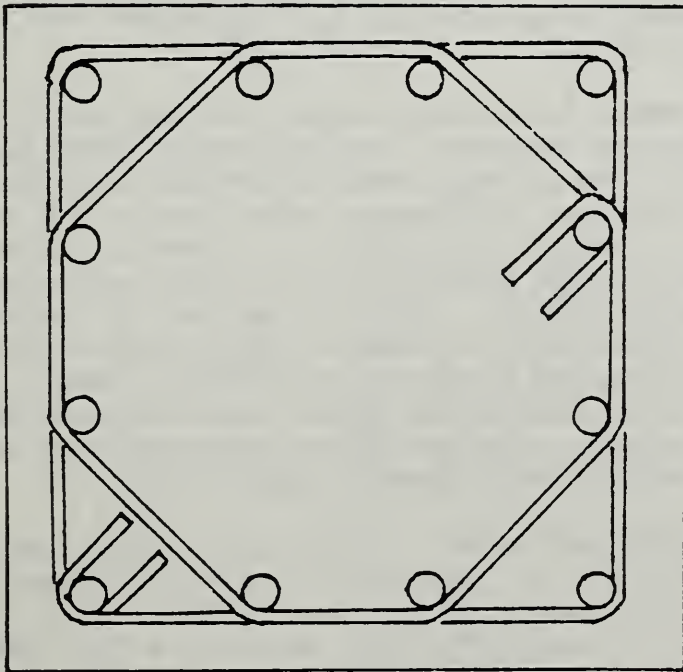
The yield displacement obtained experimentally equalled 0.2 in. (5 mm). Ng determined yield displacement in a manner similar to that used by Munro, except that the model was initially loaded to a displacement ductility of 0.75 instead of 0.6. Stable load-displacement and moment-rotation loops were obtained up to a displacement ductility of 8, at which point the test was stopped. No buckling of the longitudinal bars was observed, but extensive yielding of the spiral reinforcement up to 5.1 in. (130 mm) above the base was noted at the end of the test. It was evident that a displacement ductility of greater than 8 could have been achieved even though the spiral had yielded as no longitudinal bar buckling was noted. At 1.38 in. (35 mm) from the base, a maximum hoop strain of 6120 microstrain was recorded. This strain equalled 6 times the yield strain. It was concluded that if the amount of transverse steel used had been that recommended by the code, buckling of the longitudinal bars would have occurred. The plastic hinge length calculated experimentally was about 5.3 in. (135 mm) or about 0.5 H where H was the overall column diameter. Again no increase in plastic hinge length with increase in ductility factor was noted.

A series of four full size columns were tested by Gill [10] for different levels of axial load. These columns were designed in accordance with the New Zealand's code of practice, DZ 3101, first draft [7]. The cross sections of the columns were square with the sides equal to 21.7 in. (550 mm). The column is shown in Fig. 2.2. Twelve DH24, 0.94 in. (24 mm) diameter deformed bars made up the longitudinal reinforcement. Round bars were used for the transverse reinforcement. The transverse steel requirement was modified to reflect the level of axial load as required by the code. Spiral steel reinforcement, ρ_s , for the columns ranged from 0.015 to 0.0349. The arrangement of the ties is shown in Fig. 2.3. The specimens were held pinned at both ends. Axial stress ranged from $0.21 f'_c$ to $0.60 f'_c$. Axial load was provided by a DARTEC Universal Testing Machine (UTM) with a 2,248 kip (10 MN) capacity. The lateral load was applied at mid-height of the column through a heavily reinforced stub. This heavy reinforcement forced hinging to occur above and below the stub.

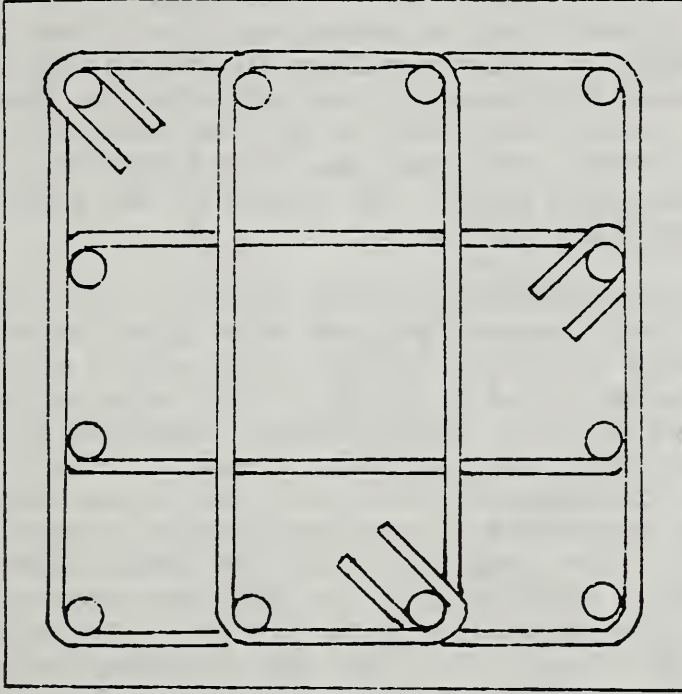


Gill's Model Dimensions [10]

FIGURE 2.2



(a) Specimen One and Two



(b) Specimen Three and Four

Gill's Tie Arrangement [10]

FIGURE 2.3

The data from the tests showed good stability of the load-displacement loops up a displacement ductility of 6. For higher axial loads, a greater increase of the measured lateral load and moment was noted from the values predicted based on ACI methods. Yield displacements ranged from 0.1 - 0.22 in. (2.5 - 5.7 mm) with lowest displacement corresponding to the specimen with the highest axial load. No buckling of the vertical bars was observed. Maximum hoop strain achieved was 8600 microstrain for the specimen with the highest axial load. The length of the plastic hinge region increased for higher axial loads.

Potangaroa [23] tested columns similar to those of Gill [10]. This series consisted of a total of five octagonal columns with spiral reinforcement. The columns were a 2/5 scale of typical bridge columns with a diameter of 59 in. (1500 mm). Columns were 10.8 ft. (3.3 m) high with a diameter of 23.6 in. (600 mm). The longitudinal reinforcement consisted of 16 - 0.94 in. (24 mm) diameter deformed bars with a yield stress of 40 ksi (275 MPa). The spiral reinforcement consisted of round bars with sizes ranging from 0.39 - 0.63 in. (10 - 16 mm) diameters at spacings ranging from 2.16 - 2.95 in. (55 - 75 mm). Units 1 to 4 complied with the first draft code of practice, DZ 3101 [7]. Unit 5 complied with the MWD requirements [9] which were more stringent than those specified in DZ 3101 [8]. The variables in the test were the magnitude of axial load and the corresponding amount of transverse reinforcement. The range of axial stress was from $0.15 f'_c$ to $0.70 f'_c$ and the range of spiral reinforcement ratio was 0.0075 to 0.0261. The specimens were loaded in the same manner as Gill [10] and the same boundary conditions existed. The columns exhibited good stability of the load-displacement loops up to a ductility factor of 8. Although the spiral reinforcement yielded early in the test ($\mu = 2$), it still provided sufficient confinement to achieve $\mu = 8$. The extent of spiral yielding increased with increased axial load. Unit 5 sustained minimal damage for $P_e = 0.35 f'_c A_g$ while attaining a ductility of 8 and was further tested with the axial load increased to $P_e = 0.70 f'_c A_g$. The latter test began and ended at a ductility factor of 8.

Under high axial loads (Unit 5, second stage), it was found that the plastic hinge extended into the secondary confined region (where the spiral spacing was greater than in the primary confined region near the base of the column). The use of different confinement steel ratios for different sections of a column is allowed by the code [7]. However, in this test, the extension of the plastic hinge into the less-confined region permitted buckling of the longitudinal bars. This in turn led to the eventual fracture of the bars and column failure outside the primary confined area. Also, the $P - \Delta$ effects were significant for high axial loads. From the data obtained for unit 5, a conclusion drawn was that the SEAOC/ACI requirements for confinement steel quantities appeared to be excessive for low axial loads and unconservative for high axial loads.

To study the effects of different aspect ratios (L/D), Ang [5] tested two octagonal and two square columns. The details of reinforcement in the columns satisfied the requirements of the second draft of DZ 3101 [7]. These columns were similar to Potangaroa's [23] and Gill's [10] except that the diameter of the columns was reduced from 21.7 in. (550 mm) to 15.7 in. (400 mm) and the height was increased to increase the aspect ratio from 2 to 4. Fig. 2.4 shows the dimensions of these columns. The longitudinal reinforcement used for the octagonal columns was 16 deformed 0.63 in. (16

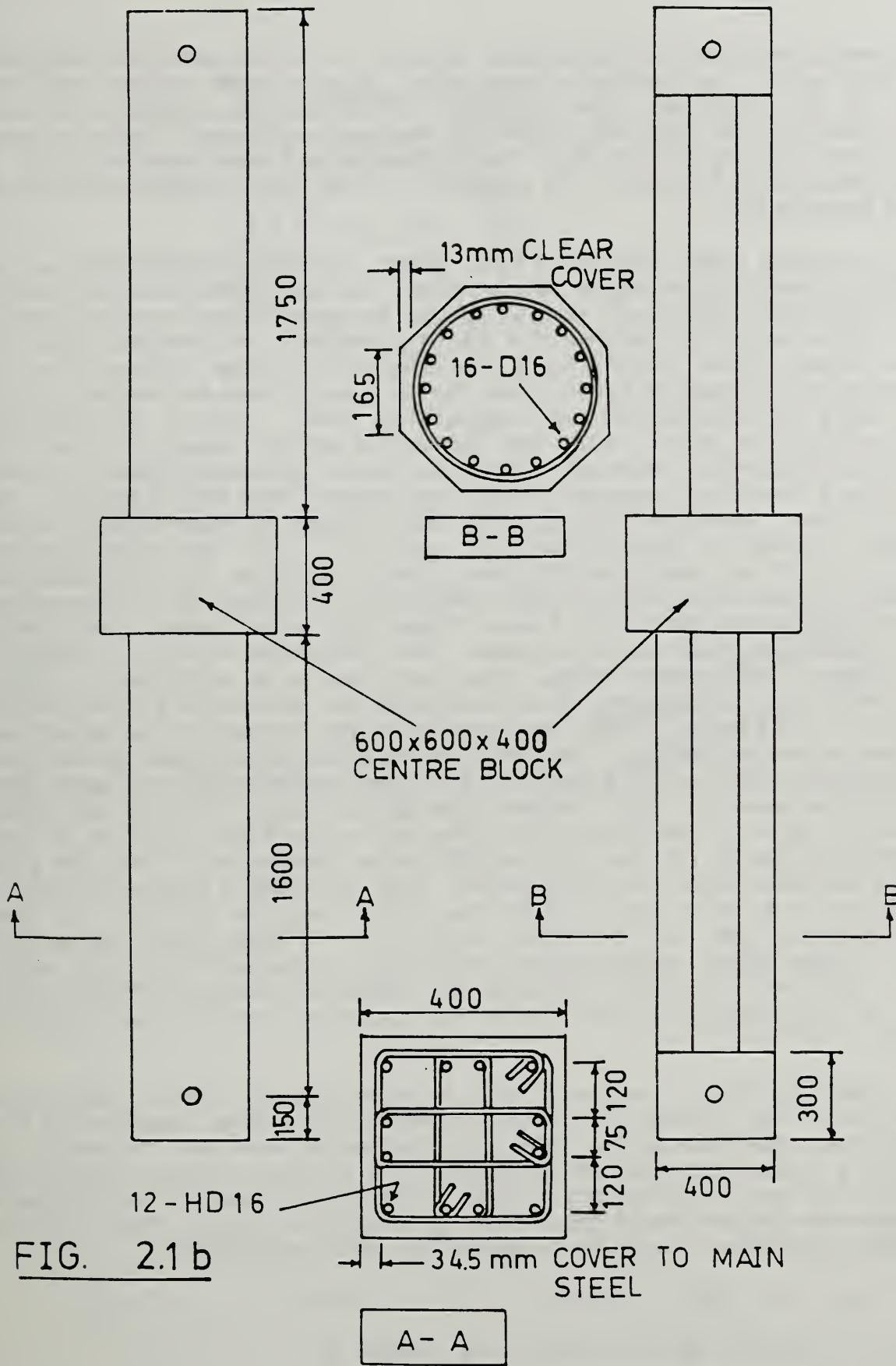


FIG. 2.1 b

DIMENSIONS OF SPECIMENS

Ang's Model Dimensions [5]

FIGURE 2.4

mm) diameter bars and for the square columns, 12 of the same size deformed bars were used. The spacing of the spiral reinforcement ranged from 1.57 - 3.94 in. (40 - 100 mm). The volumetric ratios for the octagonal columns were 0.00851 and 0.01522 and 0.0151 for the square columns. Axial stress ranged from $0.12 f'_c$ to $0.53 f'_c$. The columns were loaded statically to a displacement ductility of 8. In addition to this, the columns were further tested dynamically.

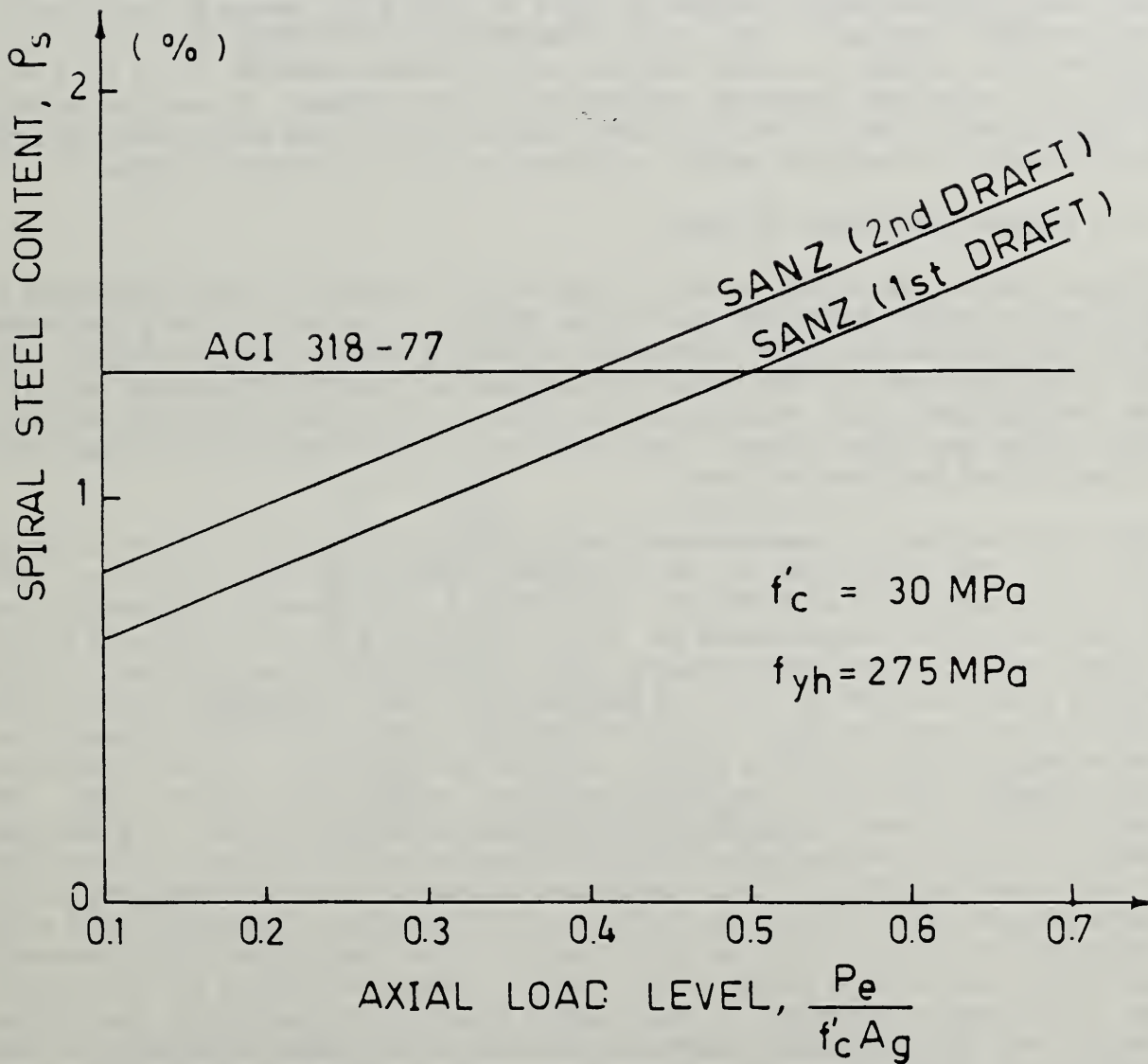
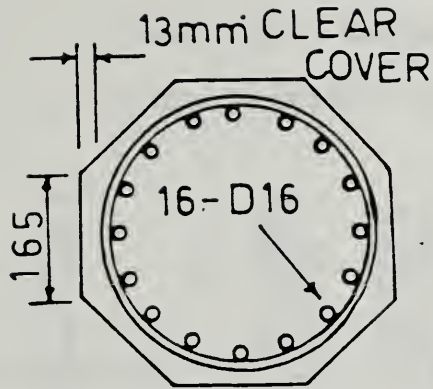
Data from these tests indicated that, where adequate confinement in the potential plastic hinge region was provided, the load-deflection hysteresis loops exhibited excellent stability (no pronounced drop in peak lateral load) up to ductility factors of 8 for the octagonal columns and 6 for the square columns. These results held true over a wide range of aspect ratios. The onset of ultimate failure under static loading was evidenced in all these tests by buckling of the longitudinal bars. Unit 2, the specimen with the highest axial load, had sustained severe damage and was not subjected to further testing. The units which underwent dynamic testing failed as a result of fracture of the longitudinal bars and/or spiral. The ductility was, therefore, affected by the increase in aspect ratio as the columns tested by Potangaroa [23] and Gill [10] had displacement ductilities of at least 8 without any visible sign of longitudinal bar buckling. Equivalent plastic hinge length was also found to be independent of the displacement ductility factor. Under high axial loads, the plastic hinge length was observed to increase. The transverse steel provided for confinement in the plastic hinge region was found to be sufficient to carry the shear. The transverse steel strength was determined from design equations in the code [8] and the shear strength carried by the column was obtained experimentally. The performance of these specimens showed that reinforcement detailed in accordance with the second draft was sufficient for ductile behavior for low and high axial loads. Due to the lower volumetric ratio of confining steel required by the first draft of DZ 3101 [7] and ACI 318-77 [2] for high axial loads, it was felt that the same ductile behavior might not be achieved. Fig. 2.5 shows a comparison of the volumetric ratios as required by the first draft of DZ 3101 [7], the second draft of DZ 3101 [8] and ACI 318-77 [2]. A significant increase in strain in the spiral reinforcement was noted in specimens with high axial load. This was initially evidenced by extensive yielding of the spiral steel at low ductility levels and strain hardening during later stages of testing.

Some common findings from these studies were that the moment capacities predicted by ACI column charts were conservative when compared to the values found experimentally. This was reasoned to have been the result of adopting a conservative value of 0.003 for the ultimate concrete strain and a result of strain hardening of the reinforcing steel. The ultimate concrete strain was found to be much greater than 0.003. The confined concrete stress was calculated using the following equations:

$$f'_{cc} = f'_c + 4.1 f_1 \quad (2.1)$$

where f_1 is defined assuming spiral has yielded as

$$f_1 = \frac{2 f_{yh} A_{sp}}{d_s s_h} \quad (2.2)$$



Confinement Steel Comparison [5]

FIGURE 2.5

A_{sp} = area of spiral reinforcement

f_{yh} = yield strength of spiral reinforcement

d_s = diameter of column to outside of spiral

s_h = spiral pitch

Combining equations (1) and (2) will result in

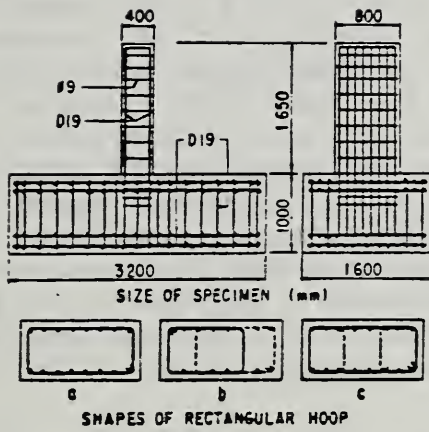
$$f'_{cc} = f'_c \left(1 + 2.05 \rho_s \frac{f_{yh}}{f'_c} \right) \quad (2.3)$$

It was found that these equations would result in a better estimate of the ultimate strength than that determined by means of the ACI column charts. The plastic hinge length ranged from 0.4 H to 0.64 H, where H was equal to the column diameter, and could reasonably be taken as 0.5 H [22]. Although the spirals or ties yielded early in the tests at $\mu = 2$ or $\mu = 4$, they still provided adequate confinement of the column. It was the opinion of the authors that it was not justifiable to provide additional spiral reinforcement to maintain spiral stresses within the elastic range.

2.2.2 Studies Performed in Japan

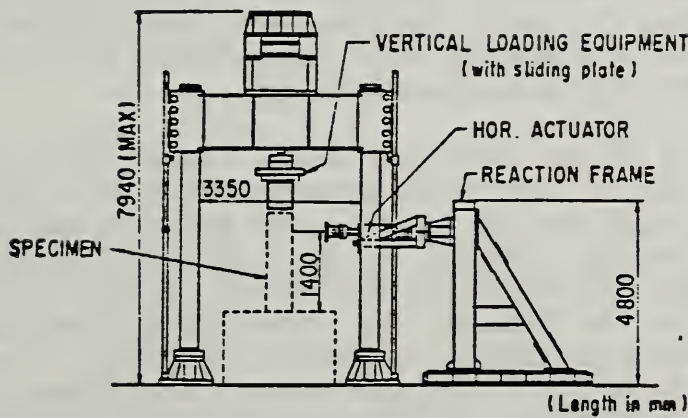
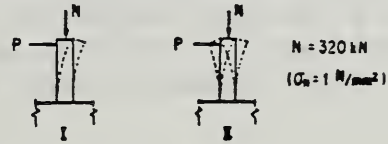
Seismic testing of bridge models in Japan has principally been conducted at the Public Works Research Institute (PWRI). The following paragraphs describe some of the work performed on models under static loading. The yield displacement in the tests was defined as that displacement at which the longitudinal bars reached yield strain. A specimen was considered to have failed when the lateral load fell below the initial yield load after ultimate load had been achieved.

Ohta [18] tested six specimens of rectangular cross sections as shown in Fig. 2.6. The dimensions of the specimens were 15.75-in by 31.5-in. (400-mm by 800-mm) and had a height of 5-ft-5-in (1650-mm). The shear-span ratios for these models were 4. The shear-span ratio was defined as the column height to column diameter ratio (L/d) and is equivalent to the aspect ratio as used in the New Zealand studies. Configurations of the hoops were singular, double, and combined single hoop with cross-ties. These hoop configurations are also shown in Fig. 2.6. The volumetric reinforcement ratio for the confining steel ranged from 0.04 to 0.16. The longitudinal steel ratio for all the models was 0.0082. The maximum spacing of the ties was the minimum dimension of the column as specified in the Japan Society of Civil Engineers standards 1974. The spacing of the hoops ranged from 3.93 in. to 15.75 in. (100 to 400 mm). Deformed bars with a diameter of 0.75 in. (19 mm) were used for the longitudinal reinforcement and round bars with a diameter of 0.35 in. (9 mm) were used for the hoops. One of the units (specimen A) was tested under uni-directional (monotonic) loading and the others were tested cyclically. The axial load applied was 71.94 kip (320 kN). Based on a concrete compressive strength of 4234 psi (29.2 MPa), $P_e/(f'_c A_g) = 0.03425$.



SPECIMEN	SHEAR SPAN RATIO	HOOP SPACING (cm)	HOOP RATIO ρ_w (%)	SHAPE OF HOOP	LONGITUDINAL BAR RATIO ρ_l (%)	HISTORY	$\sigma_u = N/A_c$ (N/mm ²)
A	4.0	20	0.08	a	0.82	I	10
B		20	0.08	a			
C		10	0.16	a			
D		20	0.16	b			
E		20	0.16	c			
F		40	0.04	a			

* LOADING I ONE DIRECTION: 10 CYCLES AT $\delta_1, 2\delta_1, 3\delta_1, \dots$
 LOADING II REVERSAL: 10 CYCLES AT $\delta_1, 2\delta_1, 3\delta_1, \dots$



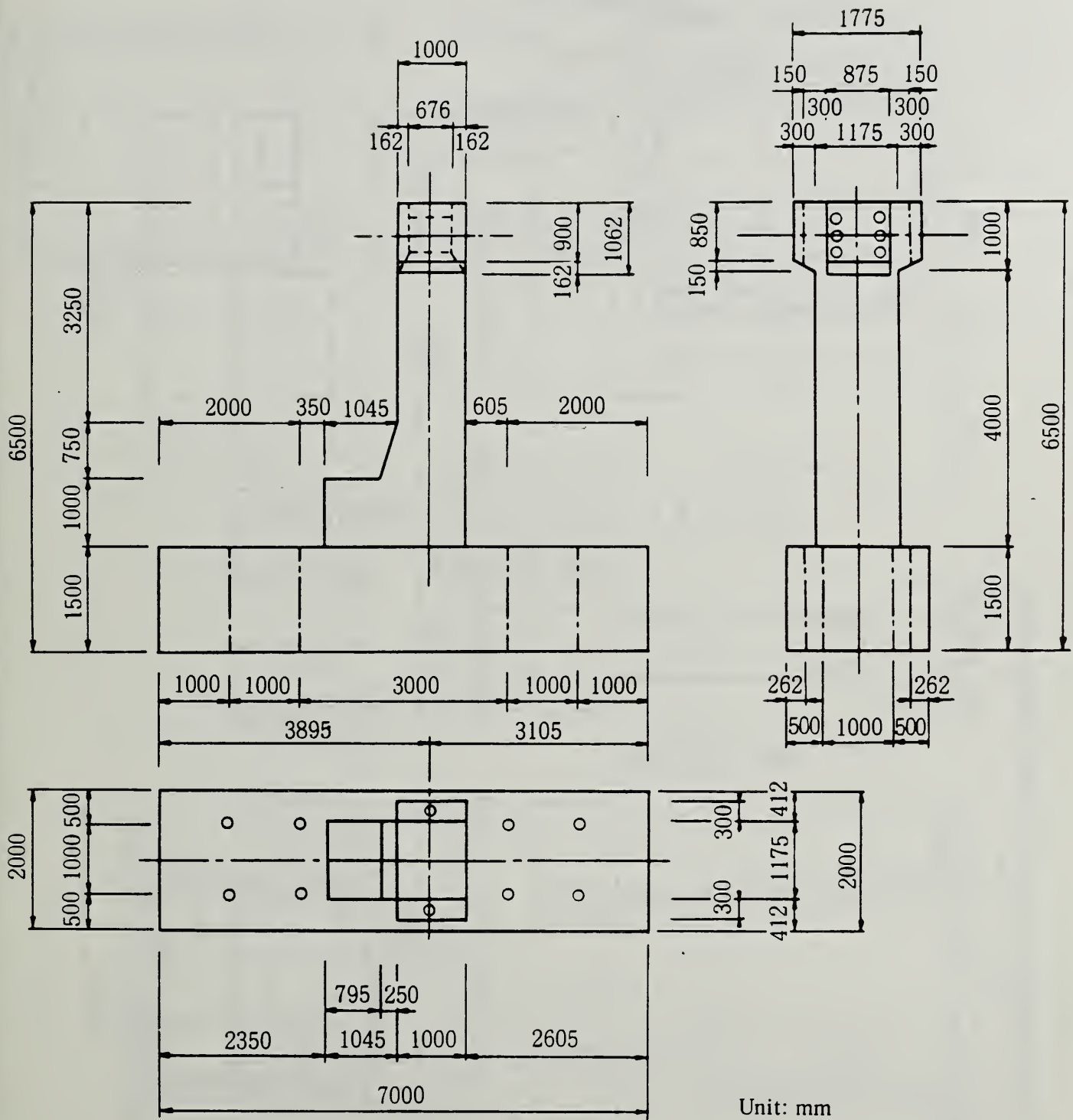
Ohta's Model Dimensions and Test Set-Up [18]

Fig. 2.6

The columns were cyclically loaded to yield displacement, $2\Delta_y$, $3\Delta_y$ etc. with the number of cycles equal to 10 for each displacement ductility. Stable loops were obtained for specimens loaded cyclically up to a displacement ductility of 3, except for Specimen F which had the largest hoop spacing [15.75 in. (400 mm)] and the smallest confining steel ratio (0.04). Specimen F had stable load-deflection hysteresis loops (no significant drop in maximum lateral load) up to a displacement ductility of 2. Specimen A reached a displacement ductility of 12, however, the axial load was removed at $8\Delta_y$ due to the difficulty in maintaining the axial load. At displacement ductilities of 3 or less, only flexural cracks formed for specimen A. These cracks became inclined with greater displacement ductilities. The other specimens had horizontal cracks forming completely through the column core upon loading to Δ_y . Diagonal cracks formed at 2-3 times Δ_y . The specimen with single hoops at a spacing of 3.94 in. (100 mm) and the specimen with the double hoops absorbed more energy than did the others and were therefore considered to be superior to single hoops with cross ties. It was also concluded that a maximum spacing of 1/2 the minimum column dimension would be adequate for hoops in the plastic hinge region.

Models of a Ban-no-su Bridge pier of the Honshu-Shikoku Bridge were tested by Kuribayashi et. al. [11] at the Public Works Research Institute. The scales of these models were 1/4 scale for one and $1/(4\sqrt{2})$ for six others. The dimensions of the models are shown in Figs. 2.7 and 2.8. Arrangement of the steel is shown in Figs. 2.9 to 2.13. Table 2.1 shows the test conditions of the models. The objectives of the study were to observe the effects of loading conditions [uni-directional (monotonic) vs. cyclic], the effects of a haunch (see Fig. 2.9) at the column base, the effects of the size of the longitudinal reinforcement without transverse reinforcement, the dynamic behavior of a concrete column reinforced with steel frame elements (SRC) as compared with a standard reinforced concrete column, and the effects of studs attached to the base of the steel frame. Specimen No. 1 was cycled 3 times for each displacement ductility while the other specimens were cycled 10 times for each displacement ductility. The aspect ratios for all the models were approximately 4.

In general, yielding of the confining spiral had no significant impact on the performance of the column. Only after fracture of a spiral bar in the plastic hinge region did maximum lateral load begin to decrease noticeably. Specimens No. 1 (monotonic loading) and No. 4 (large diameter longitudinal reinforcement with no transverse reinforcement), failed in shear while the other specimens failed in flexure. The strength and ductility of Specimen No. 4 were also lower than that of the other specimens. The stiffness at yield was found to be 1/3 - 1/4 of the initial stiffness. The yield and ultimate load of specimen No. 1 and specimen No. 3 (basic model - with haunch, no axial load, reversed loading) was about equal. However, the ultimate displacement of No. 3 was 40% that of No.1. Due to this observed reduction, the displacement ductility of specimens loaded cyclically was 1/3 - 1/2 that of specimens loaded monotonically. The yield and ultimate capacities of Specimen No. 3 was 20 - 30 % larger than Specimen No. 2 (without haunch). Specimen No. 7 (with axial load corresponding to the superstructure weight) had a 20 % larger yield load, a 10 % larger ultimate load and a 10 - 20 % smaller displacement ductility than did specimen No. 3. The maximum lateral load was observed to decrease significantly during the second cycle at a particular displacement ductility. This was followed



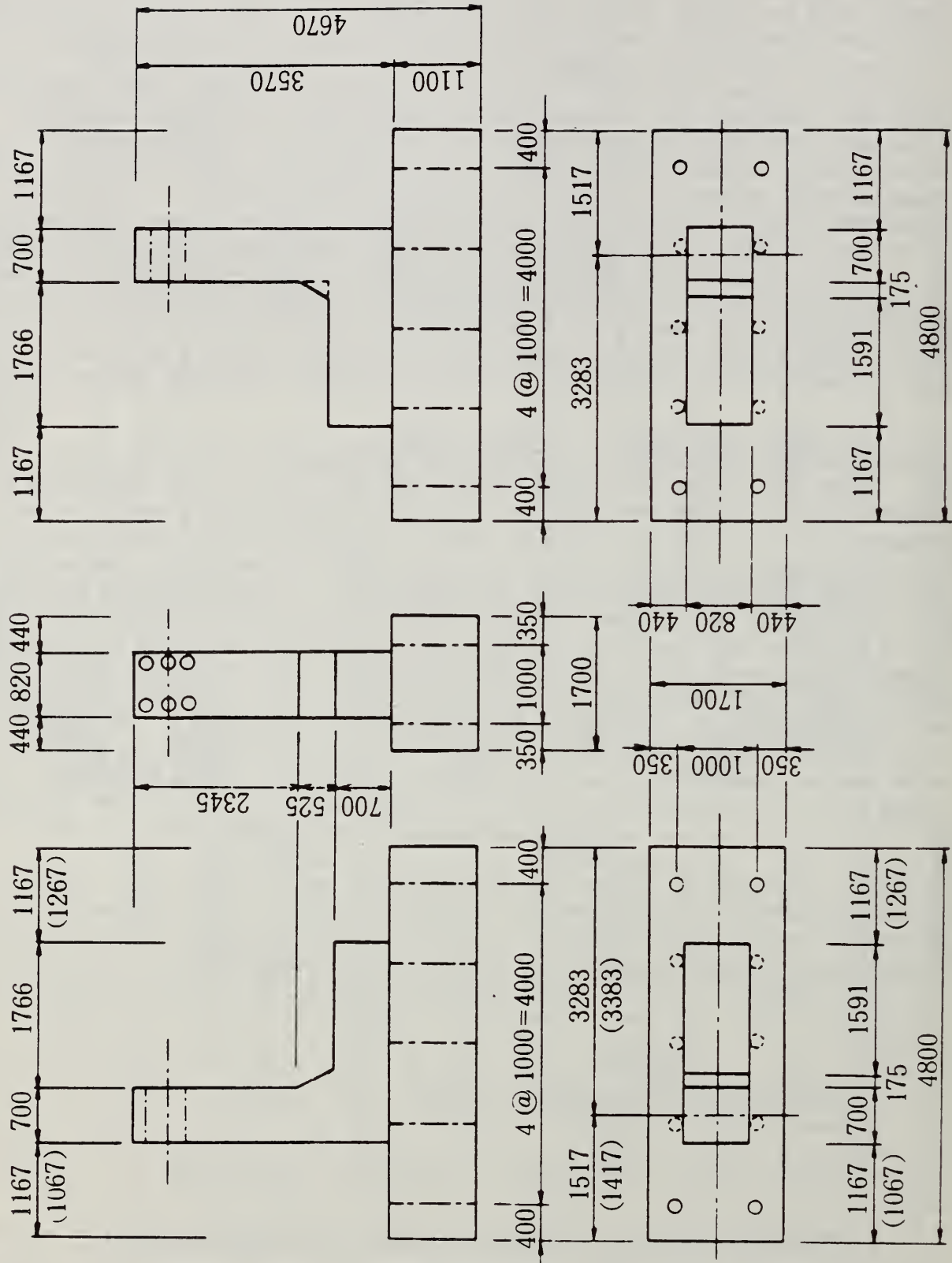
Kuribayashi's 1/4 Scale Model Dimensions [11]

FIGURE 2.7

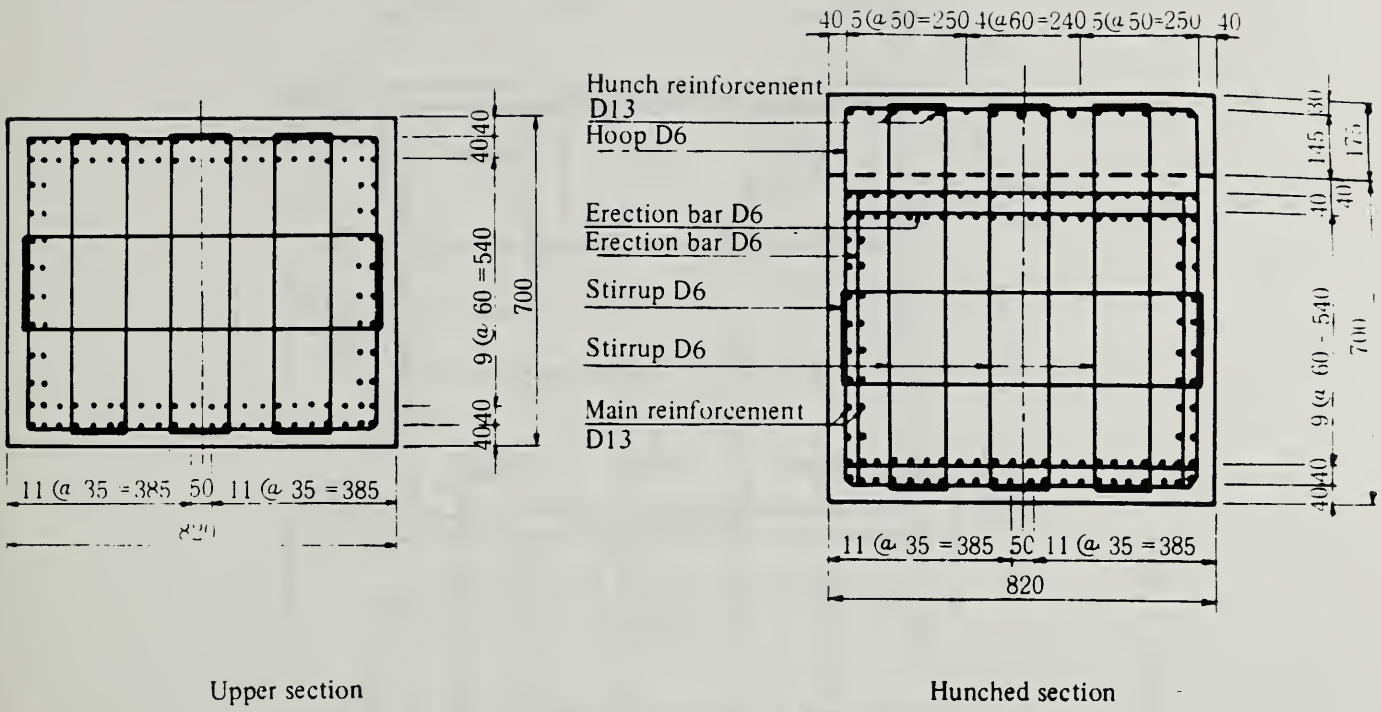
Type A

Type B

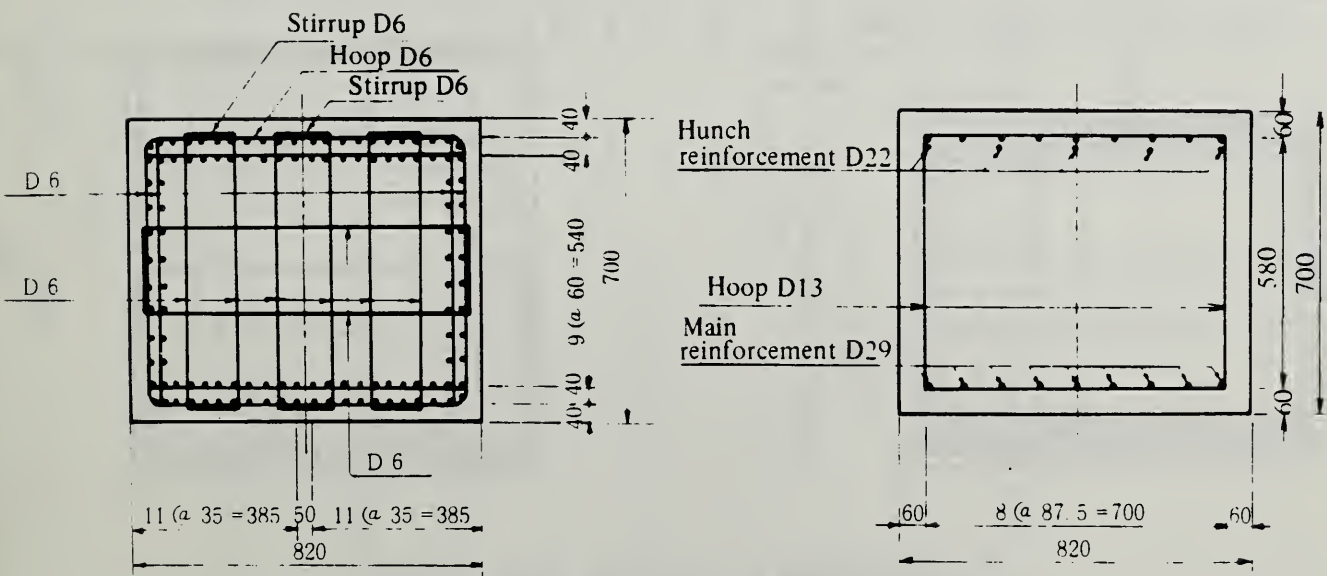
() shows dimensions of one-directional loading model



Unit: mm

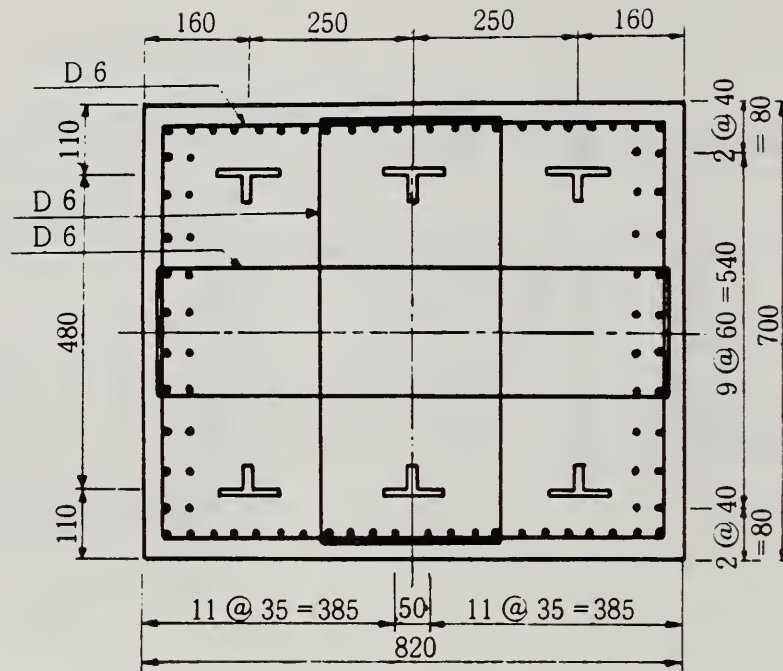


Kuribayashi's Column Nos. 1 & 3 [11]
FIGURE 2.9

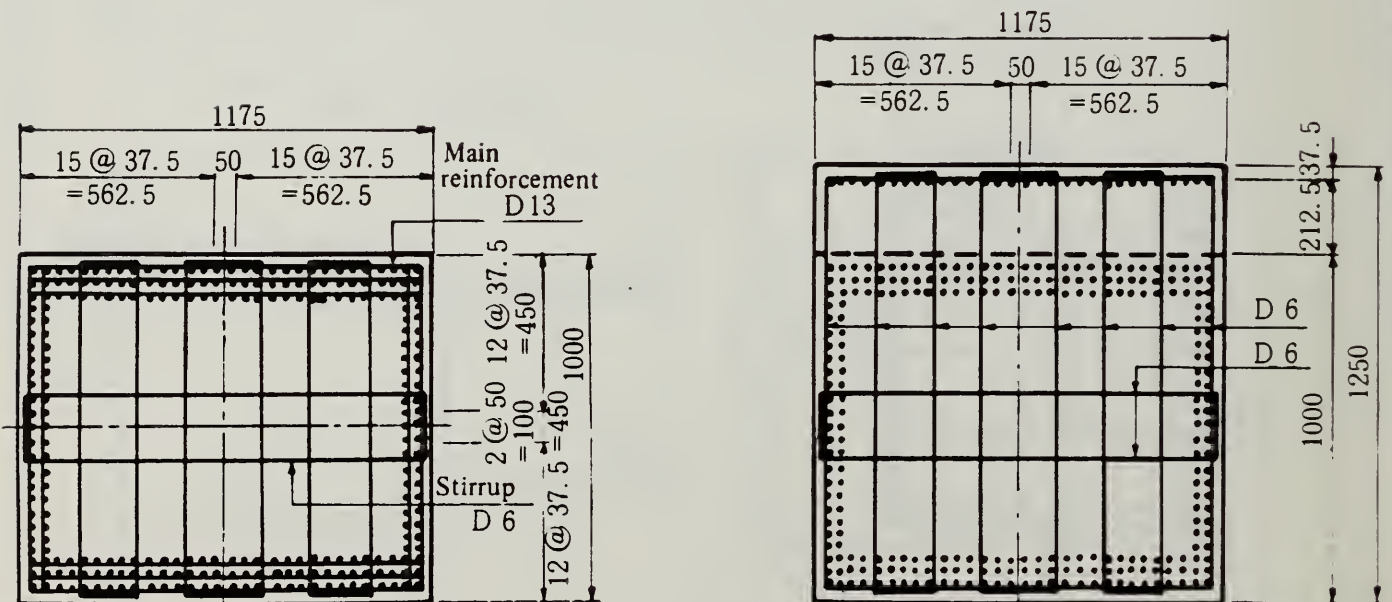


Kuribayashi's Column No. 2 [11]
FIGURE 2.10

Kuribayashi's Column No. 4 [11]
FIGURE 2.11



Kuribayashi's Column Nos. 5 & 6 [11]
FIGURE 2.12



Kuribayashi's Column No. 7 [11]
FIGURE 2.13

Model	Test Conditions
No. 1 $1/(4\sqrt{2})$ one-directional loading model	one-directional loading, other conditions are the same as basic model.
No. 2 $1/(4\sqrt{2})$ without hunch model	without hunch, other conditions are the same as basic model.
No. 3 $1/(4\sqrt{2})$ basic model	same structural conditions as the actual bridge (main reinforcement—D13, reversed cyclic loading)
No. 4 $1/(4\sqrt{2})$ large-diameter reinforcement, without side reinforcement	large-diameter reinforcement and without side reinforcement (main reinforcement—D29, reversed cyclic loading)
No. 5 $1/(4\sqrt{2})$ SRC-without stud model	SRC without stud (CT shape steel + D13 reinforcement, reversed cyclic loading)
No. 6 $1/(4\sqrt{2})$ SRC-with stud model	SRC with stud (CT shape steel + D13 reinforcement, reversed cyclic loading)
No. 7 $1/4$ model	same structural conditions as the actual bridge (main reinforcement—D13, reversed cyclic loading)

Note: Axial load of 118t corresponding to the dead load of the superstructure was applied to $1/4$ model, but no axial load was applied to $1/(4\sqrt{2})$ models.

Kuribayashi's Test Conditions [11]
TABLE 2.1

by a more gradual decrease in maximum lateral load for the succeeding cycles. The aseismic behaviors of RC and SRC columns were found to be similar. The shear studs were determined to be ineffective in preventing the pull-out of the steel frames in SRC columns.

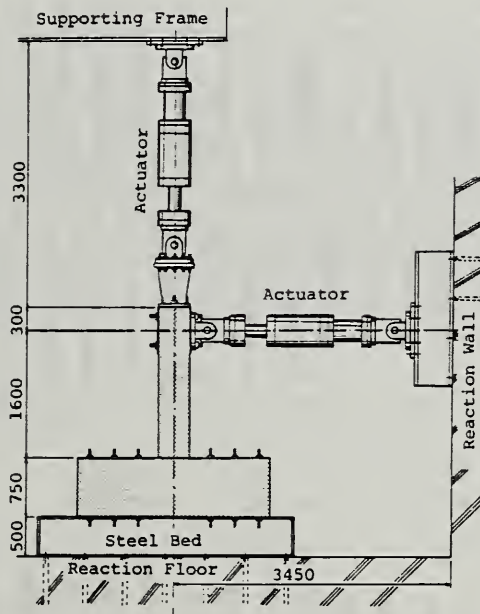
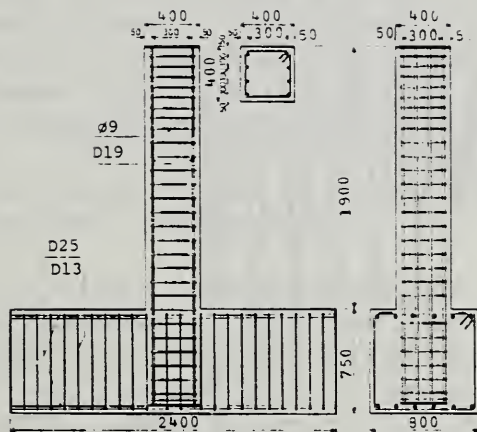
Ohno and Nishioka [17] studied the effect of the number of loading cycles at a ductility level on the energy absorption capacity of the column. Five specimens with square cross sections, Fig. 2.14, were constructed. The sides of the columns were 15.75 in. (400 mm) and the height was 74.8-in (1900 mm). The aspect ratios for all the models were 4. Deformed bars of 0.75 in. (19 mm) in diameter and round bars of 0.35 in. (9 mm) in diameter spaced at 3.94 in. (100 mm) were used for longitudinal and transverse reinforcement respectively. The confining reinforcement ratio was 0.0032. The longitudinal reinforcement ratio was 0.0082. The applied axial stress for all specimens was 142 psi (0.98 MPa) except for Specimen No. 4 which had an applied axial stress of 284 psi (1.96 MPa). This corresponded to $P_e/(f'_c A_g) = 0.079$ for Specimen No.4 and $P_e/(f'_c A_g) = 0.032$ for all the other specimens. The compressive strength of the concrete was 3596 psi (24.8 MPa).

The loading sequence for Specimen No. 1, L-1, was one cycle each at 1, 5, and 8 times Δ_y . The loading sequence for specimen No. 2, L-2, was one cycle each at 1, 2, 3, ... , 8 Δ_y . The loading sequence for specimens Nos. 3 and 4, was 1 cycle to Δ_y followed by 5 cycles each at 2, 3, 4, ... Δ_y . L-4, loading sequence for Specimen No. 5 was 1 cycle to Δ_y followed by 10 cycles each at 2, 3, 4, etc. Δ_y . These loading sequences are shown schematically in Fig. 2.15.

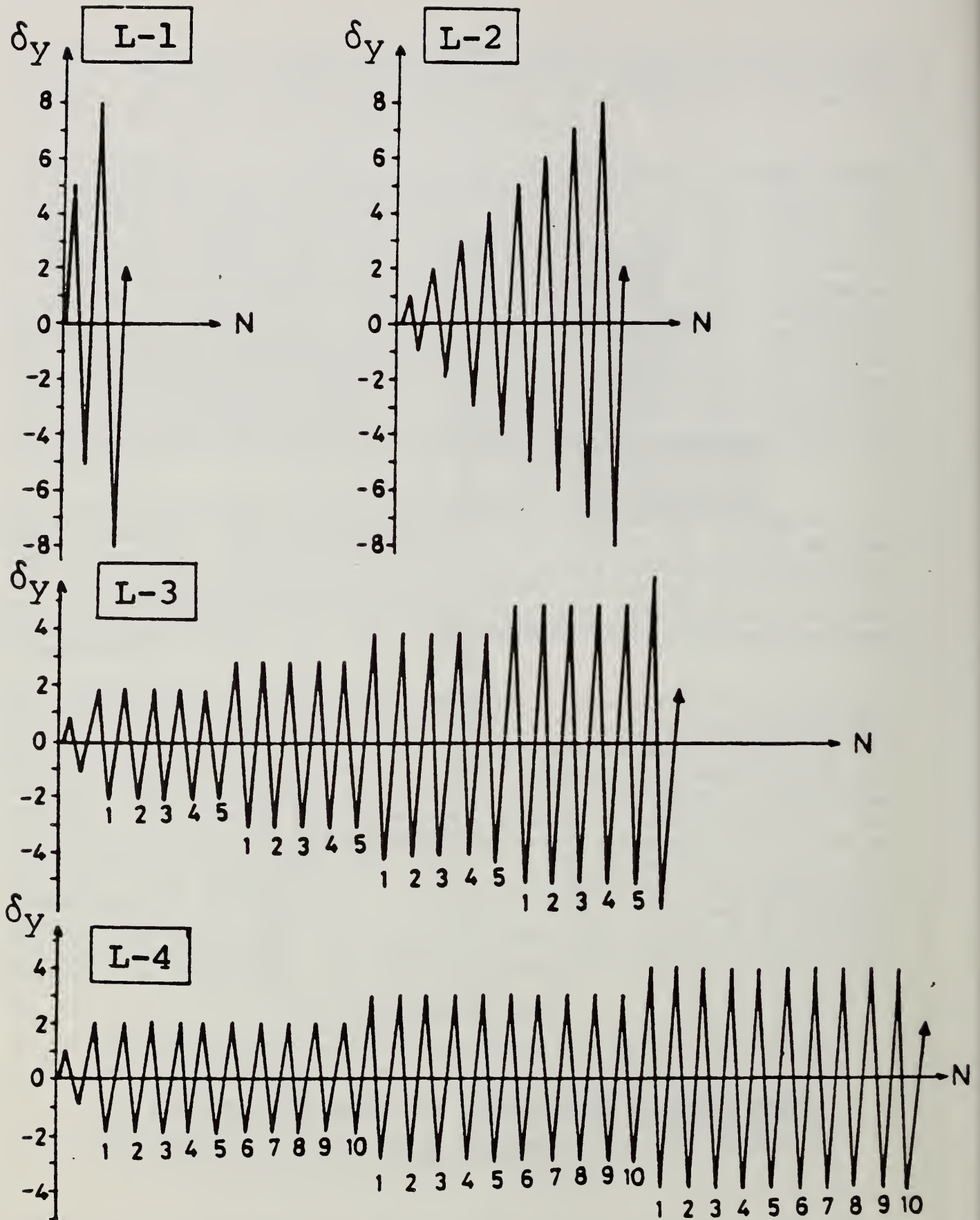
The length of the plastic hinge was found to be about 15.75 in. (400 mm) which was equal to the width of the column. This distance was measured from the base. The center of rotation was at about 7.9 in. (200 mm) from the base. The ultimate displacement was the displacement corresponding to the failure load as described previously. For all specimens, the maximum strength was obtained in the first cycle at 2 times delta y. The cumulative absorbed energy, the sum of the energy absorbed by the column up to ultimate failure, was about equal for Specimens Nos. 3 to 5. The average of the three values is 128.5 ft-kip (95 kN-m). The cumulative energy absorbed for Specimen No. 3 was 126.4 ft-kip (93.2 kN-m) as compared with Specimen No. 4 which had a cumulative absorbed energy of 123.8 ft-kip (91.3 kN-m) and an axial stress double that of Specimen No. 3. Two major findings from this study were :

- . The axial stress was felt to have had no effect on the energy absorption capacity of the column in this study.
- . Total energy absorbed by the specimens was not influenced by the number of loading cycles although the ultimate ductility was influenced by the the number of cycles.

Studies [20] have also been carried out on the seismic resistance of concrete bridge piers through the use of the Dynamic Structural Testing Facility at PWRI. Some of the conclusions from these tests are presented in brief.



Ohno's Model Dimensions and Test Set-up [17]
 FIGURE 2.14



Ohno's Loading sequence [17]

FIGURE 2.15

In a study [20] done in 1982 on the effect of dynamic loading and longitudinal reinforcement ratio, both static and dynamic testing of model piers were conducted.

- . Yield and maximum strengths and yield displacements increased with increasing longitudinal reinforcement ratio.
- . Although no significant differences in behavior were observed between dynamic loading and static loading, the maximum strength, ultimate displacement, and ductility factor for specimens subjected to dynamic loading were slightly larger than those subjected to static loading.
- . Plastic hinge length increased proportional to the amount of longitudinal reinforcement.

A study in 1983 [20] investigated the effect of column aspect ratio (height/column diameter). Test results for a column with an aspect ratio of 2.2 indicated that failure was dominated by shear. Models with aspect ratios of 3.8 and 5.4 had failure modes dominated by flexural effects. These models were tested dynamically. Ductility factor (maximum lateral displacement at failure/ yield displacement) was found to decrease as the aspect ratio decreased.

A study [20] performed in 1984 showed that for high aspect-ratio columns (dominated by flexural effects) under dynamic loading the effect of cross sectional shape was insignificant if cross sectional area, height, longitudinal and tie reinforcements were equal. Tests on small aspect ratio columns (dominated by shear effects) indicated that circular columns performed better than square columns.

Reference 20 also discusses a series of tests which investigated the effectiveness of continuous spiral reinforcement vs individual ties in bridge columns. The test specimens were model columns with a diameter of 22-in (0.56) meters and aspect ratios of 4.7 and 3.3. The spiral pitch was 1 in. (25 mm) and was continuous from the column base to a height of 19.7 in. (500 mm). These showed significantly greater ductility factors than similar models reinforced with individual ties at the same spacing. The effect of spiral hoop on the maximum strength of the model was minor. These findings were reported in a study done on the effect of spiral hoops for columns piers with circular cross sections [20] in 1984.

2.2.3 Tests Performed in Yugoslavia

A series of four circular model columns were subjected to cyclic lateral loads with constant axial load. Variables included the effect of magnitude of axial load and the effect of column aspect ratio (L/D: height/diameter). Two column heights were chosen: one to achieve a failure mode predominated by flexural effects and a second to achieve failure in shear.

The column heights (from footing to point of lateral load application) were 6' - 6.74" (200 cm) and 3' - 3.37" (100 cm) for the column heights of the flexure and shear models respectively. The column diameter was 12.09 in. (30.7 cm), the same for all specimens. The column aspect ratio (L/D) for

the flexure models was 6.51 and 3.26 for the shear models. The dimensions of the footing were 47.2 x 15.75 x 19.7 in. (1.20 x .40 x .50 m). Fig. 2.16 and 2.17 show the dimensions, steel layout and test set-up for the model tests.

The longitudinal reinforcement for all models consisted of 12 - 0.472 in. (12 mm) diameter bars. This resulted in a $\rho_t = 0.0183$. The transverse reinforcement consisted of individual circular hoops (not spirals) made from 0.236 in. (6 mm) in diameter wire. The spacing of the hoops for the flexure models was 2.95 in. (7.5 cm) near the fixed (cantilevered) end and was 5.91 in. (15 cm) for the remainder of the column height. [No specifications were given in the report as to the extent of the more heavily confined region]. A uniform hoop spacing of 2.95 in. (7.5 cm) was used for the shear models. The confining steel volumetric ratio, ρ_s , was 0.00628.

The aggregate used in the construction of the models was a river gravel with a nominal maximum size of 0.630 in. (16 mm). The average concrete compressive strength obtained from 7.87 x 7.87 x 7.87 in. (20 x 20 x 20 cm) cubes was 3260 psi (463 kp/cm²).

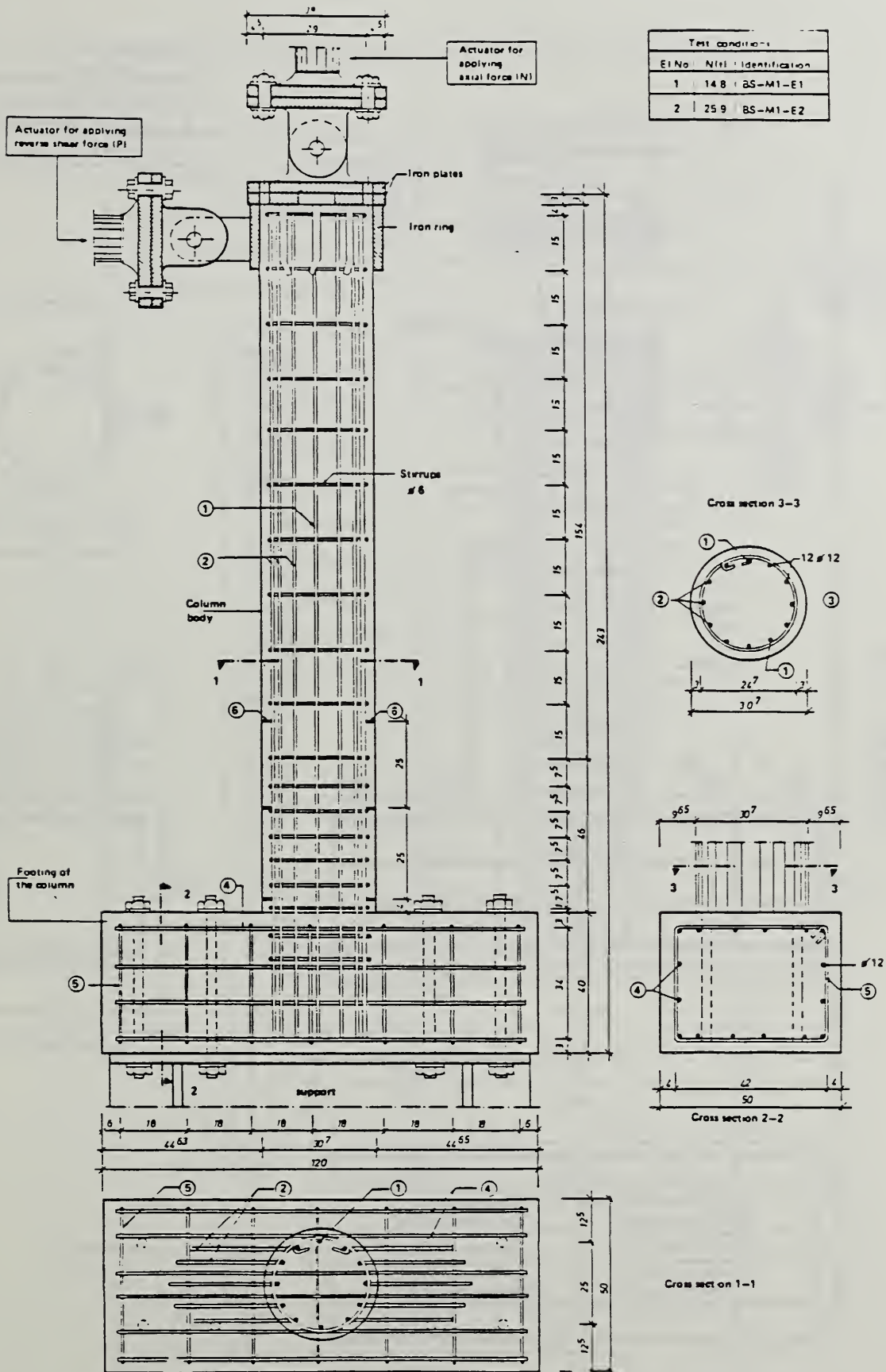
In each test set, flexure and shear, one of the models was subjected to an axial load of 16.1 kips (14,805 kp) while the other was loaded to 28.2 kips (25,908 kp). This resulted in a $P_e/f'_c A_g$ ratio of 0.043 for the lower axial load and 0.075 for the higher axial load.

The models were cycled three times while in the elastic range (displacements less than yield displacement) and 5 times while in the inelastic range (displacements greater than yield displacement). The load histories for the flexure and shear models are shown in Figs. 2.18 through 2.21. The displacement increments while in the elastic range were very small [0.04 in. (1 mm) for the shear models and 0.08 in. (2 mm) for the flexure models] so that the yield displacements could be determined more accurately. The yield displacement was defined as the displacement at which no increase in lateral load was observed for an increase in displacement.

The experimentally measured yield displacement for the flexure model subjected to the lower axial load (BS-M1-E1) was 0.59 in. (15 mm) and that of the flexure model subjected to the higher axial load (BS-M1-E2) was 0.63 in. (16 mm). The ultimate ductility for BS-M1-E1 was 4.58 and 3.31 for BS-M1-E2. The criteria for determining ultimate failure not defined in the paper.

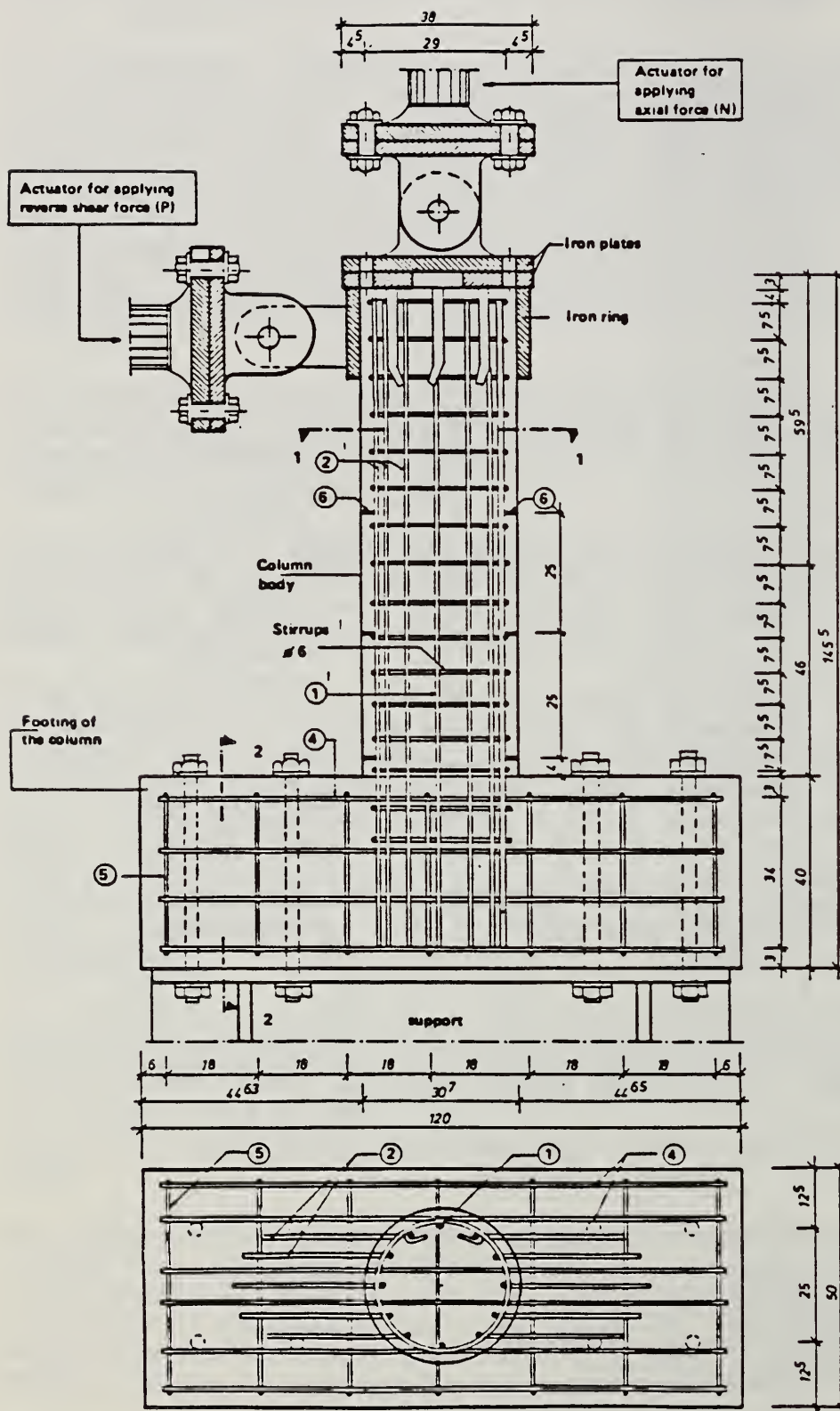
The experimentally measured yield displacement for the shear model test series was the same for both low axial load (BS-M2-E1) and high axial load (BS-M2-E2): 0.22 in. (5.5 mm). The ultimate displacement ductility for BS-M2-E1 was 5.96 and 5.73 for BS-M2-E2. The damage for the flexure models was due to nearly pure bending effects while failure of the shear models was due to combined bending and shear effects.

The experimental maximum moment obtained for BS-M1-E1 was 40.75 kip-ft (5.63 t-m) and 45.24 kip-ft (6.25 t-m) for BS-M1-E2. The experimental maximum moment values for the shear model BS-M2-E1 was 52.33 kip-ft (7.23 t-m) and for BS-M2-E2 was 55.80 kip-ft (7.71 t-m).



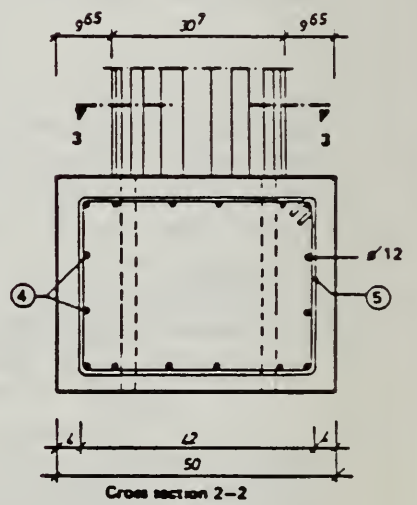
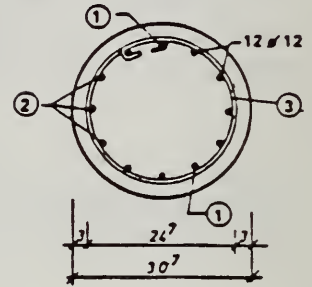
Petrovski's Flexure Model Dimensions and Steel Arrangement [35]

FIGURE 2.16



Test conditions		
EI No	N(t)	Identification
1	14.8	BS-M2-E1
2	25.9	BS-M2-E2

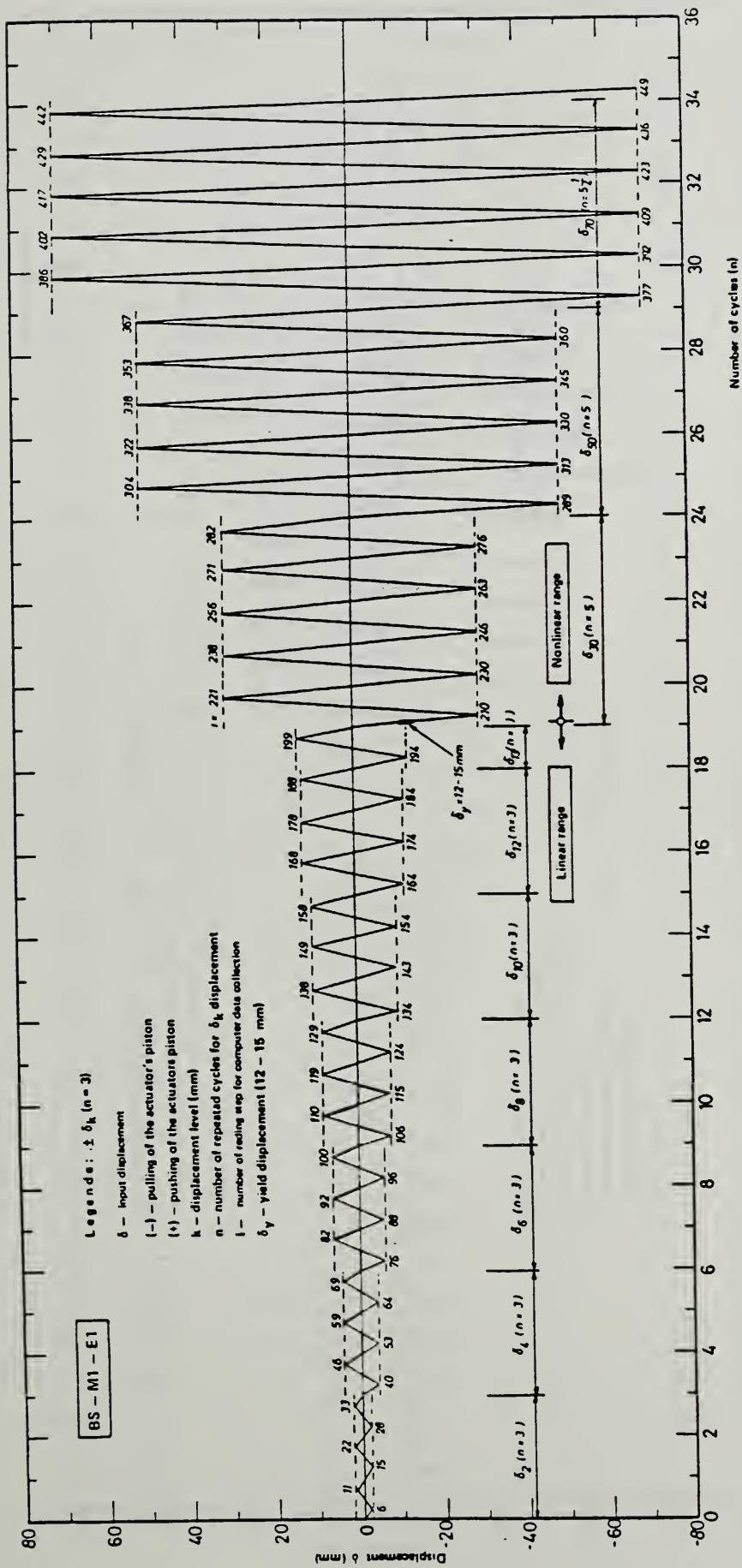
Cross section 3-3



Cross section 1-1

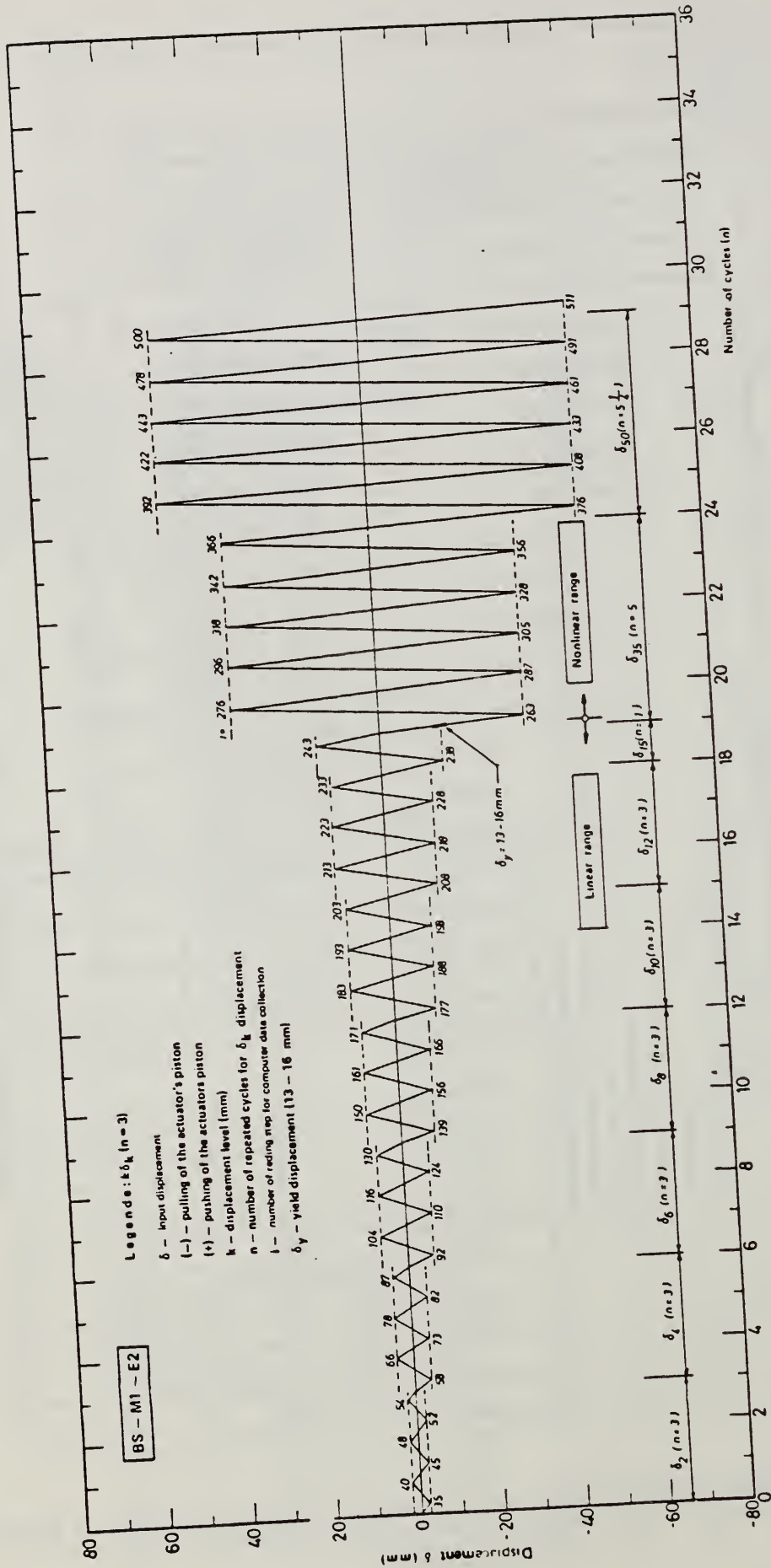
Petrovski's Shear Model Dimensions and Steel Arrangement [35]

FIGURE 2.17

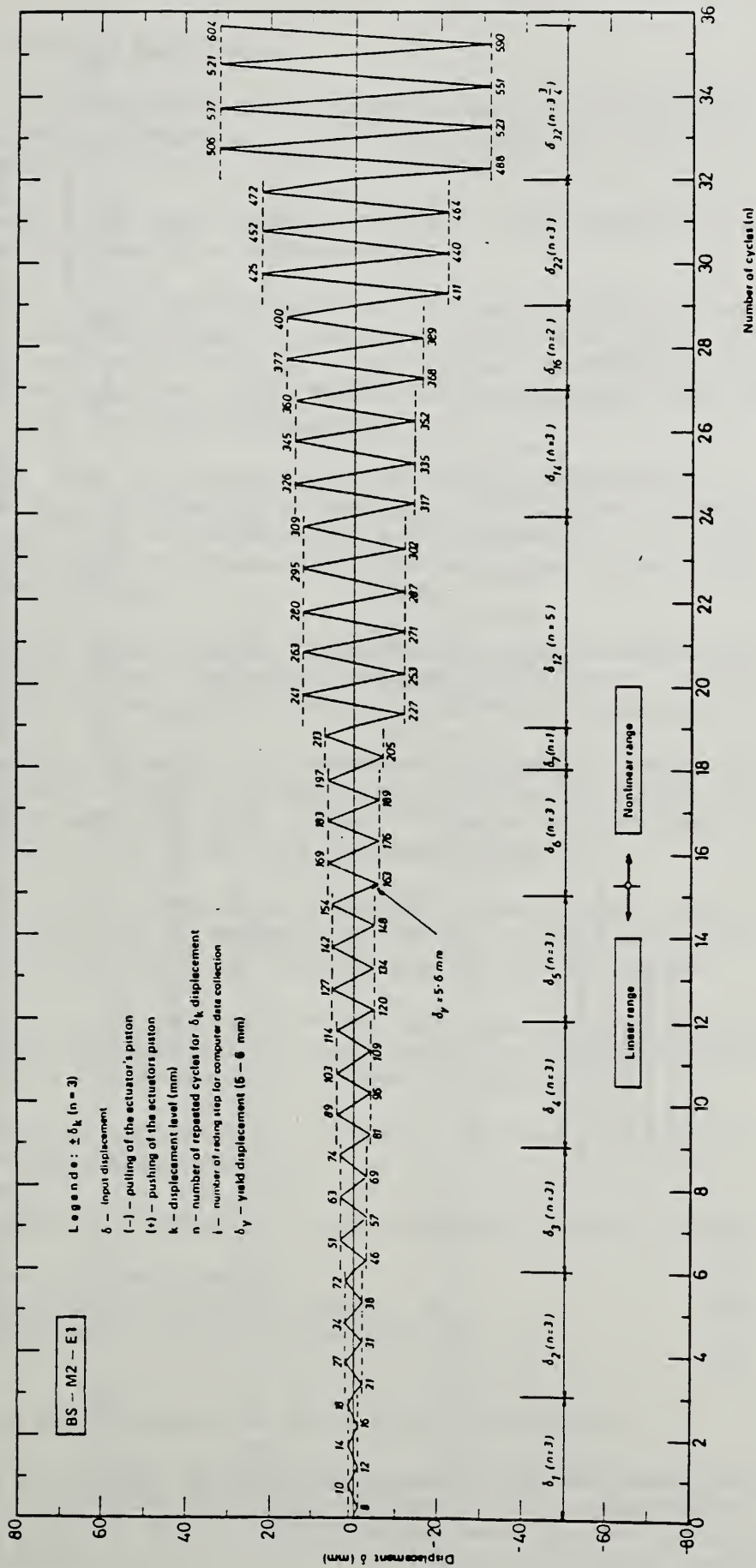


Petrovski's Load History for Flexure Model Under Low Axial Load [35]

FIGURE 2.18

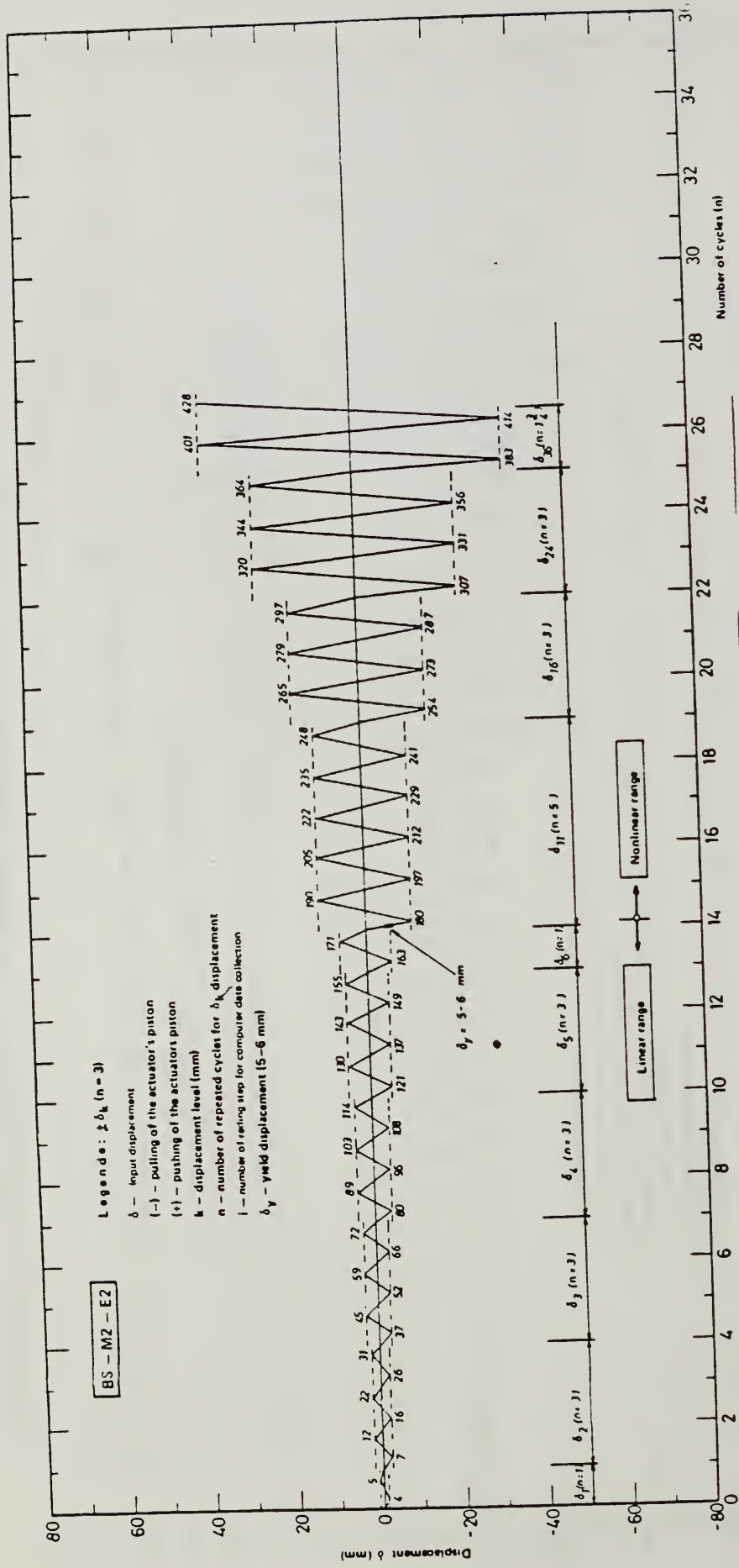


Petrovski's Load History For Flexure Model Under High Axial Load [35]
FIGURE 2.19



Petrovski's Load History For Shear Model Under Low Axial Load [35]

FIGURE 2.20



Conclusions from the tests were:

1. P - Δ relationship for the models could be categorized into 4 ranges: Range I, $0 < \Delta < \Delta_L$; Range II $\Delta_L < \Delta < \Delta_y$; Range III $\Delta < \Delta_y < \Delta_c$; and Range IV $\Delta < \Delta_c < \Delta_u$.
2. Range I is the elastic range of the structure and is characterized by a constant slope.
3. Range II is characterized by the slightly nonlinear relationship between P and Δ with the initial point at Δ_L and the end point at Δ_y . The P - Δ relationship may be approximated by a line with a slope less than the slope of the line in the elastic range.
4. Range III is characterized by plastic deformation in which $P_y = P_{max}$ is considered constant. The initial point of this range is at Δ_y and the end point is at Δ_c . Δ_c is defined as the point at which the lateral force begins to decrease significantly.
5. Range IV is the regime characterized by significant decreases in the lateral load with increased displacement. The initial point of this regime is at Δ_c and the end point is at Δ_u .
6. Based on ranges of displacements, two general ranges could be defined. The first one up to yield point (conditionally linear behavior) with a small range of deformations and the second one up to failure (nonlinear behavior).
7. Only fine cracks were observed in the linear range at the most critical cross-sections and the element would still be considered functional without any structural repair.
8. Lateral load decreases in the nonlinear range with increased displacements thereby increasing the damage to the element leading to the eventual failure of the element.
9. The number of cycles at a constant ductility also affects the stiffness deterioration.
10. Assessment of damage due to an earthquake should include:
 - a. Δ_u of the element.
 - b. Ultimate ductility level, Δ / Δ_y
 - c. Number of cycles to ultimate ductility.

2.3 Confining Reinforcement in the Plastic Hinge Region

This section highlights current code requirements for transverse steel in the plastic hinge zone of bridge columns. The requirements are those specified by ACI 318-77 [2], CALTRANS [28], and the New Zealand code [8]. The requirements of ACI 318-77 [2] are discussed because these

specifications were part of the latest version of the ACI building code when the design of the prototype columns began. The Japanese practice is not discussed as no translated version of the design code was available to the authors. However, in a paper by Kuribayashi, et.al. [36] which outlines the Japanese Road Association's 1980 specification for earthquake-resistant design of highway bridges, a displacement ductility of 2 was recommended for design of reinforced concrete (RC) bridge piers. This factor of 2 is based on an analytically determined value of approximately 6 for RC bridge piers. The analytical method was also based on monotonic loading. As noted in reference 11, the displacement ductility is smaller for specimens loaded cyclically than for specimens loaded monotonically. Therefore, using a factor of safety of 3, the value of 2 was recommended for design purposes. Also, it is not common practice in Japan to use spirals in circular bridge columns [38], but rather to use circular hoops. This is due to the difficulty of constructing large diameter spirals.

The focus of the discussions which follow will be on the requirements for circular concrete columns.

2.3.1 ACI 318-77 [2]

Confining reinforcement is required for moment resisting connections for a distance from the face of the connection that is equal to or greater than:

1. The diameter of the column or the larger dimension of a rectangular column.
2. One-sixth the clear height of the column.
3. 18 in. (457.2 mm)

The spiral reinforcement ratio is the greater of

$$\rho_s = 0.45 (A_g/A_c - 1) f'_c / f_y \quad (2.4)$$

or

$$\rho_s = 0.12 (f'_c / f_y) \quad (2.5)$$

where f_y is the yield strength of the spiral not to exceed 60,000 psi (414 MPa). These equations remain unaltered in the ACI 318-83 code [3]. The size of the spiral should be greater than or equal to a #3 bar (0.375 in [9.5-mm] diameter). The clear spacing between spirals should not exceed 3 in. (76.2 mm) nor be less than 1 in. (25.4 mm).

2.3.2 CALTRANS [28]

CALTRANS provisions for bridge column reinforcement [28,34] can be regarded as a superset of current AASHTO provisions [32,33]. Since they are generally more conservative and specific than AASHTO specifications (see Table 2.2 for a summary comparison) the 1983 CALTRANS requirements will be discussed in this section.

TABLE 2.2 COMPARISON OF AASHTO AND CALTRANS 1983 SPECIFICATIONS VERSUS THOSE PRIOR TO 1971

TOPIC	AASHTO 1969 [32]	AASHTO 1983 [33]	CALTRANS 1969 [34]	CALTRANS 1983 [28]
Long. Steel Requirements	$0.01 \leq A_s^1/A_g^2 \leq 0.08$	$0.01 \leq A_s/A_g \leq 0.08$	$0.007 \leq A_s/A_g \leq 0.08$	$0.01 \leq A_s/A_g \leq 0.08$
Size of Longitudinal Reinforcement	Min. diameter of longitudinal reinforcement is 5/8 in.	Min. diameter of longitudinal reinforcement is 5/8 in. A min. of 6 bars required for circular arrangement and 4 for rectangular arrangement.	Min. diameter of longitudinal reinforcement is 5/8 in. A min. of 6 bars are required spirally reinforced and 4 bars for tied columns.	Min. diameter of longitudinal reinforcement is 5/8 in. A min. of 6 bars are required for circular arrangement and 4 for rectangular arrangement.
Spacing of Longitudinal Reinforcement	No provisions	No provisions	Clear spacing of longitudinal bars is the greater of 1-1/2 times the max. size of the coarse aggregate. Nor shall the center-to-center spacing be greater than 2-1/2 times the long. bar diameter.	Max. spacing of the longitudinal bars is 8 in.
Spiral Spacing	Max. pitch of spirals is 1/6 the core diameter. Clear spacing of spirals is a max. of 3 in. and a min. of the greater of 1 in. or 1-1/3 times the max. size of the coarse aggregate.	Clear spacing of spirals is a max. of 3 in. and a min. of the greater of 1 in. or 1-1/3 times the max. size of the coarse aggregate.	Clear spacing of spirals max. of 3 in. for $d_{sp} < 5/8$ in. and of 5 in. for $d_{sp} \geq 5/8$ in. Min. spacing is the greater of 1-3/8 in. or 1-1/2 times the max. size of the coarse aggregate.	Clear spacing of spirals is a min. of the greater of 1 in. or 1-1/3 times the max. size of the coarse aggregate.
Min. Size of Spiral Reinforcement	No provisions	Min. size of spiral is 3/8 in.	Min. size spiral is 3/8 in. for col. diam. ≤ 30 in. and 1/2 in. for col. diam. > 30 in.	Min size of spiral is W3.5 (0.21 in.) for col. diam. < 20 in. and W9.5 (0.35 in.) for col. diam. > 20 in.

1 A_s = Area of steel reinforcement
 2 A_g = Gross area of the section
 3 d_{sp} = Diameter of the spiral

CONTINUED

TABLE 2.2 COMPARISON OF AASHTO AND CALTRANS 1983 SPECIFICATIONS VERSUS THOSE PRIOR TO 1971 (Continued)

TOPIC	AASHO 1969 [32]	AASHTO 1983 [33]	CALTRANS 1969 [34]	CALTRANS 1983 [28]
Spirals in Spirals	Splices in spirals have to be welded or lapped 1-1/2 turns.	Splices in spirals have to be welded or lapped a 48dsp or lapped a min. of 12 in.	Splices in spirals have to be welded or lapped 80dsp for deformed bars or lapped 120dsp for smooth bars.	Splices in spirals have to be welded or lapped 80dsp but no less than 12 in.
Longitudinal Reinforcement	Locations of lapped splices along the member are not specified. Lap splices in the plastic hinge region is therefore assumed to be permitted. The length of lap is dependent on the type of stress (i.e. tensile or compressive), yield reinforcement, surface characteristics of the reinforcement (i.e. plain or deformed), concrete compressive strength, and reinforcement size.	Locations of lapped splices along the member are not specified. Lap splices in the plastic hinge region is therefore assumed to be permitted. Staggering of splices a min. dist. is required. The lap length is dependent on the type of stress, class of splice, yield strength of the reinforcement, concrete compressive strength, amount of transverse reinforcement, the reinforcement size and development length of the reinforcement.	Locations of lapped splices along the member are not specified. Lap splices in the plastic hinge region is therefore assumed to be permitted. The lap length is dependent on the size of the reinforcement, and yield strength of the reinforcement.	Lap splices are not permitted for columns of 34 ft. or less. For column heights greater than 34 ft., lap splices are permitted in the region from the ftg to 2/3 of the column height for fixed columns greater than 34 ft., lap splices are not allowed in the region 10 ft. above the col. ftg. and in the area 10 ft. below the cap soffit. Staggering of the splices is also required. The length of lap is dependent on the type of steel, yield strength, yield reinforcement, and the size of the reinforcement.

CONTINUED

TABLE 2.2 COMPARISON OF AASHTO AND CALTRANS 1983 SPECIFICATIONS VERSUS THOSE PRIOR TO 1971 (Continued)

TOPIC	AASHTO 1969 [32]	AASHTO 1983 [33]	CALTRANS 1969 [34]	CALTRANS 1983 [28]
Anchorage of Spiral Ends	No provisions	Spirals anchored at each end of the unit by an extra 1-1/2 turns.	No provisions	Anchorage of spiral ends. 1. Terminated by 135° that is hooked around an intersecting long. bar. 2. Min. length of hook is 6 in. for $d_{sp} \leq 0.34$ in. and 10 in. for $d_{sp} > 0.34$ in.
Extension of Spiral into Cap	Spiral extends from ftg. to level of lowest horizontal reinforcement of member supported by column.	Spiral extends from ftg. to level of lowest horizontal reinforcement of member supported by column.	Spiral extends from ftg. to level of lowest horizontal reinforcement of member supported by column.	Lateral reinforcement extends into cap a distance equal to the lesser of 1. 1/2 confined core diameter of the cap soffit.

CONTINUED

TABLE 2.2 COMPARISON OF AASHTO AND CALTRANS 1983 SPECIFICATIONS VERSUS THOSE PRIOR TO 1971 (Continued)

TOPIC	AASHO 1969 [32]	AASHTO 1983 [33]	CALTRANS 1969 [34]	CALTRANS 1983 [28]
Extension of Spiral into Cap (Continued)				<p>2. l_d for straight main reinforcement bars for compression members.</p> <p>3. Straight portion of hooked reinforcement for compression members.</p> <p>Lateral reinforcement may be discontinued at the bottom flexural reinforcement of the cap⁵.</p>
Extension of Spiral into Footing	No provisions	No provisions	No provisions	Lateral reinforcement shall extend at the same spacing into the ftg. to the point of tangency of col. bar hooks but may be discontinued at the top of the ftg. reinforcement.

⁴ l_d = Development length of the bar

⁵ The spiral may be terminated at the bottom of the column and may begin again at the top of the footing/bottom of the cap as long as both ends of the spiral are properly anchored as discussed in an earlier section.

CONTINUED

TABLE 2.2 COMPARISON OF AASHTO AND CALTRANS 1983 SPECIFICATIONS VERSUS THOSE PRIOR TO 1971 (Continued)

TOPIC	AASHTO 1969 [32]	AASHTO 1983 [33]	CALTRANS 1969 [34]	CALTRANS 1983 [28]
Confining steel content	$\rho_s \geq 0.45(A_g/A_c - 1)f'_c/f_{sy}^6$	$\rho_s \geq 0.45(A_g/A_c - 1)f'_c/f_{sy}$	$\rho_s \geq 0.45(A_g/A_c - 1)f'_c/f_{sy}$	1. $\rho_s \geq 0.45(A_g/A_c - 1)f'_c/f_{sy}$
Confining Steel Content in the Plastic Hinge	No provisions	No provisions	No provisions	In the plastic hinge region, 2. $\rho_s \geq 0.45(A_g/A_c - 1)f'_c/f_{sy}^*$ for cols. with diameters less than or equal to 3 ft. 3. $\rho_s \geq 0.12 f'_c/f_{sy} [0.5 + 1.25^*(P_e/f'_{cA_g})]$ for cols. with diameters greater than 3 ft. The values from either equations (2) or (3) can not be less than equation (1).
Definition of Plastic Hinge Region	No provisions	No provisions	No provisions	Potential plastic hinge region is defined as: 1. Max. horizontal dimension 2. 1/6 column length 3. 24 in.

6 A_g = Area of the concrete core
 f'_c = Concrete compressive strength
 f_{sy} = Yield strength of the spiral reinforcement

The potential plastic hinge zone is defined as the greater of the following:

1. The maximum horizontal dimension of the column.
2. One-sixth the column length.
3. 24 in. (609.6 mm)

For the flared end of a flared column, the plastic hinge length is equal to the flare length plus the greater of 1, 2, or 3 above.

For columns with diameters less than or equal to 3 ft. (914mm), the required confining reinforcement ratio is given by:

$$\rho_s = 0.45 \left[\frac{A_g}{A_c} - 1 \right] \frac{f'_c}{f_y} \left[0.5 + 1.25 \frac{P_e}{f'_c A_g} \right] \quad (2.6)$$

For columns with diameters greater than 3 ft. (914 mm),

$$\rho_s = 0.12 \frac{f'_c}{f_y} \left[0.5 + 1.25 \frac{P_e}{f'_c A_g} \right] \quad (2.7)$$

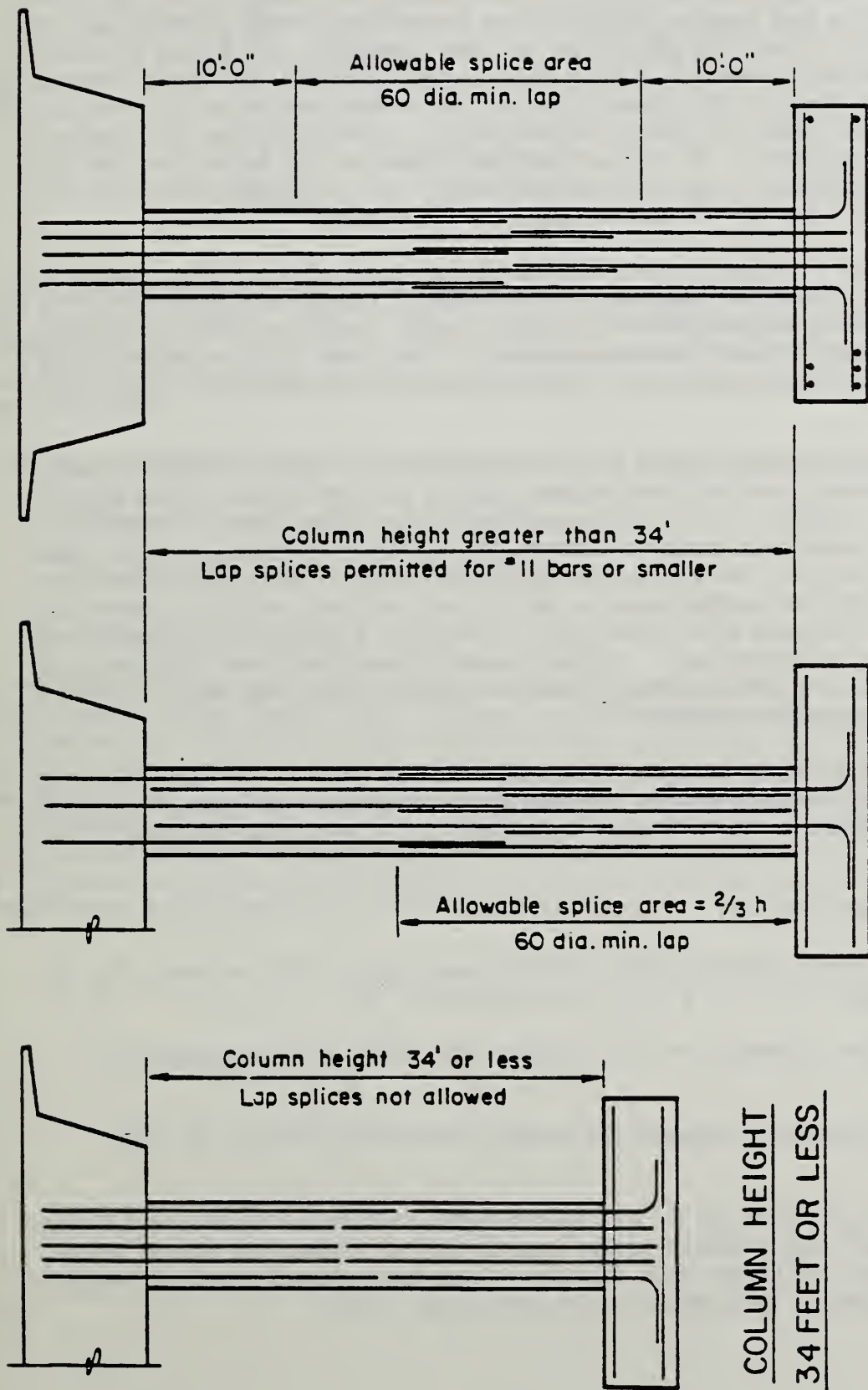
However, ρ_s from either Eqs. (2.6) or (2.7) can not be less than

$$\rho_s = 0.45 \left[\frac{A_g}{A_c} - 1 \right] \frac{f'_c}{f_y} \quad (2.8)$$

The minimum spiral is a steel wire of size W3.5 (0.221 in. [5.6 mm] diameter) for columns with a minimum dimension less than or equal to 20 in. (508 mm). For columns greater than 20 in. (508 mm) in diameter, the minimum spiral is a wire of size W9.5 (0.348 in. [8.8 mm] diameter). The maximum clear spacing of spirals is limited to 3 in. (76.2 mm) and the minimum clear spacing is the greater of 1 in. (25.4 mm) or 1-1/3 times the maximum size of the aggregate.

Table 2.2 summarizes AASHTO and CALTRANS provisions which are pertinent to the design of bridge columns. These are presented for two cases: specifications which were in effect prior to the 1971 San Fernando Earthquake, and those which are currently in effect. The most important changes occur in the specification of allowable conditions for lap splices in longitudinal reinforcement and in the recognition of the importance of confining reinforcement within potential plastic hinge regions.

Prior to 1971 the permitted locations of lapped splices in longitudinal reinforcement along the height of a bridge column were not specified by either AASHTO or CALTRANS. The 1983 CALTRANS code recognizes the problem of potential column failure within plastic hinge regions by stating that "Lap splices are not permitted [at all] for columns of 34 feet (10 m) or less" (see Fig. 2.22). For column heights greater than 34 feet (10 m) lap



FIXED

COLUMN HEIGHT GREATER THAN 34 FEET

HINGED

COLUMN HEIGHT
34 FEET OR LESS

Lap Splices in Vertical Column Reinforcement
FIGURE 2.22

splices are permitted in the region from the footing to 2/3 of the column height for columns whose base has been designed as a hinge. For fixed columns (cantilevered) greater than 34 feet (10 m) in height, lap splices are not allowed in the region 10 feet (3 m) above the column footing and in the area within 10 feet (3 m) of the column cap soffit. Since plastic hinge length generally falls within one column diameter for cantilevered systems, the 10 foot (3 m) no-splice region seems adequate to prevent longitudinal bar pullout within a potential plastic hinge for common diameter bridge columns. It is furthermore important to note that no lap splices at any location along the column height are permitted when #14 and #18 (1.7 and 2.25 in. -- 43 and 57 mm) bars are used.

A new requirement for the content of confining (spiral) reinforcement in potential plastic hinge regions has been added which reflects need for additional confining reinforcement at higher axial loads to prevent lateral buckling of longitudinal reinforcement. The new confining content requirements are equivalent to those presently recommended in the New Zealand code.

Another new provision deals with the end anchorage of spiral reinforcement. In order to prevent loss of confinement during an earthquake, when spiral reinforcement cover is likely to have spalled away, specific recommendations have been made to assure positive end anchorage which does not depend on bond for development of bar strength. This has taken the form of a mechanical anchorage in which all spiral reinforcement is terminated by a minimum 135° bend that is hooked around an intersecting longitudinal reinforcing bar. Recent specifications have limited the use of 135° bends for construction reasons. Welded splices, which require a backing bar, are also permitted.

Finally, the 1983 CALTRANS specification defines the potential plastic hinge region as the greater of: the maximum horizontal column dimension (equal to the diameter for circular columns); 1/6 the column height; or 24 in. (0.6m).

2.3.3 New Zealand Code [8]

The potential plastic hinge for a column bearing an axial stress, P_e , of less than or equal to $\phi 0.3 f'_c A_g$ is the greater of:

1. The column diameter or the larger dimension of a rectangular column
2. Where the moment exceeds 0.8 times the maximum moment at that end.

For $P_e \geq \phi 0.3 f'_c A_g$ (where ϕ is the strength reduction factor = 0.9 for confined members), the plastic hinge length is 1.5 times the above value. This requirement reflects the finding that the plastic hinge length generally increases in proportion to column axial load.

The volumetric ratio for columns using spirals or hoops is the greater of:

$$\rho_s = 0.45 \left[\frac{A_g}{A_c} - 1 \right] \frac{f'_c}{f_{yh}} \left[0.5 + 1.25 \frac{P_e}{\phi f'_c A_g} \right] \quad (2.9)$$

or

$$\rho_s = 0.12 \frac{f'_c}{f_{yh}} \left[0.5 + 1.25 \frac{P_e}{\phi f'_c A_g} \right] \quad (2.10)$$

The maximum column load, P_e , allowed is $0.7 \phi f'_c A_g$ unless it is shown that P_e is less than $0.7 \phi P_o$, where P_o is the axial load of the column corresponding to zero eccentricity. A displacement ductility capacity of 8 can be expected if this required amount of transverse reinforcement were to be provided.

The center-to-center spacing of the spiral or hoops is the lesser of:

1. One-fifth the least lateral dimension.
2. 6 times the longitudinal bar diameters.
3. 7.9 in. (200 mm).

Longitudinal bars are spaced a maximum of 7.9 in. (200 mm) on centers in the plastic hinge zone. Lap splices in the longitudinal reinforcement in the potential plastic hinge region is not permitted by the code. The center of the splices is to be located in the middle quarter of the column height unless it can be shown that plastic hinging cannot develop at the column end. Anchorage of the transverse reinforcement in the potential plastic hinge zone is specified by full strength lap welds or by at least a 135° hook around a longitudinal bar with an extension of 8 times the transverse bar diameter into the concrete core.

3.0 SIMILITUDE

3.1 General

Many design codes are based on tests conducted using structural models to predict the behavior of the prototype structure. This is the result of the impracticality of construction, the difficulty of testing, and costs involved in the use of large or full scale specimens. As stated earlier, one of the objectives of this study was to determine the effects of changes in scale, if any.

A true model is one which exhibits complete similitude to the prototype [25]. Obtaining a true model of a reinforced concrete structure is difficult due to the inelastic nature of concrete and to it being a composite material. Sabnis et. al [25] proposed that a "practical true model" could be used for modelling reinforced concrete structures. The similitude requirements for this modelling and for the true model are listed in Table 3.1. The scale factors in Table 3.1 relate a model quantity to a prototype quantity. The scale factors for stress and strain, s_σ and s_ϵ , respectively are both equal to unity for the practical true model. s_ϵ is equal to one if the material of the prototype and model is the same. For true modelling, the following conditions apply

$$s'_\epsilon = s_\epsilon = s_\sigma \quad (3.1)$$

and

$$s'_\sigma = s_\epsilon \quad (3.2)$$

where the primed variables are the scale factors for the reinforcing steel. Steel was used for the model reinforcement for this test and this, therefore, results in $s'_\epsilon = 1$.

The requirement for geometrical similitude is such that linear dimensions of model and prototype are related by a constant, s_1 . Prototype loads and model loads are related in the following manner for $s_\epsilon = s_\sigma = 1$:

$$\text{Concentrated load, } Q: \quad (s_1)^2 Q_m = Q_p \quad (3.3)$$

$$\text{Line load, } w: \quad s_1 w_m = w_p \quad (3.4)$$

$$\text{Pressure, } q: \quad q_m = q_p \quad (3.5)$$

$$\text{Moment, } M: \quad (s_1)^3 M_m = M_p \quad (3.6)$$

where the subscripts "m" and "p" represent model and prototype quantities respectively.

TABLE 3.1 SIMILITUDE REQUIREMENTS FOR REINFORCED CONCRETE
MODELS [25]

	QUANTITY	DIMENSION	TRUE MODEL	PRACTICAL TRUE MODEL
MATERIAL RELATED PROPERTY	Concrete stress	FL^{-2}	S_{σ}	1
	Concrete strain	-	1	1
	Modulus of concrete	FL^{-2}	S_{σ}	1
	Poisson's ratio	-	1	1
	Mass density	FL^{-3}	S_{σ}/S_1	$1/S_1$
	Reinforcing stress	FL^{-2}	S_{σ}	1
	Reinforcing strain	-	1	1
	Modulus of reinforcing	FL^{-2}	S_{σ}	1
	Bond stress	FL^{-2}	S_{σ}	1
	GEOMETRY	Linear dimension	L	S_1
Displacement		L	S_1	S_1
Angular displacement		-	1	1
Area of reinforcement		L^2	$(S_1)^2$	$(S_1)^2$

3.2 Material

3.2.1 Reinforcement

Similitude requirements for model reinforcement are [6]:

1. The stress-strain curve for the model reinforcement must be similar to that for the reinforcement used in the prototype
2. Equal yield strength for both model and prototype reinforcement
3. Similar bond characteristics for both model and prototype reinforcement

The use of deformed wire for model reinforcement is recommended to simulate proper bond characteristics. The only available deformed wire that was suitable for the longitudinal reinforcement was D6 deformed wire [27]. The deformations of the D6 wire were in the form of indentations rather than raised ribs as in the prototype reinforcement. It was, however, not possible to obtain deformed wire for the other required wire sizes. As a result of using the D6 wire for the model longitudinal reinforcement, the scale factor, s_1 , was:

$$\begin{aligned} s_1 &= D_p/D_m \\ &= 6.1 \end{aligned}$$

where D_p = Diameter of a #14 bar = 1.693 in. (43 mm)

D_m = Diameter of a D6 wire = 0.276 in. (7 mm)

All other reinforcement and dimensions were then scaled using $s_1 = 6.1$.

The yield stress of the prototype steel was approximately 70,000 psi (483 MPa). When tested, the yield stress of the D6 wire was found to be around 88,000 psi (607 MPa). It was also noted that the stress-strain curve for the model steel had a rounded shape with no well-defined yield point. The prototype steel had a well defined yield point. As a result the model bars had to be heat-treated to lower their yield stress and to change the characteristic stress-strain curve of the model steel to match that of the full-scale reinforcing steel.

A heat treatment of 1162° F for 1 hour was determined to produce the desired changes in model steel properties during tests at the bureau of standards using a precision furnace. The bulk of the model steel was then processed at a commercial facility. This resulted in a well defined yield stress of 57,000 psi (393.1 MPa), somewhat lower than the desired value.

A similar procedure was used to treat the model spiral reinforcement, which had an initial yield point of 113,600 psi (783 MPa). Heat treating this steel for 1 hour at 1013° F produced a yield stress of 80,000 psi (552 MPa). An additional 20 minutes at 1036° F further reduced the yield stress to 69,000 psi (476 MPa). This was considered sufficiently close to that

for the prototype [64,000 psi (441 MPa)] to satisfy similitude requirements. These differences in steel yield were accounted for when comparing the behavior of model and prototype specimens.

3.2.2 Concrete

3.2.2.1 MICROCONCRETE

Classical structural modelling theory calls for scaling of all components of a structure, including materials characteristics. In the case of a composite material such as concrete, similitude considerations generally result in scaling of aggregates such that the aggregate gradation curve for the model specimen is related to the prototype aggregate gradation curve by the scale factor s_1 . Concrete designed by means of such scaling procedures is referred to as microconcrete. It was used in this test series for the construction of specimens N1, N2 and N3.

Large aggregate used for the full-scale specimen was a 3/4 in. (19 mm) nominal maximum size river gravel. Fig. 3.1 shows the gradation of the prototype aggregate and the acceptable limits, shown by the lighter dashed lines, as specified by CALTRANS. Fig. 3.1 also shows the gradation of sand (labelled "White Marsh Concrete Sand") which was used as aggregate for the microconcrete. This gradation, represented by the heavy solid line in Fig. 3.1, generally fell within the scaled down acceptable limits, represented by the lighter solid lines in the Fig. 3.1, except for the high number (finer) sieve sizes. The difficulty of achieving high volumetric percentages of very fine particle sizes is typical in microconcrete design and variance from the gradation limits in the high number sieve sizes is generally considered acceptable.

A mix design was developed to produce a 4000 psi (27.6 MPa) 27-day compressive strength concrete. Due to the fineness of the aggregate, it was difficult to achieve good workability without greatly increasing the water/cement (W/C) ratio. Rather than increase water content, however, a superplasticizer (conforming to requirements of ASTM C494-F) was used to increase workability. The concrete for the model columns was mixed at NBS following casting of the base beams using a similar strength ready-mix concrete. Amounts of materials produced in the laboratory for casting the columns are given in Table 3.2.

Microconcrete Vs. Prototype Gradation

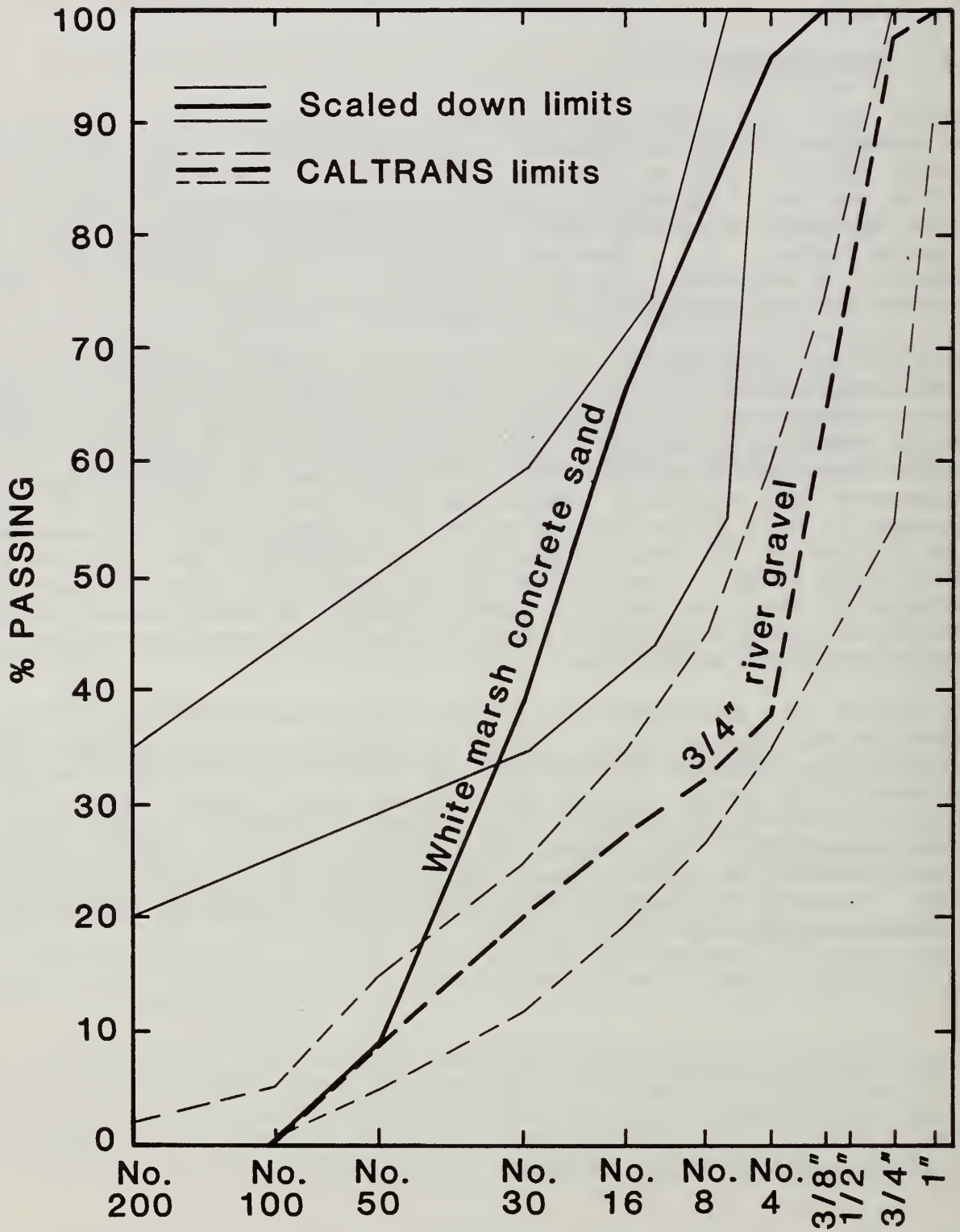


Fig. 3.1

TABLE 3.2 Microconcrete Mix Design

Material/Property	LB/CY	(kg/m ³)
Cement (Type I, Portland Cement)	699.3	(2016.2)
Sand (dry)	2724.3	(7854.6)
Water	461.0	(1329.2)
w/c	0.61	
Slump without superplasticizer	1/2 in. (12.7 mm)	(Flexure)
	1 - 3/16 in. (30.2 mm)	(Shear)
Slump with superplasticizer	2 - 1/2 in. (63.5 mm)	(Flexure)
	5 - 1/4 in. (133.3 mm)	(Shear)

Due to the small volume of concrete produced during laboratory casting operations, 3 by 6 in. (76.2 by 152.4 mm) cylinders were used instead of standard 6 by 12 in. (152.4 by 304.8 mm) cylinders. The use of the smaller cylinders has been shown [14] to produce the same compressive strengths as the standard size cylinders. Fifteen of the 3 by 6 in. (76.2 by 152.4 mm) were cast for each column specimen so that a minimum of three cylinders would be available for strength testing at 3, 7, 14, and 28 days age. The three remaining cylinders were tested on the day of the column test. Table 3.3 presents the compressive strengths and their standard deviations for column specimens N1, N2, and N3.

Table 3.3 Cylinder Test Data (compressive strength in psi) for Model Test Specimens*

Model No.	N1	N2	N3	N4	N5	N6
Age (days)						
3	2242	2242	2042	2653	3013	2653
S.D.	28	28	22	111	7	111
7	2858	2858	3082	3169	3534	3169
S.D.	90	90	78	107	71	107
14	3209	3209	3431	3492	3839	3492
S.D.	137	137	39	46	157	46
28	3393	3393	3537	3643	3822	3643
S.D.	119	119	130	46	66	46
Test	3490	3490	3681	3545	3534	3367
S.D.	99	77	75	108	170	79

* Each test represents the average of three 3 x 6 in. (76.2 by 152.4 mm) cylinder breaks. 1 psi = 6.9 KPa ; S.D. = standard deviation of three cylinder tests; "Test" = compressive strength on day of column test.

3.2.2.2 PEA GRAVEL CONCRETE

As an alternative to microconcrete a ready-mix concrete was used for three of the column specimens. These specimens were cast using a nominal 3/8 in. (9.5 mm) maximum size washed river gravel aggregate (known as "pea gravel") with a specified 28 day strength of 4000 psi (27.6 Mpa). The gradation for this aggregate is shown in Fig. 3.2. The amounts of the materials used for the pea gravel mix are shown in Table 3.4. Compressive strengths and standard deviations for each column specimen are presented in Table 3.3 (specimens N4, N5, and N6).

Pea Gravel Gradation

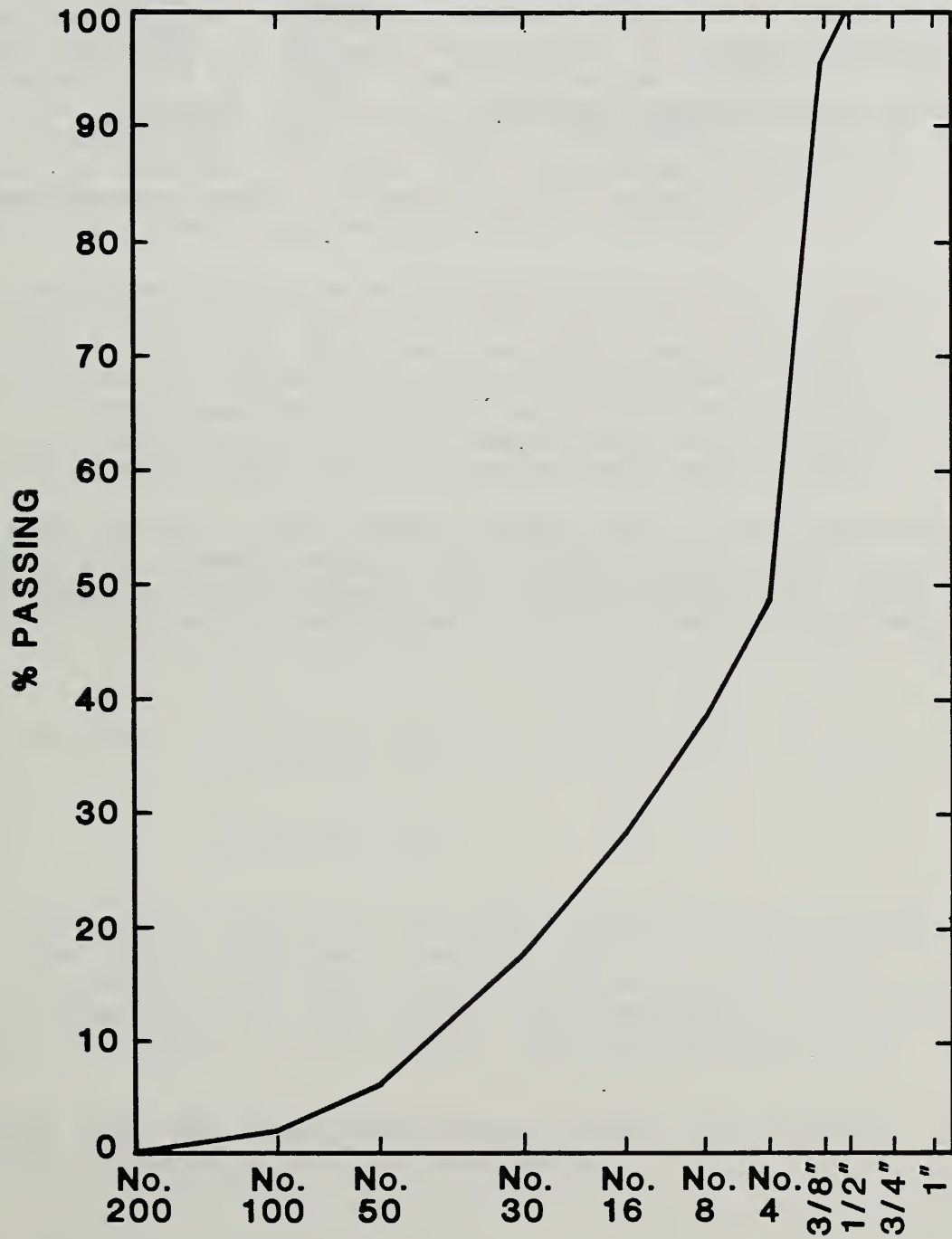


Fig. 3.2

TABLE 3.4 Pea Gravel Mix Design

Material/Property	LB/CY	(kg/m ³)
Cement (Type I, Portland Cement)	605.7	(1746.4)
Water	370.4	(1067.9)
Sand (dry)	1460.0	(4209.5)
Pea gravel (dry)	1575.0	(4541.1)
w/c	0.61	
Slump without superplasticizer	4 in.	(101.6 mm)

4.0 SPECIMEN DESIGN AND CONSTRUCTION

4.1 Design

The prototype columns (see Fig. 1.1) were designed based on CALTRANS specifications effective in 1983. The longitudinal reinforcement for both prototype columns (flexure and shear) consisted of 25 # 14 [1.7 in.; 43mm] grade 60 deformed bars. These bars were spaced at 6.82 in. (173.2 mm) center-to-center around the column. The longitudinal reinforcement ratio was 0.0199. The transverse reinforcement for the flexure prototype column consisted of spirals made from # 5 [0.625 in.; 16mm] grade 60 deformed bar spaced at 3.5 in. (88.9 mm) on center. The transverse reinforcement for the prototype shear column consisted of spirals made from # 6 [0.75 in.; 19mm] grade 60 deformed bar spaced at 2.125 in. (53.97 mm) on center.

The spirals extended into the base (footing) to the point of tangency of the longitudinal bar hooks. The steel arrangement for the prototype is shown in Figs. 4.1 and 4.2. This was one of the modifications in the CALTRANS provisions [28] since the San Fernando earthquake. Prior to this earthquake, the spiral was not required to extend into the footing of the column. The volumetric spiral reinforcement ratio was 0.00633 for the prototype flexure column and 0.01479 for the prototype shear column.

Due to the availability of the D6 model deformed wire for the longitudinal reinforcement (the closest match to an integer scale factor of the prototype longitudinal reinforcement) a 1/6.1 scale was obtained. Refer to ASTM A-496 [27] for the wire properties. The axial loads for the models were:

$$N1, N2, N4, N5: \quad P_e / f'_c A_g = 0.09$$

$$N3, N6: \quad P_e / f'_c A_g = 0.18$$

based on a design $f'_c = 4000$ psi (27.6 MPa). Actual concrete strengths obtained in the lab from compression tests of 3 by 6 in. cylinders for the models were approximately 3500 psi (24.1 MPa) on the average. These tests were conducted when the models were tested. The longitudinal reinforcement ratio for all the models was $\rho_t = 0.0199$. This was provided by 25 - D6 bars.

The transverse steel requirement was governed by Eqs. (2.7) and (2.8). The volumetric ratio required by Eq. (2.7) resulted in

$$\begin{aligned} \rho_s &= 0.12 \frac{f'_c}{f_y} \left[0.5 + 1.25 \frac{P_e}{f'_c A_g} \right] \\ &= 0.12 \frac{3.5}{57} [0.5 + 1.25 (0.09)] \\ &= 0.0045 \qquad \qquad \qquad \text{for N1, N3, N4 and N6} \end{aligned}$$

Prototype Steel Arrangement - Side View

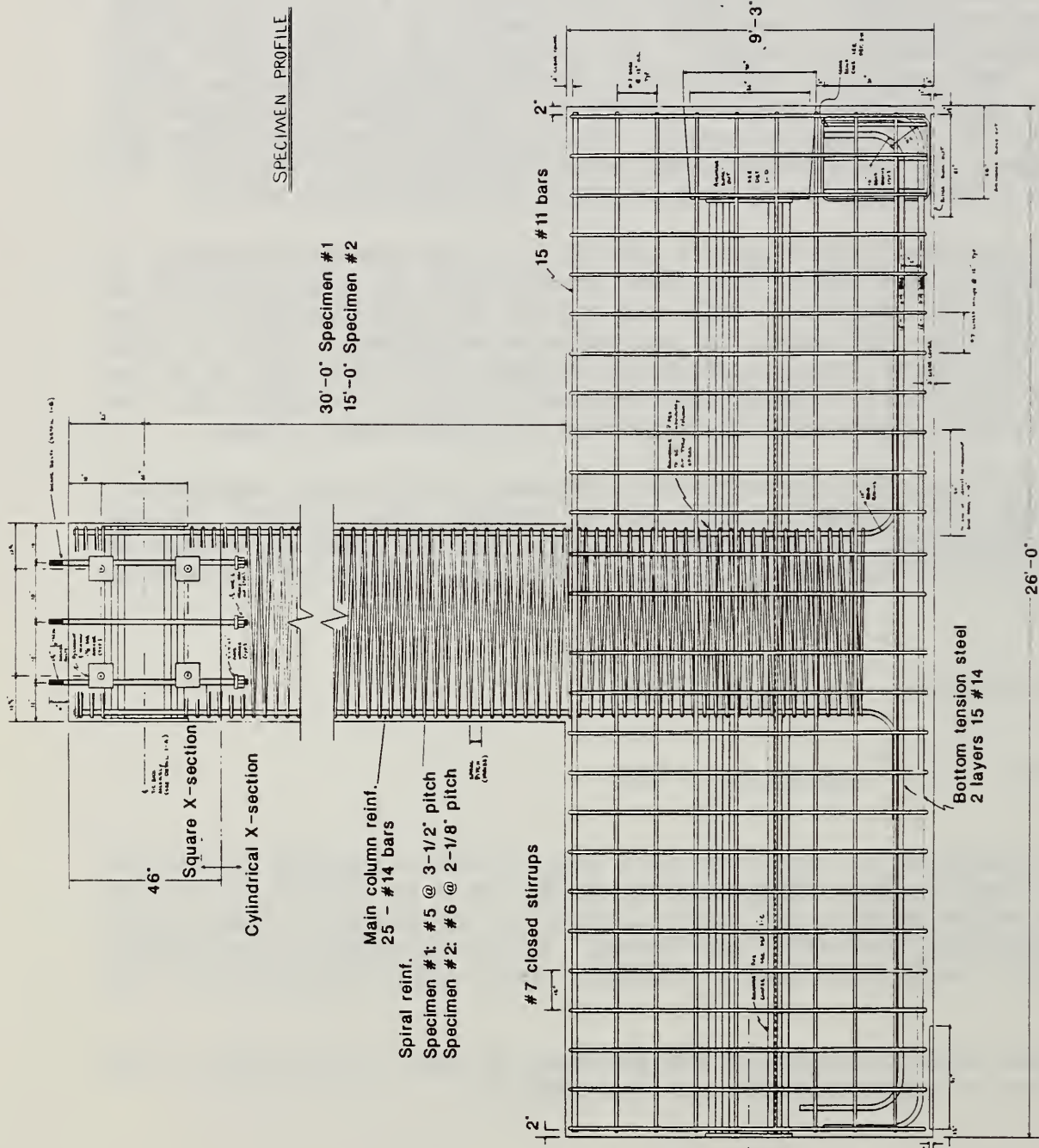
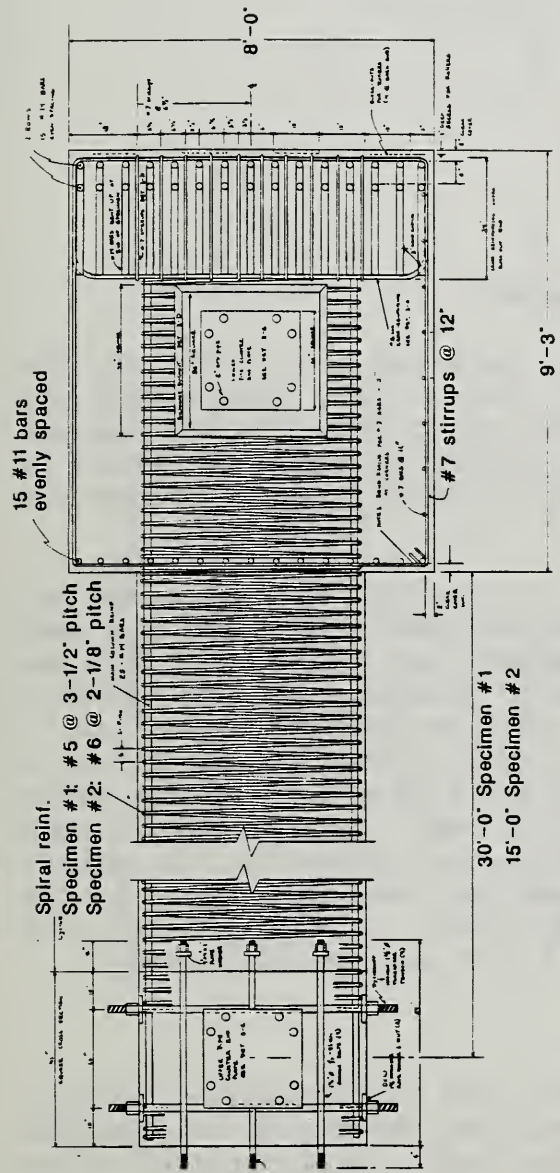


FIGURE 4.1

Prototype Steel Arrangement - End and Plan Views

SPECIMEN END PROFILE



SPECIMEN PLAN

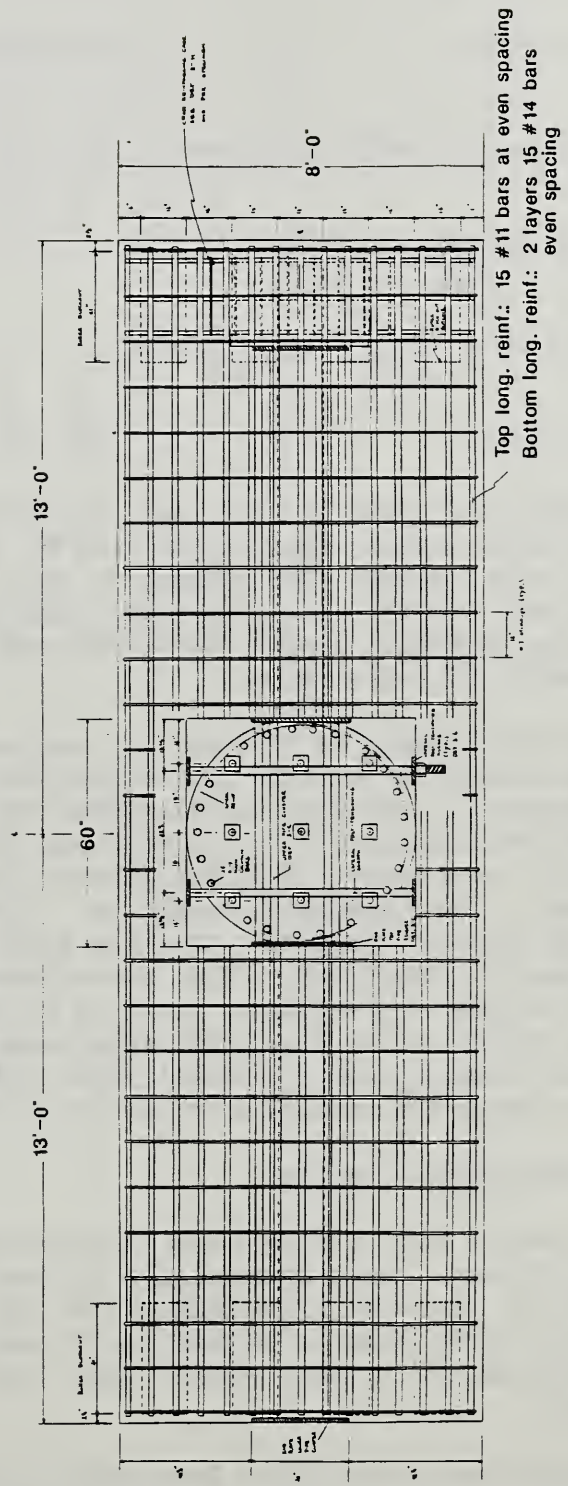


FIGURE 4.2

$$\rho_s = 0.12 \frac{3.5}{57} [0.5 + 1.25 (0.18)]$$

$$= 0.0053 \quad \text{for N2 and N5}$$

The volumetric ratio required by Eq. (2.8) resulted in

$$\rho_s = 0.45 \left[\frac{A_g}{A_c} - 1 \right] \frac{f'_c}{f_y}$$

$$= 0.45 \left(\frac{75.43}{65.61} - 1 \right) \frac{3.5}{57}$$

$$= 0.0041 \quad \text{for all models}$$

The final volumetric ratio was therefore governed by Eq. (2.7) for the models with lower axial load and by Eq. (2.8) for the models with the higher axial load. The actual ρ_s provided was 0.00694 for the flexure models and 0.01452 for the shear models. These values are a result of following standard design practices used by CALTRANS. Table 4.1 summarizes the details of the models.

The footing (base) of the column was heavily reinforced to prevent any failure occurring to it. The dimensions of the base were not scaled down by a factor of one-sixth as required for geometrical similitude. This was because the base had to be compatible with an existing structural testing facility (see Appendix C) to prevent any uplift during the test and to simulate a fixed boundary condition. The depth of the base was chosen so that the models would fit into the testing facility with a minimum amount of relocation required of the servo-hydraulic rams. These changes in base dimensions were considered to have no detrimental effects on the results of the tests since the prototype base was designed to operate in the elastic range under actual test conditions. The amount of base reinforcement was scaled down at $(1/6.1)^2$ of that used in the prototype.

4.2 Construction Process

The formwork for the base was constructed using high-density, plastic-coated plywood. This type of plywood was selected because of its strength, durability, non-stick qualities, and for the smooth finish imparted to the concrete which aided in detection of cracking. The joints in the formwork were sealed by a water-proof tape and the forms were oiled prior to casting.

The column was formed using Sonotubes, a commercially available cylindrical form made of spun paper. A 10-inch (25.4 cm) inside diameter Sonotube was selected as an initial best-estimate of the required model column diameter. This was then split down its length, and the circumference reduced by the amount needed to result in a 9.8 in. (24.89 cm) diameter. Metal strapping was used to seal the split tube. Water-proof was used to seal the seam prior to casting.

TABLE 4.1 MODEL PROPERTIES

MODEL	LONG. STEEL A _s (in ²)	LONG. YIELD f _y (ksi)	SPIRAL DIAM. d _s (in.)	SPIRAL SPACING s _h (in.)	SPIRAL YIELD STRESS f _{sp} (ksi)	ρ _s	f' _c (psi)	P _e (kips)	P _e f' _c A _g
N1	1.50	57	0.120	0.35	64	0.01452	3490	26.87	0.10
N2	1.50	57	0.120	0.35	64	0.01452	3349	53.75	0.20
N3	1.50	57	0.106	0.57	69	0.00694	3681	26.87	0.10
N4	1.50	57	0.120	0.35	64	0.01452	3545	26.87	0.10
N5	1.50	57	0.120	0.35	64	0.01452	3534	53.75	0.20
N6	1.50	57	0.10	0.57	69	0.00694	3367	26.87	0.10

The base reinforcement, consisting of stirrups, shrinkage, tension and compression steel, was tied first. The D6 deformed wires used to model the longitudinal column reinforcement were mounted in a separate jig. Pre-formed spiral coils were then tied to the longitudinal reinforcement (see Fig. 4.3) to form the finished column. The longitudinal bars were instrumented with electrical strain gages prior to tying the spiral. The gages on the spiral were placed after the column cage was completely tied. Fig. 4.4 shows a close up of an instrumented column cage. The locations of the various strain gages are shown on Figures 4.8 and 4.9. The instrumented column cage was then tied to the base cage as shown in Fig. 4.5. Fig. 4.6 shows the sizes of the steel wires used in the model and the arrangement of the steel.

4.3 Model Casting

The casting of the models was done in two phases. The bases in each set were cast first and then the columns were cast a few days later creating a cold joint at the column-base joint, as is common practice in industry. The microconcrete for the bases of models N1 - N3 was mixed without the use of superplastizers and as a result substantial vibrating was necessary to ensure that the concrete flowed between the tightly spaced reinforcement. The casting of one of the microconcrete bases is shown in Fig. 4.7.

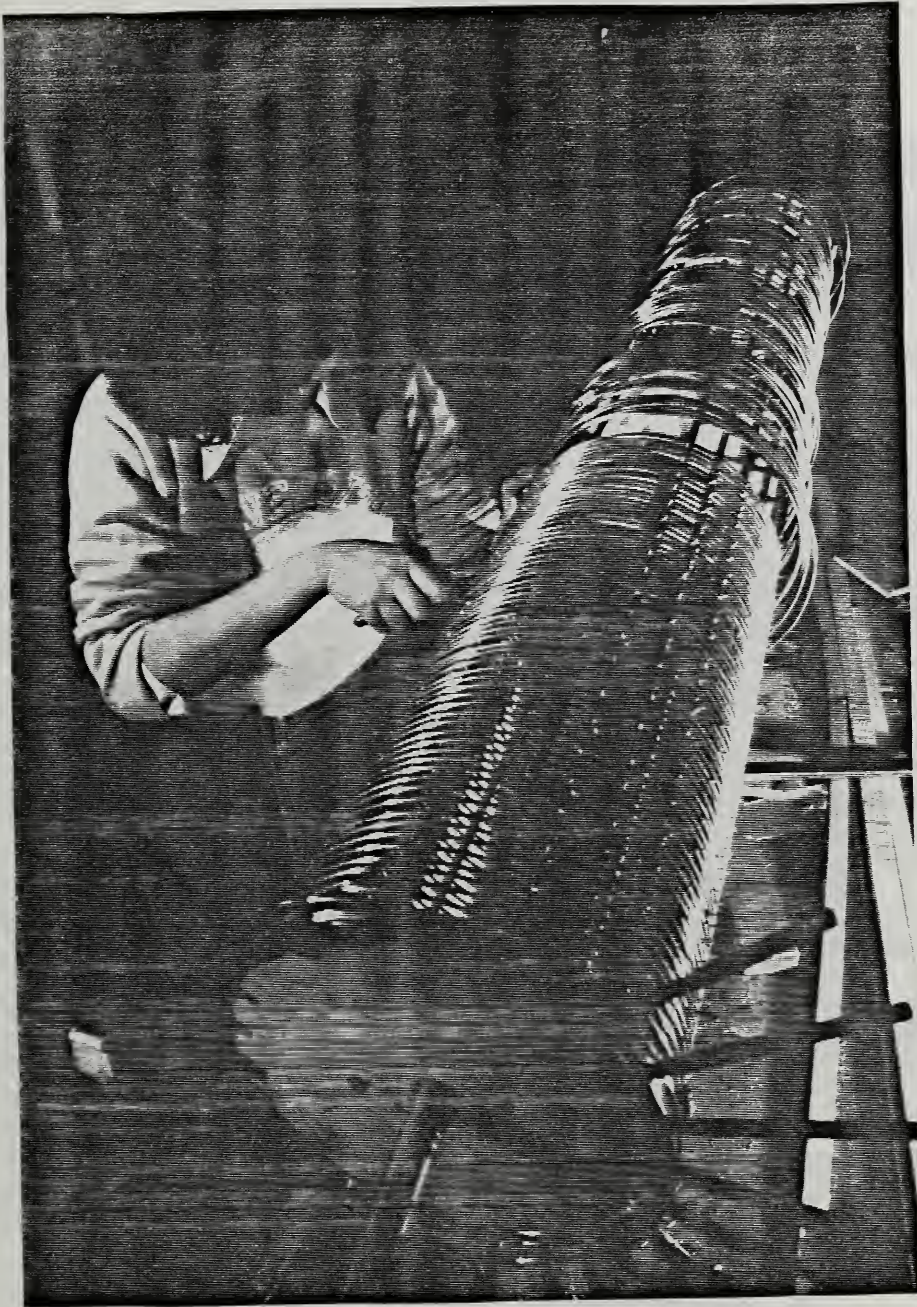
The pea gravel mix was easier to place and no problems were encountered with premature set. Superplastizer was not included in the pea gravel mix. Slump tests were used as a guide to determine the workability of the concrete. The air content was also measured.

4.4 Instrumentation

A total of 49 strain gages were used for each model. The majority of the gages were placed in the potential plastic hinge region. Figs. 4.8 - 4.10 show the location of these strain gages. The gages in the base and outside the potential plastic hinge region were used to monitor the progression of yielding in both longitudinal and confining spiral reinforcement. Figure 4.11 shows typical strain gage placements in the model columns. Type 2 gages were redundant backups for the "Type 1" gages applied to the longitudinal reinforcement in the anticipated plastic hinge region. Both Type 1 and 2 gages were aligned parallel to the reinforcement to measure axial strain. Type 3 gages were placed at 45° off the axis of loading (see Fig. 4.11) to monitor any eccentric bending during the test.

Five embedment strain gages, oriented vertical, and parallel to the axis of loading, were placed across the width of the column-base joint, along the column centerline, and were used to monitor the axial strain variation through the column. Fig. 4.12 shows a sketch of a typical flexure-compensating embedment gage used in the models.

Two LVDTs were used to measure the rotation at the base of the column. These were attached to the column by means of a piece of all-thread bar. The all-threads were inserted into a hole drilled into the column and then held in place by an epoxy for the microconcrete models. The all-threads were screwed into anchors placed in the column formwork prior to casting of



Tying of spiral cage

Fig. 4.3



Instrumented column cage

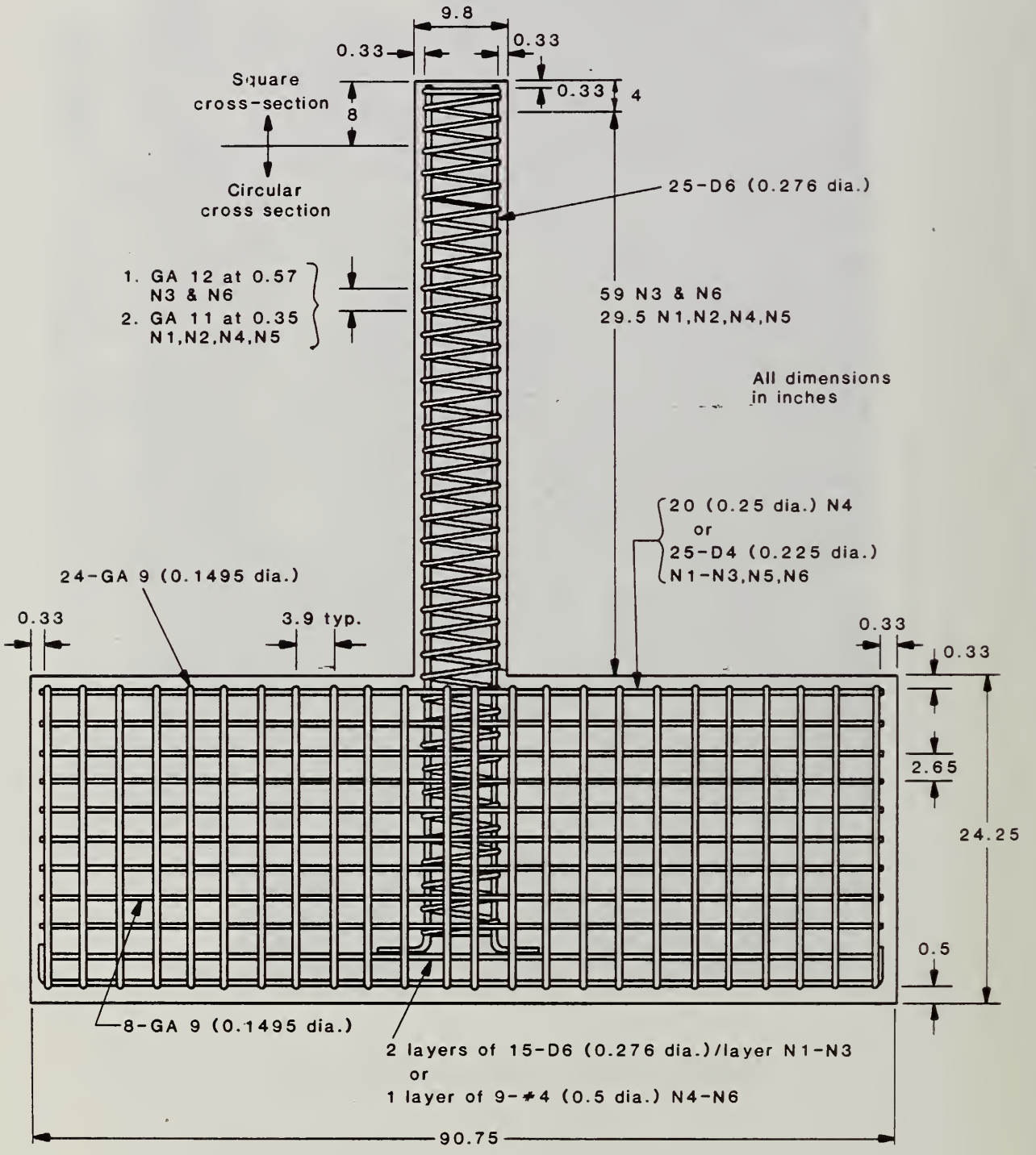
Fig. 4.4



Tying column cage to base cage

Fig. 4.5

COLUMN DIMENSIONS AND STEEL LAYOUT



NOTE: Width of the base is 28.375

FIGURE 4.6



Casting of microconcrete bases

Fig. 4.7

FLEXURE COLUMN AXIAL STRAIN GAGE LOCATION AND REINFORCEMENT SCHEDULE

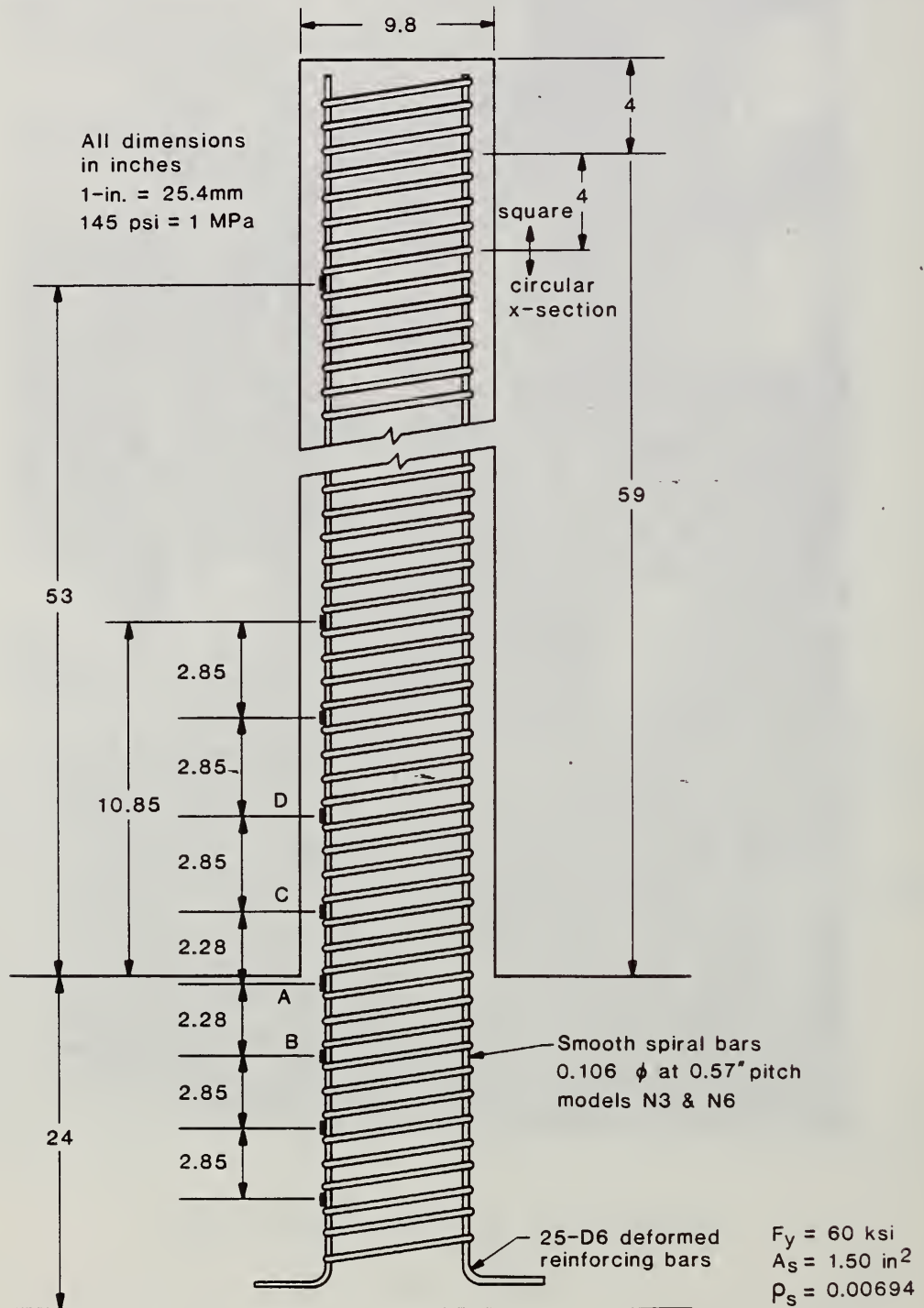


FIGURE 4.8

SHEAR COLUMN AXIAL STRAIN GAGE LOCATION AND REINFORCEMENT SCHEDULE

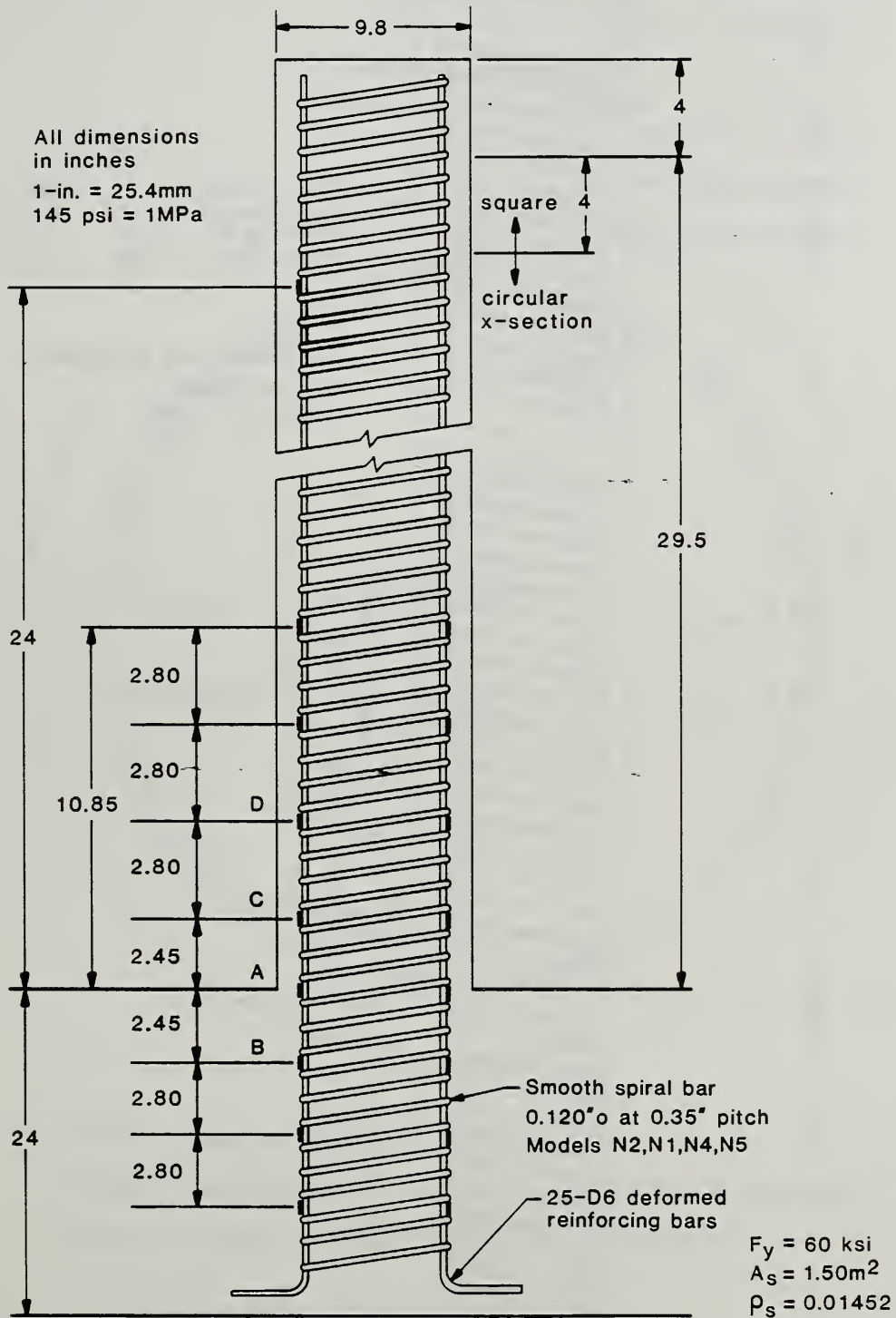


FIGURE 4.9

FLEXURE AND SHEAR SPIRAL GAGE LOCATION

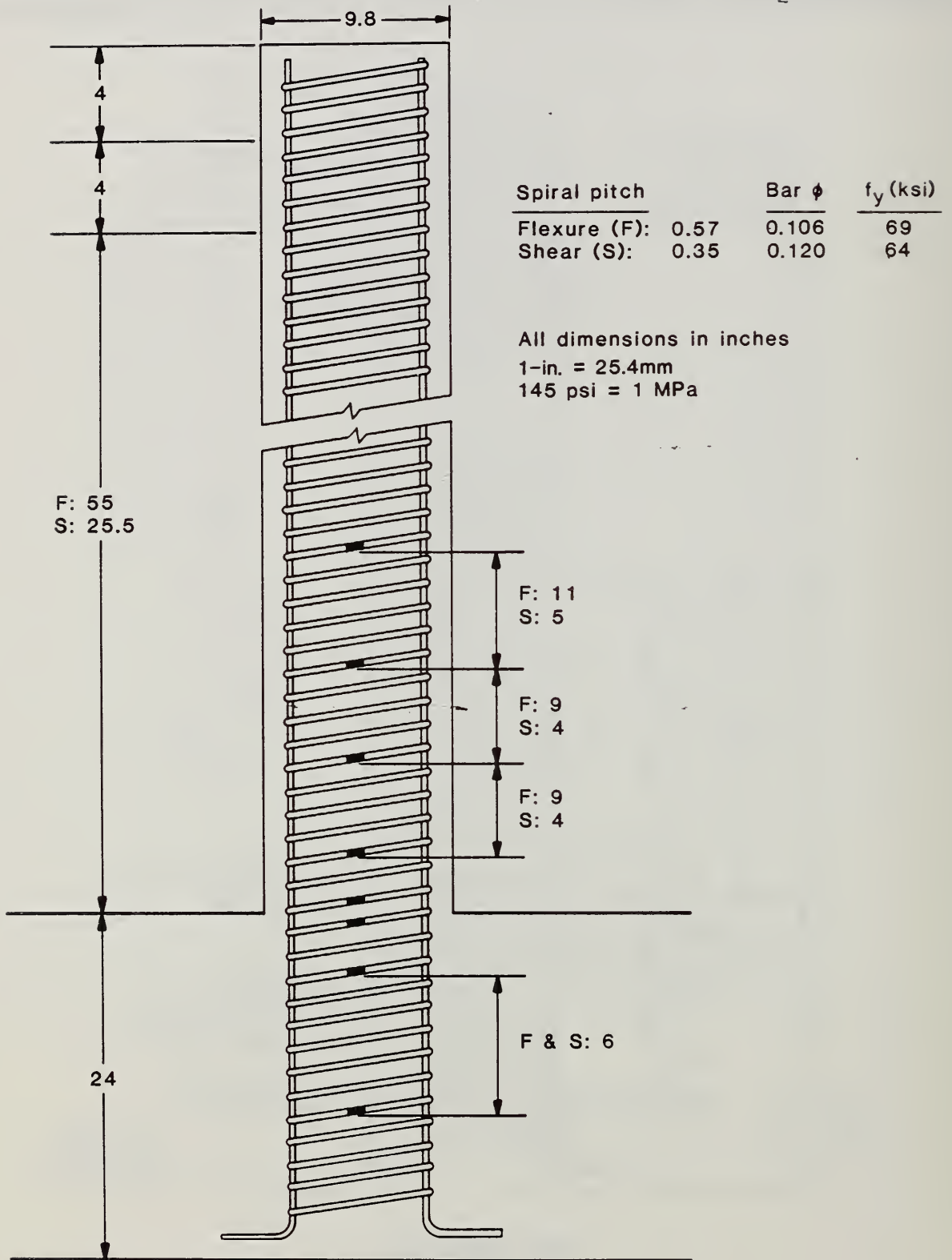
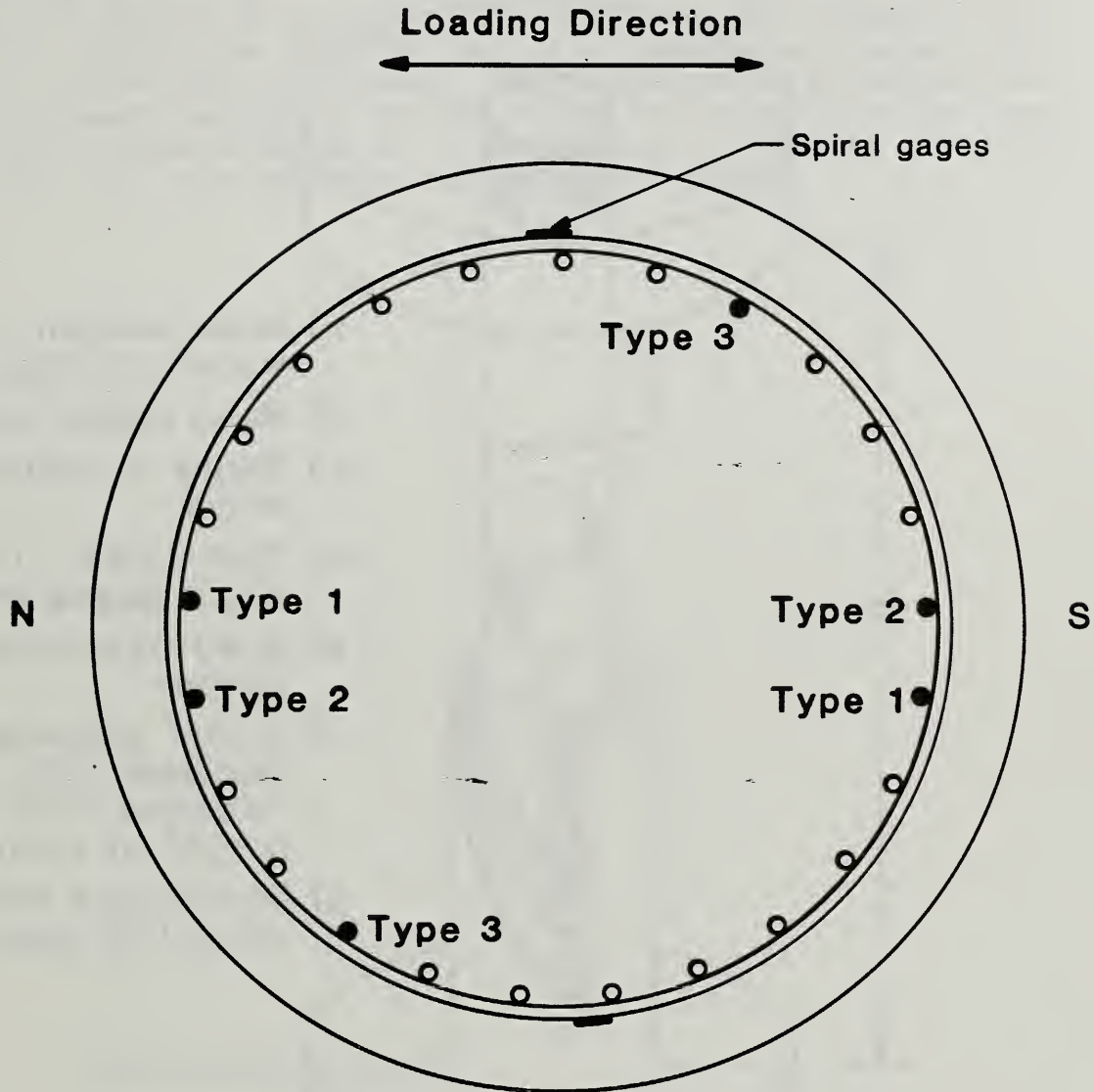


FIGURE 4.10

**STRAIN GAGE LOCATIONS
(Top View)**



Type 1 bars have 9 gages

Type 2 bars have 4 gages in positions A-D*

Type 3 bars have 1 gage in position A*

* Refer to Figs. 4.8 and 4.9

Fig. 4.11

EMBEDMENT GAGE

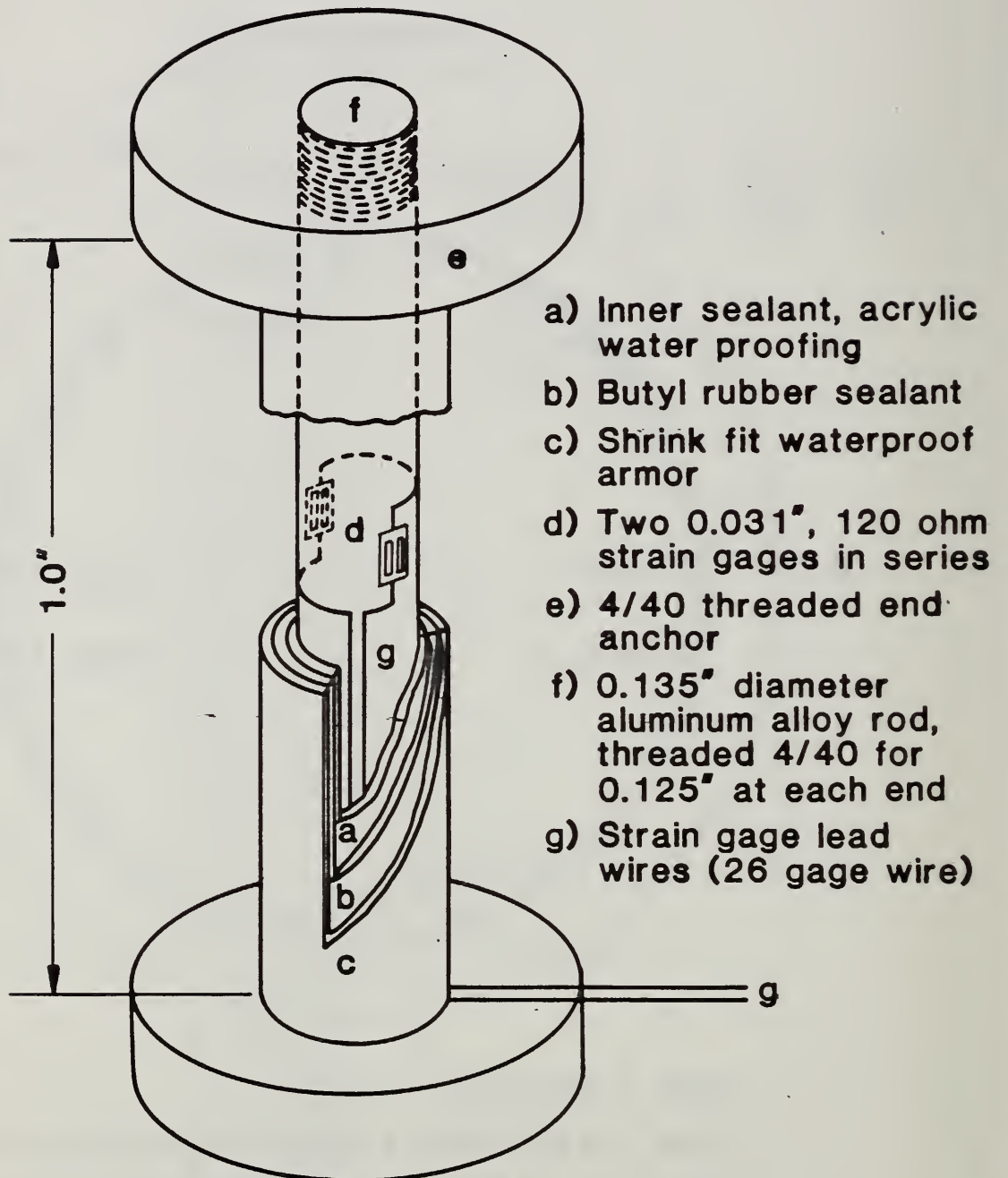


Fig. 4.12

Two LVDTs were used to measure the rotation at the base of the column. These were attached to the column by means of a piece of all-thread bar. The all-threads were inserted into a hole drilled into the column and then held in place by an epoxy for the microconcrete models. The all-threads were screwed into anchors placed in the column formwork prior to casting of the concrete for the pea gravel models. Two or four additional LVDTs were used along the height of the column for the shear and flexure models respectively. One of the LVDTs for each of the models was placed at the same height as the point of lateral load application to measure the maximum displacement experienced by the column. The other LVDTs were used to measure the displacement of the column at various heights along the column. Figs. 4.13 - 4.14 show the location of the LVDTs.

LVDT LOCATIONS FOR SHEAR COLUMNS

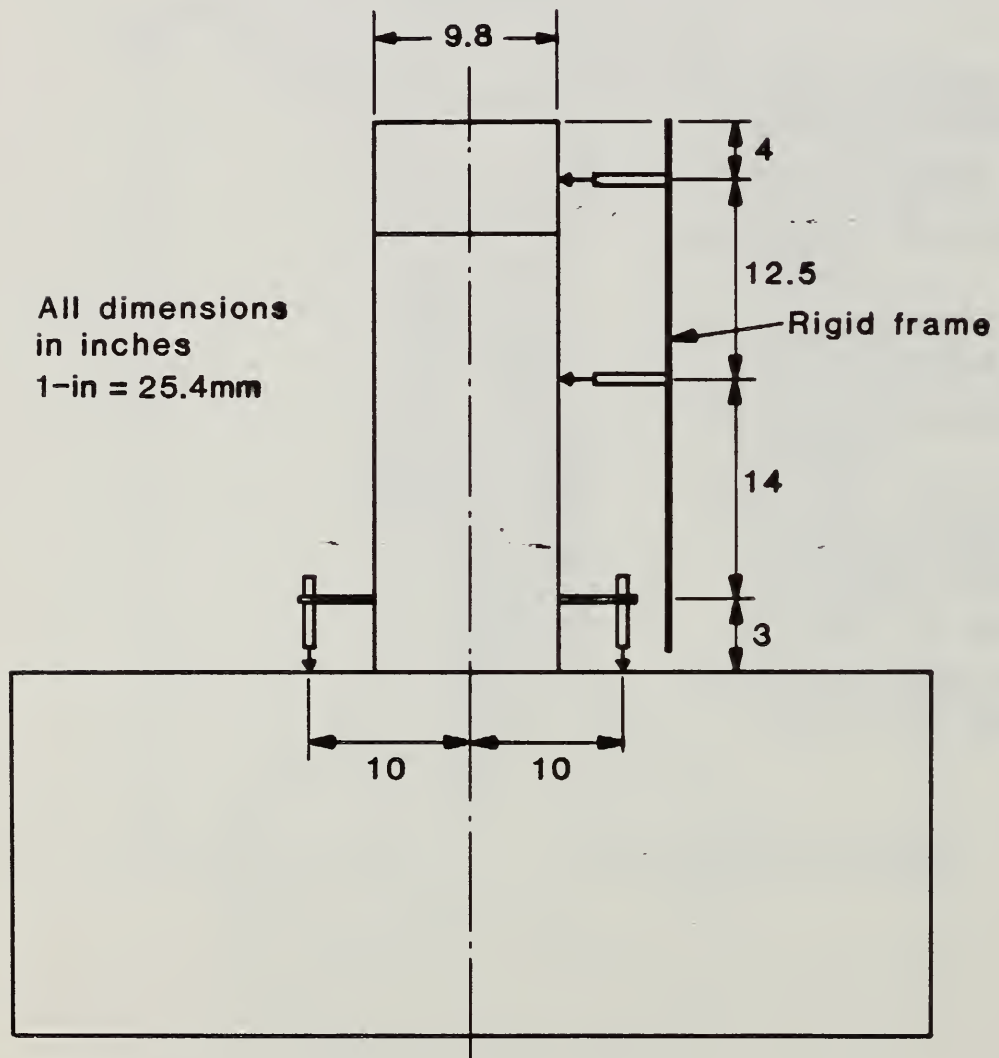


Fig. 4.13

LVDT LOCATIONS FOR FLEXURE COLUMNS

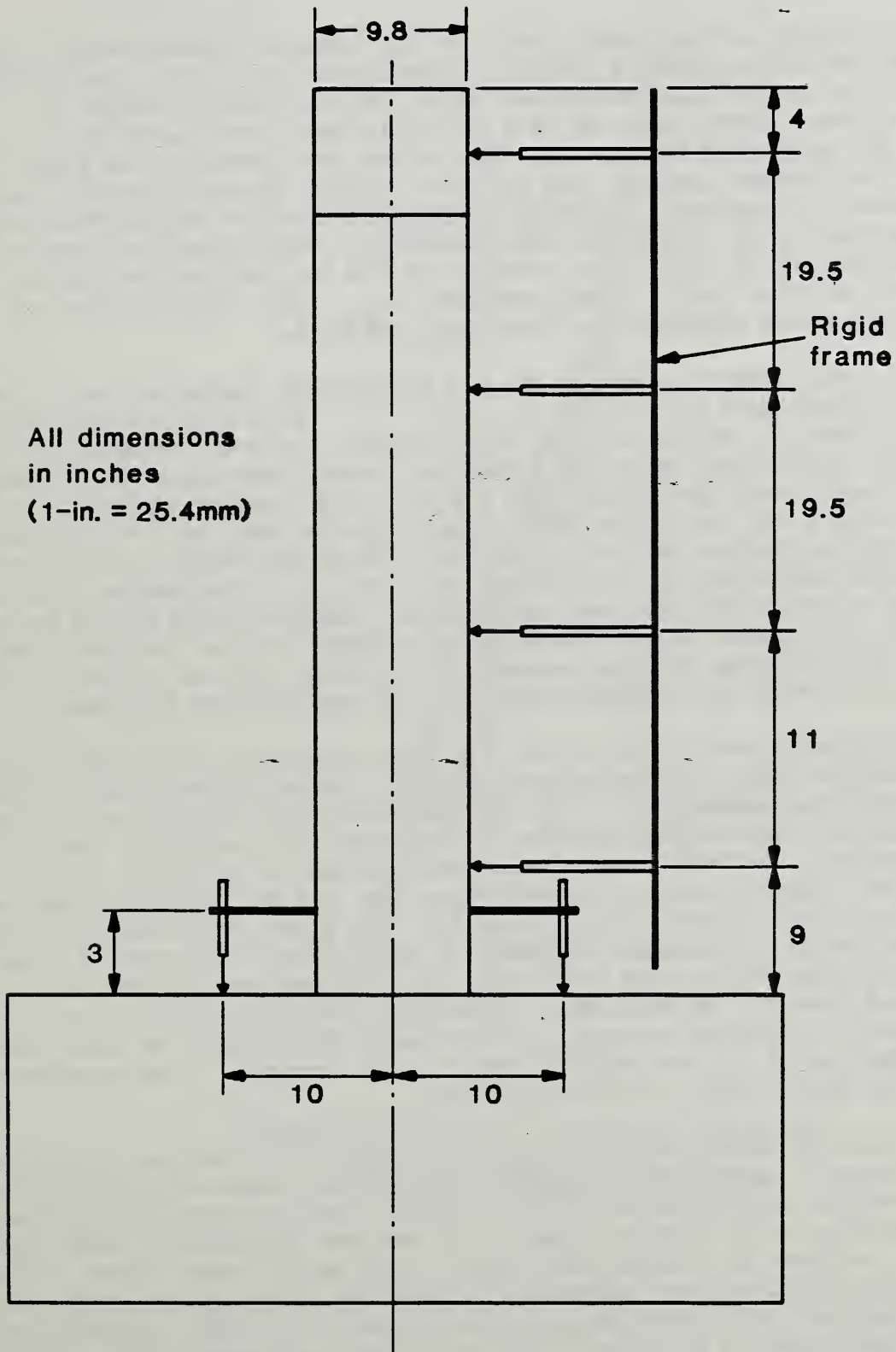


Fig. 4.14

5.0 TEST RESULTS AND OBSERVATIONS

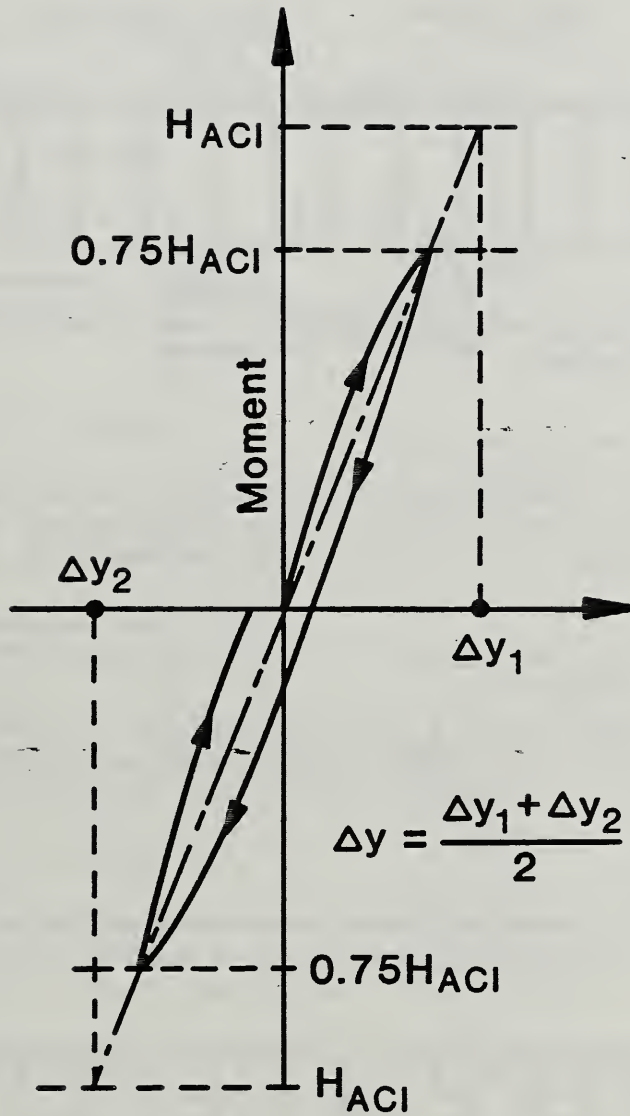
5.1 Introduction

The determination of the yield load and the loading sequence are the same as the method and procedure used by Priestley et. al. [37]. The ultimate moment of the column was calculated using the ACI column charts [4]. The yield load was assumed equal to 75 % of the lateral load which would induce ultimate ACI moment in the column. The column was loaded to the yield load in both the forward (south) and reverse (north) directions and the two displacements measured. The "yield" displacement in each direction was then obtained by dividing the experimentally determined deflection (as described above) by 0.75. The average of the two deflection values was then used as the yield displacement, Δ_y . The calculation of the experimental yield displacement is shown in Fig. 5.1.

In general, the loading sequence for the shear model tests was one cycle at Δ_y , two cycles each at $u = \pm 2, \pm 4, \pm 6, \dots$. If a significant drop in the moment capacity of the column in the second cycle as compared with the first cycle at the same ductility level was noted, the column was subjected to a third cycle at that ductility level. The loading history for the flexure models was one cycle at Δ_y , two cycles each at $\mu = +2$ and ± 3 . Instead of two cycles at $\mu = \pm 4$ as with the shear models, the flexure models were subjected to 10 cycles at $\mu = \pm 4$. The reason for this deviation was that the maximum achievable μ as governed by the maximum stroke of the hydraulic ram for model N3 was 5. It was decided then to consider the effects of the number of loading cycles on the column behavior. The tests were stopped when most of the bars had fractured.

The model columns were tested in the TTF (Tri-Directional Test Facility), a general purpose three axis structural testing system at the National Bureau of Standards (See Appendix C). The columns were first loaded axially to a pre-determined force which simulated the gravity loading of the bridge superstructure. Lateral force was then increased to yield load. The direction of loading was north-south (see Fig. 5.2 for specimen test set-up) with the first excursion to the south. The first cycle was conducted under load control (loadcell feedback to the closed loop servo-hydraulic actuator system) while the remainder of the test was conducted under displacement control (displacement transducer feedback to the closed loop servo-hydraulic actuator system). Cracks were highlighted as they formed so that they could be seen more clearly in photographs. Photographs were taken at the end of most of the excursions.

The remainder of this chapter presents a detailed discussion of test specimen properties and observations of behavior made during each test. The observations are presented in the form of a cycle-by-cycle log keyed to figures showing significant changes in column appearance (e.g. crack extension, failure of reinforcement etc.). The reader should bear in mind that the test specimen was mounted in a loading system in which lateral load was applied in a direction parallel to the north-south magnetic axis. The first excursion in any load cycle was always southward, followed by a return to the initial position, a subsequent northward excursion, and a return to initial position which completed the cycle.



**EXPERIMENTAL DEFINITION OF
YIELD DISPLACEMENT**

Fig. 5.1

TTF TEST SET-UP

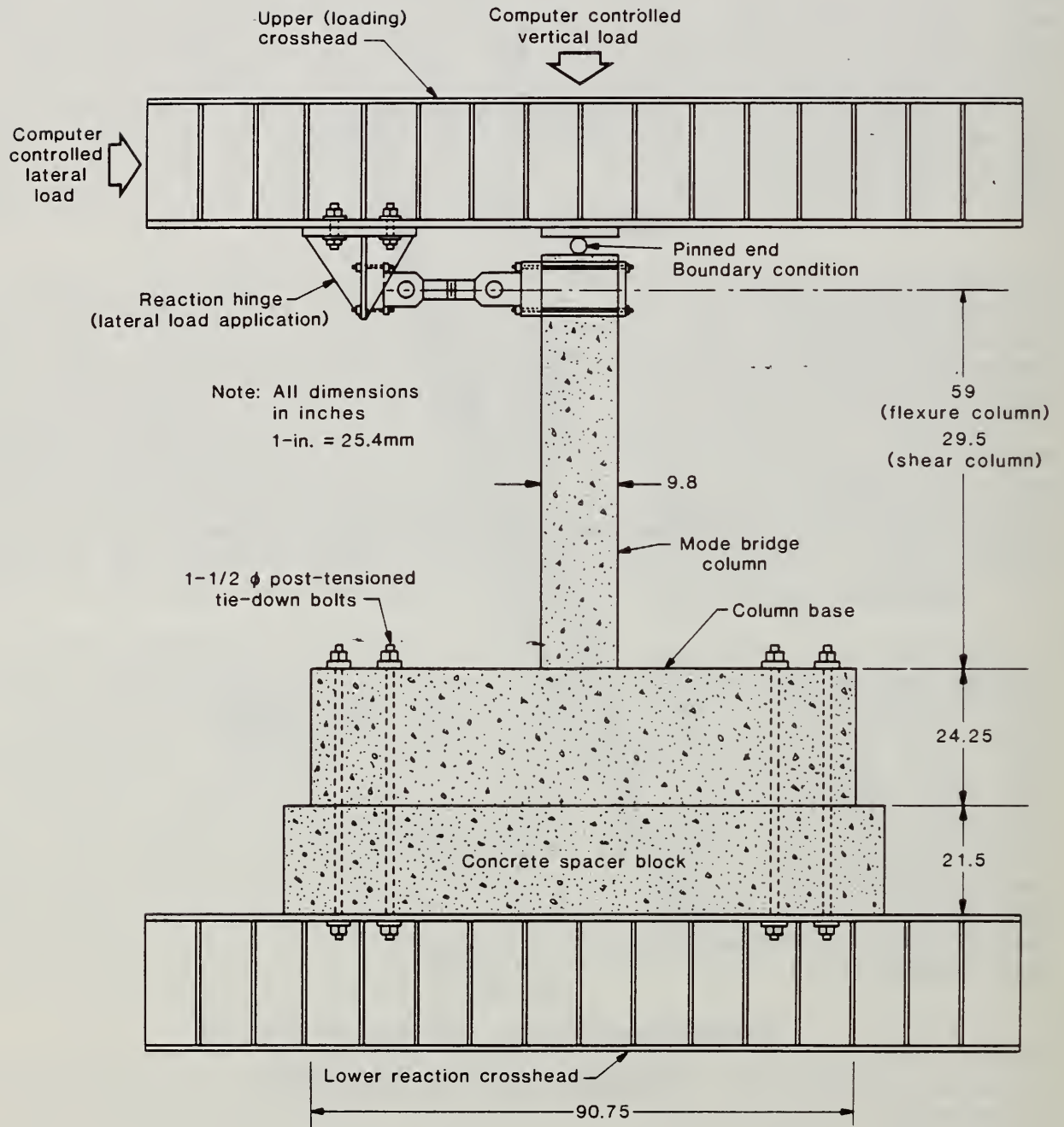


FIGURE 5.2

5.2 Model N1

5.2.1 MODEL PROPERTIES

$$f'_c = 3490 \text{ psi (24.08 MPa)}$$

$$P_e = 26.87 \text{ kips (119.6 KN)}$$

$$M_u \text{ (experimentally)} = 38.35 \text{ ft-kip (52.0 kN-m)}$$

$$P_h = 10.8 \text{ kips (48.06 KN)}$$

$$\Delta_y \text{ (experimentally)} = 0.38 \text{ in. (9.65 mm)}$$

where P_h is the lateral "yield" load. The load history is shown in Fig. 5.3.

5.2.2 DUCTILITY FACTOR = 1, CYCLE 1

Hairline flexure and shear cracks appeared when the lateral load was equal to 7.5 kips (33.37 KN) or approximately 69 % of the calculated yield load. Cracks were observed up to a height of 1' - 8" (50.8 cm) above the base. See Fig. 5.4.

5.2.3 DUCTILITY FACTOR = 2, Cycles 2 & 3

Existing cracks propagated and new cracks formed - both flexure and shear. On the excursion south, second cycle, very minor crushing appeared to be occurring at the base of the south side of the column.

5.2.4 DUCTILITY FACTOR = 4, CYCLES 4 & 5

Cycle 4: Crushing of the column base on the south side was evident during the southward excursion with flaking occurring on the excursion north. See Fig. 5.5.

Cycle 5: Pieces of concrete, one about 1 in. X 2 in. (2.54 X 5.08 cm) fell off the south side on the excursion south. All spall dimensions are width x height. This is shown in Fig. 5.6. Additional shear cracks formed. Some flexure crack widths were approximately 0.375 in. (9.5 mm). An area in the base foundation beam adjacent to the south side of the column began to spall, as if the column was pulling out.

5.2.5 DUCTILITY FACTOR = 6, CYCLES 6 & 7

Cycle 6: On the excursion south, some crack widths on the north side of the column were about 1/4 in. (6.35 mm). The base around the column on the north side showed signs of uplifting also. A radial crack, Fig. 5.7, at about a distance of 2.5 - 3 in. (64 - 77 mm) out from column, appeared in the base on the south side. On the subsequent excursion north, the column base on the north began to spall. A few additional cracks formed.

LOADING HISTORY FOR MODEL N1

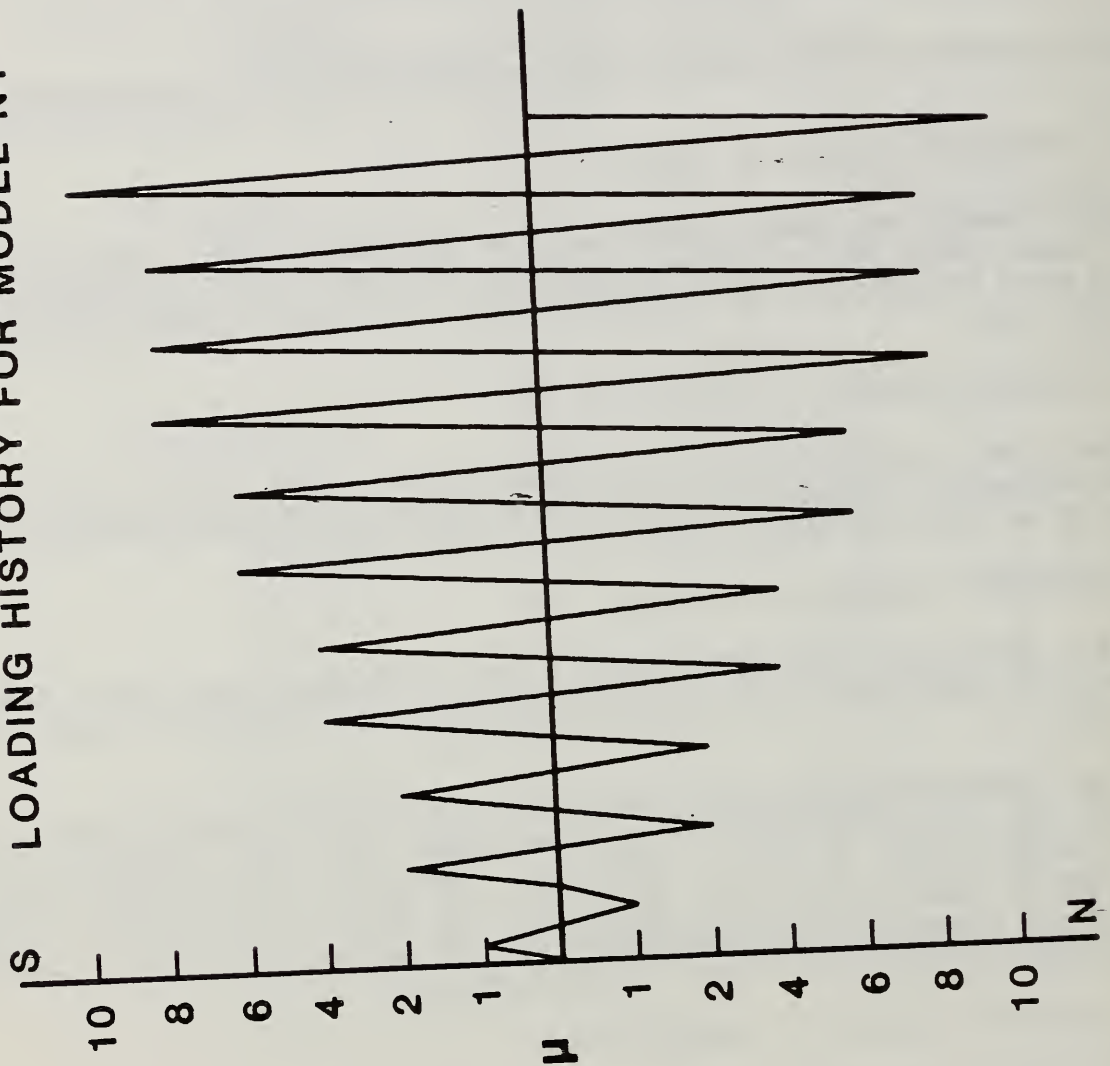
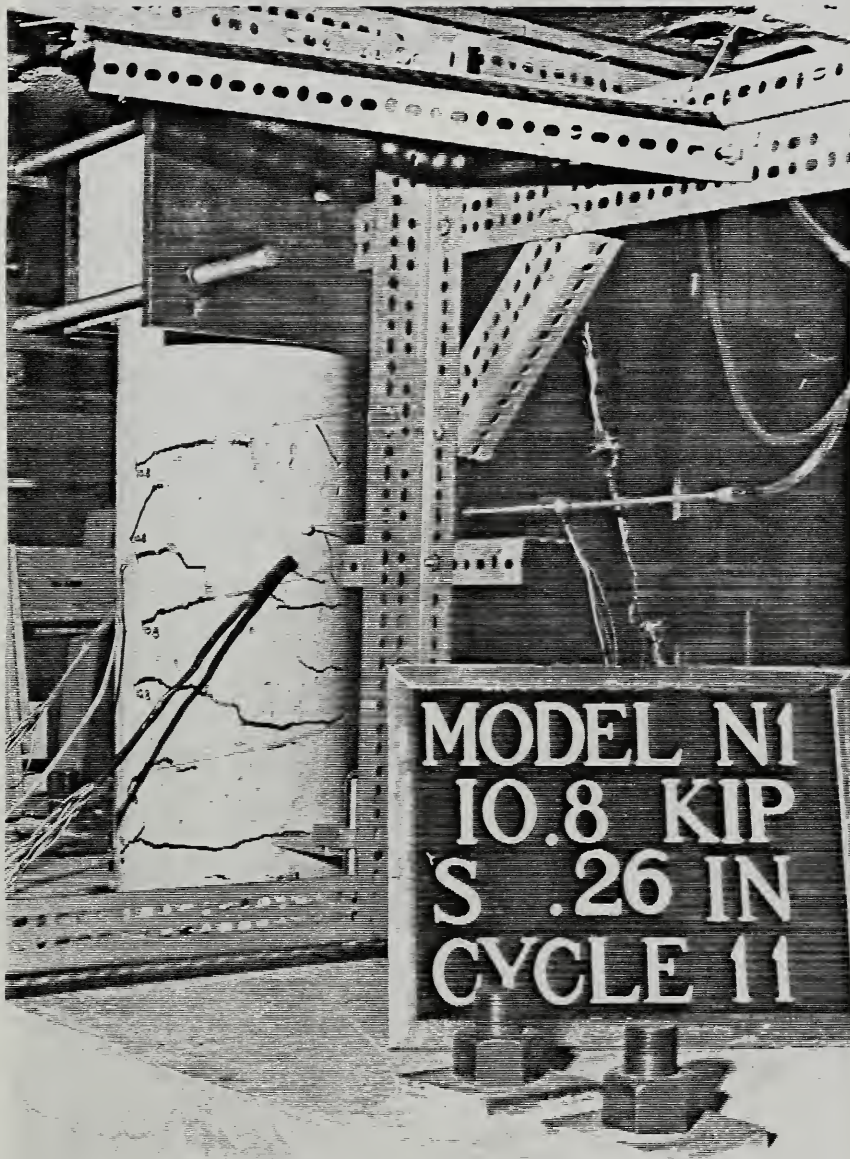
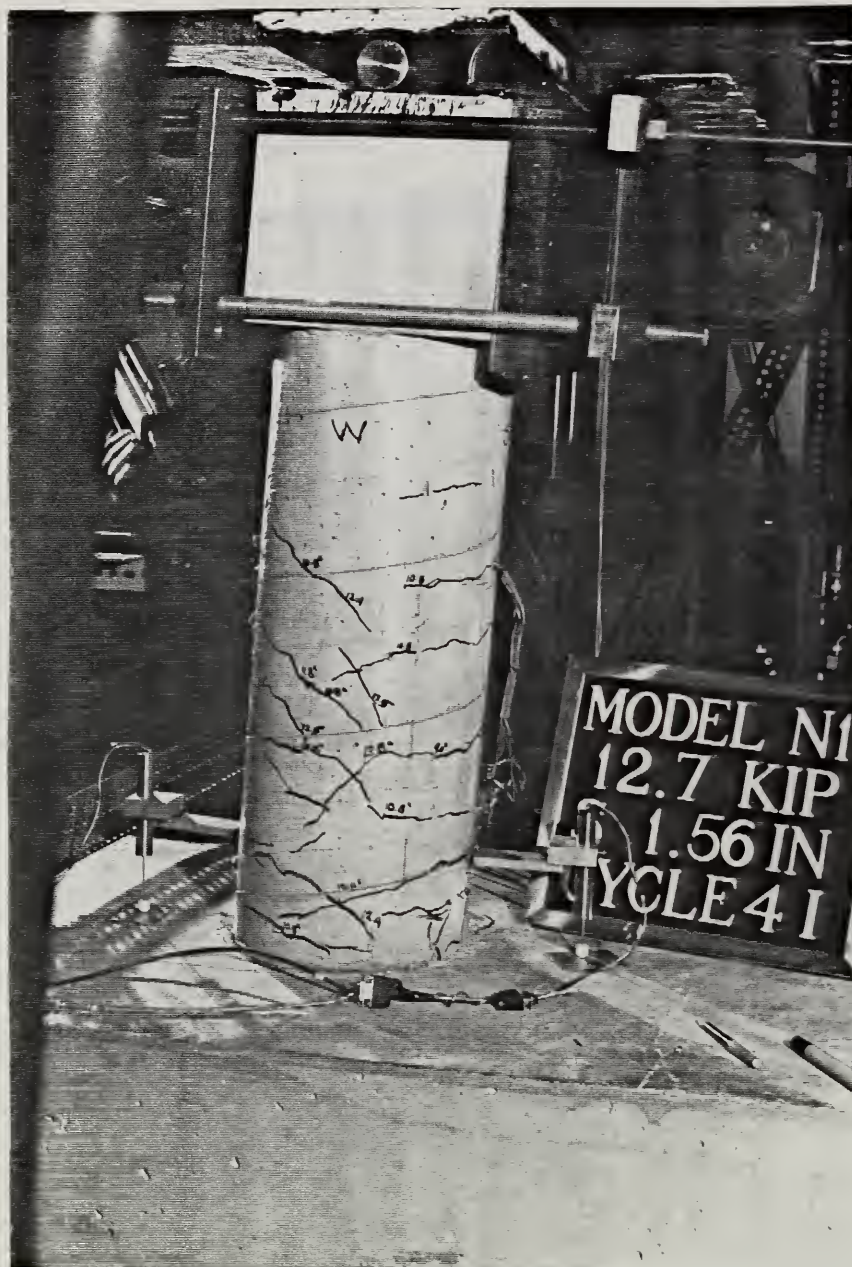


Fig. 5.3



Model N1, DF = 1, Cycle 1

Fig. 5.4



Model N1, DF = 4, Cycle 4

Fig. 5.5



Model N1, DF = 4, Cycle 5

Fig. 5.6



Model N1, DF = 6, Cycle 6

Fig. 5.7

Cycle 7: On the excursion south, the column base on the north spalled off. The spall areas on both the north and south sides of the column were approximately 6 X 2 in. (15.24 X 5.08 cm). A few additional cracks formed.

5.2.6 DUCTILITY FACTOR = 8, CYCLES 8, 9 & 10

Cycle 8: Three pops were heard during the first southward excursion. No visible sign of fracture could be seen as the concrete obscured the longitudinal bars from view. These sounds could have been the breaking of ties used to tie the longitudinal bars to the spiral cage, as was observed in another test. Severe crushing of the column base on the south side was noted. Buckled longitudinal bars were visible on both the north and south sides of the column. The lateral load on the excursion south was about 66% of the yield load.

Cycle 9: Again, the sound of fracturing "bars" was heard twice. The longitudinal bars had buckled out by approximately an inch (25.4 mm). The spiral was still intact but had yielded. This was most likely due to it sliding up along the buckled longitudinal bars, allowing it to reduce its stress.

Cycle 10: Ten longitudinal bars had buckled and one was completely fractured on the south side of the column.

5.2.7 DUCTILITY FACTOR = 10, CYCLE 11

Six longitudinal bars on the north side and seven on the south side had fractured. Fig. 5.8 shows the entire column and a close-up showing the fractured bars is shown in Fig. 5.9.

5.3 Model N2

5.3.1 PROPERTIES

$$f'_c = 3349 \text{ psi (23.11 MPa)}$$

$$P_e = 53.75 \text{ kips (239.2 kN)}$$

$$M_u \text{ (experimental)} = 46.52 \text{ ft-kip (63.07 kN-m)}$$

$$P_h = 11.15 \text{ kips (49.6 kN)}$$

$$\Delta_y \text{ (experimental)} = 0.22 \text{ in. (5.59 mm)}$$

The loading history is shown in Fig. 5.10.

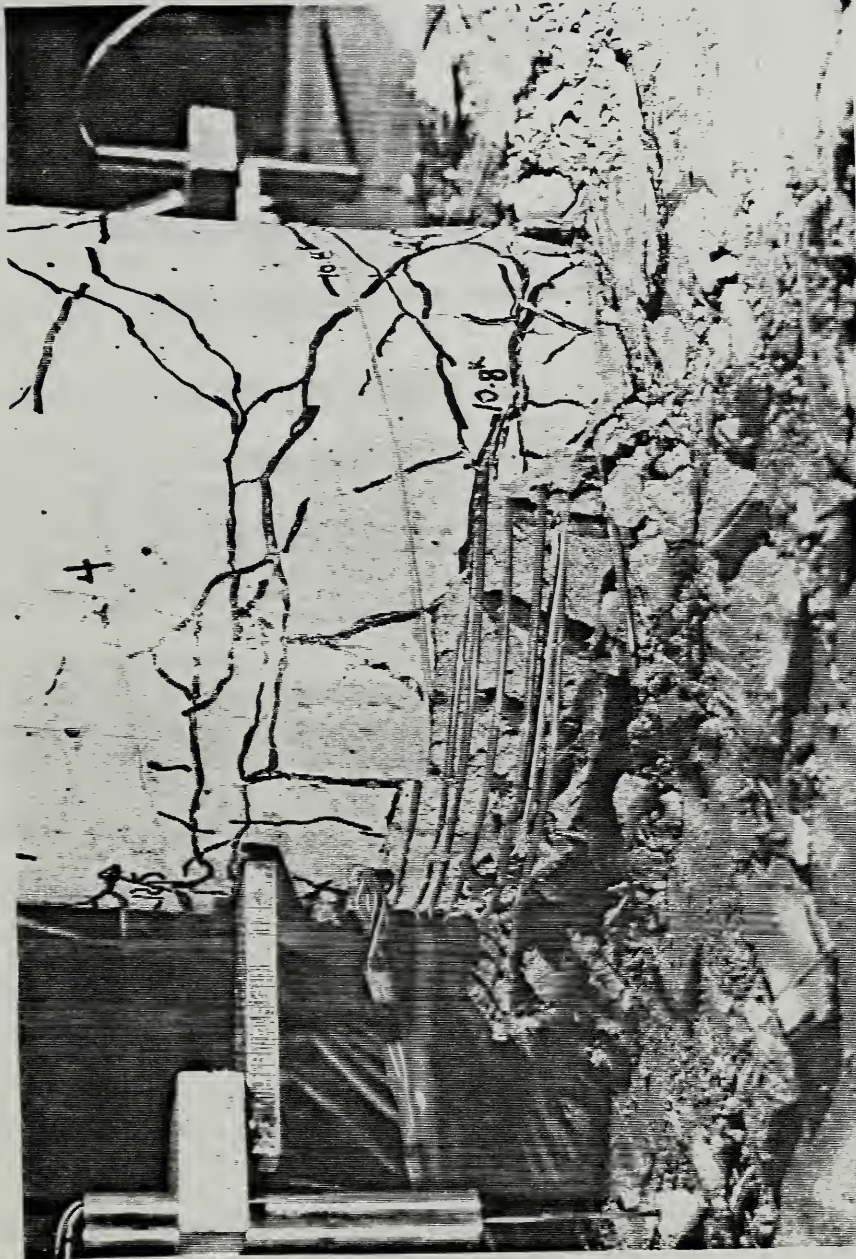
5.3.2 DUCTILITY FACTOR = 1, CYCLE 1

Only flexure cracks were noted upon loading the column to the yield load. These appeared as horizontal cracks initiating at the north and south centerlines of the column and propagating to the east and west centerlines.



Model N1, DF = 10, Cycle 11

Fig. 5.8



Model N1, DF = 10, Cycle 11

Fig. 5.9

LOADING HISTORY FOR MODEL N2

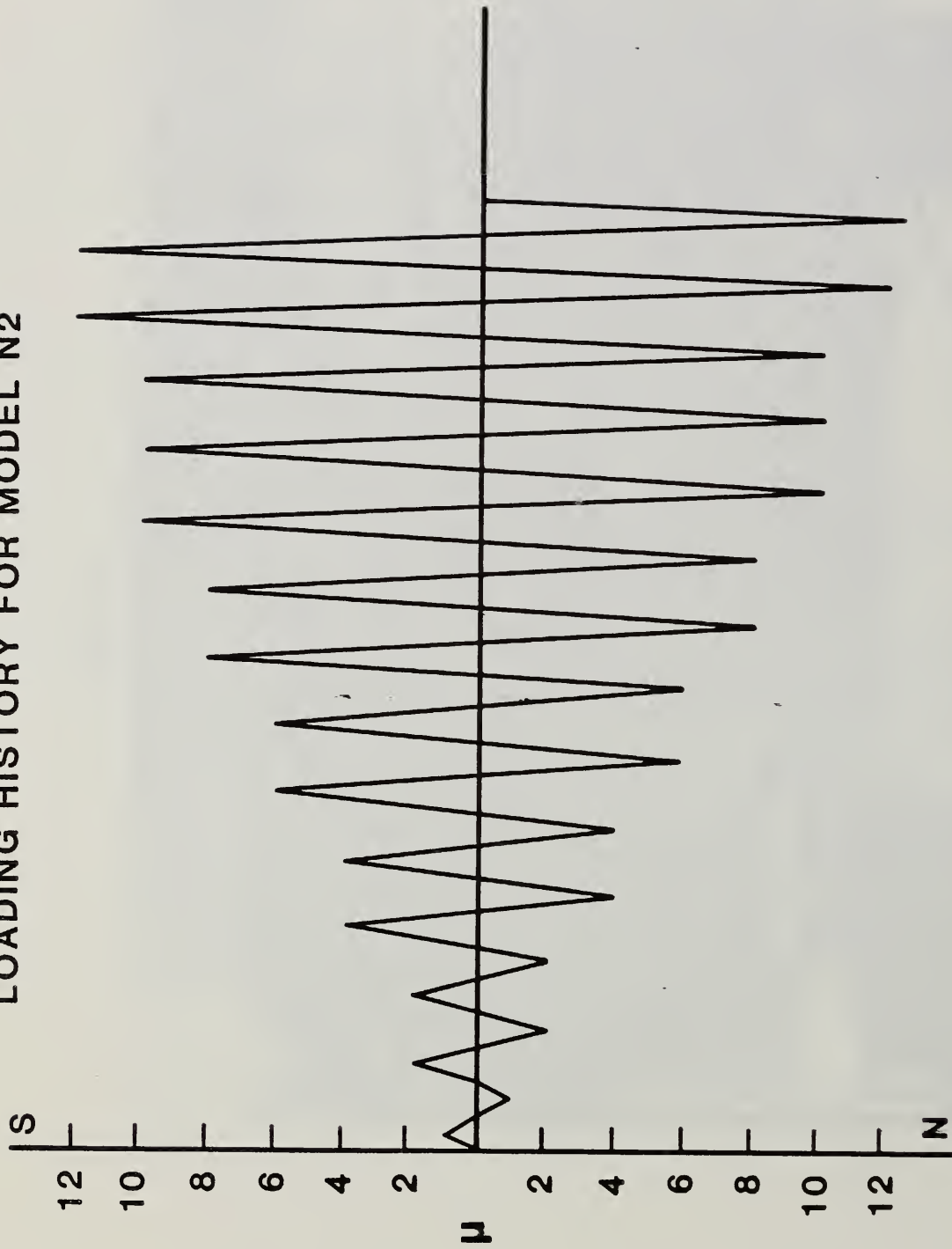


Fig. 5.10

These reached a height of 1' - 2" (35.6 cm). The load at first cracking was to 7.8 kips (34.69 kN) or approximately 70 % of the calculated yield load. The crack initial pattern is shown in Fig. 5.11.

5.3.3 DUCTILITY FACTOR = 2, CYCLES 2 & 3

Shear cracks evidenced by propagation of previously horizontal flexure cracks at a pronounced inclination (approximately 45°). This is shown in Fig. 5.12. Flexure cracks had formed to a height of 1' - 10" (55.9 cm) above the base of the column.

5.3.4 DUCTILITY FACTOR = 4, CYCLES 4 & 5

Crushing of the concrete and formation of vertical cracks about 1 - 2 in. (25.4 - 50.8 mm) in length were noted. The column could be seen to be separating from the base by about 0.1 in. (2.5 mm) and the width of cracks was about 0.1 in. (2.5 mm).

5.3.5 DUCTILITY FACTOR = 6, CYCLES 6 & 7

Cycle 6: More crack propagation was observed with new cracks forming. Additional crushing of the column base on the north and south sides with spalling on the south side occurred. Some of the flexure cracks near the base of the column were about 3/16 in. (4.8 mm) wide. The crack pattern is shown in Fig. 5.13.

Cycle 7: Spalling on both the north and south sides occurred. A piece of concrete about 5 X 3 in. (12.7 X 7.6 cm) fell off on the south side. Unfortunately, the LVDT measuring the rotation came off along with it. The spiral did not appear to have yielded.

5.3.6 DUCTILITY FACTOR = 8, CYCLES 8 & 9

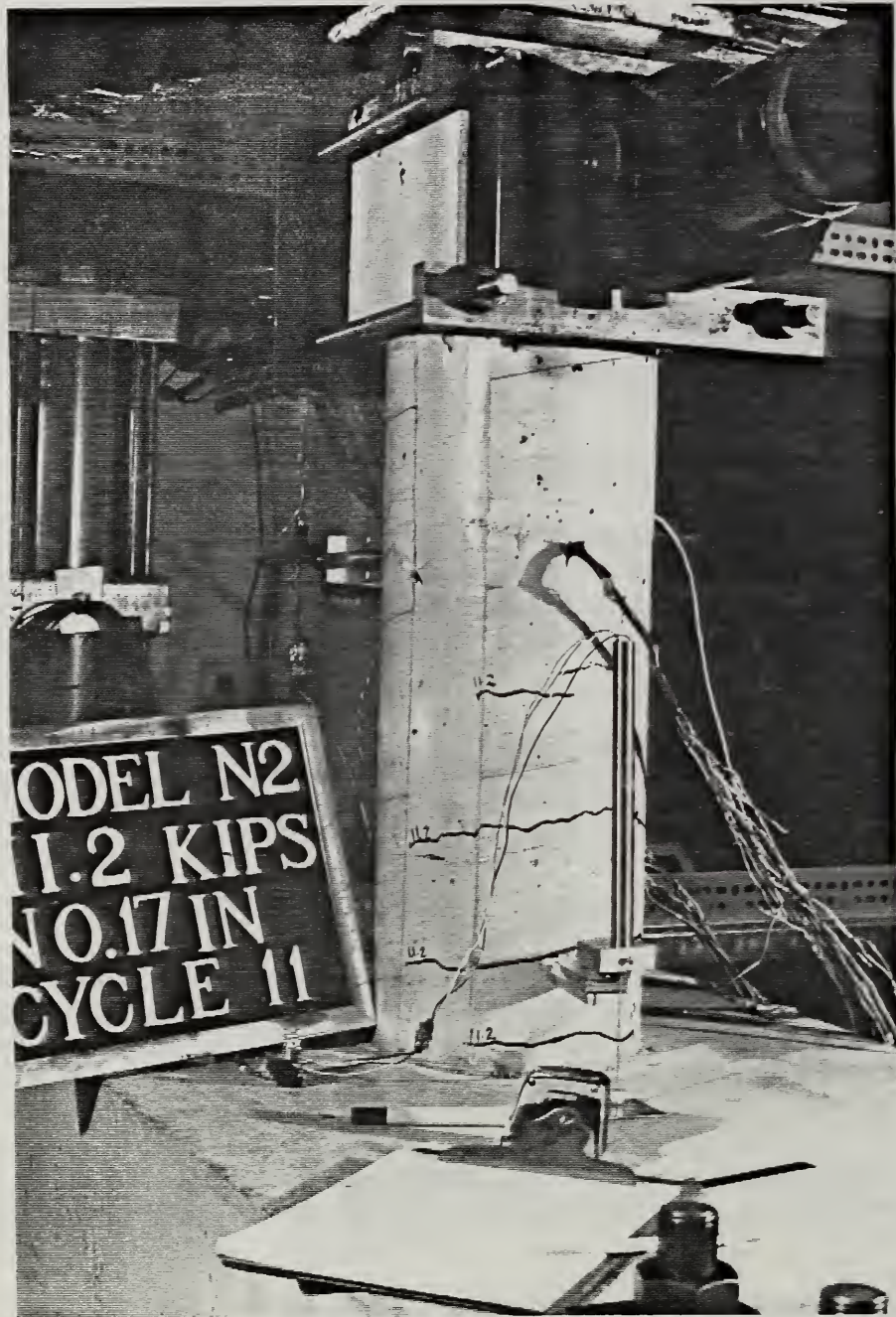
CYCLE 8: New flexure and shear cracks formed. The widths of some cracks ranged from 3/16 in. - 1/4 in. (4.8 - 6.3 mm). Some uplifting of the base on the northeast side was noted. A spiral about 2 in. (5.08 cm) up from the base on the south could be seen to have yielded. Fig. 5.14 shows the spall area and the yielded spiral.

CYCLE 9: A longitudinal bar on the south side buckled. Spirals above and below the previously yielded spiral on the south also appeared to have yielded.

5.3.7 DUCTILITY FACTOR = 10, CYCLES 10, 11, & 12

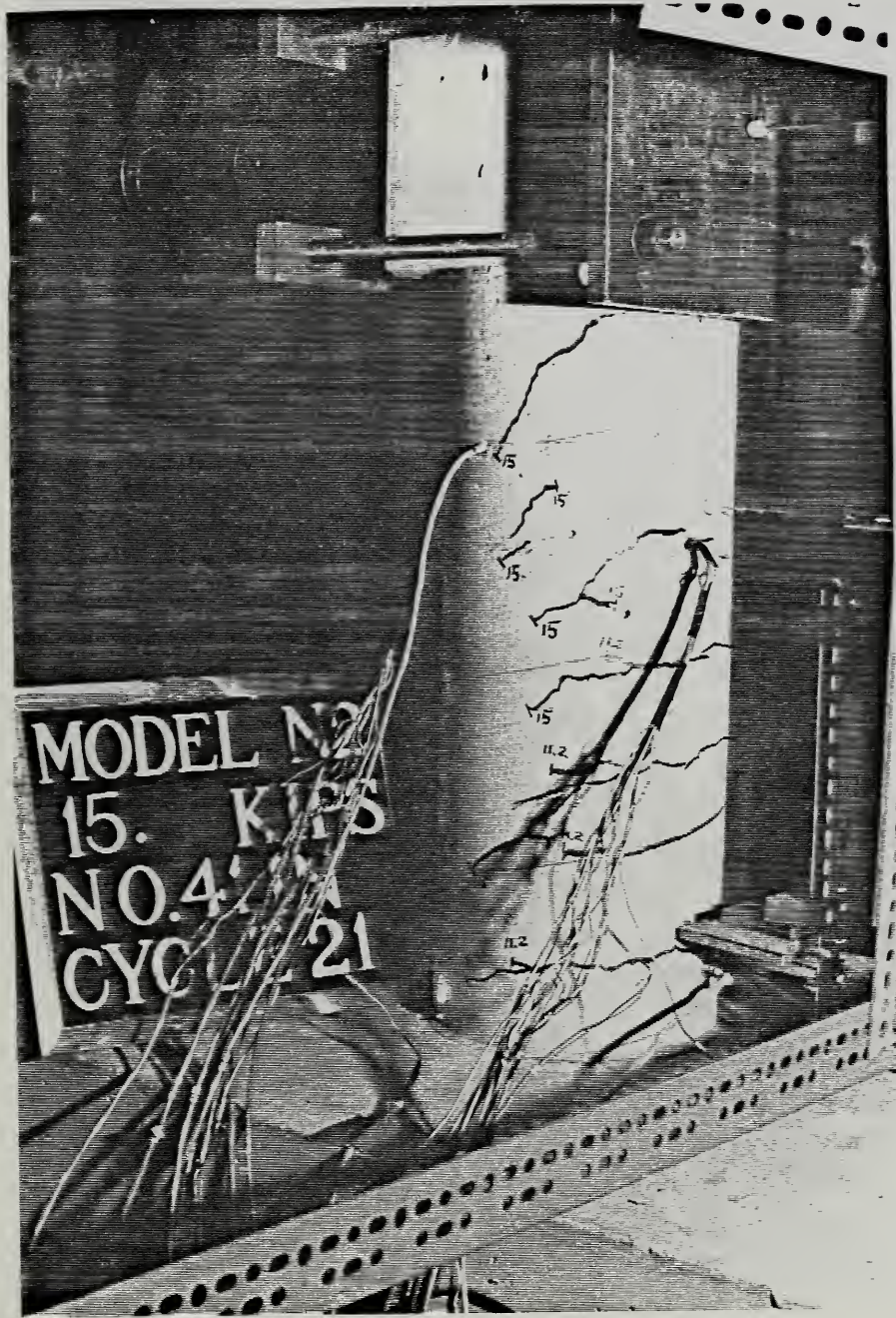
CYCLE 10: A total of six bars on the south side and a total of five bars on the north side were observed to have buckled at this point. Spalling on the north side was noted in this cycle. A spiral 2 in. (5.08 cm) from the base on the north side appeared to have yielded. The spiral 2 in. (5.08 cm) from the base on the south side fractured.

CYCLES 11 & 12: Eight longitudinal bars were observed to have buckled on the south side. The spall area on the south side measured approximately about 9 X 4 in. (22.9 X 10.2 cm) and 10 X 4 in. (25.4 X 10.2 cm) on the



Model N2, DF = 1, Cycle 1

Fig. 5.11



Model N2, DF = 2, Cycle 2

Fig. 5.12



Model N2, DF = 6, Cycle 6

Fig. 5.13



Model N2, DF = 8, Cycle 9

Fig. 5.14

north side. Three longitudinal bars on the south fractured in cycle 12. The lateral load was reduced to $0.78 P_y$ in the 12th cycle.

5.3.8 DUCTILITY FACTOR = 12, CYCLE 13

Three longitudinal bars on the north broke and two additional bars broke on the south in this cycle. Fig. 5.15 shows the fractured bars on the south and Fig. 5.16 shows the spall area on the south side.

5.4 Model N3

5.4.1 MODEL PROPERTIES

$$f'_c = 3681 \text{ psi (25.4 MPa)}$$

$$P_e = 26.87 \text{ kips (119.6 kN)}$$

$$M_u \text{ (experimental)} = 43.79 \text{ ft-kip (59.37 kN-m)}$$

$$P_h = 5.4 \text{ kips (24 kN)}$$

$$\Delta_y \text{ (experimental)} = 1.01 \text{ in. (25.6 mm)}$$

The loading history is shown in Fig. 5.17.

5.4.2 DUCTILITY FACTOR = 1, CYCLE 1

Flexure cracking began at 2.7 kips (12.0 kN) or approximately 50 % of the calculated yield load. No shear cracking was observed. Fig. 5.18 shows the crack pattern.

5.4.3 DUCTILITY FACTOR = 2, CYCLES 2 & 3

Few additional cracks formed at this ductility level. The crack widths ranged from 0.08 - 0.1 in. The severity and number of cracks were similar on both the north and south sides. Very minor crushing of the south side occurred.

5.4.4 DUCTILITY FACTOR = 3, CYCLES 4 & 5

Some spalling on the south side occurred. The LVDT used to measure the south rotation came off along with the concrete cover. Some spalling also occurred on the north side. The crack widths were approximately 0.16 in. (4 mm). A few vertical cracks about one inch (25.4 mm) in length formed. A spiral about 3 in. (7.6 cm) above the was noted to have fractured when the cover spalled off. The fracturing of the spiral was unexpected. However, upon inspection of the spiral, the south bar was observed to been damaged during the drilling of the column to install the LVDTs used to measure the rotation. The influence which this had on the energy absorption performance is discussed in section 6.2. Fig. 5.19 shows the spalling of the south side.



Model N2, DF = 12, Cycle 13
Fig. 5.15



Model N2, DF = 12, Cycle 13

Fig. 5.16

LOADING HISTORY FOR MODEL N3

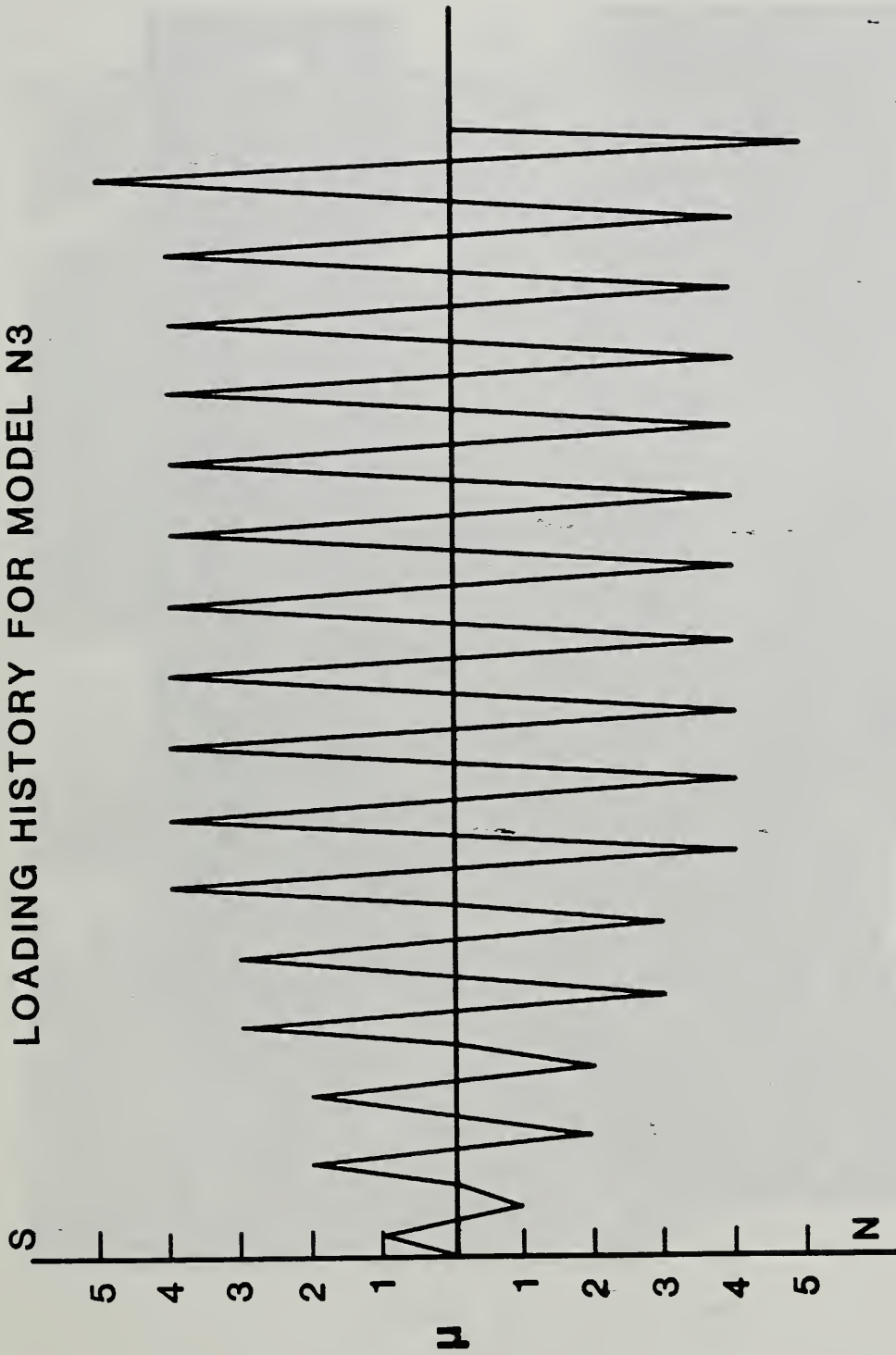
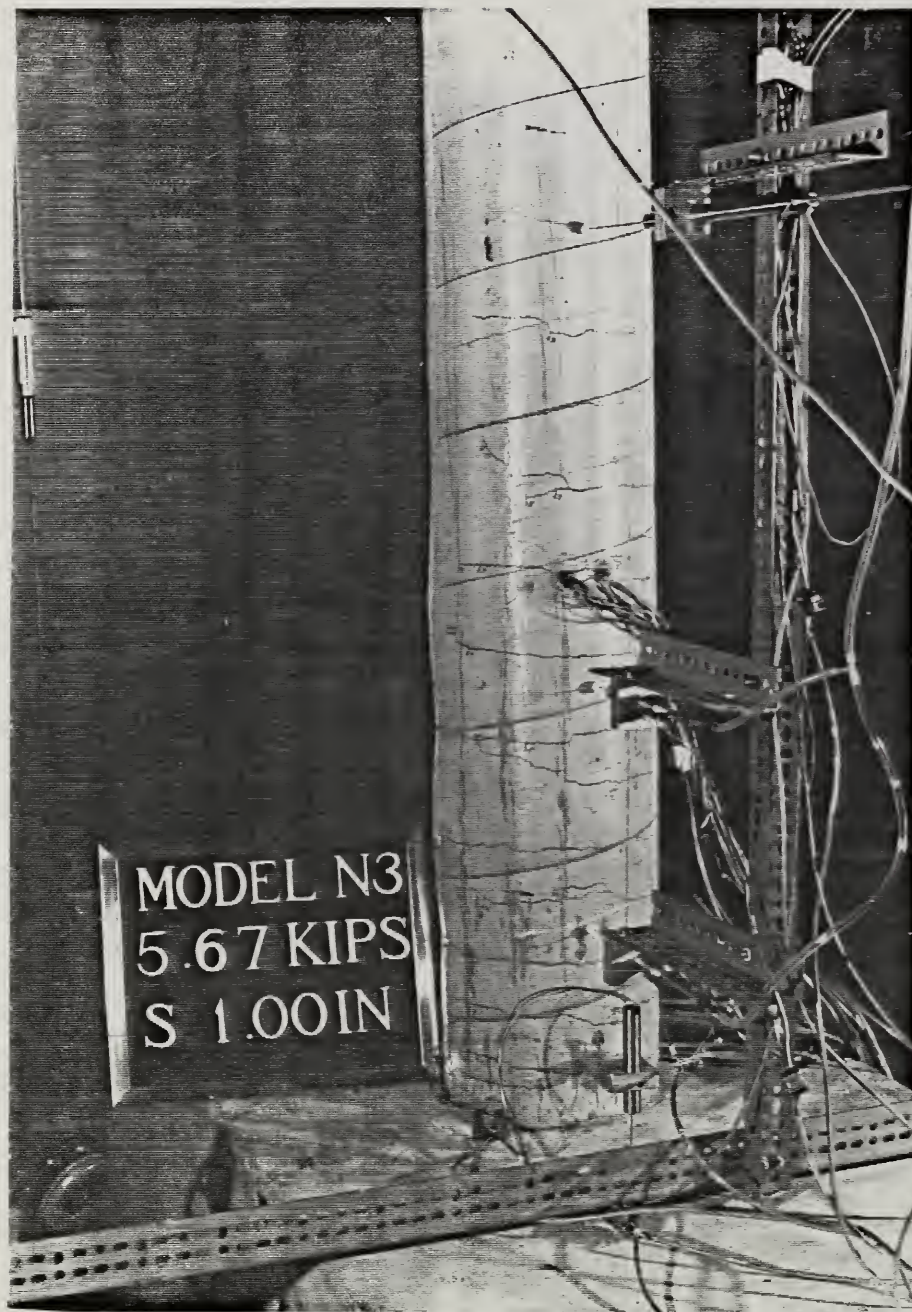
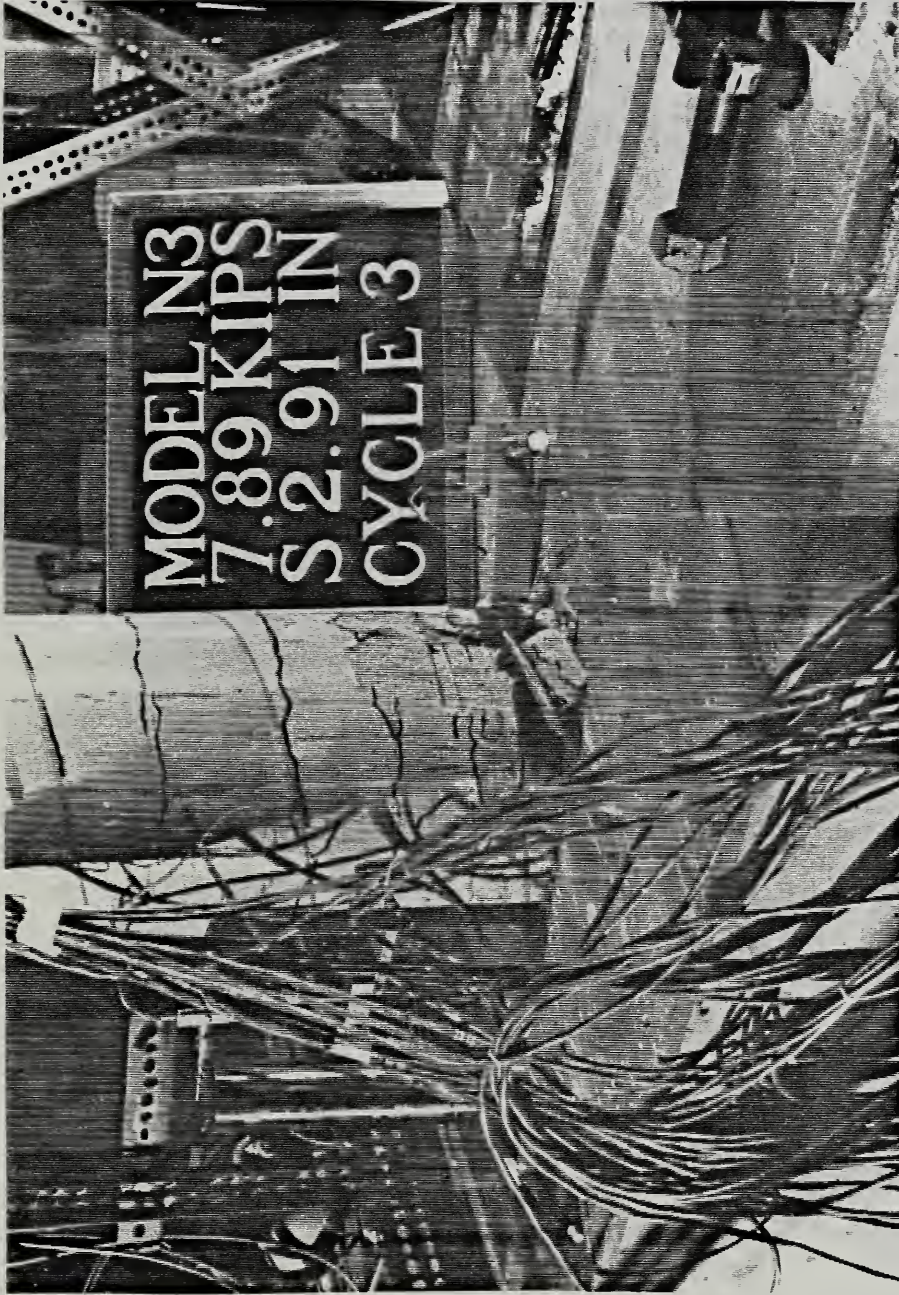


Fig. 5.17



Model N3, DF = 1, Cycle 1
Fig. 5.18



Model N3, DF = 3, Cycle 4

Fig. 5.19

5.4.5 DUCTILITY FACTOR = 4, CYCLES 6 - 15

CYCLE 6: Formation of additional vertical cracks occurred. The crack pattern is shown in Fig. 5.20 for the south side following the excursion to the south. The spiral about 3 in. (7.62 cm) above the base fractured on the north side. Upon inspection, the spiral had also sustained minor damage during the drilling process. Additional spalling was also observed.

CYCLES 7 - 10: Vertical bars on both the north and south sides were observed to have buckled. Spalling up to a height of 5 in. (12.7 cm) from the base was noted. Figs. 5.21 and 5.22 show the fractured spiral and the buckled bars respectively.

CYCLES 11 - 15: The column had spalled almost entirely around its circumference. Three longitudinal bars on the north and three on the south fractured with the first fracture occurring on the eleventh cycle on the north side.

5.4.6 DUCTILITY FACTOR = 5, CYCLE 16

A 4th longitudinal bar on the south fractured in this cycle. The lateral load had decreased to approximately 0.30 P_y . The extent of damage is shown in Fig. 5.23.

5.5 Model N4

5.5.1 MODEL PROPERTIES

$$f'_c = 3545 \text{ psi (24.46 MPa)}$$

$$P_e = 26.86 \text{ kips (119.53 kN)}$$

$$M_u \text{ (experimental)} = 37.48 \text{ ft-kip (50.82 kN-m)}$$

$$P_h = 10.87 \text{ kips (48.37 kN)}$$

$$\Delta_y \text{ (experimental)} = 0.21 \text{ in. (5.33 mm)}$$

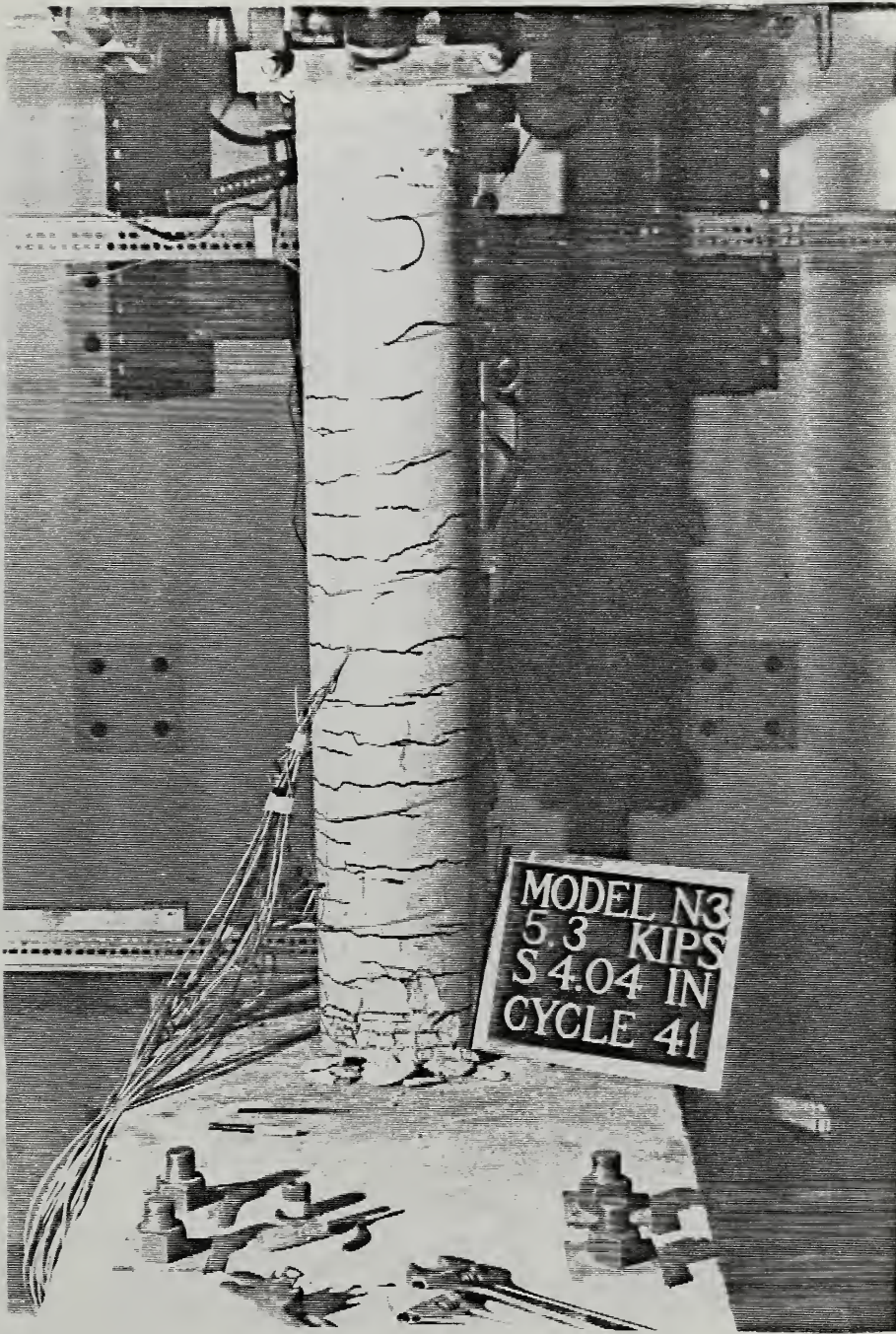
The loading history is shown in Fig. 5.24.

5.5.2 DUCTILITY FACTOR = 1, CYCLE 1

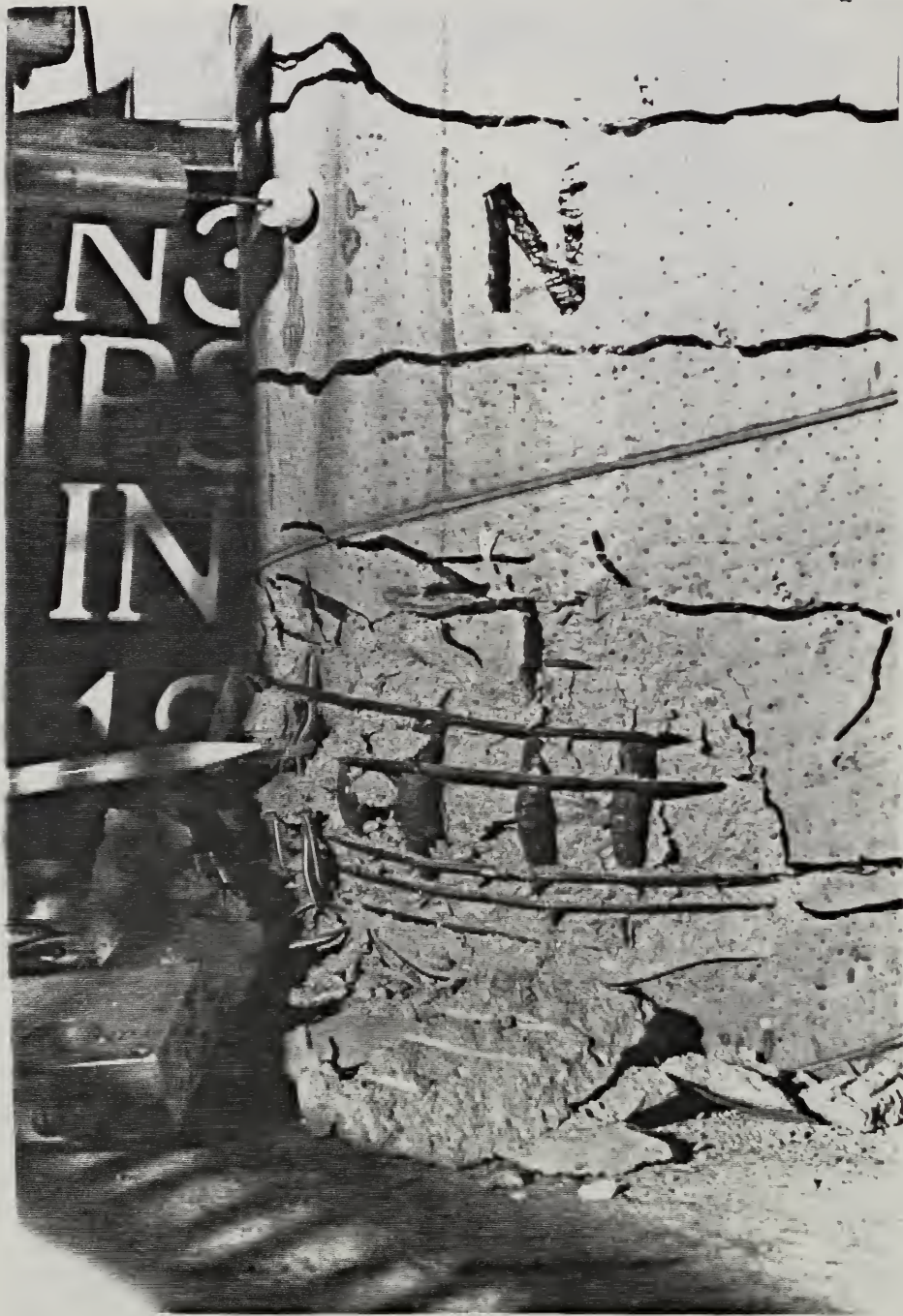
Lateral load at first cracking was 9 kips (40.0 kN) or approximately 83 % of the calculated yield load. The cracks were hairline flexure cracks which reached a height of about 1' - 2" (35.56 cm) on both the north and south sides. Fig. 5.25 shows the cracked column.

5.5.3 DUCTILITY FACTOR = 2, CYCLES 2 & 3

The flexure cracks propagated to the east and west sides of the column and additional cracks appeared up to a height of 1' - 8.5" (52.1 cm). Crack propagation and formation occurred mainly during the second cycle. The new crack pattern is shown in Fig. 5.26.

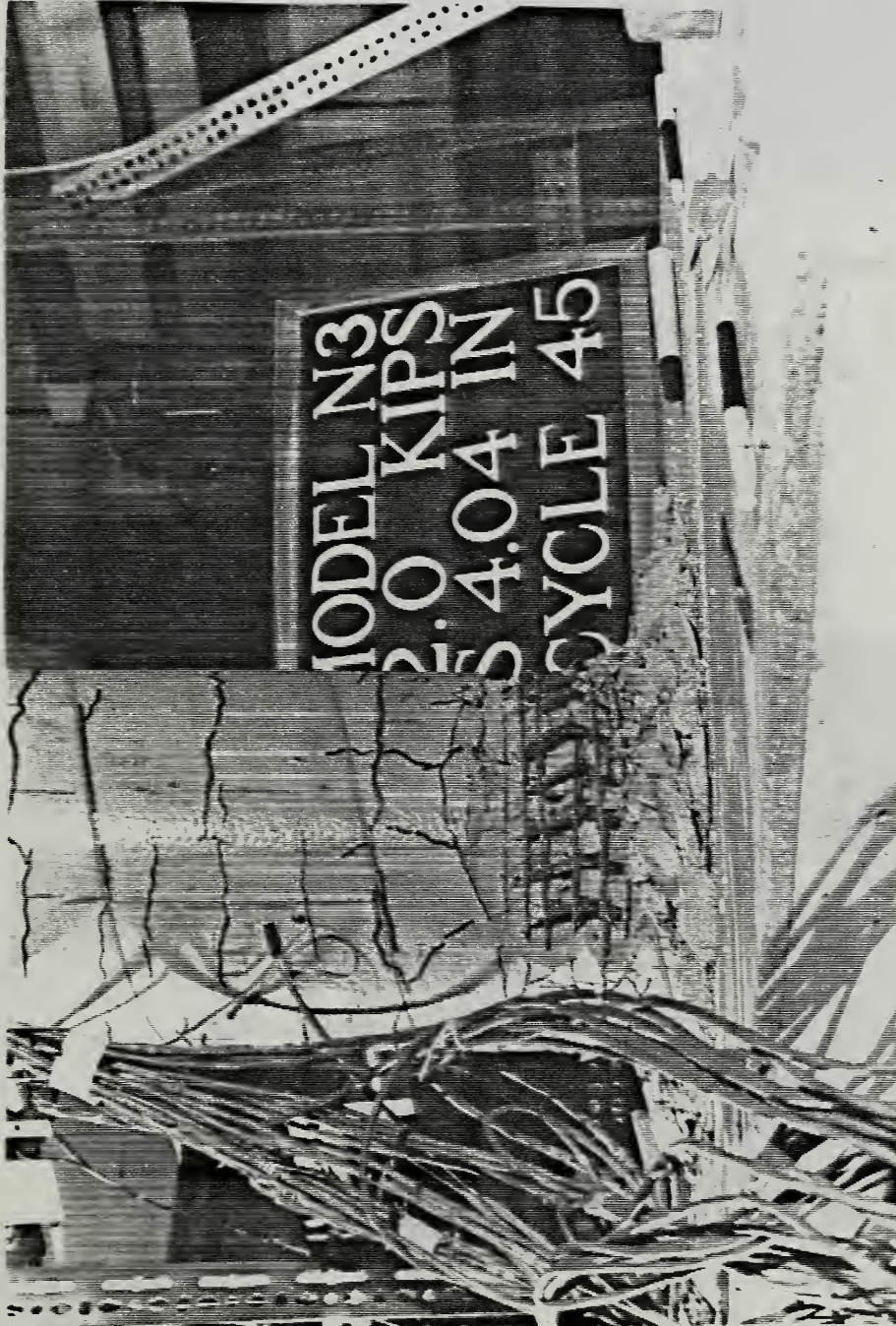


Model N3, DF = 4, Cycle 6
Fig. 5.20



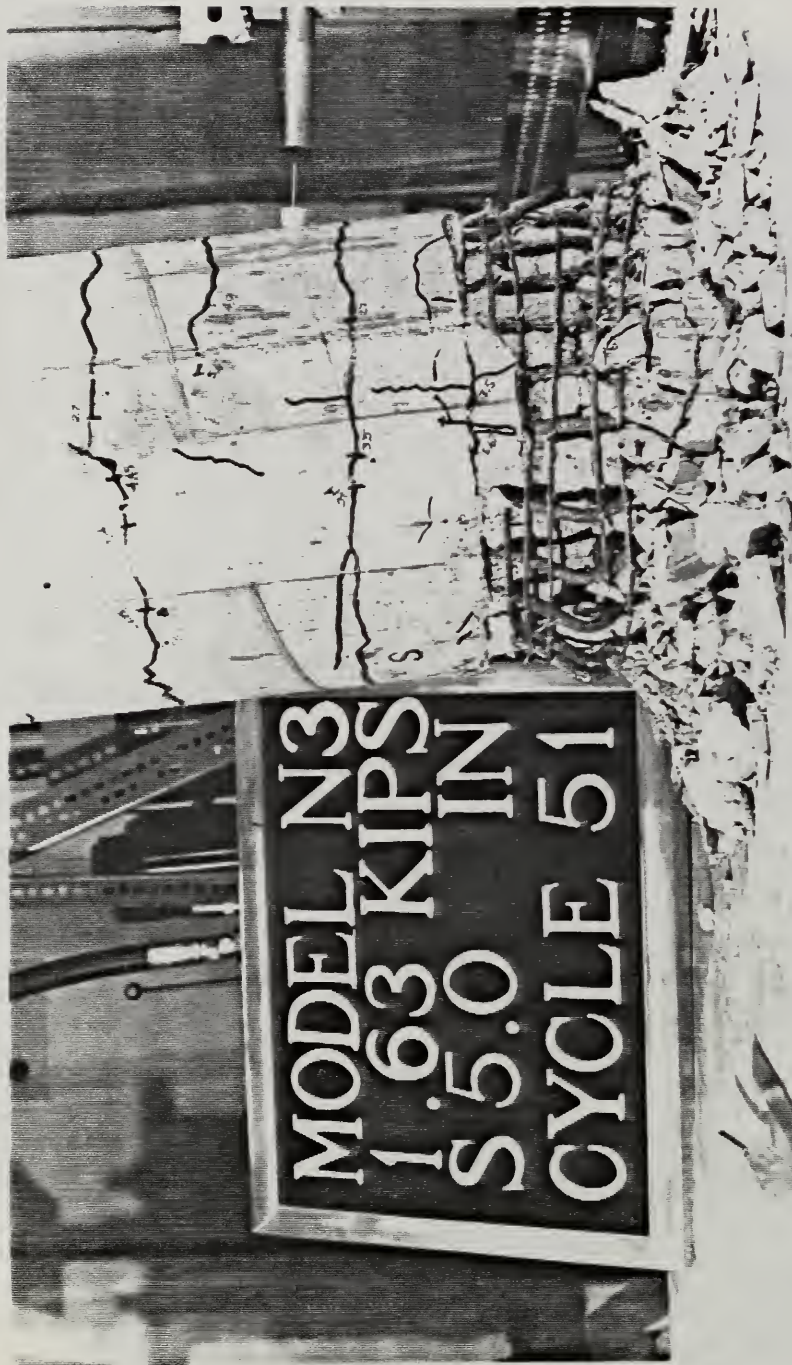
Model N3, DF = 4, Cycle 7

Fig. 5.21



Model N3, DF = 4, Cycle 10

Fig. 5.22



Model N3, DF = 5, Cycle 16

Fig. 5.23

LOADING HISTORY FOR MODEL N4

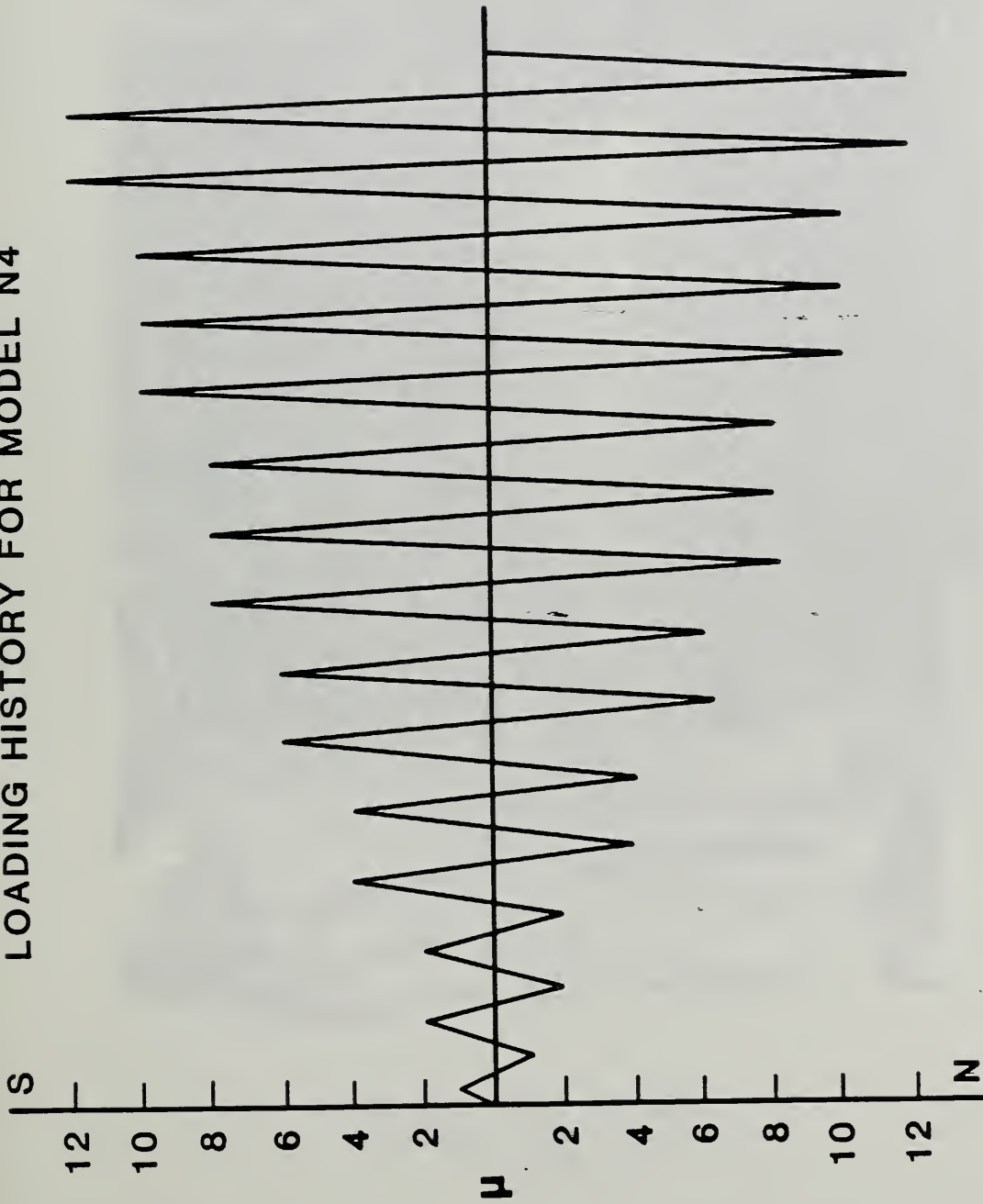


Fig. 5.24



Model N4, DF = 1, Cycle 1

Fig. 5.25



Model N4, DF = 2, Cycle 2

Fig. 5.26

5.5.4 DUCTILITY FACTOR = 4, CYCLES 4 & 5

Minor crushing of the base on the south side occurred. Additional flexure cracks appeared near the base of the column. Some of the cracks began to proceed downwards at an angle of about 20° - 30° as they propagated towards the east and west sides of the column as shown in Fig. 5.27. Most of the cracking occurred during the fourth cycle.

5.5.5 DUCTILITY FACTOR = 6, CYCLES 6 & 7

Spalling on the south side of the column occurred with a piece about 1-1/2 X 1-1/2 in. (3.8 X 3.8 cm) falling off. The spalling did not expose the spiral at this stage. Separation of the column from the base was about 0.04 - 0.08 in (1 - 2 mm). Few additional cracks formed at this load stage.

5.5.6 DUCTILITY FACTOR = 8, CYCLES 8, 9, & 10

Spalling on the north began during the 8th cycle. The spall area on the south was about 9 X 2.5 in. (22.9 x 6.3 cm). The spall area on the north was about 7-1/2 X 1-1/2 in. (19.1 X 3.8 cm) at the end of the 10th cycle. No additional cracks were observed. No lateral load drop was noted after the 9th cycle. However, a third cycle at DF = 8 was carried out since the counterpart of this model, N1, was cycled three times at DF = 8. The objective in doing this was to precisely replicate loading history in an effort to isolate possible differences in energy absorption performance between the two columns.

5.5.7 DUCTILITY FACTOR = 10, CYCLES 11, 12 & 13

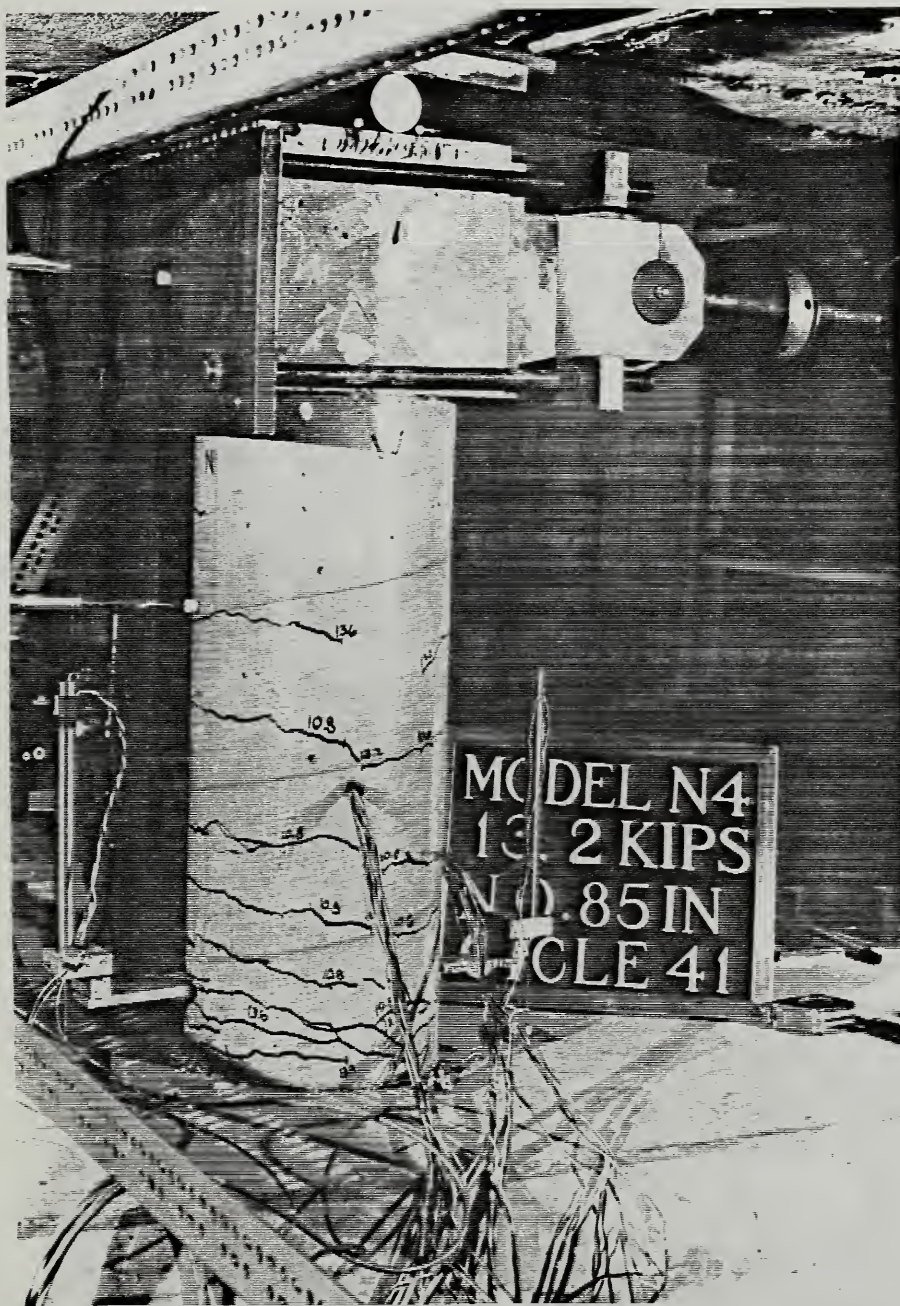
CYCLE 11: Yielding of spirals at the column-base joint was observed during this cycle. Four buckled bars on the south side were also noted.

CYCLE 12: A spiral on the north side approximately 0.5 in. (12.7 mm) above the base fractured. A total of 8 longitudinal bars and 7 longitudinal bars on the north and south sides, respectively, had buckled at this load stage as shown in Fig. 5.28.

CYCLE 13: A longitudinal bar on the north side fractured while two on the south side fractured. The peak lateral load was reduced to $0.56 P_y$ in this cycle.

5.5.8 DUCTILITY FACTOR = 12, CYCLES 14 & 15

During the 14th cycle, three additional longitudinal bars fractured on the north which increased the total number of fractured bars on the north to four. An additional longitudinal bar on the south fractured during the 15th cycle. These fractured bars are shown in Fig. 5.29.



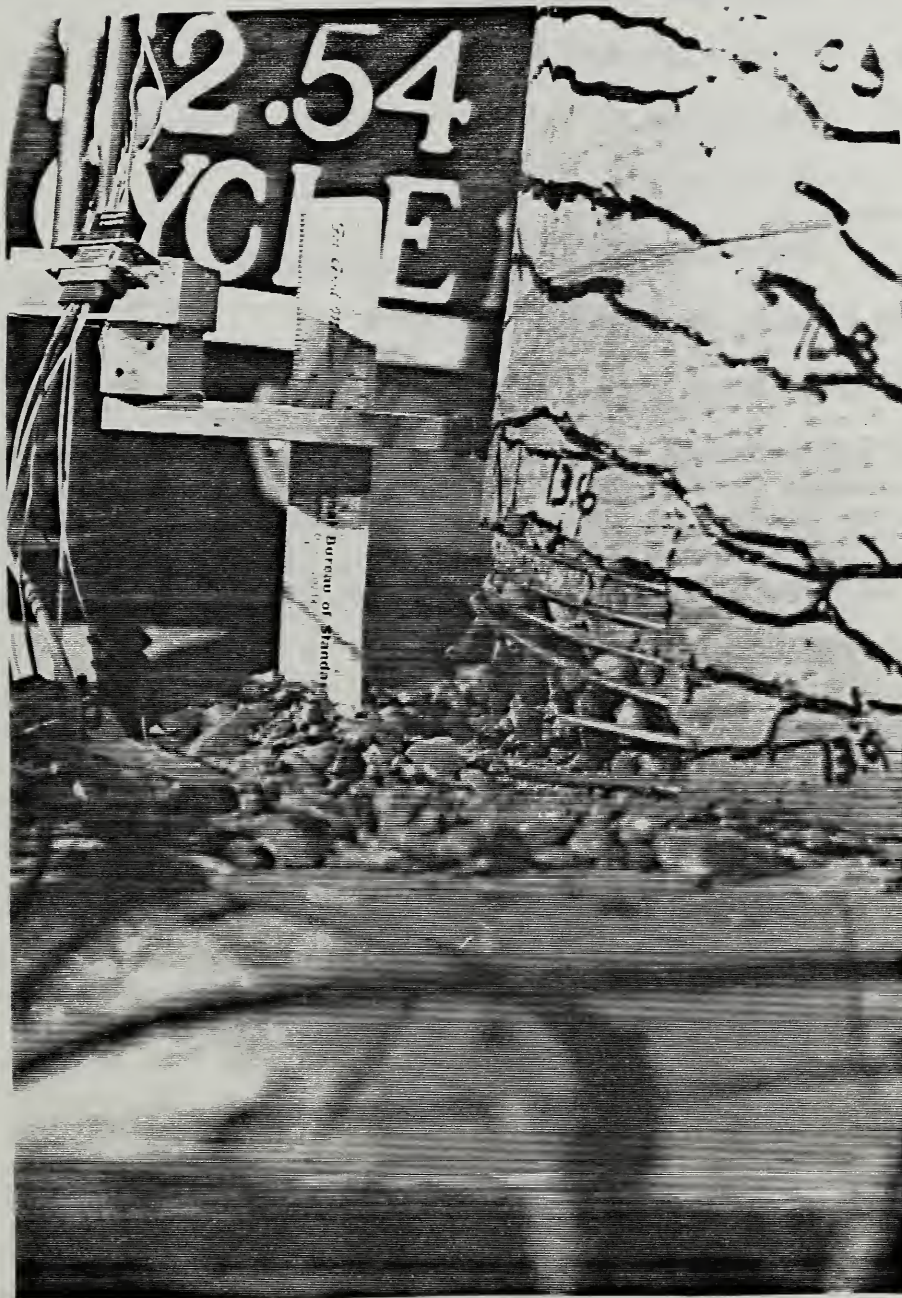
Model N4, DF = 4, Cycle 4

Fig. 5.27



Model N4, DF = 10, Cycle 12

Fig. 5.28



Model N4, DF = 12, Cycle 15

Fig. 5.29

5.6 Model N5

5.6.1 MODEL PROPERTIES

$$f'_c = 3534 \text{ psi (24.38 MPa)}$$

$$P_e = 53.75 \text{ kips (239.19 kN)}$$

$$M_u \text{ (experimental)} = 46.61 \text{ ft-kip (63.23 kN-m)}$$

$$P_h = 11.15 \text{ kips (49.61 kN)}$$

$$\Delta_y \text{ (experimental)} = 0.19 \text{ in. (4.83 mm)}$$

The loading history is shown in Fig. 5.30.

5.6.2 DUCTILITY FACTOR = 1, CYCLE 1

Hairline flexure cracks, six on the north side and five on the south side, appeared at this load stage. Two shear cracks were also observed on the south side of the column. The cracks reached a height of 1' - 4 1/2" (41.9 cm) on the south side and 1' - 2" (35.6 cm) on the north side of the column. The crack pattern on the south is shown in Fig. 5.31.

5.6.3 DUCTILITY FACTOR = 2, CYCLES 2 & 3

The flexure cracks began to proceed downwards at angles of about 20° - 30° as they propagated to the east and west sides of the columns. Additional flexure cracks appeared up to a height of 1' - 8" (50.8 cm) on the south side of the column.

5.6.4 DUCTILITY FACTOR = 4, CYCLES 4 & 5

Minor crushing occurred at the base of the column on both the north and south sides. Some additional shear cracks formed on the east and west sides of the column. The crack pattern for this load stage is shown in Fig. 5.32.

5.6.5 DUCTILITY FACTOR = 6, CYCLES 6 & 7

More crushing was observed at the base of the column on both the north and south sides. Additional shear and flexure crack formation were also noted. Some of the crack widths were about 0.08 in. (2 mm). The south side spalled off on the 7th cycle with the spall area approximately equal to 5 X 1-1/2 in. (12.7 X 3.8 cm).

5.6.6 DUCTILITY FACTOR = 8, CYCLES 8 & 9

Some additional flexure cracks were noted on the north side of the column. Some new shear cracks were also observed on the east and west sides of the column. The north side of the column began to spall off with the area of spall measured approximately 6 X 2 in. (15.2 X 5.1 cm).

LOADING HISTORY FOR MODEL N5

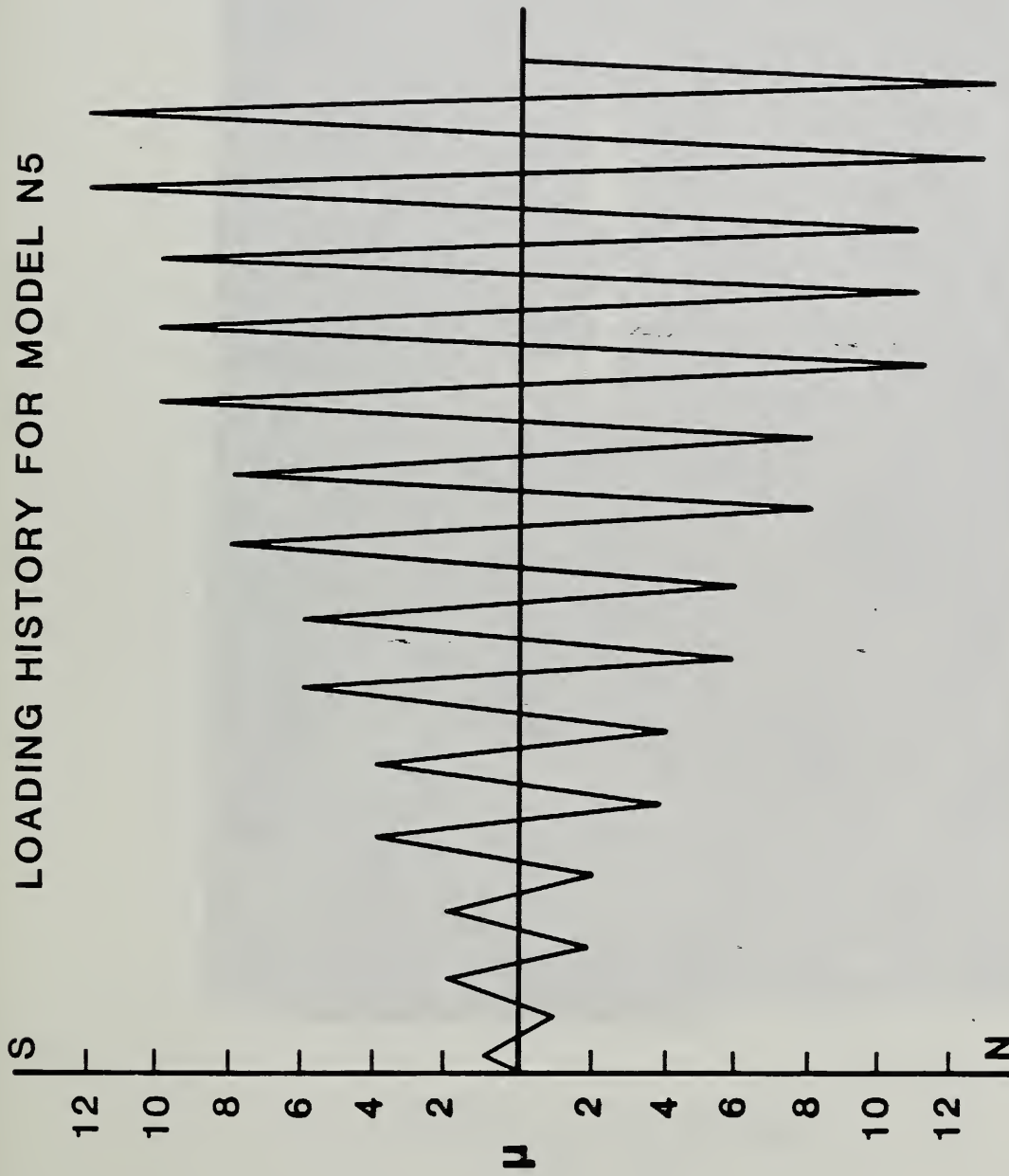
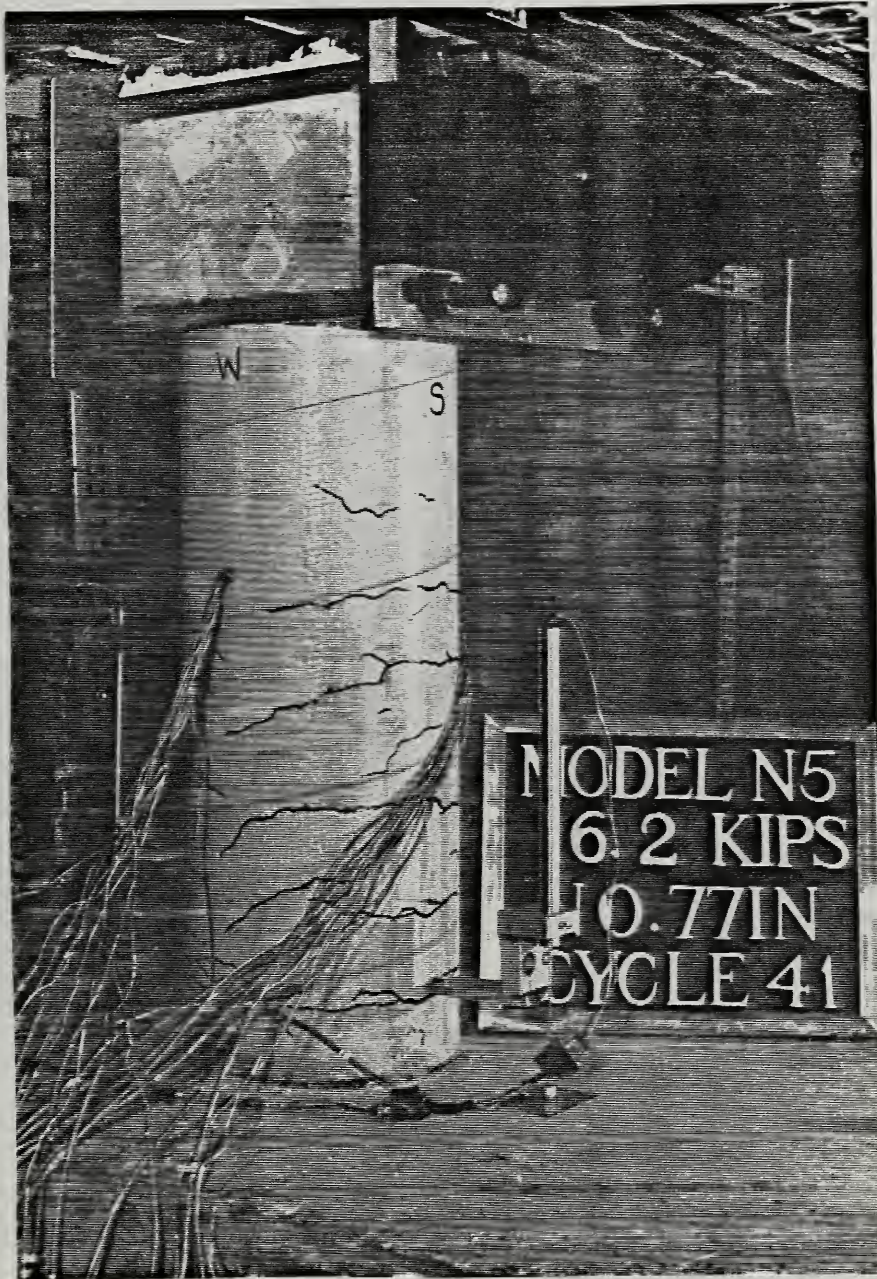


Fig. 5.30



Model N5, DF = 1, Cycle 1

Fig. 5.31



Model N5, DF = 4, Cycle 4

Fig. 5.32

5.6.7 DUCTILITY FACTOR = 10, CYCLES 10, 11 & 12

CYCLE 10: A succession of cracking sounds was heard like that which would be produced by three bars fracturing although no visual verification was possible. The spall areas on the north and south sides of the column were 8 X 2 in. (20.3 x 5.1 cm) and 6 X 2 in. (15.2 X 5.1 cm) respectively. Two longitudinal bars were observed to have buckled on the south side of the column. The spiral at the column-base joint on the south side and the three spirals immediately above appeared to have yielded.

CYCLE 11: A spiral on the south side of the column at about 2 in. (5.1 cm) above the base fractured as indicated in Fig. 5.33. One bar on the northeast side of the column was noted to have fractured, probably in the previous cycle. Four and six longitudinal bars on the south and north sides of the column, respectively, had buckled. Four spirals on the north side of the column appeared to have yielded. The spall area on the south was about 9 X 2 in. (22.9 X 5.1 cm) with the spall area on the north unchanged.

CYCLE 12: The spall area on the south increased to about 9 X 3 in. (22.9 X 7.6 cm). A spiral on the northwest side of the column about 3/8 in. (9.5 mm) above the base fractured. The fractured spiral is shown in Fig. 5.34.

5.6.8 DUCTILITY FACTOR = 12, CYCLES 13 & 14

Four longitudinal bars fractured in succession on the north side of the column making a total of five fractured bars on the north side. Three longitudinal bars broke in succession on the south and two more a little later on. A longitudinal bar on the south was observed to have fractured, probably one of the snaps heard earlier. A total of 6 fractured bars were observed on the south side. The spall area and the fractured bars on the south side are shown in Fig. 5.35. The peak lateral load in the 13th cycle was reduced to approximately 0.60 P_y .

5.7 Model N6

5.7.1 MODEL PROPERTIES

$$f'_c = 3367 \text{ psi (23.22 MPa)}$$

$$P_e = 26.87 \text{ kips (119.53 kN)}$$

$$M_u \text{ (experimental)} = 36.87 \text{ ft-kip (49.99 kN-m)}$$

$$P_h = 5.4 \text{ kips (24.0 kN)}$$

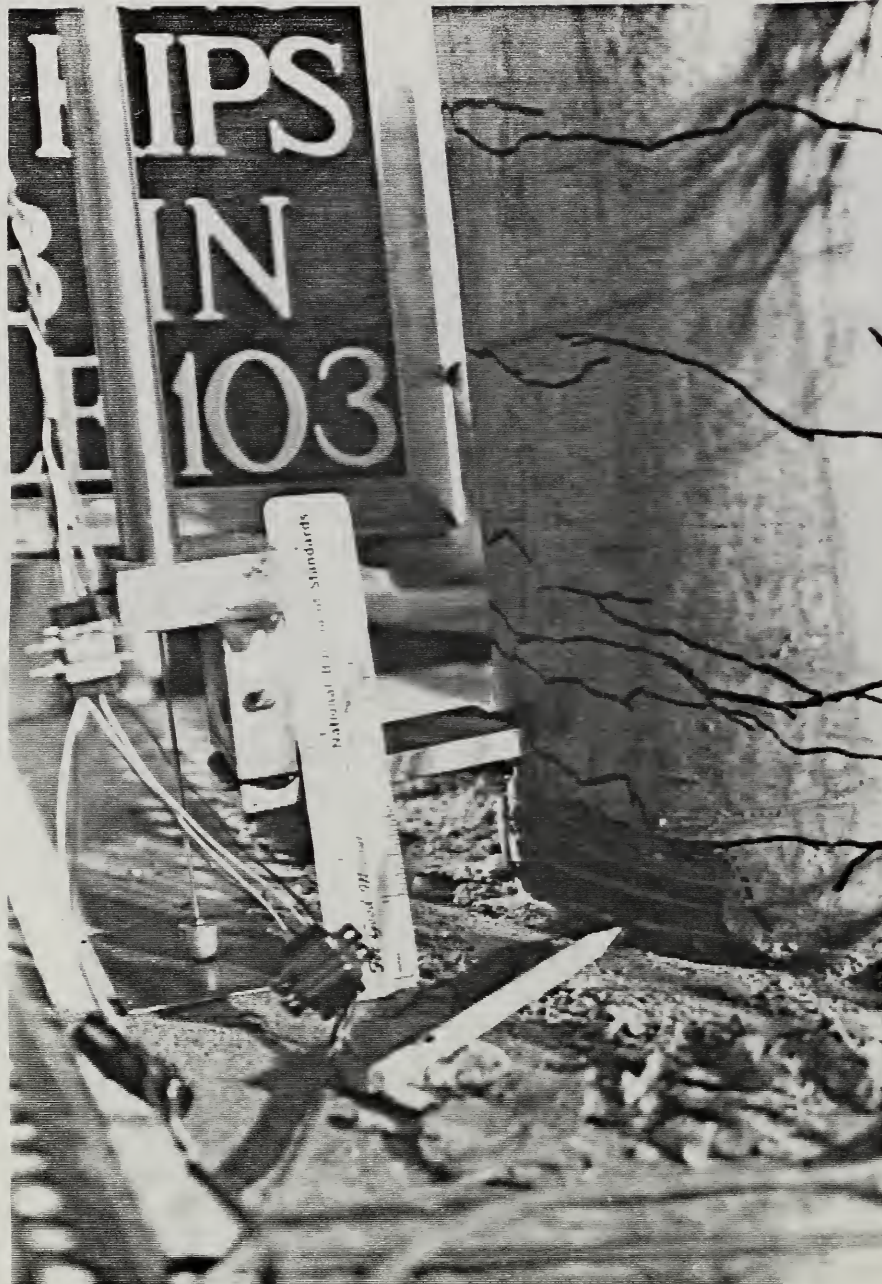
$$\Delta_y \text{ (experimental)} = 0.66 \text{ in. (16.8 mm)}$$

The loading history is shown in Fig. 5.36.



Model N5, DF = 10, Cycle 11

Fig. 5.33



Model N5, DF = 10, Cycle 12

Fig. 5.34



Model N5, DF = 12, Cycle 13
Fig. 5.35

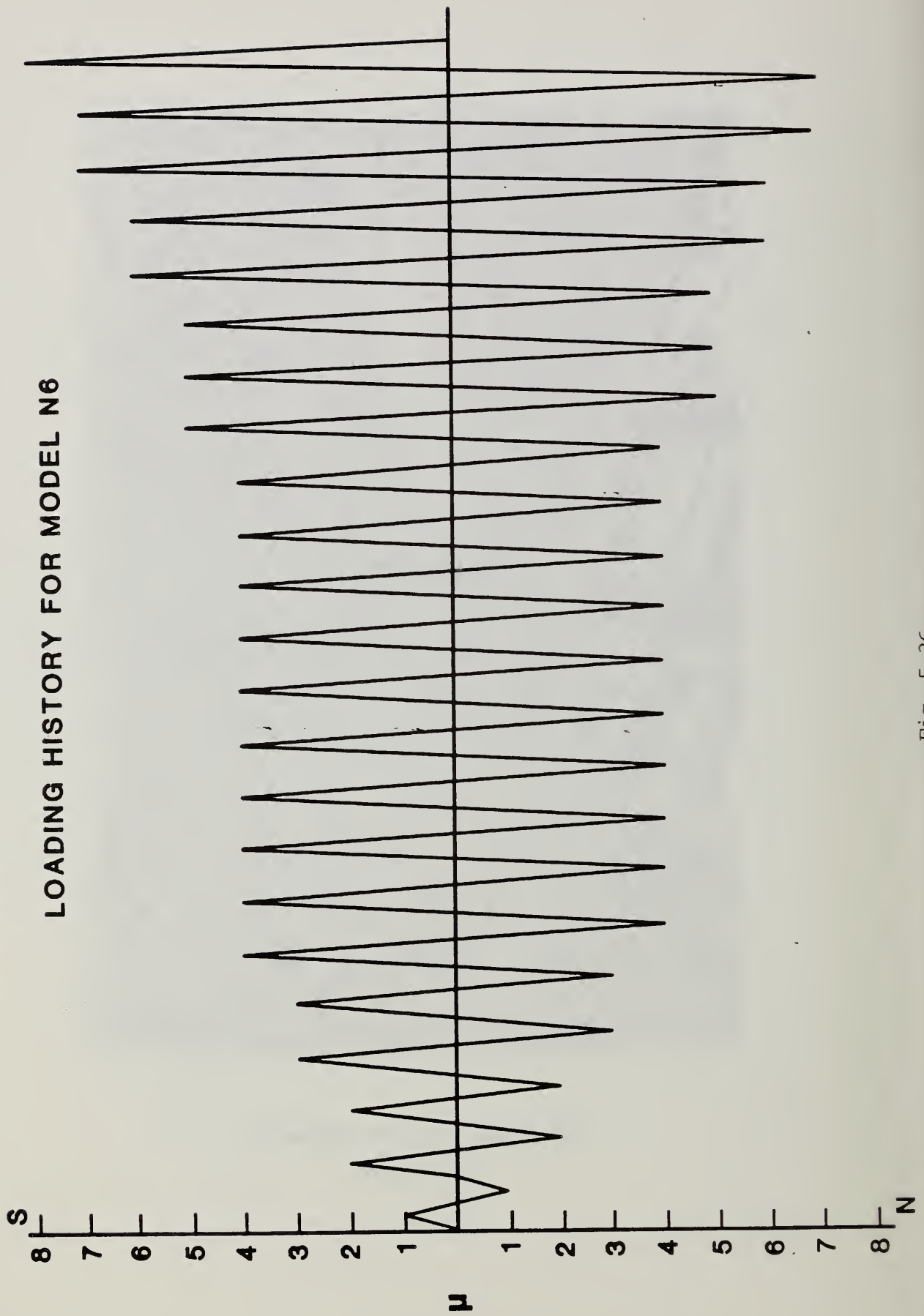


Fig. 5.36

5.7.2 DUCTILITY FACTOR = 1, CYCLE 1

Hairline flexure cracks were observed at a lateral load of 2.25 kips (10 kN) on the first excursion south and at a load of 2.64 kips (11.7 kN) on the first excursion north. These loads are 41.7 % and 48.9 % of the calculated yield load for the lateral load to the south and north respectively. Cracks formed up to a height of 2'-0" (61 cm) on the north side and up to 2'-2" (66 cm) on the south side. The south side of the column is shown in Fig. 5.37.

5.7.3 DUCTILITY FACTOR = 2, CYCLES 2 & 3

More flexure cracks appeared on both the north and south sides of the column. The existing cracks propagated to the east and west sides of the column as shown in Fig. 5.38. A crack was noted at the column-base joint. Very minor crushing of the column at the base on the south side was also noted.

5.7.4 DUCTILITY FACTOR = 3, CYCLES 4 & 5

Minor flaking of the south side began at a lateral load of 5.8 kips (25.8 kN) and at a lateral load of 6.6 kips (29.4 kN) on the north side. Both occurrences were in the 4th cycle. Two additional flexure cracks were observed on the north side of the column. The width of cracks ranged from 0.08 in to 0.12 in. (2 - 3 mm). The column appeared to be hinging at approximately 3 in. (7.6 cm) above the base on the north side.

5.7.5 DUCTILITY FACTOR = 4, CYCLES 6 - 15

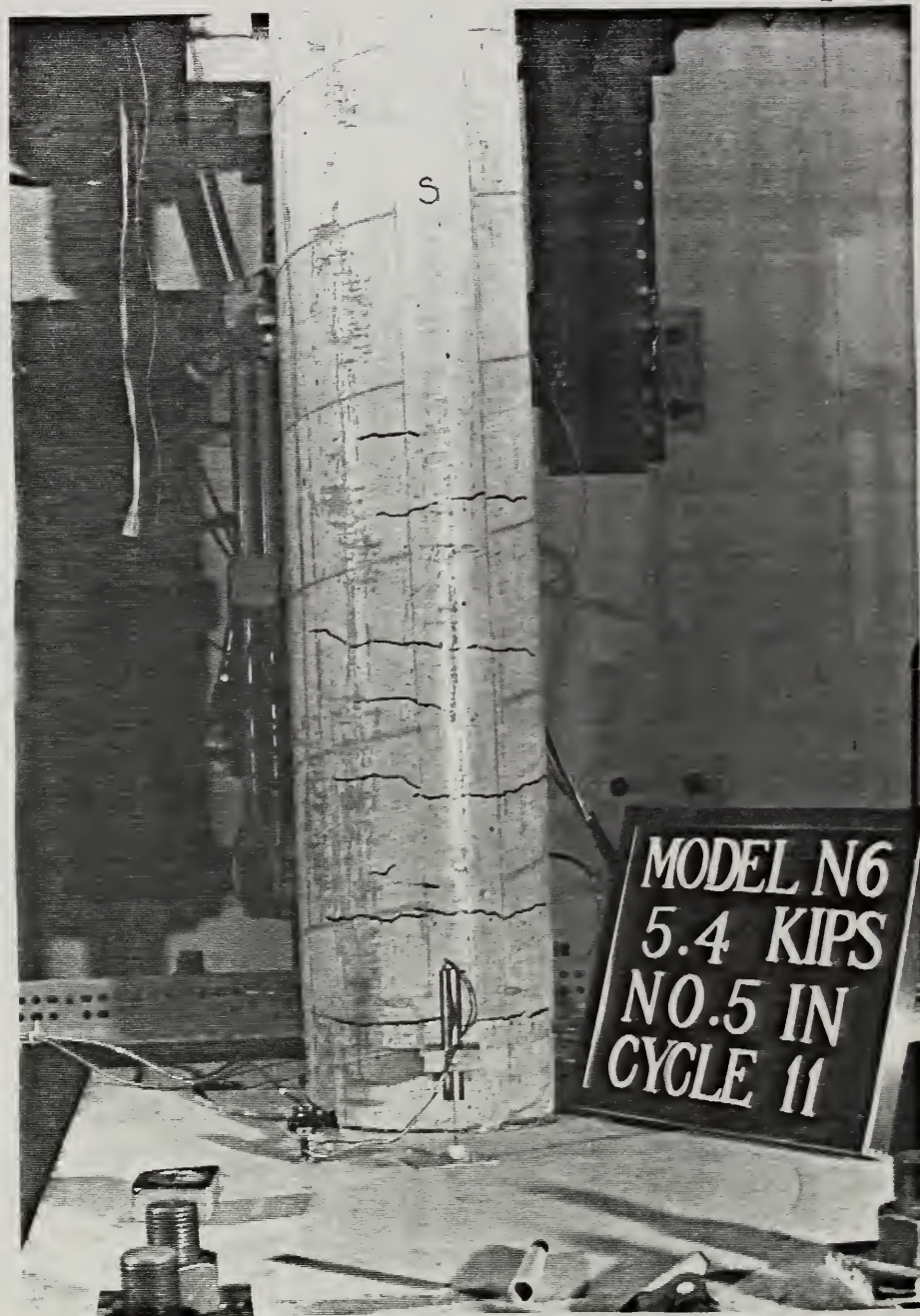
CYCLES 6 - 9: Formation of some shear cracks was observed on the east side of the column. Increased flaking on both the north and south sides of the column occurred. This is shown in Fig. 5.39. A piece of concrete cover about 2 X 2 in. (5.1 X 5.1 cm) spalled off on the south side of the column during the 6th cycle. Maximum crack width measured was approximately 0.25 in. (6.3 mm).

CYCLES 10 -12

Spalling on both the north and south sides continued. Spall areas were about 8 X 2 in. (20.3 X 5.1 cm) on the south and 5 X 2 in. (12.7 X 5.1 cm) on the north. The spalling exposed the spiral on the north side of the column. The LVDT measuring the rotation on the south came off along with the cover concrete when it spalled during the 12th cycle. The spiral on the south was exposed when this occurred and two of the spirals, one about 2 in. (5.1 cm) above the base and the one above that, showed signs of straightening out between the longitudinal bars.

CYCLE 13: One longitudinal bar on the south was noted to have buckled. A third spiral on the south began to straighten out between the vertical bars. Additional cover concrete on the north side appeared to be ready to spall off. The concrete core seemed to be intact (i.e. no cavities in the core were noted).

CYCLE 14: Two longitudinal bars on the south side were noted to have buckled. The spiral 2 in. (5.1 cm) above the base on the south fractured



Model N6, DF = 1, Cycle 1

Fig. 5.37



Model N6, DF = 2, Cycle 2

Fig. 5.38



Model N6, DF = 4, Cycle 6

Fig. 5.39

on the excursion south. The spiral 2.75 in. (7.0 cm) above the base on the north fractured on the excursion north. Three longitudinal bars on the north side could be seen to have buckled. In general, the buckling of bars proceeded in accordance with their distances from the column E-W centerline. That is to say, the southern most longitudinal bar which lies on the N-S centerline typically buckled first following a sufficiently large excursion to the south. Subsequently, the two adjacent bars to either side would buckle next. Fig. 5.40 shows the fractured and the buckled bars. The spall areas on the south was 8 X 4.5 in. (20.3 X 11.4 cm) and 7 X 4.5 in. (17.8 X 11.4 cm) on the north.

CYCLE 15: Three additional longitudinal bars on the south buckled. The spiral below the previously fractured spiral on the south fractured. The location of the second fracture was directly below that of the first fracture. Five longitudinal bars on the north had buckled by this load stage. Spall areas were 9 X 4.75 for the south side in. (22.9 X 12.1 cm) and 8 X 4.5 in. (20.3 X 12.1 cm) on the north side. A cavity on the south side was beginning to form in the concrete core.

5.7.6 DUCTILITY FACTOR = 5, CYCLES 16 - 18

More spalling occurred with the spall areas increasing to 12 X 4.5 in. (30.5 X 11.4 cm) on the south side and 11 X 5 in. (27.9 X 12.7 cm) on the north side. Eight longitudinal bars each on the south and the north sides had buckled. The extent of the spall area and the buckling of the bars is shown in Fig. 5.41. In the 17th cycle, the peak lateral load dropped to approximately 0.50 P_y . This indicated, for all practical purposes, the useful end of the test.

5.7.7 DUCTILITY FACTOR = 6, CYCLES 19 & 20

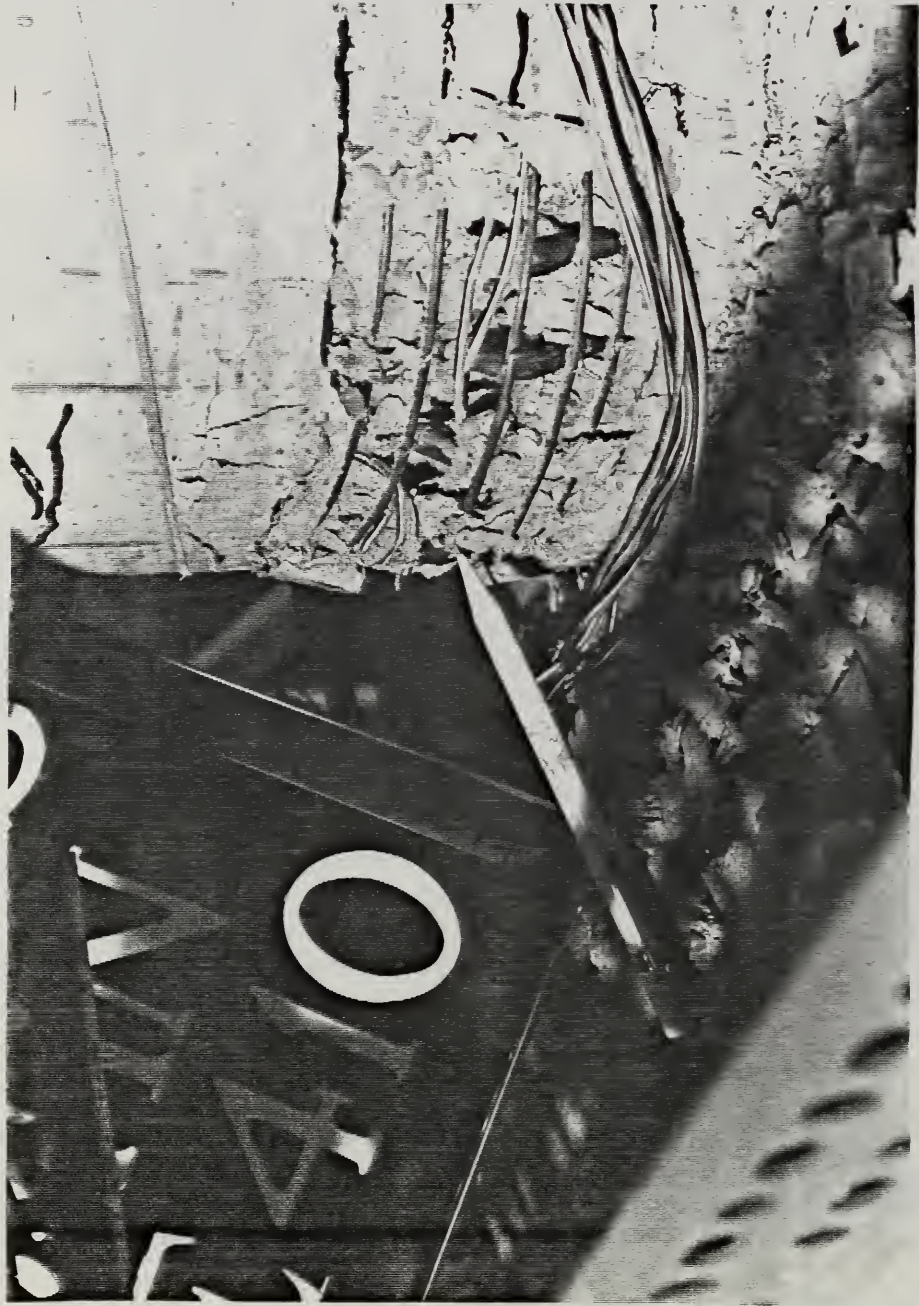
Two longitudinal bars fractured during the 19th cycle on the south side as depicted in Fig. 5.42. A longitudinal bar on the north side fractured during the 20th cycle, and two other bars on the north appeared to be necking down. The cover concrete around the base of the column had essentially spalled off entirely up to a height of about 5 in. (12.7 cm)

5.7.8 DUCTILITY FACTOR = 7, CYCLES 21 & 22

Three additional bars on the north fractured during the 21st cycle. Hinging appeared to have occurred at about 2 in. (5.1 cm) above the base. With the exception of two bars, one on the east and the other on the west sides, all the longitudinal bars had either fractured or buckled at this load stage.

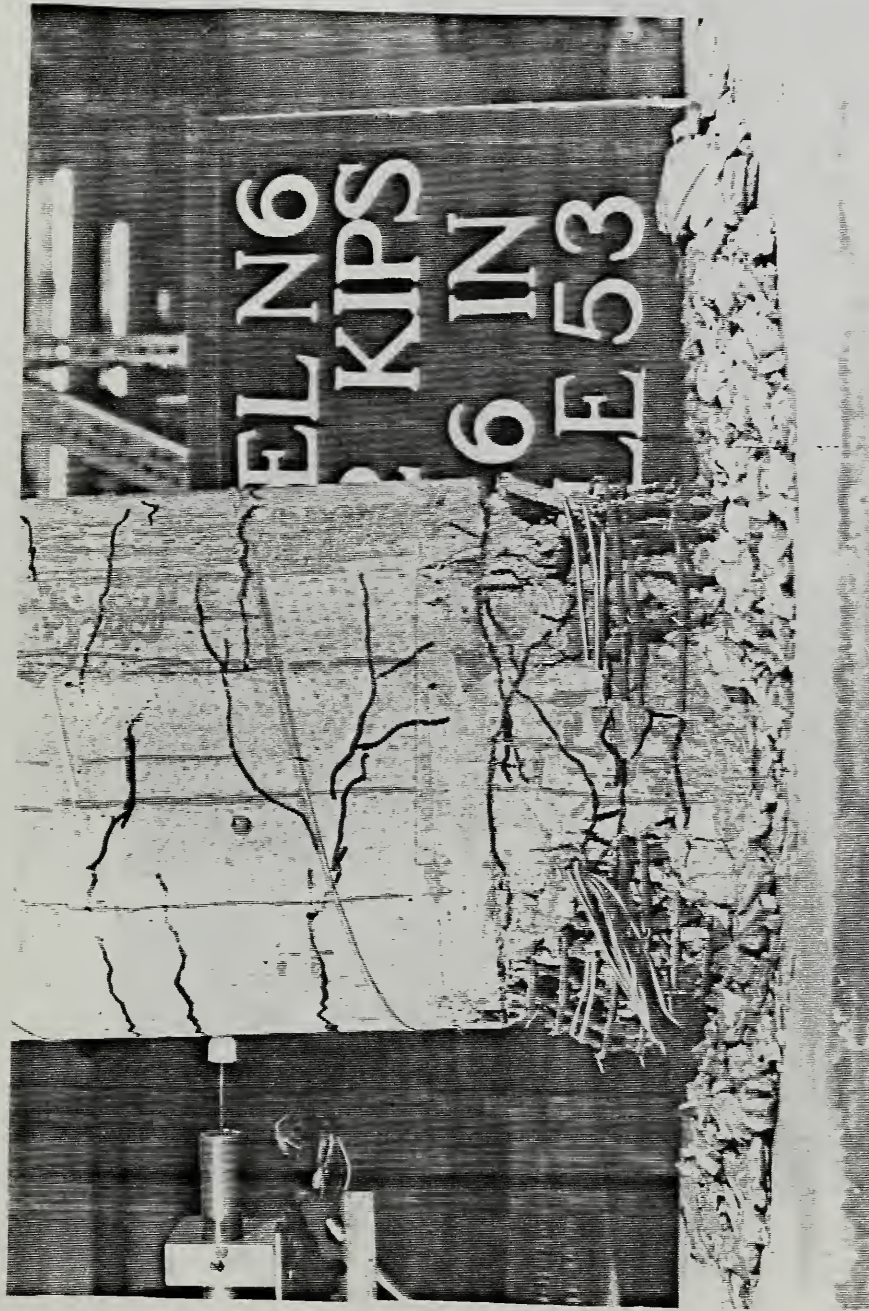
5.7.9 DUCTILITY FACTOR = 8, CYCLE 23

Only one excursion (half a cycle) was made at this ductility level before the test was stopped. An additional longitudinal bar on the north fractured making a total of 5 fractured bars on the north side. Fig. 5.43 shows the north side of the column and Fig. 5.44 shows the south side of the column at the end of the test.



Model N6, DF = 4, Cycle 14

Fig. 5.40



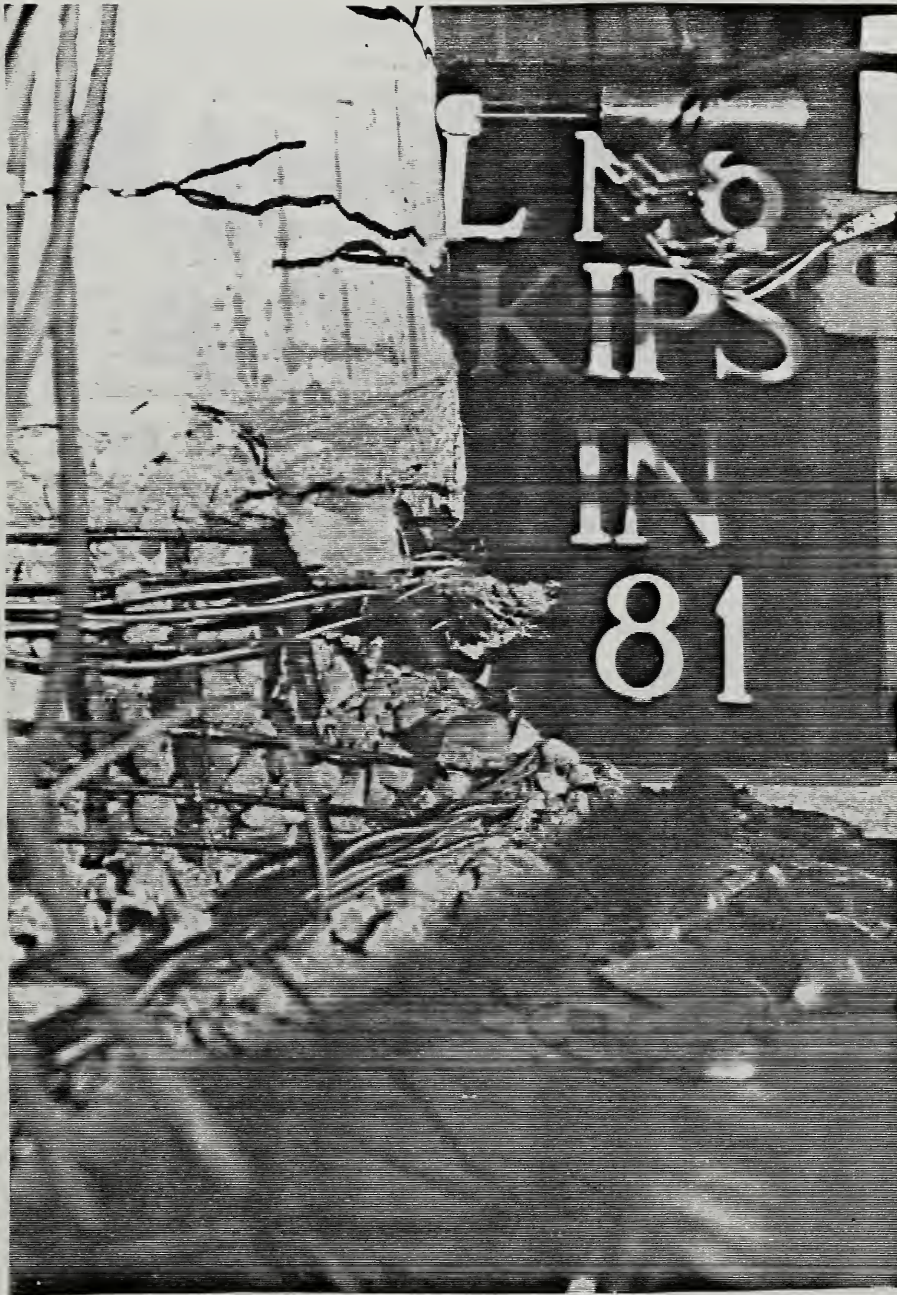
Model N6, DF = 5, Cycle 18

Fig. 5.41



Model N6, DF = 6, Cycle 20

Fig. 5.42



Model N6, DF = 8, Cycle 23

Fig. 5.43



Model N6, DF = 8, Cycle 23

Fig. 5.44

6.0 DISCUSSION OF RESULTS

6.1 Column Deflection

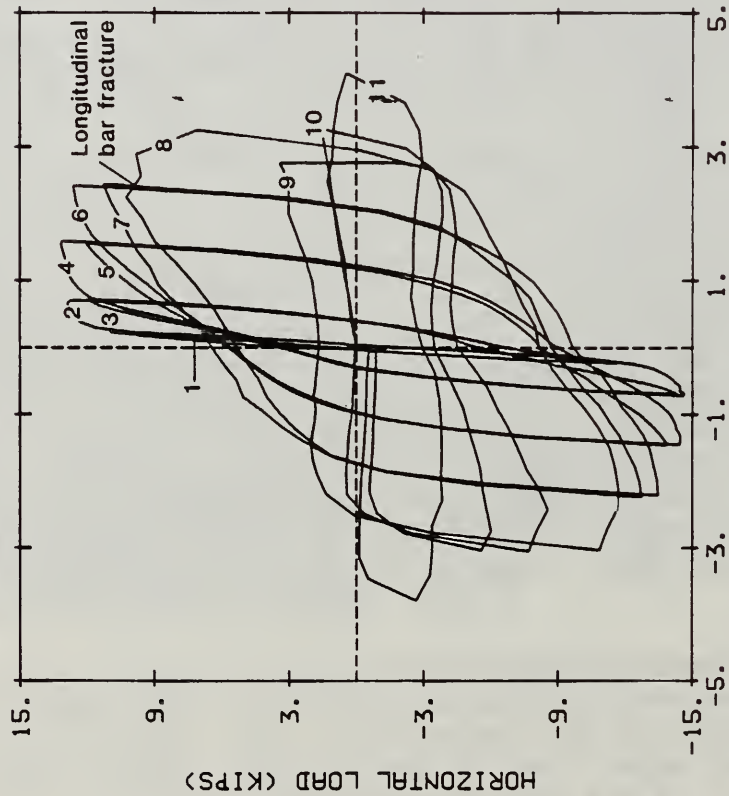
The best measure of column performance in cyclic load tests is a plot of the lateral load as a function of maximum lateral deflection. For the cantilevered bridge column tests conducted in this experimental program the lateral load was applied at the top of the column, as would be the case when inertial loads from the highway superstructure are imposed in a real earthquake. Column lateral displacements were measured at several locations along the height of the column (see Figs 4.13-4.14), and thus many load-deflection histories are available for study. To expedite comparison of performance between different column tests, we will use only the maximum lateral deflection record, corresponding to the displacement at the point of application of the lateral load. Hereafter, the phrase "load-deflection curve" or "load-deflection history" will refer to experimentally obtained plots of these loads and displacements during the conduct of cyclic load tests.

The load deflection curves for all the models tested in this study exhibited stable behavior until fracture of either the spiral or longitudinal bars occurred as indicated in Figs. 6.1 to 6.6. In these figures, the overall performance of the column was measured by plotting the lateral displacement at the top of the column as a function of the lateral load. The spiral fractured in all the models except for model N1. The spiral in N1 slid upward along the longitudinal bars thereby relieving the stress in the spiral and leaving it intact. Fracture of a longitudinal bar was marked by a significant drop in lateral load. This type of behavior is visible in Figs. 6.1 - 6.6 as a vertical drop on the load-deflection plots near the point of maximum lateral load for a given cycle.

The displacement ductilities at ultimate column failure are given in Table 6.1. The column was considered to have "failed" (reached ultimate) when the moment, including the P - Δ effect, resisted by the model was smaller than the greater of 80 % of the maximum (north or south) moment measured during the first cycle to $\mu = +2$. This definition of the ultimate failure was the same as that used in a study by Zahn et. al. [30]. Ultimate failure as defined by the Japanese researchers in section 2.2.2, results in the same displacement ductilities as those obtained using Zahn's definition. Displacement ductilities obtained for the shear models (L/d = 3) were 10 and 12 for models N4 and N5 respectively as compared with 8 and 10 for the shear models constructed from microconcrete, N1 and N2 respectively. Displacement ductility for the flexure model (L/D = 6) constructed from ready-mix concrete was 5 as compared with 4 for the microconcrete model.

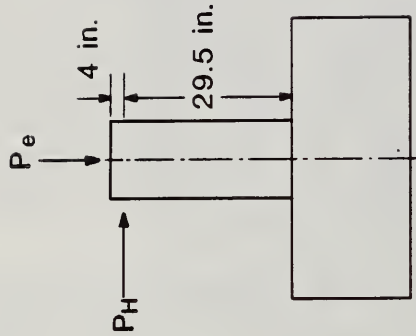
The measured yield displacements for the microconcrete models with the lower axial load were much greater than those for the models constructed from ready-mix concrete with the lower axial load. Yield displacements of models with the higher axial load, N2 and N5, were, however, the same. The displacement profiles of the models are shown in which 6.7 - 6.12.

- 1 - 1 delta y, cycle 1
- 2 - 2 delta y, cycle 1
- 3 - 2 delta y, cycle 2
- 4 - 4 delta y, cycle 1
- 5 - 4 delta y, cycle 2
- 6 - 6 delta y, cycle 1
- 7 - 6 delta y, cycle 2
- 8 - 8 delta y, cycle 1
- 9 - 8 delta y, cycle 2
- 10 - 8 delta y, cycle 3
- 11 - 10 delta y, cycle 1



COLUMN DISPLACEMENT (INCHES)

LOAD CYCLES FOR MODEL N1



$$P_e = 0.1 f'_c A_g = 26.87 \text{ kips}$$

- $A_g = 75.43 \text{ in}^2$
- $A_s = 1.5 \text{ in}^2$
- $\rho_t = 0.0199$
- $\rho_s = 0.01452$
- Spiral = 0.120 in.
- Bars = 0.276 in.
- 1 in. = 25.4 mm

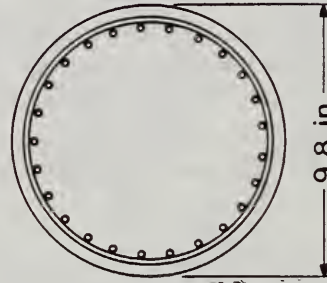
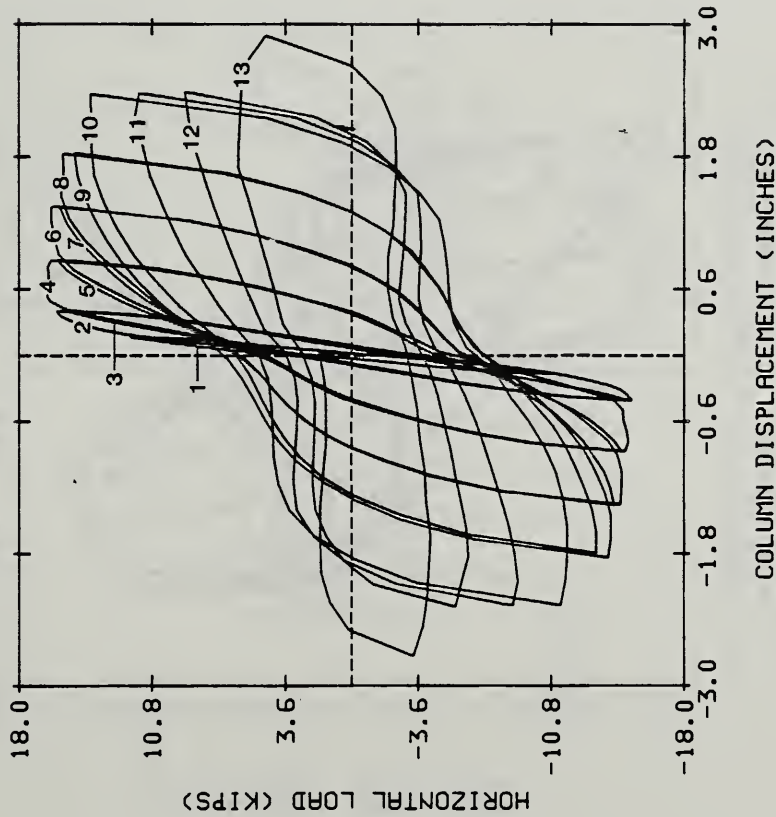


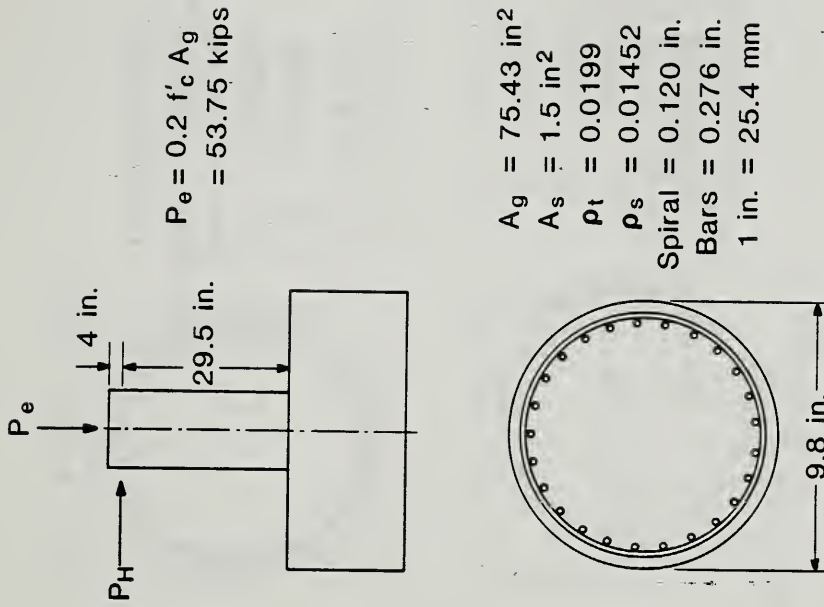
FIGURE 6.1

- 1 - 1 delta y, cycle 1
- 2 - 2 delta y, cycle 1
- 3 - 2 delta y, cycle 2
- 4 - 4 delta y, cycle 1
- 5 - 4 delta y, cycle 2
- 6 - 6 delta y, cycle 1
- 7 - 6 delta y, cycle 2
- 8 - 8 delta y, cycle 1
- 9 - 8 delta y, cycle 2
- 10 - 10 delta y, cycle 1
- 11 - 10 delta y, cycle 2
- 12 - 10 delta y, cycle 3
- 13 - 12 delta y, cycle 1

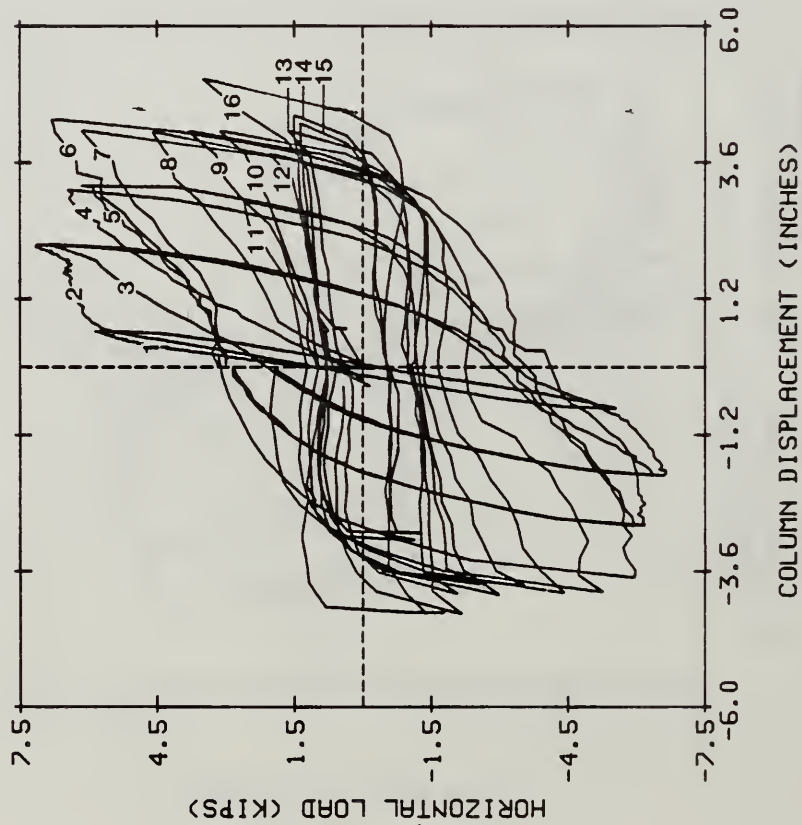


LOAD CYCLES FOR MODEL N2

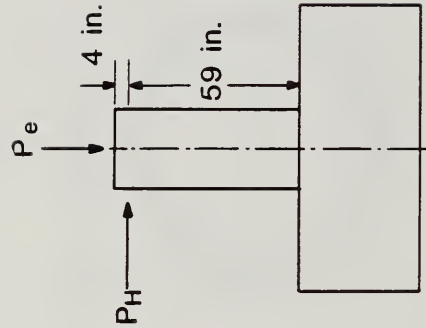
FIGURE 6.2



- 1 - 1 delta y, cycle 1
- 2 - 2 delta y, cycle 1
- 3 - 2 delta y, cycle 2
- 4 - 3 delta y, cycle 1
- 5 - 3 delta y, cycle 2
- 6 - 4 delta y, cycle 1
- 7 - 4 delta y, cycle 2
- 8 - 4 delta y, cycle 3
- 9 - 4 delta y, cycle 4
- 10 - 4 delta y, cycle 5
- 11 - 4 delta y, cycle 6
- 12 - 4 delta y, cycle 7
- 13 - 4 delta y, cycle 8
- 14 - 4 delta y, cycle 9
- 15 - 4 delta y, cycle 10
- 16 - 5 delta y, cycle 1



LOAD CYCLES FOR MODEL N3



$$P_e = 0.1 f'_c A_g$$

$$= 26.87 \text{ kips}$$

- $A_g = 75.43 \text{ in}^2$
- $A_s = 1.5 \text{ in}^2$
- $\rho_t = 0.0199$
- $\rho_s = 0.00694$
- Spiral = 0.106 in.
- Bars = 0.276 in.
- 1 in. = 25.4 mm

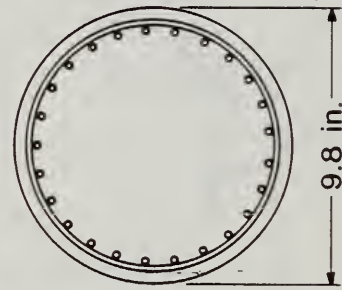
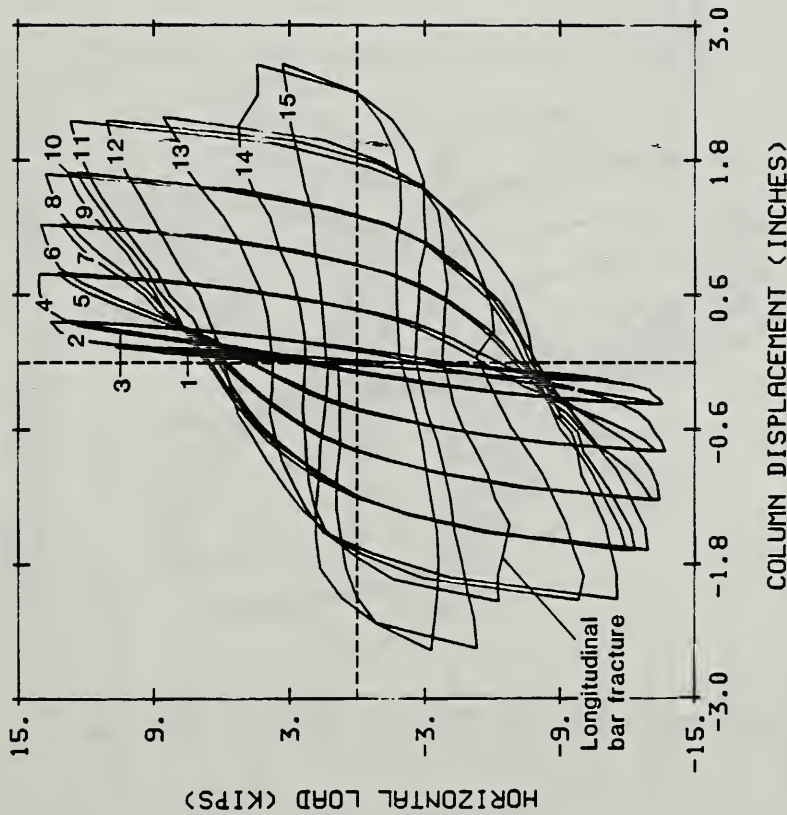


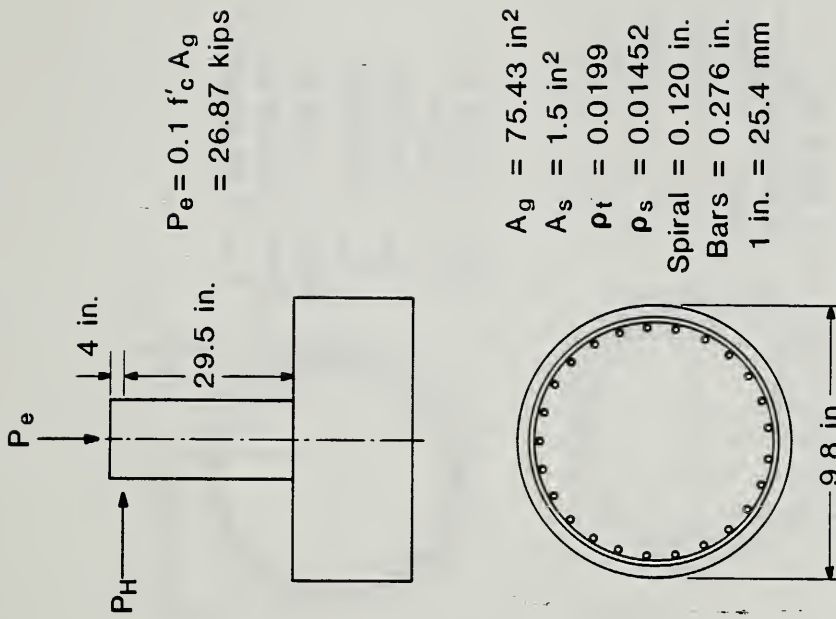
FIGURE 6.3

- 1 - 1 delta y, cycle 1
- 2 - 2 delta y, cycle 1
- 3 - 2 delta y, cycle 2
- 4 - 4 delta y, cycle 1
- 5 - 4 delta y, cycle 2
- 6 - 6 delta y, cycle 1
- 7 - 6 delta y, cycle 2
- 8 - 8 delta y, cycle 1
- 9 - 8 delta y, cycle 2
- 10 - 8 delta y, cycle 3
- 11 - 10 delta y, cycle 1
- 12 - 10 delta y, cycle 2
- 13 - 10 delta y, cycle 3
- 14 - 12 delta y, cycle 1
- 15 - 12 delta y, cycle 2



LOAD CYCLES FOR MODEL N4

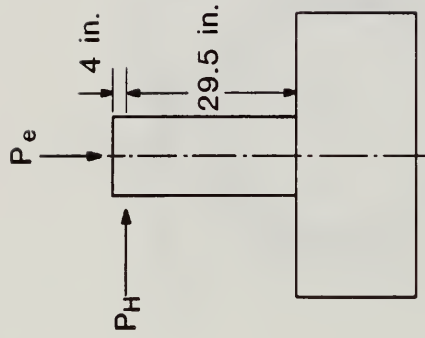
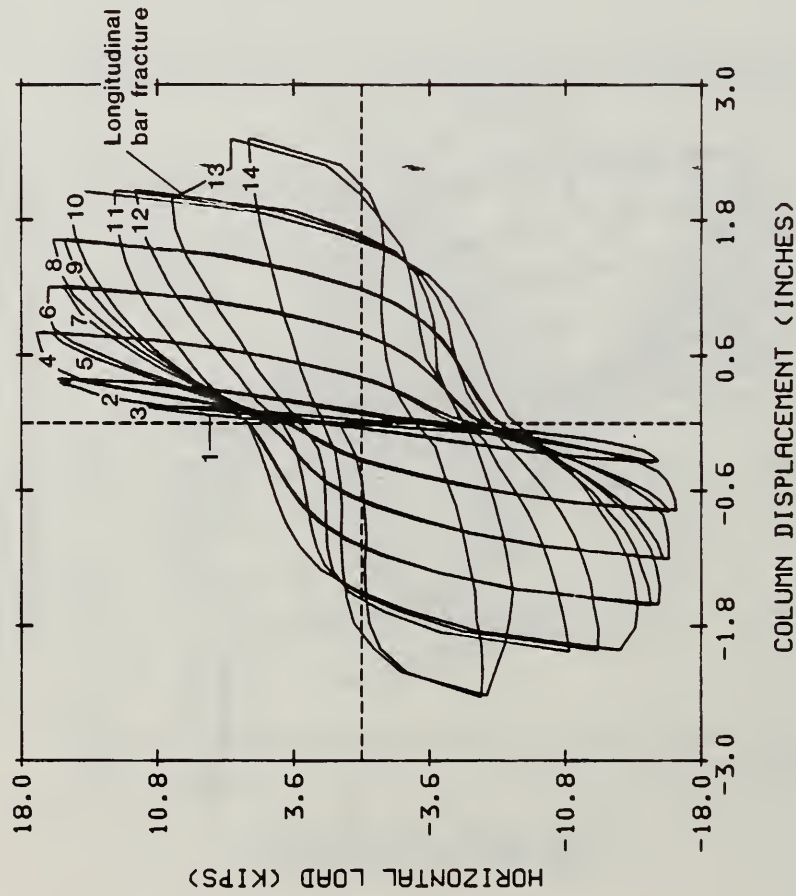
FIGURE 6.4



$$P_e = 0.1 f'_c A_g = 26.87 \text{ kips}$$

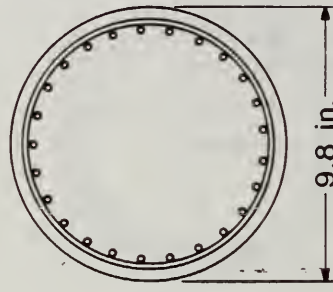
- $A_g = 75.43 \text{ in}^2$
- $A_s = 1.5 \text{ in}^2$
- $\rho_t = 0.0199$
- $\rho_s = 0.01452$
- Spiral = 0.120 in.
- Bars = 0.276 in.
- 1 in. = 25.4 mm

- 1 - 1 delta y, cycle 1
- 2 - 2 delta y, cycle 1
- 3 - 2 delta y, cycle 2
- 4 - 4 delta y, cycle 1
- 5 - 4 delta y, cycle 2
- 6 - 6 delta y, cycle 1
- 7 - 6 delta y, cycle 2
- 8 - 8 delta y, cycle 1
- 9 - 8 delta y, cycle 2
- 10 - 10 delta y, cycle 1
- 11 - 10 delta y, cycle 2
- 12 - 10 delta y, cycle 3
- 13 - 12 delta y, cycle 1
- 14 - 12 delta y, cycle 2



$$P_e = 0.2 f'_c A_g = 53.75 \text{ kips}$$

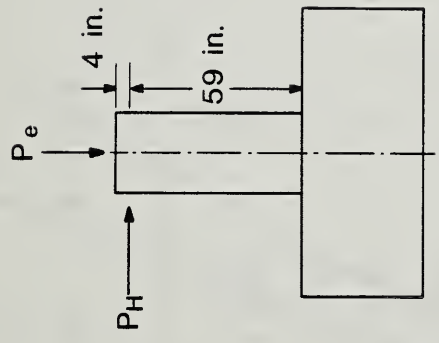
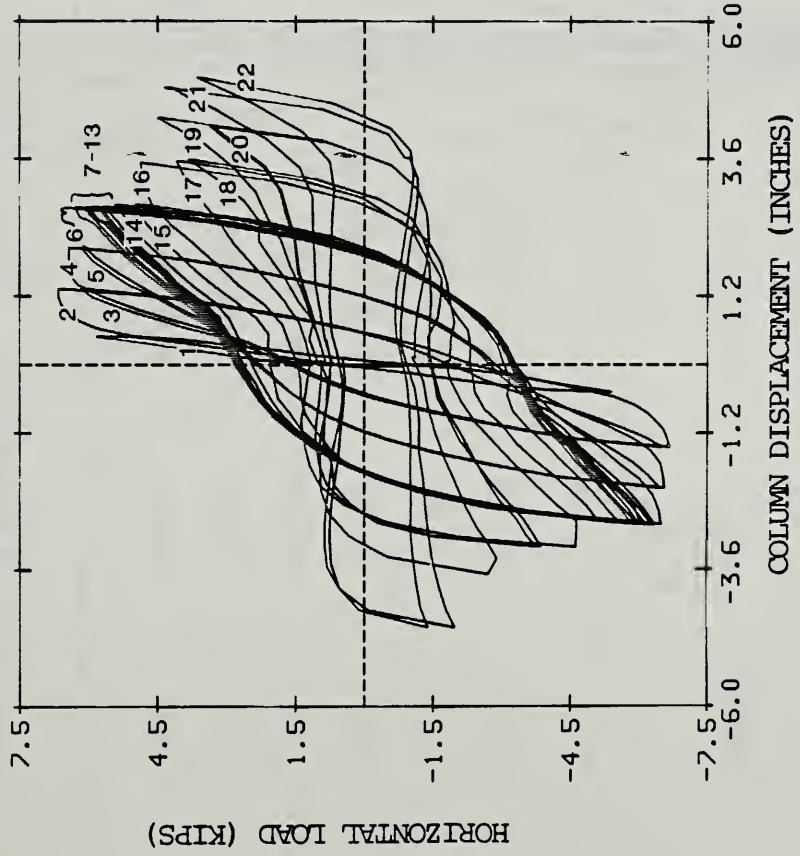
- $A_g = 75.43 \text{ in}^2$
- $A_s = 1.5 \text{ in}^2$
- $\rho_t = 0.0199$
- $\rho_s = 0.01452$
- Spiral = 0.120 in.
- Bars = 0.276 in.
- 1 in. = 25.4 mm



LOAD CYCLES FOR MODEL NS

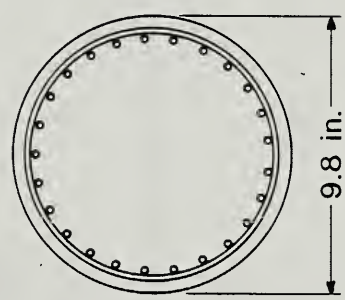
FIGURE 6.5

- 1 - 1 delta y, cycle 1
- 2 - 2 delta y, cycle 1
- 3 - 2 delta y, cycle 2
- 4 - 3 delta y, cycle 1
- 5 - 3 delta y, cycle 2
- 6 - 4 delta y, cycle 1
- 7 - 4 delta y, cycle 2
- 8 - 4 delta y, cycle 3
- 9 - 4 delta y, cycle 4
- 10 - 4 delta y, cycle 5
- 11 - 4 delta y, cycle 6
- 12 - 4 delta y, cycle 7
- 13 - 4 delta y, cycle 8
- 14 - 4 delta y, cycle 9
- 15 - 4 delta y, cycle 10
- 16 - 5 delta y, cycle 1
- 17 - 5 delta y, cycle 2
- 18 - 5 delta y, cycle 3
- 19 - 6 delta y, cycle 1
- 20 - 6 delta y, cycle 2
- 21 - 7 delta y, cycle 1
- 22 - 7 delta y, cycle 2



$P_e = 0.1 f'_c A_g$
 $= 26.87 \text{ kips}$

- $A_g = 75.43 \text{ in}^2$
- $A_s = 1.5 \text{ in}^2$
- $\rho_t = 0.0199$
- $\rho_s = 0.00694$
- Spiral = 0.106 in.
- Bars = 0.276 in.
- 1 in. = 25.4 mm



LOAD CYCLES FOR MODEL N6

FIGURE 6.6

TABLE 6.1 YIELD DISPLACEMENTS

MODEL	$\frac{P_e}{f'_c A_g}$	ρ_s	γ (lb/ft ³)	E_c^1 (ksi)	L/D	Δ_y (IN.)	Δ_u / Δ_y
N1	0.10	0.01452	132	2,957	3	0.38	8
N2	0.20	0.01452	132	2,896	3	0.22	10
N3	0.10	0.00694	132	3,036	6	1.01	4
N4	0.10	0.01452	145	3,431	3	0.21	10
N5	0.20	0.01452	145	3,425	3	0.19	12
N6	0.10	0.00694	145	3,343	6	0.66	5

$$1 \quad E_c = w^{1.5} (33) \quad f'_c \quad [3]$$

COLUMN DISPLACEMENTS FOR MODEL N1

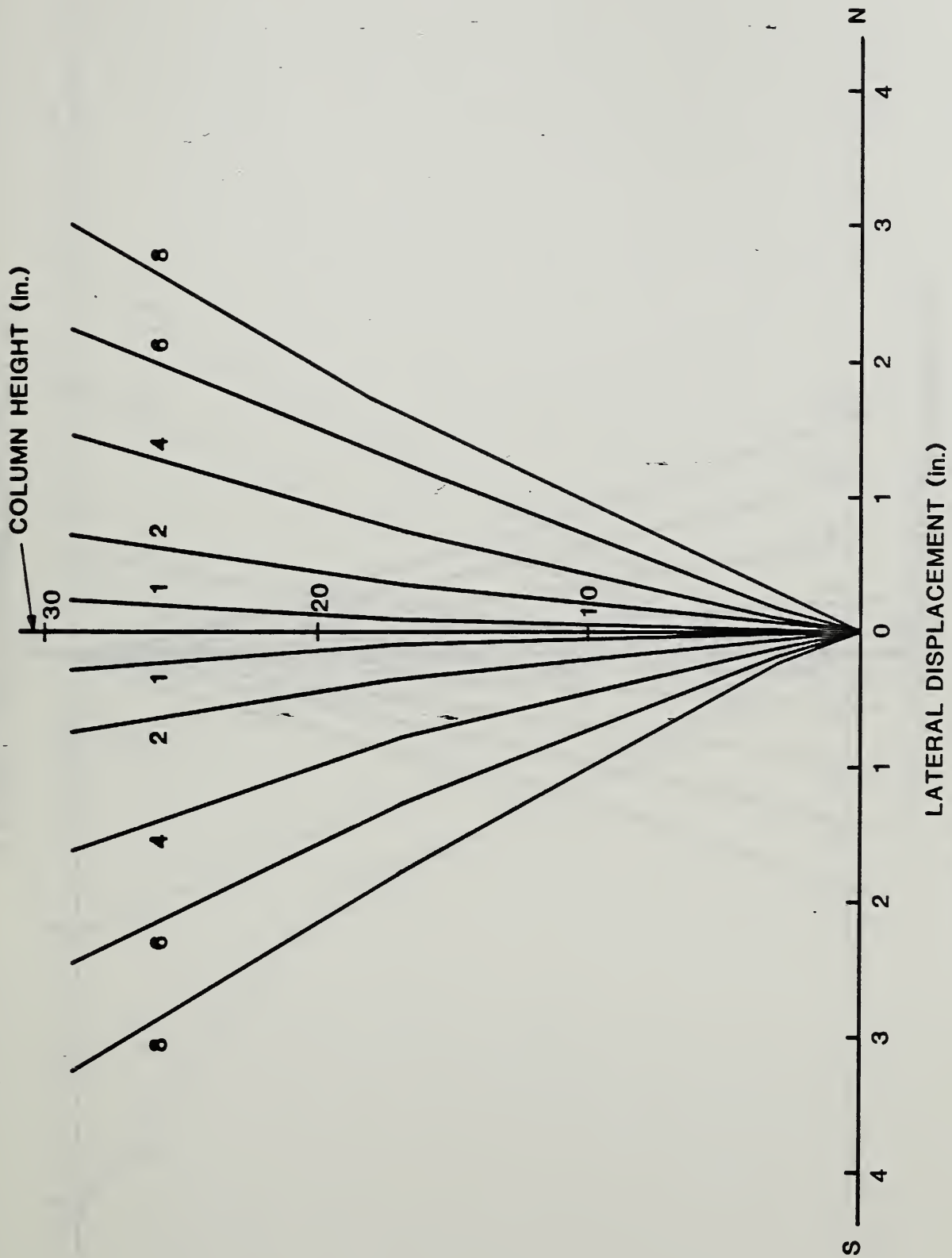
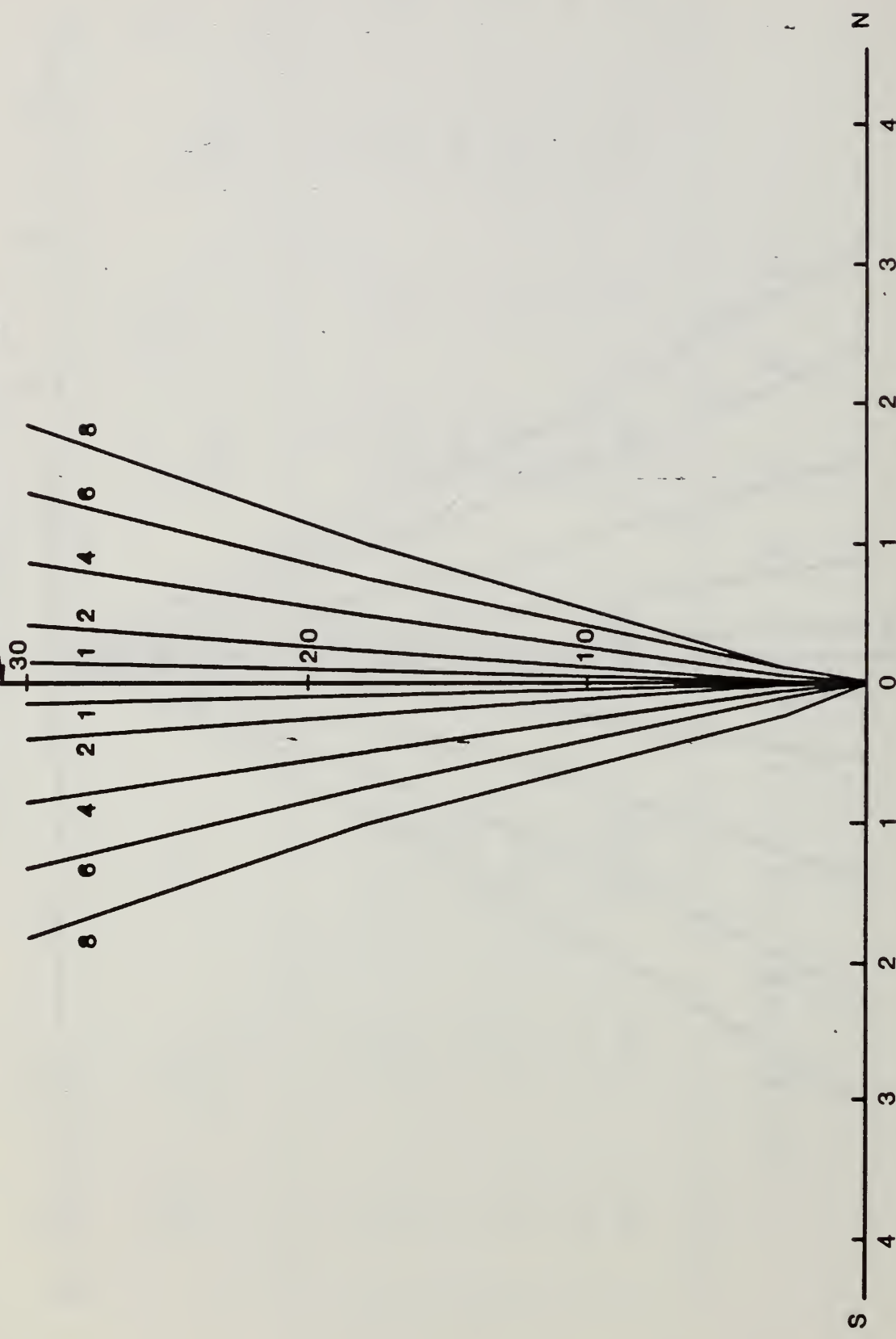


Fig. 6.7

COLUMN DISPLACEMENTS FOR MODEL N2

COLUMN HEIGHT (in.)



LATERAL DISPLACEMENT (in.)

Fig. 6.8

COLUMN DISPLACEMENTS FOR MODEL N3

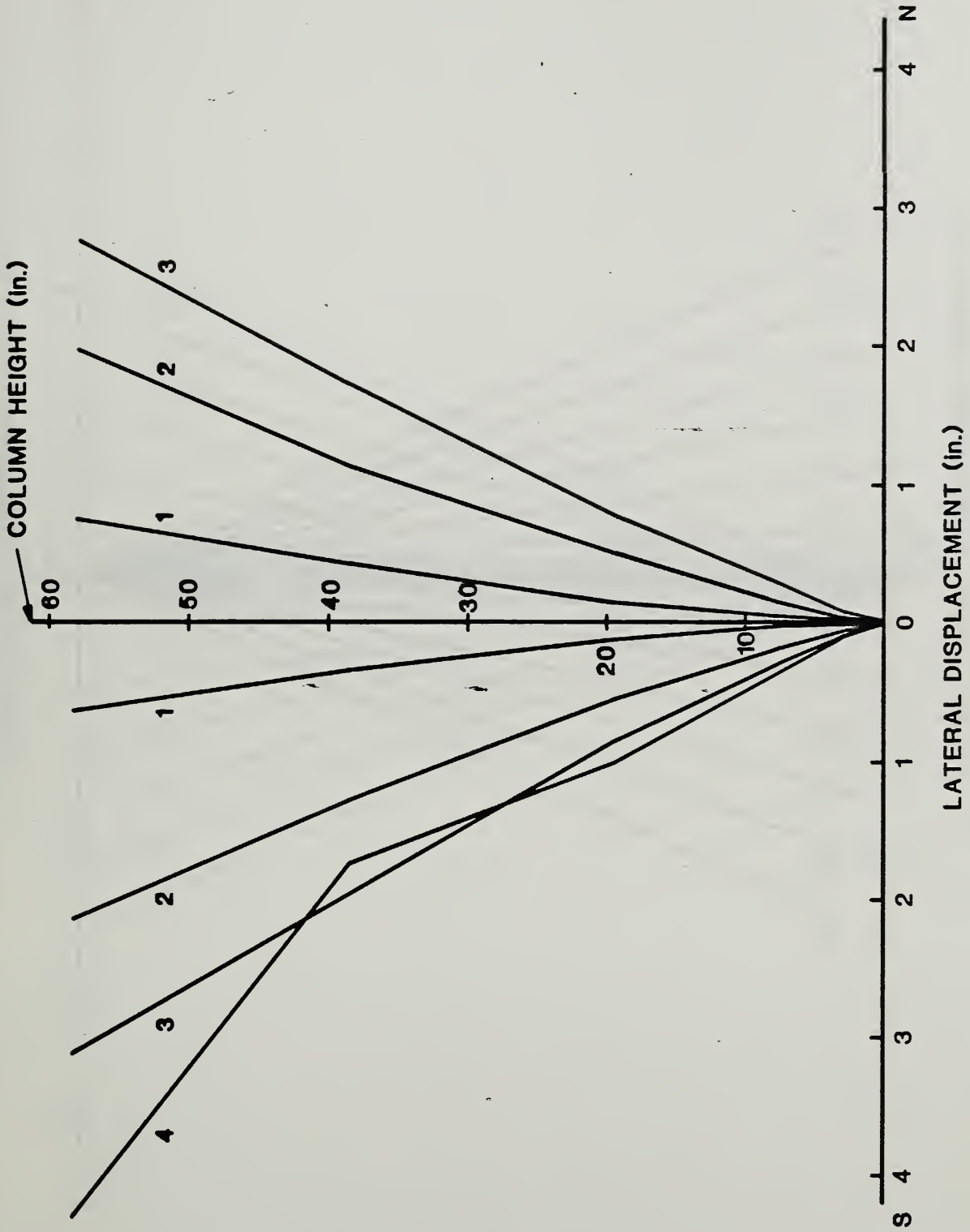


Fig. 6.9

COLUMN DISPLACEMENTS FOR MODEL N4

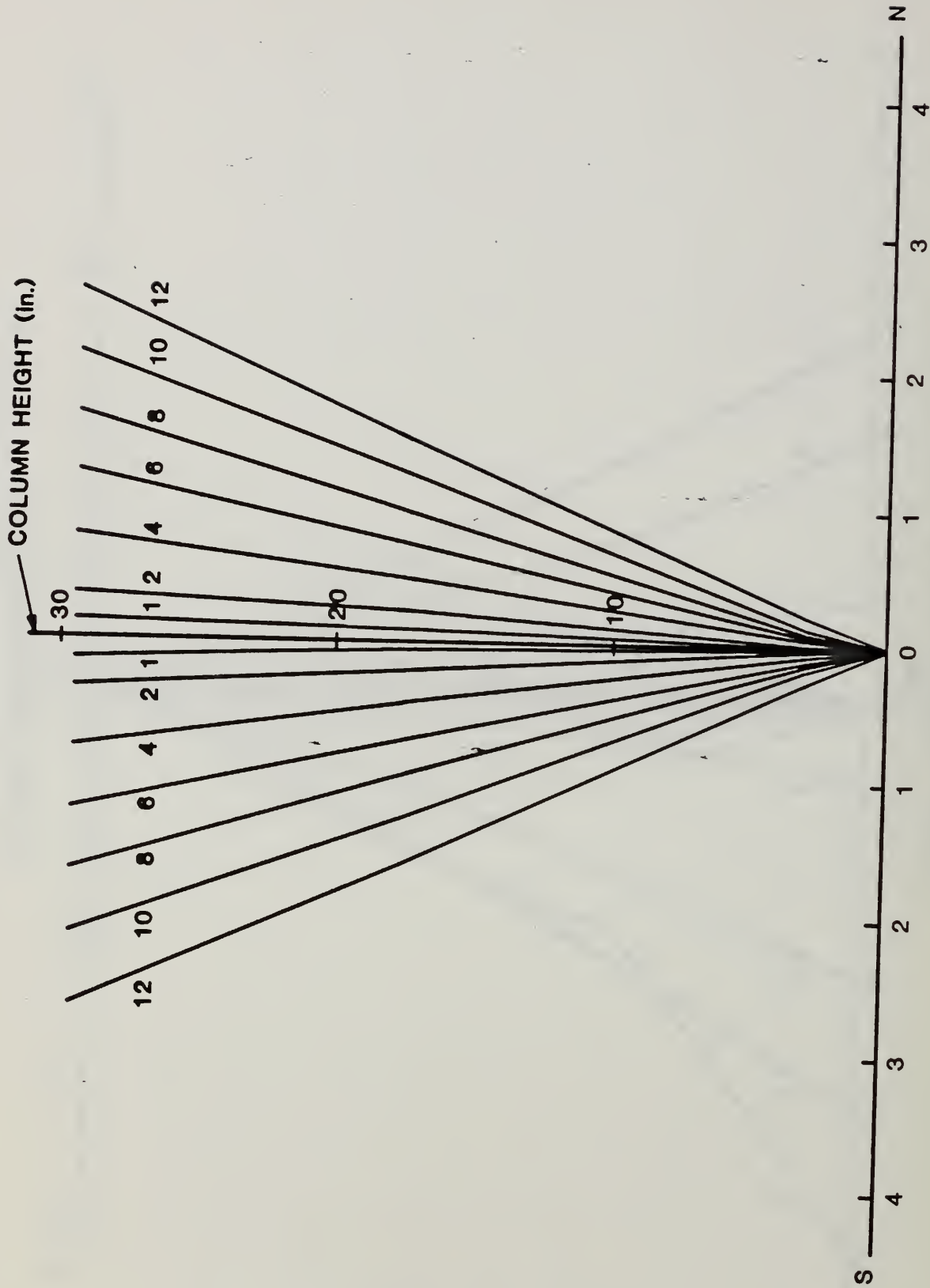


Fig. 6.10

COLUMN DISPLACEMENTS FOR MODEL N5

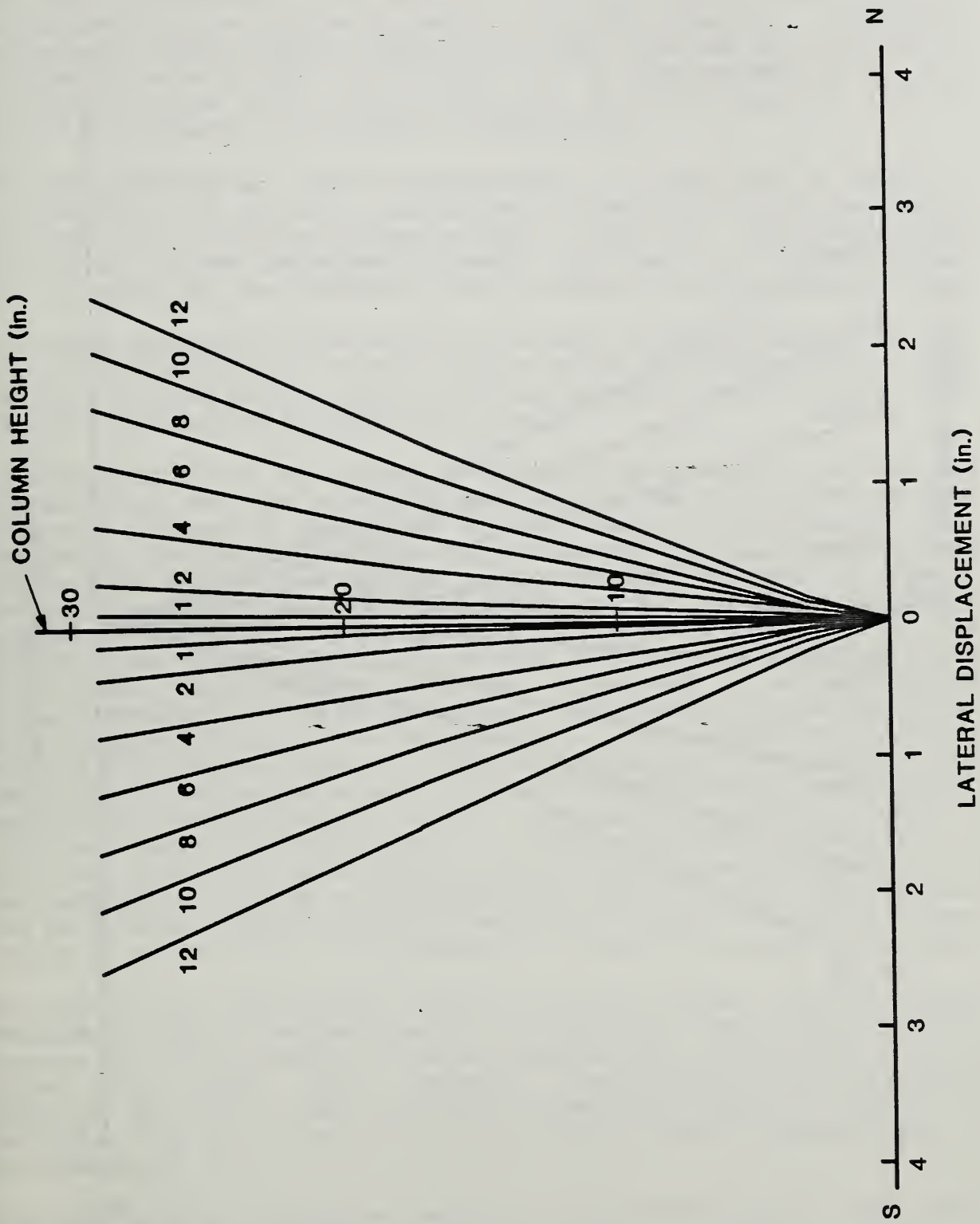


Fig. 6.11

COLUMN DISPLACEMENTS FOR MODEL N6

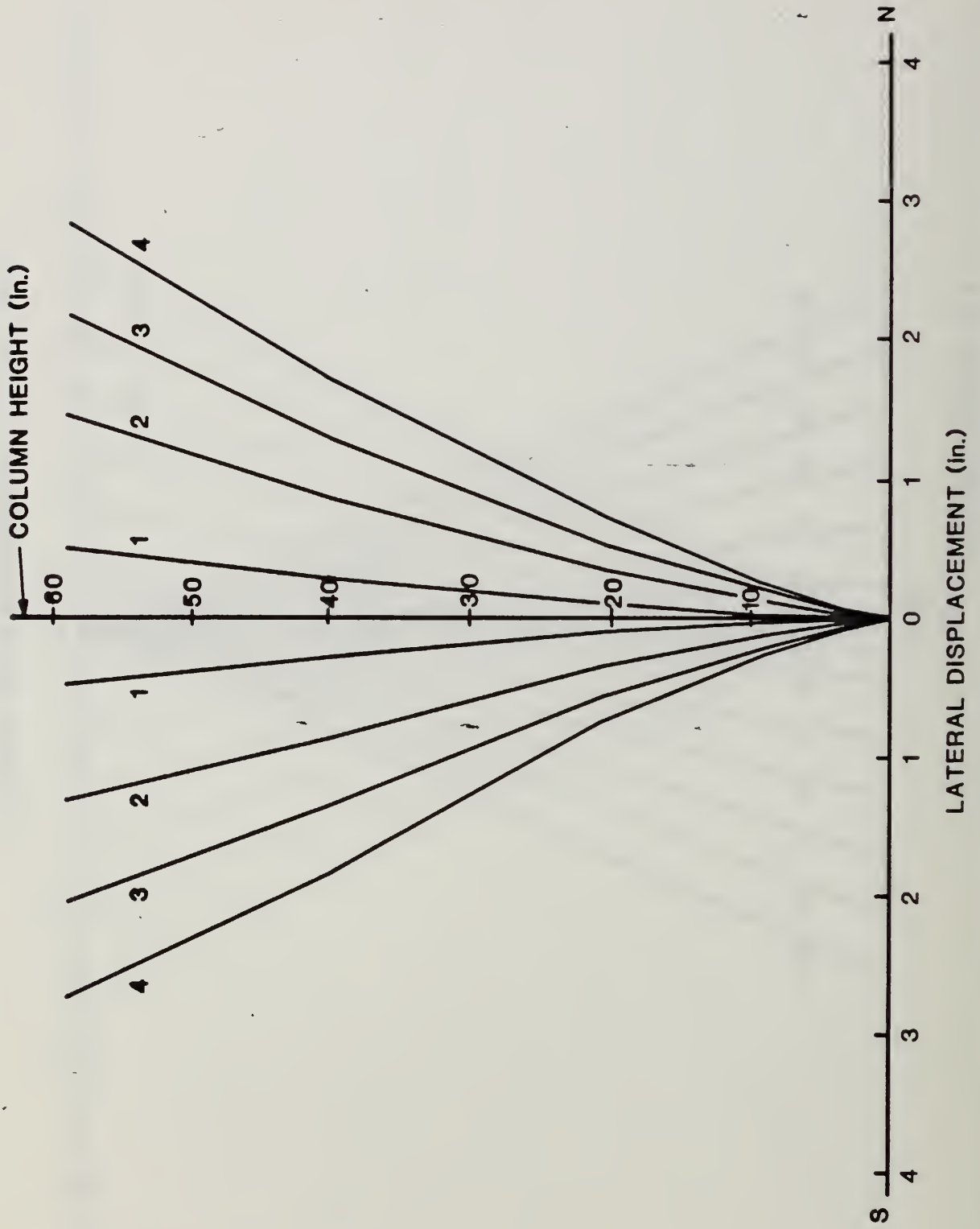


Fig. 6.12

6.2 Energy Absorption

One means of measuring the ability of a structure to withstand an earthquake is to calculate its energy absorption capacity. The energy absorbed by a column during a particular load cycle can be determined by integrating the area within the lateral load vs. displacement curve. This was done in this study by the use of a special computer graphic integration procedure, as described in Appendix A.

The energy absorbed per cycle for each model up to completion of testing is shown in Figs. 6.13 - 6.18. A comparison of the total energy absorbed by the models up to ultimate failure is shown in Fig. 6.19. The total energy for a given test was determined by summing individual cycle energies up to the cycle which met the ultimate failure criteria previously described.

The energy absorbed by the models can be seen to decrease markedly upon fracture of the spiral. This is shown graphically in Figs. 6.14 - 6.19. Also, as indicated in the figures, ultimate failure of the columns occurred soon after fracture of the confining spiral.

As shown in Fig. 6.13, the absorption capacity of the models constructed with ready-mix concrete is greater than that of the microconcrete models. The energy absorbed by specimen N4 is approximately 12% greater than that absorbed by specimen N1, and the energy absorbed by N5 is 8% greater than that absorbed by N2. This increase may result from aggregate interlock in the pea gravel models, a phenomenon not found in microconcrete models because of the small aggregate size. The energy absorbed by the microconcrete flexure model, N3, is much less than that absorbed by the flexure model, constructed with ready-mix concrete N6, as was expected due to the premature failure of the spiral. The energy absorbed up to the point of spiral fracture, $\mu = 4$ first cycle, for model N3 was 151.5 kip-in. (2.46 N-m) compared with 86.9 kip-in. (1.41 N-m) for model N6 up to the same ductility and cycle as model N3. This difference was a result of the measured yield displacement, 0.66 in. (16.8 mm), for model N6 as compared with a measured yield displacement of 1.01 in. (25.6 mm) for model N3. If the energy absorbed by model N6 was multiplied by the ratio of these yield displacements ($1.01/0.66 = 1.53$) this would result in 133.0 kip-in. (2.16 N-m) which would indicate that the behavior of model N3 would have been comparable to that of N6 if the spiral in N3 had not prematurely fractured.

The models with higher axial load, N2 and N5, showed a greater energy absorption capacity than the models with lower axial load, N1 and N4. This increase in energy absorption was not found by Ohno and Nishioka [17] for higher axial loads. It is, however, reflected in their proposed equations, Eqs. (6.1) & (6.3), to predict energy absorption of columns. In particular Eq. (6.1) predicts that the ultimate moment is proportional to the axial load.

This difference in energy absorbed due to the different axial loads would have been greater if the P - Δ effect had been included in the energy absorption calculation. This is due to the greater influence of the P - Δ effect on the flexural strength of a column for higher axial load as shown in Tables 6.2 to 6.7 and as observed by Potangaroa [23]. The variables in these tables were defined as:

INDIVIDUAL CYCLE ENERGY FOR MODEL N1

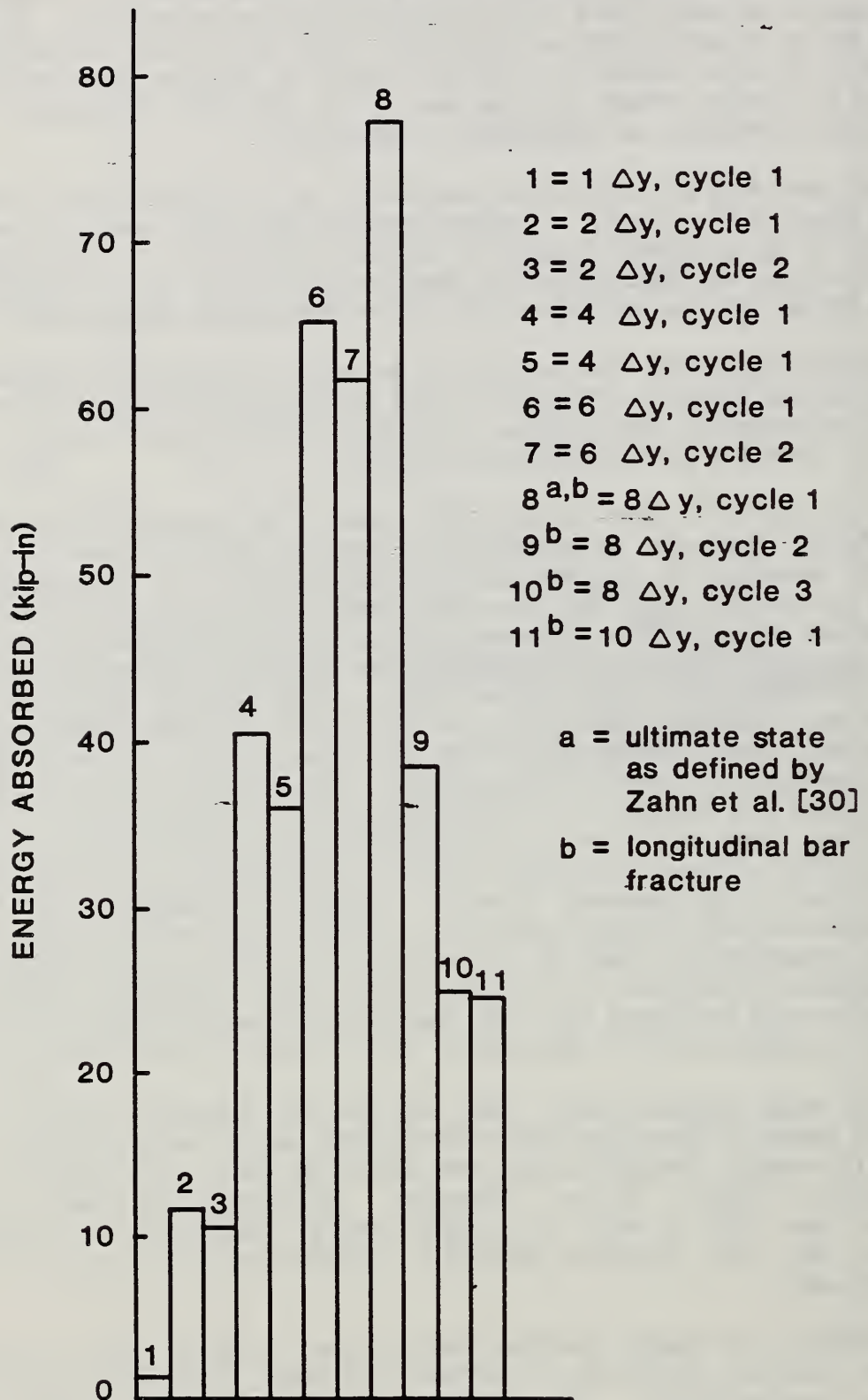


Fig. 6.13

INDIVIDUAL CYCLE ENERGY FOR MODEL N2

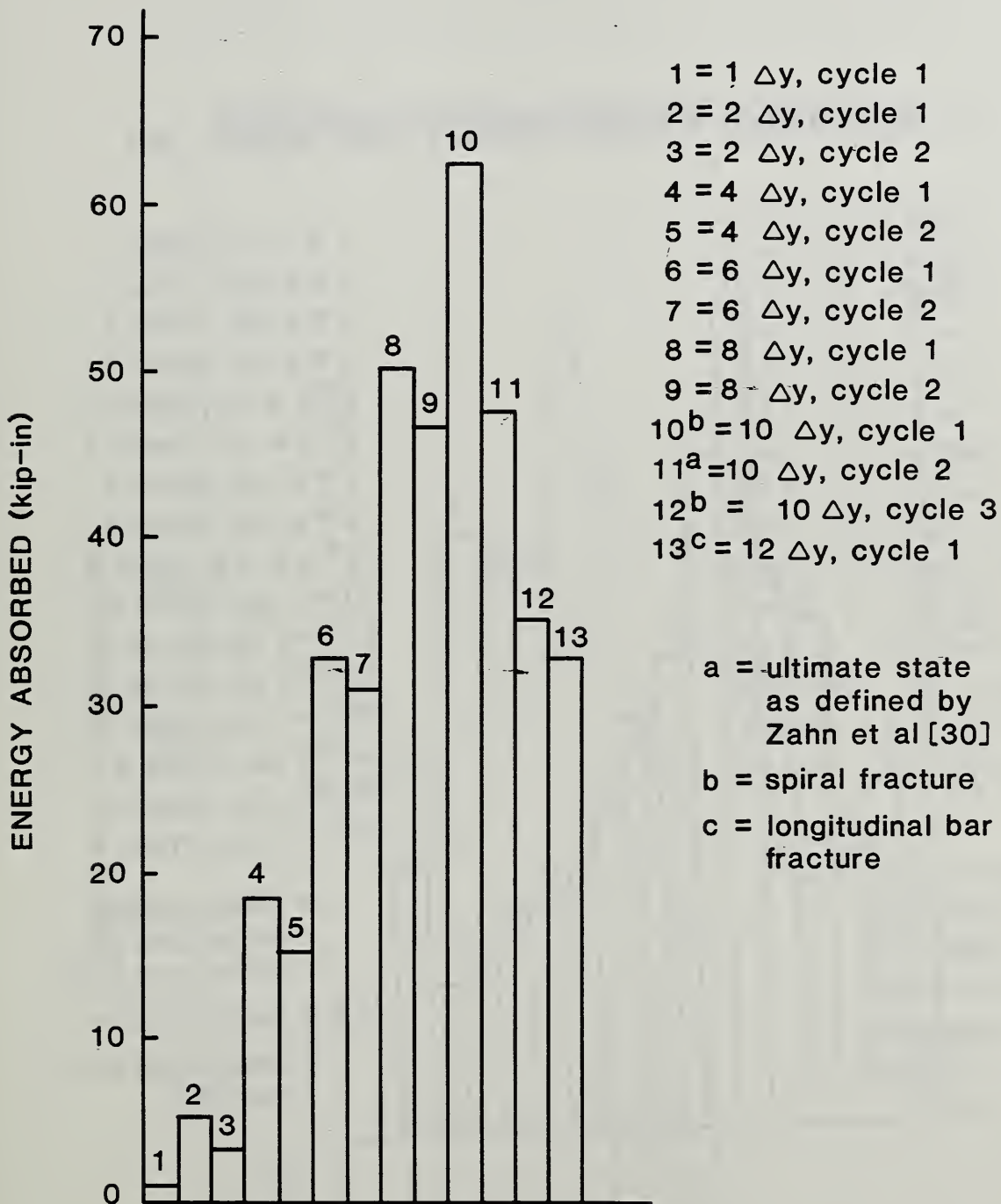


Fig. 6.14

INDIVIDUAL CYCLE ENERGY FOR MODEL N3

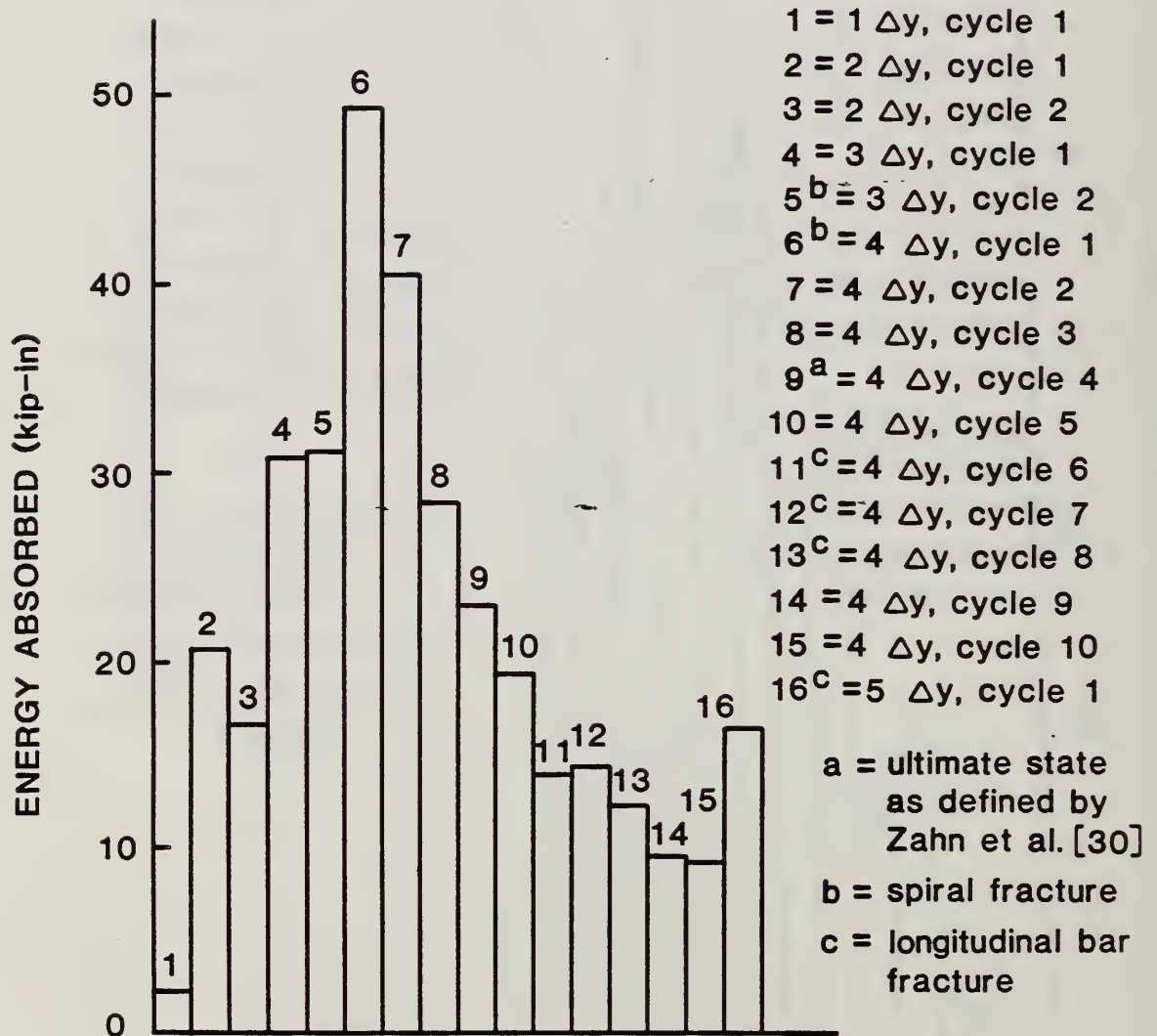


Fig. 6.15

INDIVIDUAL CYCLE ENERGY FOR MODEL N4

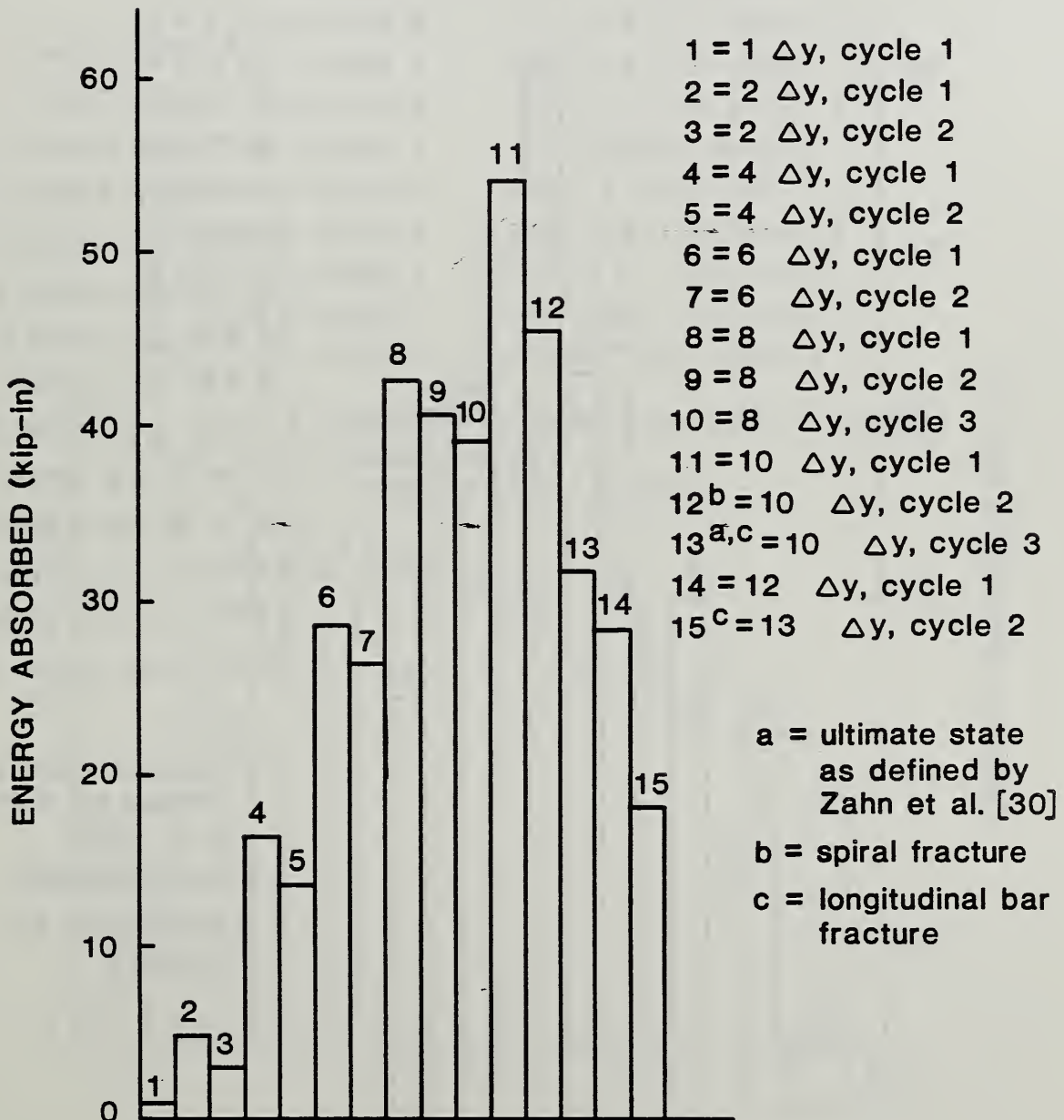


Fig. 6.16

INDIVIDUAL CYCLE ENERGY FOR MODEL N5

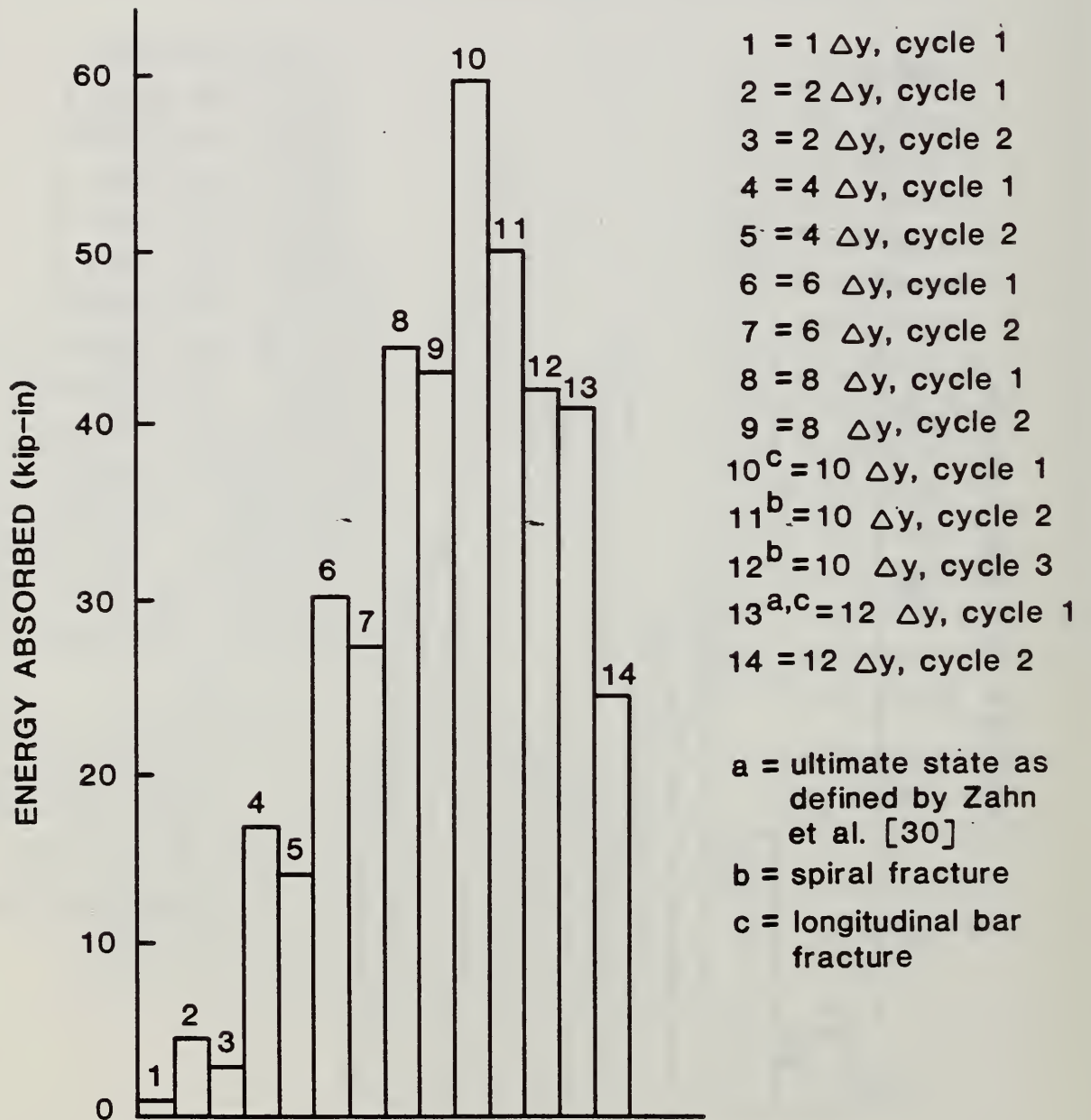


Fig. 6.17

INDIVIDUAL CYCLE ENERGY FOR MODEL N6

1 = 1 Δy , cycle 1	12 = 4 Δy , cycle 7
2 = 2 Δy , cycle 1	13 = 4 Δy , cycle 8
3 = 2 Δy , cycle 2	14 ^b = 4 Δy , cycle 9
4 = 3 Δy , cycle 1	15 ^b = 4 Δy , cycle 10
5 = 3 Δy , cycle 2	16 = 5 Δy , cycle 1
6 = 4 Δy , cycle 1	17 ^a = 5 Δy , cycle 2
7 = 4 Δy , cycle 2	18 = 5 Δy , cycle 3
8 = 4 Δy , cycle 3	19 ^c = 6 Δy , cycle 2
9 = 4 Δy , cycle 4	20 ^c = 6 Δy , cycle 2
10 = 4 Δy , cycle 5	21 ^c = 7 Δy , cycle 1
11 = 4 Δy , cycle 6	22 = 7 Δy , cycle 2

a = ultimate as defined by Zahn et al. [30]
 b = spiral fracture
 c = longitudinal bar fracture

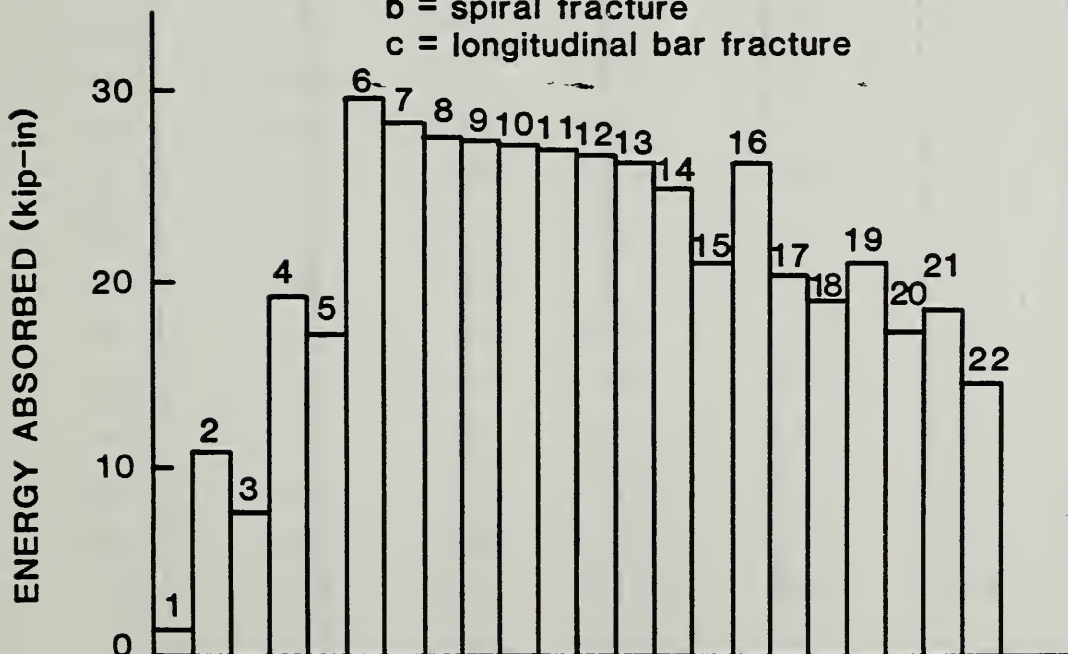


Fig. 6.18

ENERGY ABSORBED UP TO ULTIMATE STATE
AS DEFINED BY Zahn et al. [30]

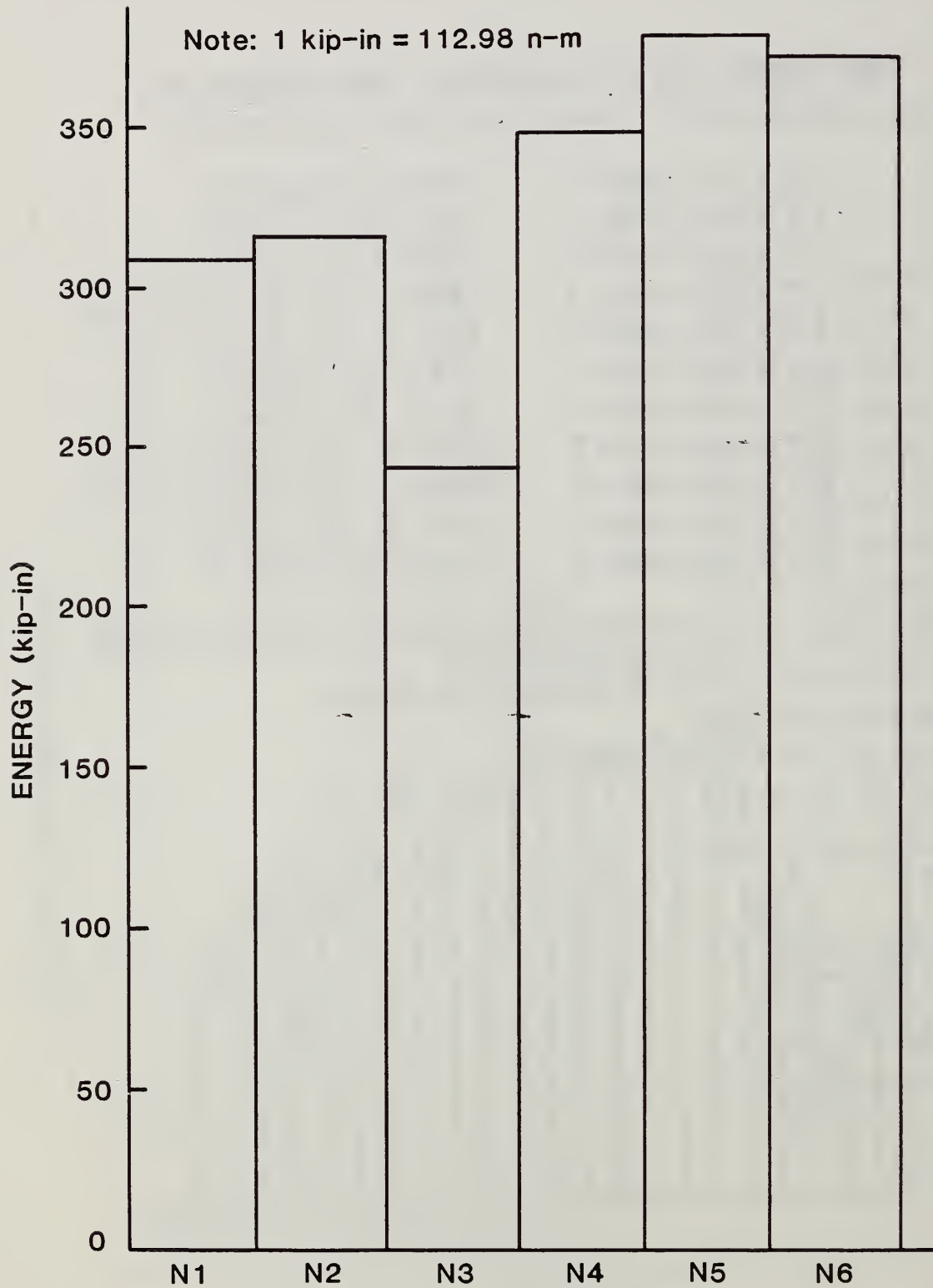


Fig. 6.19

TABLE b.2 Loads and Moments for Model N1

Cycle	H (Kip)	Δ (In.)	P_e (Kip)	M_H (Kip-Ft)	P - Δ (Kip-Ft)	M Total (Kip-Ft)
11,S	10.966	0.237	26.37	26.96	0.52	27.48
11,N	11.299	0.223	26.70	27.78	0.50	28.28
21,S	12.548	0.711	26.10	30.85	1.55	32.40
21,N	14.594	0.716	25.68	35.88	1.53	37.41
22,S	11.980	0.722	25.50	29.45	1.53	30.98
22,N	14.299	0.689	25.48	35.15	1.46	36.61
41,S	13.258	1.596	24.37	32.59	3.24	35.83
41,N	14.408	1.453	24.22	35.42	2.93	38.35
42,S	12.059	1.560	23.31	29.65	3.03	32.68
42,N	13.740	1.455	24.32	33.78	2.95	36.73
61,S	12.627	2.423	23.22	31.04	4.69	35.73
61,N	13.471	2.211	23.96	33.12	4.42	37.54
62,S	11.292	2.442	23.10	27.76	4.70	32.46
62,N	12.731	2.238	23.75	31.30	4.43	35.73
81,S	7.151	3.248	23.72	17.58	6.42	24.00
81,N	10.850	3.029	24.45	26.67	6.17	32.84
82,S	1.745	2.768	25.42	4.29	6.86	10.15
82,N	7.681	3.049	28.31	18.88	7.19	26.07
83,S	2.239	3.271	27.59	5.50	7.52	13.02
83,N	5.499	3.038	28.99	13.52	7.34	20.86
101,S	0.484	4.100	29.41	1.19	10.05	11.24
101,N	3.249	3.79	29.94	8.43	10.68	19.11

TABLE 6.3 Loads and Moments for Model N2

Cycle	H (Kip)	Δ (In.)	P_e (Kip)	M_H (Kip-Ft)	$P - \Delta$ (Kip-Ft)	M Total (Kip-Ft)
11,S	11.976	0.169	54.72	29.44	0.77	30.21
11,N	10.958	0.166	53.93	26.94	0.75	27.69
21,S	15.970	0.407	52.88	39.26	1.79	41.05
21,N	15.149	0.405	52.82	37.24	1.78	39.02
22,S	15.405	0.410	52.52	37.87	1.79	39.66
22,N	14.913	0.405	53.38	36.66	1.80	38.46
41,S	16.267	0.868	51.94	39.99	3.76	43.75
41,N	14.801	0.870	51.94	36.39	3.76	40.16
42,S	15.954	0.871	53.07	39.22	3.85	43.07
42,N	14.596	0.871	52.56	35.88	3.81	39.69
61,S	16.270	1.353	52.63	40.00	5.93	45.93
61,N	14.534	1.356	52.85	35.73	5.97	41.70
62,S	15.808	1.351	52.22	38.86	5.88	44.74
62,N	14.222	1.358	57.38	34.96	5.93	40.89
81,S	15.643	1.830	52.85	38.46	8.06	46.52
81,N	13.875	1.835	52.78	34.11	8.07	42.18
82,S	15.007	1.832	52.91	36.89	8.08	44.97
82,N	13.242	1.792	53.09	32.55	7.93	40.48
101,S	14.151	2.373	52.92	34.78	10.46	45.25
101,N	11.302	2.265	53.66	27.78	10.13	37.91
102,S	11.497	2.379	53.85	28.26	10.60	38.94
102,N	8.699	2.272	53.59	21.39	10.15	31.54
103,S	9.060	2.389	53.37	22.27	10.63	32.90
103,N	5.611	2.284	53.73	13.79	10.23	24.02
121,S	4.700	2.897	53.48	11.55	12.91	24.47
121,N	3.323	2.729	54.00	8.17	12.28	20.45

TABLE 6.4 Loads and Moments for Model N3

Cycle	H (Kip)	Δ (In.)	P_e (Kip)	M_H (Kip-Ft)	P - Δ (Kip-Ft)	M Total (Kip-Ft)
11,S	5.861	0.635	27.59	28.82	1.46	30.28
11,N	5.535	0.729	26.44	27.21	1.61	28.82
21,S	7.157	2.157	25.42	35.19	4.57	39.76
21,N	6.573	1.906	24.59	32.32	3.91	36.23
22,S	6.875	2.163	25.00	33.80	4.50	38.30
22,N	6.360	1.908	24.83	31.27	3.95	35.22
31,S	6.464	3.126	26.13	31.78	6.81	38.59
31,N	6.175	2.785	26.25	30.36	6.09	36/45
32,S	6.167	3.200	25.17	30.32	6.71	37.03
32,N	5.953	2.795	25.31	29.27	5.90	35.17
41,S	6.802	4.354	28.53	33.44	10.35	43.79
41,N	5.915	3.933	29.06	29.08	9.52	38.60
42,S	6.152	4.173	29.96	30.25	10.42	40.67
42,N	5.259	3.013	29.78	25.86	7.48	33.34
43,S	4.602	4.146	30.93	22.63	10.69	33.32
43,N	4.414	3.981	30.60	21.70	10.15	31.85
44,S	3.817	4.154	29.90	18.77	10.35	29.12
44,N	3.522	3.865	31.69	17.32	10.21	27.53
45,S	3.130	4.161	29.46	15.43	10.22	25.65
45,N	2.976	4.025	29.92	14.63	10.04	24.67
46,S	2.598	4.168	31.64	12.77	10.99	23.76
46,N	2.699	3.883	30.68	13.27	9.93	23.20
47,S	2.042	3.760	33.83	10.04	10.60	20.64
47,N	2.71	4.031	33.80	13.32	11.35	24.67
48,S	1.631	4.161	32.53	8.02	11.28	19.30
48,N	2.784	4.013	33.73	13.69	11.28	24.97
49,S	1.515	4.434	27.56	7.45	10.18	17.63
49,N	2.723	3.622	25.16	13.39	7.59	20.98
410,S	1.372	3.648	27.64	6.75	8.40	15.15
410,N	2.701	3.70	28.35	13.28	8.74	22.02
51,S	5.500	5.073	26.82	27.04	11.34	38.38
51,N	5.016	4.328	30.05	24.66	10.84	35.50

TABLE 6.5 Loads and Moments for Model N4

Cycle	H (Kip)	Δ (In.)	P_e (Kip)	M_H (Kip-Ft)	$P - \Delta$ (Kip-Ft)	M Total (Kip-Ft)
11,S	10.713	0.143	26.77	26.34	0.32	26.66
11,N	11.11	0.158	25.93	27.31	0.34	27.65
21,S	13.571	0.367	25.33	33.36	0.77	34.13
21,N	13.541	0.371	24.86	33.29	0.77	34.06
22,S	12.830	0.370	25.52	31.54	0.79	32.33
22,N	13.237	0.370	25.54	32.54	0.79	33.33
41,S	14.047	0.791	25.120	34.53	1.66	36.19
41,N	13.669	0.790	25.46	33.60	1.68	35.28
42,S	13.268	0.797	25.66	32.62	1.70	34.32
42,N	13.241	0.791	25.16	32.55	1.66	34.21
61,S	13.990	1.229	25.48	34.39	2.61	37.00
61,N	13.431	1.227	25.28	33.02	2.58	35.60
62,S	13.114	1.234	25.58	32.24	2.63	34.87
62,N	13.091	1.227	25.67	32.18	2.62	34.80
81,S	13.788	1.677	25.60	33.90	3.58	37.48
81,N	12.915	1.699	25.19	31.75	3.57	35.32
82,S	12.818	1.691	25.49	31.51	3.59	35.10
82,N	12.356	1.672	25.25	30.38	3.52	33.90
83,S	12.418	1.691	25.40	30.53	3.58	34.11
83,N	11.960	1.672	25.31	29.40	3.53	32.93
101,S	12.700	2.150	24.77	31.22	4.44	35.66
101,N	11.559	2.111	25.68	28.42	4.52	32.94
102,S	11.113	2.153	25.30	27.32	4.54	31.86
102,N	9.818	2.118	26.53	24.14	4.68	28.82
103,S	8.594	2.186	25.84	21.13	4.71	25.84
103,N	6.264	2.131	26.32	15.40	4.67	20.07
121,S	4.441	2.651	26.52	10.92	5.86	16.78
121,N	5.304	2.549	25.84	13.04	5.49	18.53
122,S	2.909	2.658	26.57	7.15	5.89	13.04
122,N	2.838	2.564	26.70	6.98	5.70	12.68

TABLE 6.6 Loads and Moments for Model N5

Cycle	H (Kip)	Δ (In.)	P_e (Kip)	M_H (Kip-Ft)	$P - \Delta$ (Kip-Ft)	M Total (Kip-Ft)
11,S	11.381	0.148	49.78	27.98	0.61	28.59
11,N	8.480	0.109	49.37	20.85	0.45	21.30
21,S	16.099	0.392	49.037	39.58	1.60	41.18
21,N	15.718	0.335	47.00	38.64	1.31	39.95
22,S	15.249	0.392	48.50	37.49	1.58	39.07
22,N	15.440	0.344	47.94	37.96	1.37	39.33
41,S	16.870	0.082	48.82	41.47	3.26	44.73
41,N	16.674	0.768	47.91	40.99	3.07	44.06
42,S	16.411	0.799	48.13	40.34	3.20	43.54
42,N	16.309	0.777	48.39	40.09	3.13	43.22
61,S	16.068	1.207	48.01	39.50	4.83	44.33
61,N	16.295	1.204	46.68	40.06	4.68	44.74
62,S	15.834	1.217	46.83	38.93	4.75	43.67
62,N	15.977	1.199	47.43	39.28	4.74	44.02
81,S	16.324	1.629	47.72	40.13	6.48	46.61
81,N	15.700	1.606	47.51	38.60	6.36	44.96
82,S	15.747	1.633	47.32	38.71	6.44	45.15
82,N	15.312	1.614	47.39	37.64	6.37	44.01
101,S	14.688	2.056	46.44	36.11	7.96	44.07
101,N	13.691	2.014	47.25	33.66	7.93	41.59
102,S	13.099	2.064	47.51	32.20	8.17	40.37
102,N	12.490	2.016	47.09	30.70	7.91	38.61
103,S	12.002	2.071	49.49	29.50	8.54	38.04
103,N	10.996	2.028	49.44	27.03	8.36	35.39
121,S	6.952	2.523	48.22	17.09	10.14	27.23
121,N	6.617	2.416	49.38	16.27	9.94	26.21
122,S	5.957	2.532	47.91	14.64	10.11	24.75
122,N	5.661	2.430	50.17	13.92	10.16	24.08

TABLE 6.7 Loads and Moments for Model N6

Cycle	H (Kip)	Δ (In.)	P_e (Kip)	M_H (Kip-Ft)	P - Δ (Kip-Ft)	M Total (Kip-Ft)
11,S	5.836	0.500	29.13	28.69	1.21	29.90
11,N	5.400	0.484	27.06	26.55	1.09	27.64
21,S	5.605	1.329	23.54	32.47	2.61	35.08
21,N	6.665	1.444	21.65	32.77	2.60	35.37
22,S	6.169	1.333	20.63	30.33	2.29	32.62
22,N	6.488	1.447	21.21	31.90	2.56	34.46
31,S	6.437	2.050	21.11	31.65	3.61	35.26
31,N	6.556	2.168	20.94	32.23	3.78	36.01
32,S	6.152	2.048	21.38	20.25	3.65	33.90
32,N	6.442	2.164	21.45	31.67	3.87	35.54
41,S	6.515	2.751	21.10	32.03	4.84	36.87
41,N	6.486	2.805	20.72	31.89	4.84	36.73
42,S	6.297	2.758	21.26	30.96	4.89	35.85
42,N	6.347	2.809	21.12	31.21	4.94	36.15
43,S	6.061	2.759	21.33	29.80	4.90	34.70
43,N	6.286	2.809	21.28	30.91	4.98	35.89
44,S	6.026	2.759	20.22	29.63	4.65	34.28
44,N	6.153	2.814	19.59	30.25	4.59	34.84
45,S	5.938	2.763	19.70	29.20	4.54	33.74
45,N	6.046	2.800	22.96	29.73	5.36	35.09
46,S	5.797	2.766	20.14	28.50	4.64	33.14
46,N	6.000	2.800	19.17	29.500	4.47	33.97
47,S	5.744	2.760	19.51	28.24	4.50	32.74

Continue TABLE 6.7

Cycle	H (Kip)	Δ (In.)	P_e (Kip)	M_H (Kip-Ft)	$P - \Delta$ (Kip-Ft)	M Total (Kip-Ft)
47,N	5.971	2.803	19.86	29.36	4.64	34.00
48,S	5.641	2.763	19.76	27.73	4.55	32.28
48,N	5.819	2.767	19.70	28.61	4.54	33.15
49,S	5.433	2.802	19.39	26.71	4.53	31.24
49,N	5.579	2.778	19.06	27.43	4.41	31.84
410,S	5.000	2.811	18.82	24.58	4.41	28.99
410,N	5.086	2.726	18.16	25.01	4.13	29.14
51,S	4.889	3.543	20.01	24.04	5.91	29.95
51,N	4.610	3.196	23.08	22.67	6.15	28.82
52,S	4.100	3.570	23.04	20.16	6.85	27.01
52,N	3.852	3.190	23.50	18.94	6.25	25.19
53,S	2.588	3.593	23.42	12.72	7.01	19.73
53,N	3.300	3.191	24.06	16.23	6.40	22.63
61,S	4.503	4.322	23.79	22.14	8.57	30.71
61,N	2.695	3.677	24.31	13.25	7.45	20.70
62,S	2.331	3.628	25.10	11.46	7.59	19.05
62,N	3.047	4.123	25.98	14.98	8.93	23.91
71,S	5.191	4.845	26.92	25.52	10.87	36.39
71,N	2.800	4.598	26.79	13.77	10.27	24.04
72,S	4.489	4.922	25.24	22.04	10.35	32.42
72,N	2.225	4.491	24.21	10.94	9.06	20.00

H = Lateral load (kips)

P_e = Axial load (kips)

M_H = Moment at the base of the column due to H (kip-ft)

$P - \Delta$ = Moment due to P_e (kip-ft)

$M_{Total} = M_H + P - \Delta$ (kip-ft)

The energy absorbed by models N4 and N6 was essentially equal. These models which were constructed using ready-mix "pea gravel" concrete, were loaded to the same magnitude of axial load, but had different aspect (moment/shear) ratios and loading sequence. This would agree with the conclusion drawn by Ohno and Nishioka [17] that the total energy absorbed by a column is independent of the loading sequence.

Ohno and Nishioka [17] proposed that the energy absorption capacity of a column could be predicted if the cross section, and the concrete and reinforcing steel properties of the column were known. The proposed method is as follows:

$$M_p = 0.8 a_t f_y D + 0.5ND [1 - N/(bDf'_c)] \quad (6.1)$$

for

$$N \leq 0.4 bDf'_c$$

$$\theta_p = 2 \{ \cos^{-1} (l_p/2x) - \cos^{-1} [(l_p + \Delta l)/2x] \} \pi/180 \quad (6.2)$$

$$W_c = M_p \theta_p \quad (6.3)$$

where

M_p = plastic moment (kN-m)

a_t = cross sectional area of tensile reinforcement
(mm^2)

f_y = yield stress of tensile reinforcement (MPa)

N = axial load (kN)

b = width of cross section (cm)

D = depth of cross section (cm)

f'_c = compressive strength of concrete (MPa)

θ_p = ultimate column rotation (rad)

l_p = plastic hinge length (cm)

$$x = \sqrt{l_p^2 + s^2} / 2 \text{ (cm)}$$

s = distance between tension and compression reinforcement (cm).

Δl = length of elongation in the tensile steel
 = (% elongation) (l_p) (cm)

W_c = energy absorption capacity (kN-m)

The percent elongation of the steel at fracture for the NBS prototype longitudinal bars was 15.5 % based on mill test reports. Since this information was not available for the D6 wire used in the models, the prototype value was used in the calculation of θ_p . The ultimate moments and the moments predicted using Eq. (6.1) are given in Table 6.8. The two values compare very well. Calculation of θ_p yielded very low values and as a result Eq. (6.3) gave low energy absorption predictions when compared with the values obtained from the integration of the hysteresis curves. This difference between the values obtained from Eq. (6.3) and the experimental values could also be because the energy obtained through the use of Eq. (6.3) is calculated as the area under the load displacement curve (monotonic curve) which was constructed from the peak lateral loads obtained from a reversed cyclic test while the NBS experimental values represented the summation of the energy dissipated in each cycle up to the ultimate failure of the column. The low values of θ_p from the analytical calculation could be due to the manner in which the plastic hinge length was measured (see section 6.3) or to the assumed value for the elongation percentage of the D6 wire.

6.3 Plastic Hinge Lengths

An attempt was made to obtain the experimental plastic hinge length for each of the models. The plastic hinge length was taken as that length over which the majority of the longitudinal bars in the column had yielded. This length was determined experimentally as the height at which the strain gages indicated yielding of the longitudinal bars had occurred. The strains were those measured for the two cycles at $\mu = 4$ for the shear models and the two cycles at $\mu = 3$ for the flexure models. The plastic hinge was assumed to have fully developed at these respective stages. These values are given in Table 6.9. In addition, the extent of observed concrete spalling is also given in Table 6.9.

Empirical equations have been developed for the prediction of plastic hinge lengths. Two such equations are by Baker and Corley [31] and are as follows:

Baker's equation [31]:

$$l_p = 0.8 k_1 k_3 (z/d)c \quad (6.4)$$

TABLE 6.8 ULTIMATE MOMENT CAPACITIES

MODEL	ULTIMATE MOMENT (KIP-FT)		$\frac{M_{exp}}{M_{ACI}}$	θ_p EQ. 6.2	ENERGY (KIP-IN)	
	ACI	EXPERIMENTAL ¹ EQ. 6.1			EQ. 6.3 ³	EXPERIMENTAL ²
N1	35.32	38.35	1.09	0.160	72.92	309.8
N2	36.55	46.52	1.27	0.220	121.81	351.5
N3	35.32	39.76	1.13	0.279	127.32	243.6
N4	35.32	37.48	1.06	0.135	61.56	348.7
N5	36.55	46.61	1.28	0.160	88.95	379.4
N6	35.32	36.87	1.04	0.279	127.06	351.0

1 Including P - Δ effect.

2 Summation of energy absorbed up to ultimate state as defined by Zahn [30].

3 Based on a plastic hinge length equal to the spalled height.

TABLE 6.9 PLASTIC HINGE LENGTHS

MODEL	$\frac{P_e}{f'_c A_g}$	(L/D)	PLASTIC HINGE BASED ON MEASURED STRAINS (IN.)	MEASURED SPALL HEIGHT (IN.)	BAKER	CORLEY
N1	0.10	3	11 ¹	3.0	5.87	6.78
N2	0.20	3	11 ¹	4.0	6.32	6.78
N3	0.10	6	11 ²	5.0	11.75	8.67
N4	0.10	3	8	2.5	5.87	6.78
N5	0.20	3	8	3.0	6.32	6.78
N6	0.10	6	11	5.0	11.75	8.67

1 Measured strains at this height exceeded 7000 $\mu\epsilon$. The height of yielding is likely to be greater than this height.

2 Measured strains at this height exceeded 5000 $\mu\epsilon$. The height of yielding is likely to be greater than this height.

where

$k_1 = 0.7$ for mild steel or 0.9 for cold-worked steel

$k_3 = 0.6$ when $f'_c = 5100$ psi (35.2 N/mm²) or 0.9 for

$f'_c = 1700$ psi (11.7 n/mm²), assuming

$f'_c = 0.85$ x cube strength of concrete

z = distance of critical section to the point of contraflexure

d = effective depth of member

c = neutral axis depth at ultimate moment

Corley's equation [31]:

$$l_p = 0.5d + 0.2\sqrt{d} (z/d) \quad (6.5)$$

The values obtained for these equations are also given in Table 6.9.

An alternative experimental method for determining plastic hinge length which has been used in New Zealand is to instrument the potential hinge region with a large number of displacement transducers (LVDTs) such that a sufficient number of data points are available to determine local curvature. Because of data channel limitations at the time of conduct of the NBS model tests, a trade-off was made between external LVDTs and strain gages placed on longitudinal reinforcement. It was felt that the extent of longitudinal bar yielding could be more precisely determined using the internal gages.

The calculated plastic hinge lengths based on measured strains were greater than those predicted by Baker and Corley [31] as shown in Table 6.9. These lengths did not appear to increase with increasing displacement ductility as indicated by the strain readings along the longitudinal bar at higher displacement ductilities. This finding was also noted in references [5], [16], and [23].

Table 6.9 shows that the extent of spalling in the plastic hinge region was greater for models subjected to higher axial load. It was also greater for models constructed using microconcrete than for those constructed with ready-mix concrete. Increased plastic hinge lengths for greater axial loads were also noted in references [5], [10], and [23].

The extent of the spalled region was also dependent on column aspect ratio. Those models dominated by flexural behavior ($L/D = 6$) exhibited spalling in the plastic hinge region to a greater height than for those models whose behavior was dominated by shear ($L/D = 3$). This phenomenon was observed irrespective of the material used for construction of the columns.

The extent of yield penetration along longitudinal bars averaged 0.3 D or 3 in. (7.6 cm) into the base. This was determined by strain gage measurements along the longitudinal bars. Yielding of one of the longitudinal bars for model N5 was noted to extend to about 0.51 D [5 in. (12.7 cm)] into the base. This yielding occurred at $\mu = 6$ with a strain of $8300 \mu\epsilon$ recorded. Plots of peak cycle strains (averaged for north and south excursions) are shown in Figs. 6.20 - 6.25. Only four cycles were plotted since the strain gages debonded during large plastic elongations of the longitudinal bars.

6.4 Confining Steel Strains

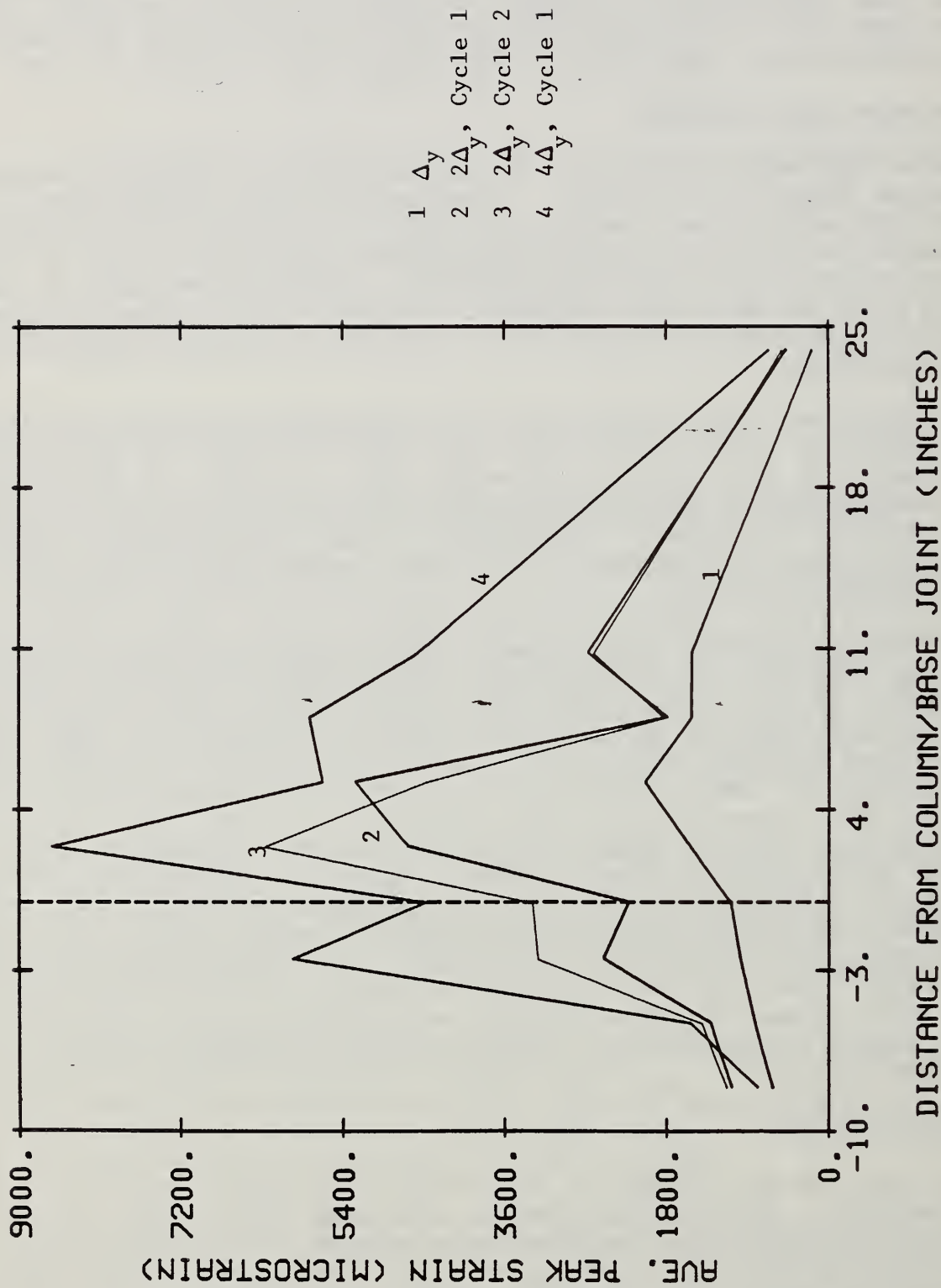
The results from model N3 will not be included in this discussion because of premature damage to the spiral. Some gages used to monitor strain in the confining spiral steel, especially those at the base of the column, were damaged during the casting of the models. The determination of the extent of yielding of spiral reinforcement was therefore based on the remaining gages and by visual inspection. A spiral was considered to have yielded if significant straightening of the spiral between longitudinal bars was observed.

Yielding of spiral reinforcement for all models was concentrated in the region beginning 0.05D [0.5 in. (12.7 mm)] into the base and extending approximately 0.2D [2 in. (5.08 cm)] above the base. Fracture of the spiral reinforcement generally occurred during the next ductility level following first yielding of the spiral. The exception to this was specimen N5, which exhibited yielding of the spiral at $\mu = 6$, with subsequent fracturing at a ductility level of $\mu = 10$.

Measured strains in spiral reinforcement averaging approximately $420 \mu\epsilon$ were noted at a height of 0.51 D [5 in. (12.7 cm)] above the base and $400 \mu\epsilon$ approximately 0.1 D [1 in. (2.35 cm)] into the base for the shear specimens. Yielding of one spiral at approximately 0.71 D [7 in. (17.8 cm)] into the base was noted for model N5 at $\mu = 6$. The recorded strain was $2700 \mu\epsilon$ at that load stage and remained practically unchanged for the remainder of the test. This would agree with the yield penetration into the base of one of the longitudinal bars in model N5 as noted earlier. Yielding of this particular spiral could have been caused by localized buckling of the longitudinal bar due to a large piece of aggregate pressing against it. The measured strain in the spiral reinforcement for model, N6 ($L/D = 6$) was approximately $200 \mu\epsilon$ at 0.2 D [2 in. (5.08 cm)] into the base and $150 \mu\epsilon$ at 1.02 D [10 in. (25.4 cm)] above the base. Based on the results of this test, it would appear that the CALTRANS requirement to extent the spiral into the footing to the point of tangency of the longitudinal bar hook is very conservative.

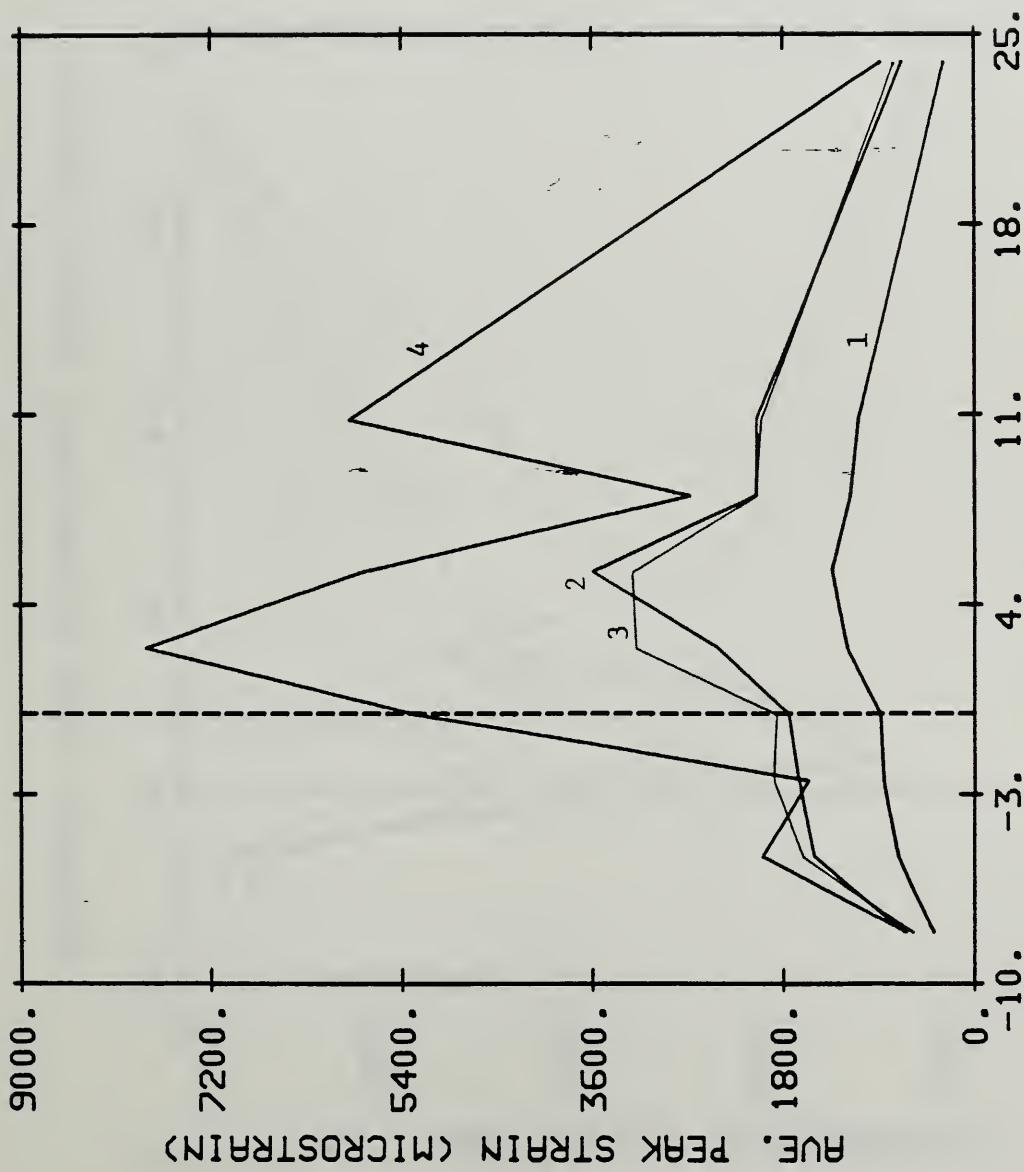
6.5 Ultimate Moment

The P-M curves for the flexure and shear models are shown in Figs. 6.26 and 6.27 respectively. The ultimate moments, including P - Δ effect, for the models with low axial load exceeded the predicted values using the ACI design charts for $\phi = 1$ by an average of 11 %. This increase from the ACI value in moment capacity was slightly greater for the microconcrete models than for those specimens constructed with ready-mix concrete. The ultimate moments for the two models (N2 and N5) with higher axial load showed an increase of 27% over those calculated using ACI procedures. This increase



PEAK STRAIN ALONG LONGITUDINAL BAR (MODEL N1)

Fig. 6.20

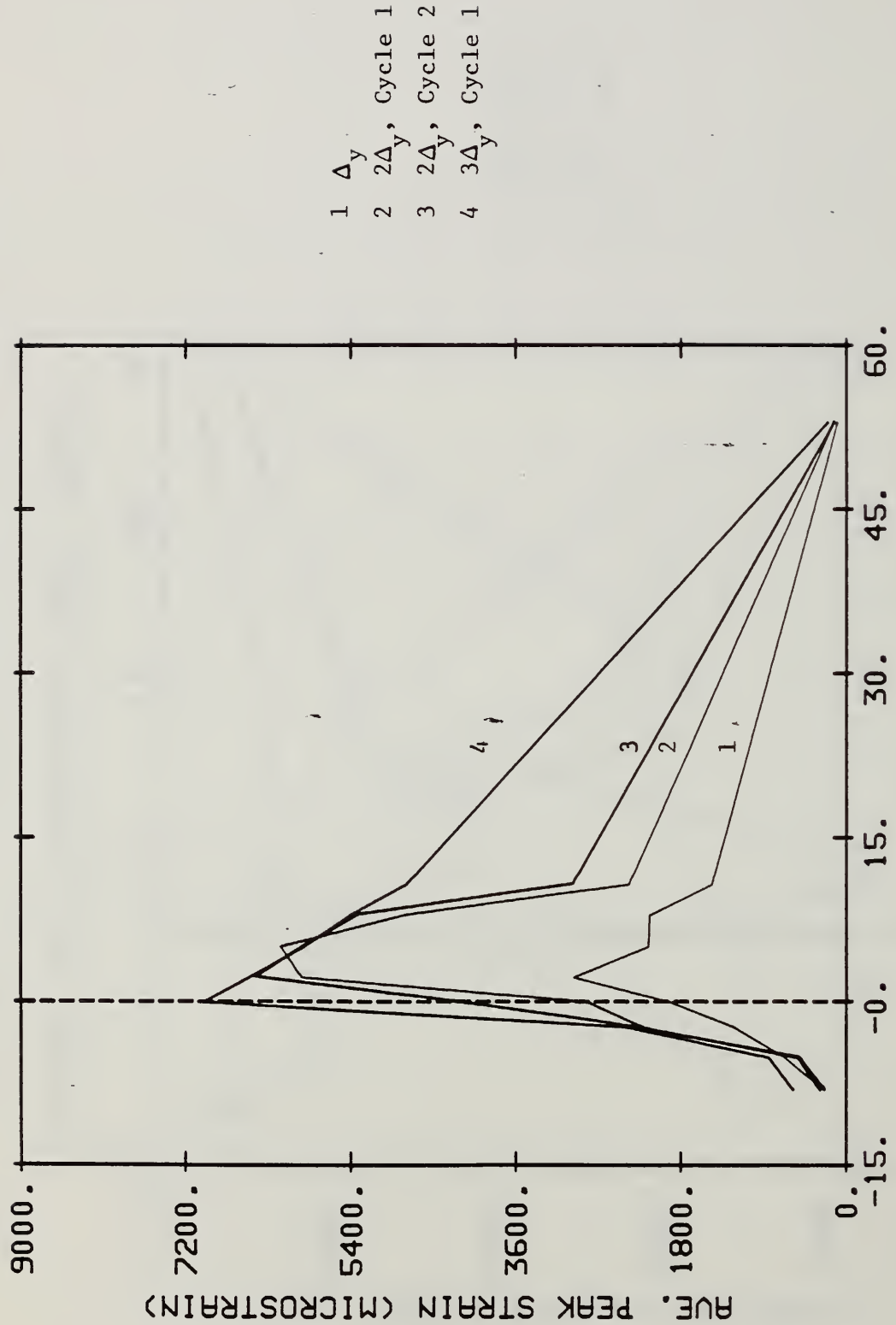


- 1 Δ_y , Cycle 1
- 2 $2\Delta_y$, Cycle 1
- 3 $2\Delta_y$, Cycle 2
- 4 $4\Delta_y$, Cycle 1

DISTANCE FROM COLUMN/BASE JOINT (INCHES)

PEAK STRAIN ALONG LONGITUDINAL BAR (MODEL N2)

Fig. 6.21

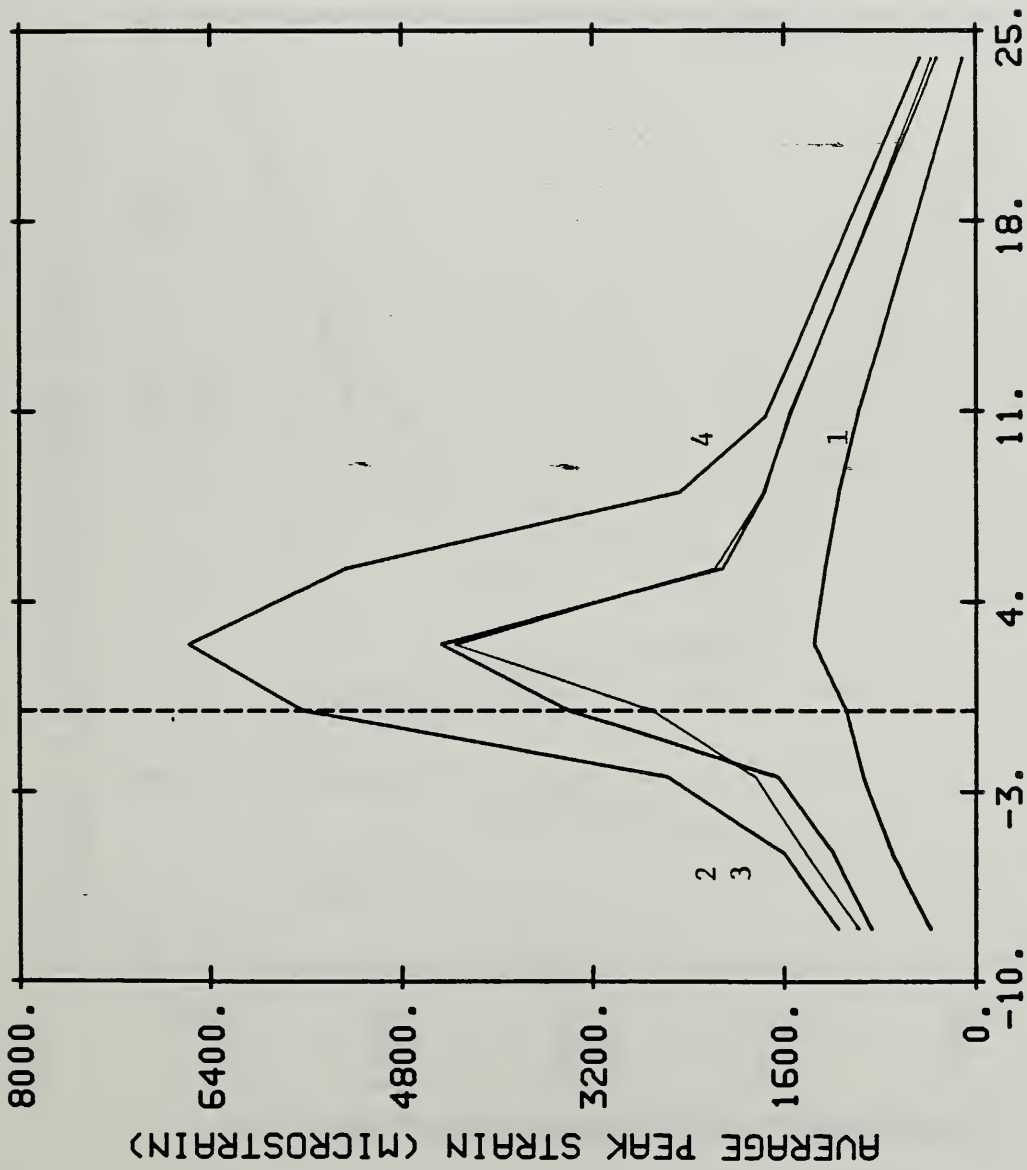


- 1 Δ_y , Cycle 1
- 2 $2\Delta_y$, Cycle 1
- 3 $2\Delta_y$, Cycle 2
- 4 $3\Delta_y$, Cycle 1

DISTANCE FROM COLUMN/BASE JOINT (INCHES)

PEAK STRAIN ALONG LONGITUDINAL BAR (MODEL N3)

Fig. 6.22

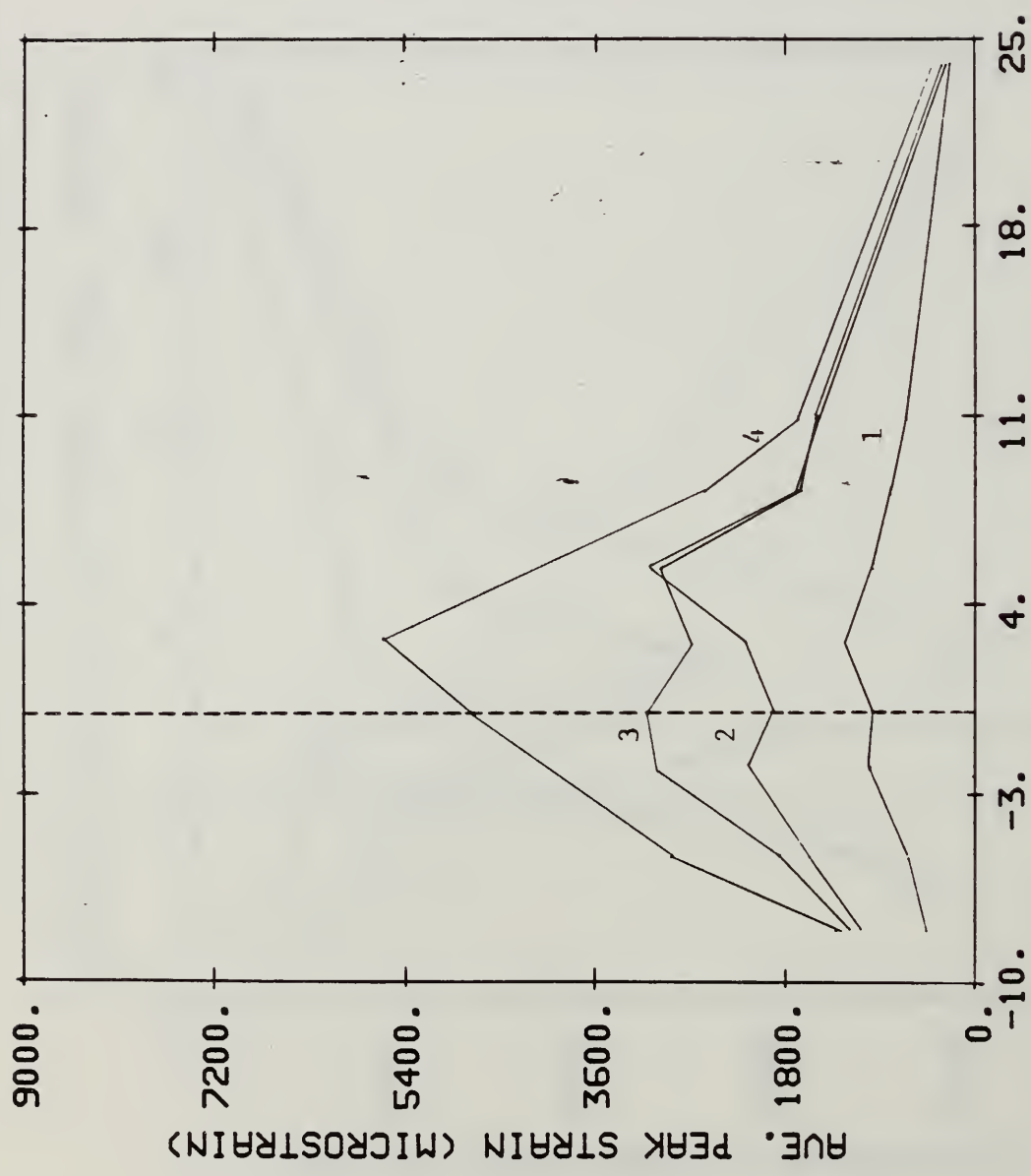


- 1 Δ_y , Cycle 1
- 2 $2\Delta_y$, Cycle 1
- 3 $2\Delta_y$, Cycle 2
- 4 $4\Delta_y$, Cycle 1

DISTANCE FROM THE COL/BASE JOINT (INCHES)

PEAK STRAIN ALONG LONGITUDINAL BAR (MODEL N4)

Fig. 6.23

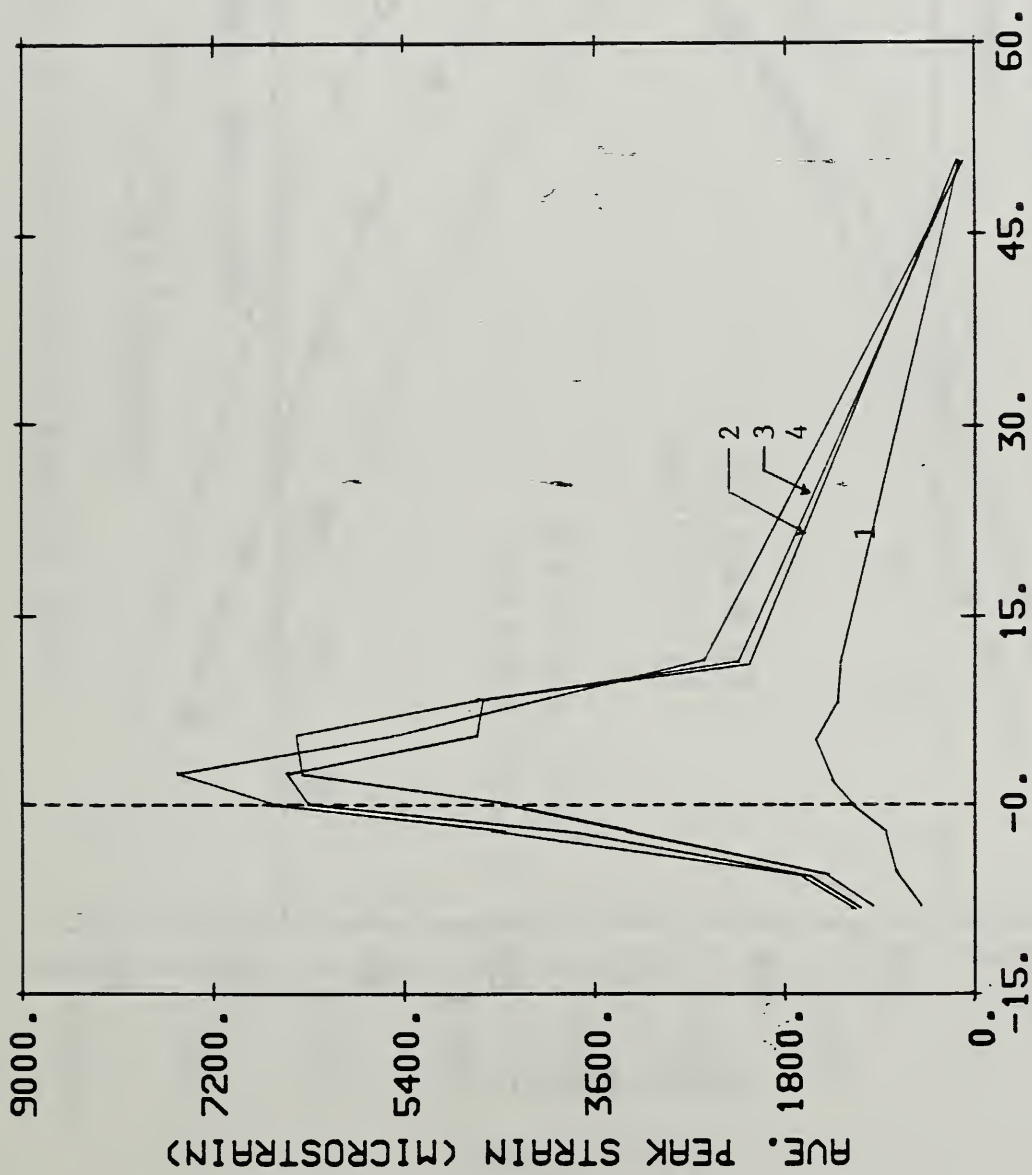


- 1 Δ_y
- 2 $2\Delta_y$, Cycle 1
- 3 $2\Delta_y$, Cycle 2
- 4 $4\Delta_y$, Cycle 1

DISTANCE FROM COLUMN/BASE JOINT (INCHES)

PEAK STRAIN ALONG LONGITUDINAL BAR (MODEL N5)

Fig. 6.24



- 1 Δ_y
- 2 $2\Delta_y$, Cycle 1
- 3 $2\Delta_y$, Cycle 2
- 4 $3\Delta_y$, Cycle 1

PEAK STRAIN ALONG LONGITUDINAL BAR (MODEL N6)

DISTANCE FROM COLUMN/BASE JOINT (INCHES)

Fig. 6.25

P-M DIAGRAM FOR FLEXURE MODELS

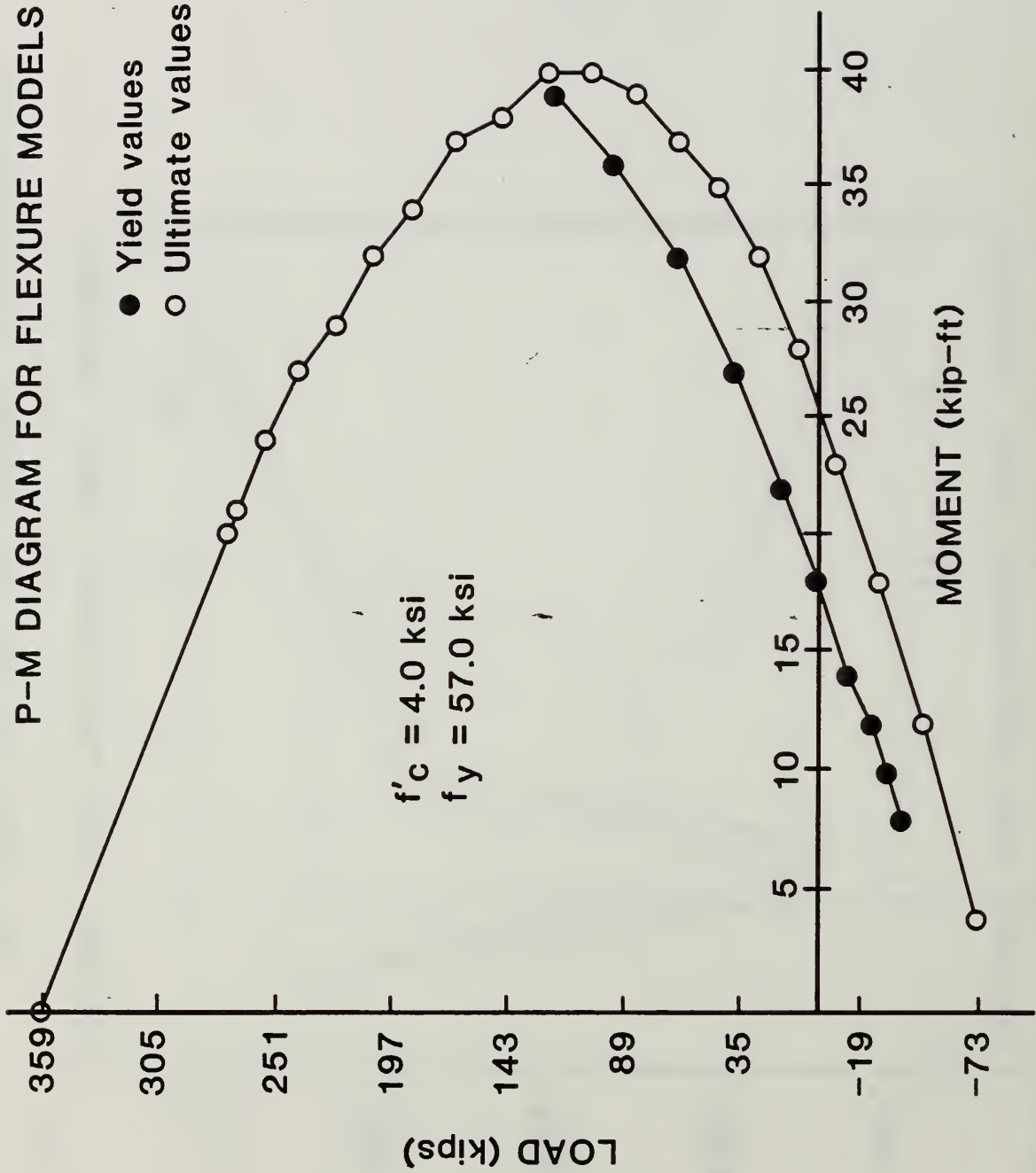


Fig. 6.26

P-M DIAGRAM FOR SHEAR MODELS

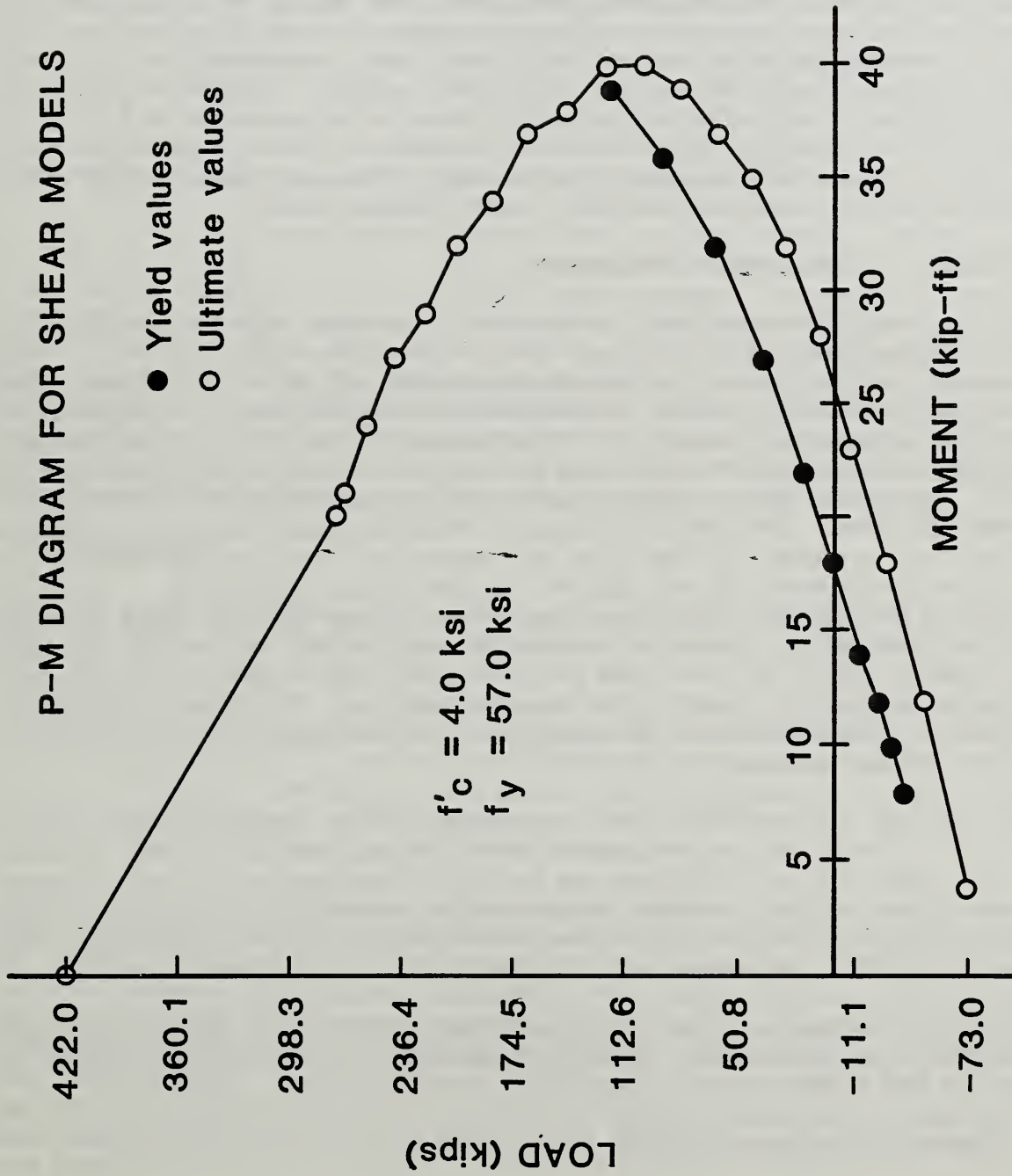


Fig. 6.27

in ultimate moment from the predicted values for higher axial loads was also noted by Gill [10] and Kuribayashi [11]. The experimentally observed ultimate moments were found to be nearly identical between companion specimens cast from microconcrete and ready-mix concrete. It also appears that the ACI design charts produce lower estimates of ultimate moment for higher axial loads. The ultimate moments obtained experimentally and those from the ACI design charts are given in Table 6.8.

As in previous studies [11], [13], and [16], a drop in lateral load was noted during the second cycle at a given ductility level. This was because the majority of the cracks formed during the first cycle. The successive decrease in lateral load was more pronounced when spiral yielding was also involved. On the average, for all six models, the maximum lateral load during any second cycle at a given ductility level decreased by 3.9 % with respect to that observed during the first cycle. This decrease was smaller for two models with higher axial load -- an average of 2.72 % as compared with an average drop of 4.47 % for the four models with the lower axial load. This could be due to the closure of cracks under higher axial loads which would permit an increase in the lateral load.

6.6 Adequacy of Transverse Confinement

The spiral reinforcement used in the model studies appears adequate to obtain displacement ductilities 10 for shear models ($L/D = 3$) and displacement ductilities of 4 for flexure models ($L/D = 6$). Beyond these ductilities fracture of spiral reinforcement and buckling of longitudinal reinforcement generally occurred. The spacing of the spirals was adequate to prevent longitudinal bar buckling as long as the spiral remained intact. It would therefore appear that in order to increase the ductility capacity for these columns, the amount of spiral reinforcement would have to be increased, or, contrarily, the size and number of longitudinal bars would have to be increased in an effort to forestall buckling. Studies performed in New Zealand [16] have shown that larger diameter bars used for spiral reinforcement, placed at a greater spacing but achieving the same reinforcement ratio as that used in this study, have resulted in higher achievable ductility factors for a given column. Further research is warranted to investigate the optimum spiral reinforcement ratio as well as the effect of bar size and pitch.

Neither ACI [2] nor CALTRANS [28] currently have a ductility requirement for bridge columns corresponding to that implemented in the New Zealand code [8]. Such a quantification can be highly subjective and will depend on, among other things, seismic history at a potential construction site, distance from active faults, local sub-surface soil conditions, and anticipated dynamic response including soil-structure interaction.

CALTRANS defines the potential plastic hinge length over which transverse reinforcement (as defined by CALTRANS; see section 2.3.2 of this paper) is required as the greater of:

1. Diameter of column = 9.8 in.

2. Required Length of Confining Spiral = Height of column / 6.0
 - a. $59 \text{ in.} / 6 = 9.8 \text{ in.} (25 \text{ cm})$ for models N3 and N6
 - b. $29.5 \text{ in.} / 6 = 4.9 \text{ in.} (12.5 \text{ cm})$ for models N1, N2, N4, and N5
3. But not less than 24 in. (full scale). For the models this requirement becomes $24 \text{ in.} / 6.1 = 3.9 \text{ in.}$, which is less than either of the above requirements.

The length over which the extra transverse confinement was required was, therefore, equal to 1.0 D [9.8 in. (25 cm)] for the flexure specimens. This value is greater than the observed maximum extent of surface spalling -- 0.51D [5 in. (13 cm)] -- but less than the calculated plastic hinge length based on measured strains. A similar situation exists for the shear specimens: the required length of spiral was 0.5D [4.9 in. (12.5 cm)]. This can be compared with an average observed spall length of 0.31D [3 in (7.6 cm) and a calculated longitudinal bar yield length of between 0.8-1.1D [8-11 in. (20-28 cm)] for the model shear columns. Given these conflicting data it is not possible to draw any definitive conclusions regarding the sufficiency of current CALTRANS recommendations as to the required length of spiral in the plastic hinge region. It should be noted, however, that the data presented in Table 6.9 indicate that the CALTRANS confinement lengths calculated above would be less than the plastic hinge lengths calculated using the procedures suggested by Corley and Baker in all but one case, that being for the flexure column ($L/D = 6$) using the Corley procedure. This would indicate a possible unconservative situation if we assume that it is desirable to have transverse confinement extending beyond the potential plastic hinge region.

6.7 FAILURE MODES

The failure mode for models N3 and N6 was dominated by flexural effects. This failure mode consisted of the formation of horizontal flexural cracks in the vicinity of the plastic hinge region, followed by gradual extension of the cracks around the circumference of the column. Increased lateral displacement resulted in spalling of concrete at the base of the column to a height of approximately one column diameter, followed by yielding of spiral reinforcement, fracture of the spiral, and, ultimately, buckling and fracture of longitudinal reinforcement in the plastic hinge region. The aspect ratio (L/D) for the flexural models was 6.

The failure mode for models N1, N2, N4 and N5 was similar to that for the flexure specimens, with the exception that extensive diagonal cracks formed on the sides of the column in the plastic hinge region prior to spalling. Despite the presence of diagonal cracking, the column aspect ratio ($L/D = 3$) was not sufficiently low to permit a pure shear failure. Japanese studies [20] have shown that columns with aspect ratios of 2.2 do exhibit failure in pure shear, while columns with aspect ratios of 3.8 and 5.4 are dominated by flexural effects. It would appear from this study that columns with aspect ratios of greater than 3 will result in a flexural failure mode.

6.8 COMPARISON OF RESULTS WITH PREVIOUS STUDIES

The column test parameters used in the New Zealand and the Japanese studies were somewhat different from those used in the NBS study. For example, higher axial loads and greater amounts of transverse steel were investigated in the studies performed in New Zealand. Different loading histories and transverse steel ratios were also a deterrent to possible comparisons of results from this study with those performed in Japan.

However, some direct comparisons between previous studies and the current NBS work can be made. For example, most researchers have observed that yielding of the transverse steel had no significant effect on the lateral load. Fracturing of the spiral did cause a significant drop in the lateral load as noted both by NBS and a Japanese study [11].

Also, a drop in the lateral load for repetitions following the first cycle at a particular ductility level was noted in the NBS study and the New Zealand and Japanese studies. In a study done by Gill [10], the yield displacement was found to decrease for higher axial loads. The yield displacement for the NBS microconcrete shear models was smaller for the model subjected to the higher axial load (0.38 in. for the lower axial load and 0.22 in. for the higher axial load). This effect was less pronounced for the models constructed using ready-mix concrete in the NBS study (0.21 for the lower axial load and 0.19 in. for the higher axial load). Finally, the failure mode for columns with an aspect ratio of 3 or greater was predominated by flexural effects.

One difference between the results of the NBS work and of a study done by Ng [6] is that for similar transverse reinforcement ratios, the model in Ng's study achieved a higher displacement ductility than the NBS models. Although the transverse reinforcement ratios were similar, the bar size used in Ng's models was larger and the spiral pitch was greater than those used in the NBS study. The longitudinal reinforcement ratio for Ng's model was also greater by approximately 25 %.

Petrovski and Ristic's [35] tests, performed in Yugoslavia, used similar transverse and longitudinal reinforcement ratios to the flexure models in the NBS study. Their loading history, however, was significantly different. Some useful comparisons between the Yugoslav and NBS tests are as follows:

1. Columns subjected to a higher axial load had a higher experimental maximum moment.
2. The experimental yield displacements were approximately equal between Petrovski's tests and those for the NBS ready-mix models. These values, specifically, were 0.61 in. and 0.22 in. (15.4mm and 5.6mm) for Petrovski's flexure and shear models, respectively and 0.66 in. and 0.20 in. (16.7mm and 5mm) for the flexure and shear models cast using ready-mix concrete at NBS. No difference in the yield displacement was noted for different axial loads in the Yugoslav tests.

3. The ultimate displacement ductilities for the Petrovski's flexure models were 4.58 and 3.31 for the models subjected to the lower and higher axial loads, respectively. These values are slightly lower than those obtained for the NBS flexure models.
4. The ultimate displacement ductilities for Petrovski's shear models were 5.96 and 5.73, for the models subjected to the lower and higher axial load, respectively. These values are much lower than those obtained for the NBS shear models and could be a result of the lower transverse steel ratio used in Petrovski's study.
5. The loading history, transverse steel ratio, and the aspect ratio for the flexure models are sufficiently similar for the Yugoslav and NBS tests to bear direct comparison. The slight difference in the ultimate displacement ductilities as noted in observation 4 would seem to indicate that the cycling of an element 5 or 10 times at a particular displacement ductility does not significantly effect the ultimate displacement ductility.

7.0 CONCLUSIONS AND FUTURE RESEARCH NEEDS

7.1 CONCLUSIONS

Current CALTRANS specifications [28] were sufficient to prevent pullout of the longitudinal bars from the footing for all specimens tested, and to prevent shear failure in columns with $L/D = 3$ for axial loads of $0.10 f'_c A_g$ and $0.20 f'_c A_g$. Ultimate displacement ductilities of 10 were achieved for shear specimens with $L/D = 3$ and displacement ductilities of five for specimens with $L/D = 6$. CALTRANS does not presently specify a minimum ductility level required for column design. However, experimentally observed ductilities for NBS model specimens compared favorably with similar columns tested in New Zealand. Specific results from the model tests are as follows:

1. Material Dependent Behavior: Microconcrete vs. Ready-Mix Concrete

- o Slightly higher ultimate displacement ductilities were obtained for models cast with ready-mix concrete. This behavior is believed to result from aggregate interlock in the ready-mix concrete, where significantly larger nominal mean sized aggregates were used.
- o Models constructed from ready-mix concrete exhibited an average of 10.25 % (the difference between models N3 and N6 was omitted in this calculation due to the premature fracture of the spiral in model N3) higher total energy absorption capacity than their microconcrete counterparts. This appears to be a consequence of the extended ductility achieved through aggregate interlock in the inelastic regime; since energy dissipated per cycle was comparable prior to ultimate failure.
- o No difference in the experimental ultimate moments between the two types of concrete was observed.

2. Effect of Magnitude of Axial Load.

Tests were conducted to determine the effect of axial load on specimens with $L/D = 3$. Two axial load levels were investigated: $P = 0.10 f'_c A_g$ and $0.20 f'_c A_g$. These tests indicated:

- o Higher energy absorption capacity for models subjected to higher axial load: a 13.5 % rise was noted for microconcrete models and an 8.8 % rise for models constructed from ready-mix concrete at axial loads of $0.10 f'_c A_g$ and $0.20 f'_c A_g$ respectively.
- o Higher displacement ductilities were achieved for models subjected to higher axial load.
- o Ultimate moments for models with higher axial load were greater than for those with the lower axial load. This is a natural consequence of moving towards the balance point on the P-M curve from an initially low axial state of stress.

- o Experimentally measured ultimate moments were greater than those predicted using ACI methods; this was particularly pronounced at higher axial loads. The percent increase from the ACI predicted values were 10.8 for the models subjected to the lower axial load and 27.4 for the models subjected to the higher axial load. It would, therefore, appear that the ACI method results in conservative ultimate moment predictions for columns under high axial loads (greater than $0.2 f'_c A_g$).
3. Plastic hinge length increases with increasing aspect ratio (L/D). It does not, however, appear to increase for increased displacement ductility.

Testing of the first full-scale prototype flexure column was completed at the end of July, 1986. Detailed results from that test were not available in time for inclusion in this report. However, the ultimate displacement ductility from the prototype specimen was approximately six. This compares favorably with the displacement ductility factor of five obtained for the flexure model constructed with ready-mix concrete.

7.2 PRACTICAL APPLICATIONS

The findings from this study point towards some practical applications for the design engineer. It was found that, in general, the spiral strains in the "foundation" base at a depth of $0.1 D$ [1 in. (25 mm)] were 400 microstrain or less, well below yield strain. This would indicate that the requirement to extend the spiral into the footing to the point of tangency of the longitudinal bar hook may be overly conservative.

The probable plastic moment as defined by CALTRANS [28] is 1.3 times the nominal ultimate moment. This represents the maximum anticipated moment that a supporting foundation would need to resist. This design factor increase of 30 % from the nominal ACI moment agrees well with the 27.4 % obtained for models subjected to higher axial load ($0.2 f'_c A_g$). However, it would seem to be conservative for models subjected to lower axial load (less than $0.1 f'_c A_g$). A reduction of this multiplier for structures subjected to lower axial loads would seem warranted and would result in smaller, less costly footings.

The maximum extent of yielding of the longitudinal bars into the footing was $0.51 D$ [5 in. (127 mm)]. The corresponding value for yield penetration into the footing for the prototype column would then be 30 in. (760 mm) for a 60 in. (1.52 m) column. The basic development length for a #14 bar (the longitudinal reinforcement used in the NBS prototype column) is 86 in. (2.18 m) based on a concrete strength of 3500 psi (24 MPa) as was the case for the models. This development length would therefore appear to be adequate for anchorage of longitudinal reinforcement.

7.3 FUTURE RESEARCH NEEDS

Comparisons between NBS model test results and similar tests conducted in New Zealand and Japan have indicated that use of larger size spiral reinforcing bars at larger spacing may prove more effective in achieving greater displacement ductility than the use of smaller diameter spiral reinforcing bar at closer spacing. Furthermore, the use of larger longitudinal bars, and/or greater numbers of longitudinal reinforcing bars, than presently required by CALTRANS specifications may stay the onset of longitudinal bar buckling, and therefore also increase ultimate ductility. Both techniques merit further detailed investigations to establish statistically useful trend information. Along these lines, use has been made in Japan of independent hoops for transverse confining reinforcement in lieu of a continuous spiral for large diameter columns. The effectiveness of this approach, as compared to the use of a continuous spiral, should be investigated.

Higher displacement ductilities and energy absorption capacities were achieved in models subjected to higher axial loads. This suggests that increasing triaxial confining forces within the plastic hinge region might lead to higher displacement ductilities, and hence greater ability to dissipate energy. One possible approach would be to use active reinforcement in the form of lateral prestress. The level of prestressing and the method used to achieve the prestress, particularly where stressing lengths are short, should be among the parameters for future investigation.

Another method to help increase the ductility of bridge columns may be to use a perforated metal casing either in addition to or instead of the spiral in the potential plastic hinge region. This is suggested as a result of observed column failure occurring soon after the fracturing of the spiral. The thickness of the casing, the toughness and type of material from which it is fabricated, and the length of of the casing should be some of the parameters considered.

Finally, the testing of the first full scale prototype specimen has proven the feasibility of conducting such tests within the laboratory. Following the results of similitude studies relating the behavior of the model to prototype specimens, it may be desirable to conduct further benchmark (full scale) tests which address the important questions of the performance of existing bridge columns designed using pre-1971 specifications, and the effectiveness of (as-yet-untested) retro-fit techniques which are now being used to bring these columns up to current standards.

REFERENCES

1. ACI Committee 318, "Building Code Requirements for Reinforced Concrete", ACI 318-71, American Concrete Institute, 1971.
2. ACI Committee 318, "Building Code Requirements for Reinforced Concrete", ACI 318-77, American Concrete Institute, 1977.
3. ACI Committee 318, "Building Code Requirements for Reinforced Concrete", ACI 318-83, American Concrete Institute, 1983.
4. ACI Committee 340, "Design Handbook", in accordance with the Strength Design Method of ACI 318-77, Vol. 2, SP-17A(78), American Concrete Institute, 1978.
5. Ang, Beng Ghee, Park, R., and Priestley, M. J. N., "Ductility of Reinforced Concrete Bridge Piers Under Seismic Loading", Department of Civil Engineering, University of Canterbury, New Zealand, Feb. 1981.
6. Carpenter, James E., Roll, Frederic, and Zelman, Maier I., "Techniques and materials for structural models" in Models For Concrete Structures, ACI Publication SP-24, 1970.
7. "Code of Practice for the Design of Concrete Structures", First Draft DZ 3101, Standards Association of New Zealand, 1978
8. "NZS 3101: 1982 'Code of Practice for the Design of Concrete Structures'" (Two volumes: code and commentary), Standards Association of New Zealand, 1982.
9. "Highway Bridge Design Brief", Ministry of Works and Development, New Zealand, Issue C, July 1973.
10. Gill, Wayne D., "Ductility of Rectangular Reinforced Concrete Columns with Axial Load", Department of Civil Engineering, University of Canterbury, New Zealand, Feb. 1979.
11. Kuribayashi, Eiichi, et. al., "Reversed Cyclic Loading Test of Bridge Pier Models", Technical Memorandum of PWRI No. 1801, Earthquake Engineering Division, Earthquake Disaster Prevention Department, Public Works Research Institute, Ministry of Construction, October, 1981.

12. Lew, H. S., Leyendecker, E. V., and Dikkers, R. D., Engineering Aspects of the 1971 San Fernando Earthquake, NBS Building Science Series #40, Dec. 1971.
13. Munro, I. R. M., Park, R., and Priestley, M. J. N., "Seismic Behaviour of Reinforced Concrete Bridge Piers", Department of Civil Engineering, University of Canterbury, New Zealand, Feb. 1976.
14. Nasser, K. W., Kenyon, J. C., "Why Not 3 X 6 Inch Cylinders for Testing Concrete Compressive Strength?" in the Journal of the American Concrete Institute, Proceedings V. 81, January-February 1984 / No. 1.
15. "New Zealand Draft Concrete Code", New Zealand National Society for Earthquake Engineering.
16. Ng, Kit Heng, Park, R., and Priestley, M. J. N., "Seismic Behaviour of Circular Reinforced Concrete Bridge Piers", Department of Civil Engineering, University of Canterbury, New Zealand, Feb. 1978.
17. Ohno, Tomonori and Nishioka, Takashi, "An Experimental Study on Energy Absorption Capacity of Columns in Reinforced Concrete Structures", in Structural Engineering/Earthquake Engineering, Proceedings of the Japan Society of Civil Engineers, Vol. 1, No. 2, Oct. 1984.
18. Ohta, Minoru, "Experimental Study on the Behavior of Reinforced Concrete Bridge Piers Under Horizontal Load Reversals", Public Works Research Institute, Ministry of Construction.
19. Park, R., and Priestley, M. J. N., "Code Provisions For Confining Steel in Potential Plastic Hinge Regions of Columns in Seismic Design", University of Canterbury, New Zealand.
20. "Performance and Strengthening of Bridge Structure and Research Needs", Proceedings - Second Joint U. S. - Japan Workshop, September, 1985.
21. Priestley, M. J. N., and Park, R., "Seismic Resistance of Reinforced Concrete Bridge Columns", University of Canterbury, New Zealand.
22. Priestley, M. J. N., and Park, R., Strength and Ductility of Bridge Substructures, RRU Bulletin 71, University of Canterbury, Dept. of Civil Engineering, Dec. 1984.

23. Priestley, M. J. N., Park, R., and Potangaroa R. T., "Ductility of Spirally Confined Concrete Columns", Journal of Structural Division, Proceedings of the ASCE, Vol. 107, Jan. 1981.
24. "Recommendations for Future Research", Applied Technology Council Workshop on Earthquake Resistance of Highway Bridges, Jan. 1979.
25. Sabnis, Gajahan M., Harris, Harry C., White, Richard N., Mirza, M. Saeed, Structural Modeling and Experimental Techniques, Prentice Hall, 1983.
26. "Seismic Design Guidelines for Highway Bridges", Applied Technology Council, FHWA RD 81/081.
27. "Standard Specifications for Deformed Steel Wire for Concrete Reinforcement", ASTM A-496, Vol. 01.04, 1984.
28. "Standard Specifications for Highway Bridges" as amended by AASHTO interims through 1984 with revisions by CALTRANS, AASHTO, 1983.
29. Woodward, Kyle and Rankin, Frank, "The NBS Tri-Directional Facility", NBSIR 84-2879, U. S. Department of Commerce, National Bureau of Standards, May 1984.
30. Zahn, F. A., Park, R., and Priestley M. J. N., "Design of Reinforced Concrete Bridge Columns For Strength and Ductility", Department of Civil Engineering, University of Canterbury, New Zealand, March, 1986.
31. Park, R., and Paulay, T., Reinforced Concrete Structures, John Wiley & Sons, New York, 1975.
32. Standard Specifications for Highway Bridges, adopted by the American Association of State Highway Officials, 10 th. ed., Nov. 1969.
33. Standard Specifications for Highway Bridges, adopted by the American Association of State Highway and Transportation Officials, 13 th. ed., 1983.
34. "Bridge Planning and Design Manual", Vol. 1 - Design Specifications, California Department of Transportation, Jan. 1971.

35. Petrovski, Jakim and Ristic, Danilo, "Reversed Cyclic Loading Test of Bridge Column Models", Report IZII 84 -- 164, Institute of Earthquake Engineering and Engineering Seismology, University of "Kiril and Metodij", Skoje, Yugoslavia, Sept. 1984.
36. Kuribayashi, Eiichi, et. al., "New Specifications for Earthquake-Resistant Design of Japanese Highway Bridges" in the Proceedings of the 12th Joint Meeting of the US-Japan Panel on Wind and Seismic Effects, NBS SP 665, Washington, D.C., 1980.
37. Personal communication with Dr. M.J.N Priestley, Universtiy of Canterbury, 1985.
38. Personal communication with Mr. Koichi Minosaku, Public Works Research Institute, 1986.

APPENDIX A: PROGRAM "TURBO-LOOP"

Measurement of the amount of energy absorbed by a bridge column subjected to reversed cyclic loading is a difficult process, involving the evaluation of the summation of the areas enclosed by the lateral load vs lateral deflection curves generated for each cycle. Because typical experimentally derived load-deflection curves exhibit noise and other irregularities (due to such physical phenomena as the fracture of reinforcing bars and sudden crushing of concrete), evaluation of the area bounded by such curves is not easily tractable through numerical integration procedures.

An alternative, rapid method for the evaluation of cyclic strain energy was developed for this project. Each hysteresis curve for a particular model test was plotted individually on a high resolution (1280 x 1024 pixel) color raster device. The area enclosed by that curve was then filled with a specified color. The number of pixels of that color was then tabulated. A conversion factor was then used to convert the tabulated number to units of energy in kip-in (kN-mm). This value represented the energy absorbed by the model for that cycle. The process of integrating each load cycle for one model test can then be completed in a matter of minutes by automating the entry of data from each cycle. A window size of 800 by 800 pixels was used to determine the energy absorption capacities. This resulted in less than 1 % error over that for a window size of 1280 by 1024 pixels while greatly increasing computational speed.

A FORTRAN program listing of "Turbo_Loop" is presented in the following pages. This was implemented on a VAX 11/750 computer system with a DMA driven Raster Technologies One/80 color raster display device. A second FORTRAN program, "Graph", is presented in Appendix B. This is a graphics post-processor written specifically for the interactive analysis of cyclic column test data. It uses as input the data produced from Turbo-Loop.

```

C *****
C
C PROGRAM TURBO_LOOP
C
C PURPOSE:
C
C CALCULATE THE ENERGY ABSORBED BY A STRUCTURE SUBJECTED
C TO CYCLIC LOADING BY INTEGRATING THE AREA WITHIN THE
C EXPERIMENTALLY OBTAINED HYSTERESIS CURVES.
C
C METHOD:
C
C THE INTEGRATION IS DONE BY "COUNTING THE DOTS" WITHIN
C A HYSTERESIS CURVE. THE HYSTERESIS CURVE IS PLOTTED ON
C A HIGH RESOLUTION COLOR GRAPHICS DEVICE. THE HYSTERESIS
C CURVE IS THEN FLOODED WITH A PARTICULAR COLOR WHICH HAS
C A COLOR INDEX, A, ASSOCIATED WITH IT AND THE BACKGROUND
C WITH A DIFFERENT COLOR WHICH HAS COLOR INDEX, B,
C ASSOCIATED WITH IT. THE PROGRAM THEN COUNTS THE NUMBER
C OF PIXELS WITH COLOR INDEX A. THIS NUMBER REPRESENTS
C THE AREA WITHIN THE HYSTERESIS CURVE IN PIXELS WHICH IS
C THEN CONVERTED TO UNITS OF ENERGY (KIP-IN).
C
C IMPLEMENTATION:
C
C GRAPHICS:
C
C THE PROGRAM MAKES USE OF A RASTER TECH MODEL ONE/80
C COLOR GRAPHICS DEVICE WHICH HAS A RESOLUTION OF 1280 BY
C 1025 PIXELS FOR OUTPUT DISPLAY. CONSULT THE RASTER
C TECHNOLOGIES HANDBOOK FOR EXPLANATION OF CALLS TO THE
C "ONELIB" LIBRARY.
C
C DATA FORMAT:
C
C DATA FOR TURBO_LOOP IS GENERATED THROUGH THE FOLLOWING
C PROCEDURE:
C
C 1) NBS SPECIFIC:
C GENERATE PLOT FILES CONSISTING OF ONE COLUMN EACH
C OF THE Y-COORDINATES ( TYPICALLY LOAD ) AND THE X-
C COORDINATES (TYPICALLY DISPLACEMENT ). THESE PLOT
C FILES ARE AUTOMATICALLY GENERATED USING PROGRAM
C UT:$DDP FROM ANY SET OF TEST DATA OBTAINED EITHER
C BY THE TTF FACILITY OR BY THE LARGE SCALE TEST
C FACILITY IN BUILDING 202. EACH PLOT FILE SHOULD
C ONLY REPRESENT ONE CYCLE.
C
C 2) NBS SPECIFIC:
C STRIP KEY DATA FROM THE PLOT FILES NEEDED BY TURBO_
C LOOP. THIS CAN BE DONE AUTOMATICALLY BY RUNNING THE
C CONVERSION PROGRAM "POLYCONV" OR "JLG" AND ENTERING
C THE NAMES OF THE TWO PLOT FILES, THE FILENAME OF THE
C CONVERTED DATA ( MUST HAVE AN ".INP" EXTENSION ) AND

```

C THE IDENTIFYING TITLE TO BE PLOTTED ON THE RASTER
C TECH ONE/80. THE CONVERTED FORMAT AFTER RUNNING
C "POLYCONV" OR "JLG" IS AS FOLLOWS:
C

- C A) TITLE (A80 FORMAT)
C B) XMIN, XMAX, YMIN, YMAX, NPTS
C

C WHERE:

C XMIN - MINIMUM VALUE OF THE X-COORDINATE IN
C (E12.5 FORMAT)
C XMAX - MAXIMUM VALUE OF THE X-COORDINATE IN
C (E12.5 FORMAT)
C YMIN - MINIMUM VALUE OF THE Y-COORDINATE IN
C (E12.5 FORMAT)
C YMAX - MAXIMUM VALUE OF THE Y-COORDINATE IN
C (E12.5 FORMAT)
C NPTS - NUMBER OF DATA (X,Y) PAIRS IN
C (I5 FORMAT)
C

- C C) EXAMPLE: THE (X,Y) PAIRS IN 2*(E12.5) FORMAT
C

C 0.1567E+00 0.0020E+00
C 0.2389E+00 0.0789E+00
C ETC.
C

C NOTE THERE MUST BE 'NPTS' NUMBER OF SUCH PAIRS
C

C [GENERAL USERS NOTE] PROGRAM WILL ACCEPT ANY
C EXTERNALLY GENERATED TEST DATA FILES PROVIDED
C THEY HAVE THE ABOVE FORMAT.
C

C 3) NBS SPECIFIC:

C LOAD A TAPE ON DRIVE MM0: (THE ONLY ONE ON THE PDP
C 11/34). THE TAPE HAS TO BE INITIALIZED AS A
C FILES-11 TAPE. THIS HAS TO BE DONE ONLY ONCE.
C

- C A) LOGIN ON THE PDP 11/34
C B) ALLOCATE MM0:
C

C GO TO STEP D IF TAPE HAS BEEN INITIALIZED.
C

C NOTE: INITIALIZATION OF THE TAPE CAN ONLY BE
C DONE FROM A PRIVILEGED ACCOUNT.
C

- C C) INS
C FILE? DL0:[1,54]INI
C INITIALIZE/DENSITY=1600 MM0:YOURLABLE_NAME (6
C CHARACTERS)
C D) MOUNT MM0:YOURLABLE_NAME
C E) COPY CONVERTED_FILENAME.INP MM0:
C (WHERE THE CONVERTED_FILENAME.INP IS THE OUTPUT
C FROM "POLYCONV" OR "JLG")
C

- C F) DISMOUNT MM0:
- C G) DEALLOCATE MM0:
- C H) LOGOUT (AND TRANSFER TAPE TO VAX TAPE DRIVE)
- C

C 4) NBS SPECIFIC
C ON THE VAX 11/750

- C A) LOAD TAPE
- C B) LOGIN
- C C) ALLOCATE MSA0:
- C D) MOUNT/OVERRIDE=(ACCESSIBILITY,IDENTIFICATION,
C OWNER_IDENT) MSA0:

C OR

C IF THE PROGRAM IS AVAILABLE TYPE:
C @PDP_TO_VAX

- C E) COPY MSA0:CONVERTED_FILENAME.EXT
- C TO? YOUR WORK DIRECTORY FOR RUNNING TURBO_LOOP
- C F) DEALLOCATE MSA0:
- C G) DISMOUNT MSA0:

C [GENERAL USERS]

- C 5) IT IS POSSIBLE (AND DESIRABLE) TO PROCESS AN ENTIRE
C CYCLIC LOAD TEST IN ONE BATCH OPERATION; TO DO THIS,
C CREATE A FILE CALLED "LIST.LIS" WHICH CONTAINS THE
C CONVERTED FILENAMES WITHOUT THEIR EXTENSIONS. EACH
C FILENAME SHOULD BE ON A DIFFERENT LINE

C EXAMPLE:

C IF A TEST HAS 5 LOAD CYCLES AND THE CONVERTED FILE
C NAMES WERE CYCLE1.INP, CYCLE2.INP, ... , CYCLE5.INP,
C THE FILE "LIST.LIS" SHOULD CONTAIN THE FOLLOWING:

C CYCLE1
C CYCLE2
C CYCLE3
C CYCLE4
C CYCLE5

- C 6) YOU ARE NOW READY TO CALCULATE THE ENERGY WITHIN A
C HYSTERESIS CURVE USING TURBO_LOOP. TO START THE
C PROGRAM TYPE:

C RUN [CHEOK.INTEG]TURBO_LOOP OR

C FOR GENERAL USERS, SIMPLY RUN THE EXECUTABLE
C (COMPILED AND LINKED) VERSION OF TURBO_LOOP.FOR

C 7) THE RESULTS WILL BE STORED IN THE FILE OR SERIES
C OF FILES CALLED "CONVERTED_FILENAME.OUT" IN THE
C FOLLOWING FORMAT:
C
C LINE 1: TITLE AS GIVEN IN THE CONVERSION PROCESS IN
C STEP 2.
C LINE 2: ICOUNT (I10 FORMAT), AREA (F10.5 FORMAT)
C
C ONE OUTPUT FILE WILL BE CREATED FOR EACH INPUT FILE
C IN "LIST.LIS".
C
C OTHER SUBROUTINES CALLED: NONE OTHER THAN THE RASTER
C TECH "ONELIB" CALLS.
C
C LAST EDIT SESSION: 8-12-86

```

C *****
C
C PARAMETER DEFINITIONS:
C
C TITLE          TITLE OF A PARTICULAR CYCLE IN A TEST
C FILENAME       FILENAMES WHICH ARE LISTED IN FILE LIST.LIS
C INFILE        FILE WHICH CONTAINS THE TITLE, MAXIMA AND MINIMA,
C              NUMBER OF DATA POINTS AND DATA FOR A PARTICULAR
C              CYCLE
C OUTFILE       FILE WHICH WILL STORE THE TITLE OF THE CYCLE AND THE
C              ENERGY DISSIPATED FOR THAT PARTICULAR CYCLE
C YSIZE        WINDOW SIZE IN Y DIRECTION
C XSIZE        WINDOW SIZE IN X DIRECTION
C VERTS(1,N)    X-COORDINATE OF POINT N IN INTEGER*2 FORMAT
C VERTS(2,N)    Y-COORDINATE OF POINT N IN INTEGER*2 FORMAT
C NVERTS(I)    NUMBER OF VERTICES IN POLYGON I
C ICOUNT       THE NUMBER OF PIXELS WITHIN THE HYSTERESIS
C              CURVE
C AREA        THE AREA WITHIN THE HYSTERESIS CURVE
C XFACTOR     (UNITS: PIXELS/UNIT OF LENGTH) THE
C              CONVERSION FACTOR TO CHANGE THE UNITS
C              OF LENGTH INTO NUMBER OF PIXELS
C YFACTOR     (UNITS: PIXELS/UNIT OF FORCE)
C              THE CONVERSION FACTOR TO CHANGE THE UNITS
C              OF FORCE TO THE NUMBER OF PIXELS
C XRANGE      THE MAXIMUM DISPLACEMENT FOR THAT CYCLE
C YRANGE      THE MAXIMUM FORCE FOR THAT CYCLE
C
C
C SUBROUTINES CALLED:  NONE OTHER THAN RASTER TECH ONE/80
C ONELIB CALLS.  SEE APPENDIX B FOR DEFINITION OF CALLS.
C
C *****
C
C CHARACTER*80 TITLE
C CHARACTER FILENAME*10,INFILE*14,OUTFILE*14
C
C DIMENSION X(1000),Y(1000)
C INTEGER*2 VERTS(2,1000),NVERTS(1)
C INTEGER*2 IX,IY,XSIZE,YSIZE
C INTEGER*4 TOTAL
C BYTE IVAL(1310720)
C
C SET PROGRAM VARIABLES
C
C PROMPT USER FOR WINDOW SIZE
C
C TYPE *, ' ENTER SIZE OF WINDOW '
C TYPE *, ' A 500 X 500 WINDOW RESULTS IN +1% ERROR'
C TYPE *, ' X SIZE = '
C READ *,XSIZE
C TYPE *, ' Y SIZE = '
C READ *,YSIZE

```

```

C
C MAXIMUM WINDOW SIZE IS 1278 BY 1022
C
      IF(XSIZE.GT.1278) XSIZE = 1278
      IF(YSIZE.GT.1022) YSIZE = 1022
      XSIZE4 = XSIZE
      YSIZE4 = YSIZE
C
C INITIALIZE THE RASTER TECH MODEL ONE/80 GRAPHICS DEVICE
C
      TYPE *, 'INITIALIZE THE GRAPHICS DEVICE'
      CALL RTSET(1,180)
      CALL RTINIT('GDA0:',5)
      CALL ENTGRA
      CALL READF(1)
C
C LOAD THE COLOR MAP
C
      CALL LUT8(0,255,135,0)      ! ORANGE
      CALL LUT8(1,0,0,255)      ! BLUE
      CALL LUT8(2,0,255,0)      ! GREEN
      CALL LUT8(3,0,0,255)      ! BLUE
      CALL LUT8(4,0,0,0)        ! BLACK
      CALL LUT8(6,255,255,255)  ! WHITE
      CALL LUT8(5,IRED,IGRN,IBLU)
C
C OPEN FILE WHICH CONTAINS THE LIST OF CYCLES TO BE
C PLOTTED
C
      OPEN(1,FILE='LIST.LIS',STATUS='OLD',ACCESS=
1 'SEQUENTIAL',FORM='FORMATTED')
C
C READ THE FILENAME
C
500 CONTINUE
C
C LOOP ON THIS READ STATEMENT UNTIL ALL THE LOAD CYCLES
C HAVE BEEN PROCESSED
C
      READ(1,FMT=1,END=1000) FILENAME
1  FORMAT(A20)
C
C VARIABLE FILENAME IS UPDATED WITH EACH CYCLE
C
      TYPE *, 'WORKING ON FILE',FILENAME
C
C ATTACH THE ".INP" AND ".OUT" EXTENSION TO THE FILENAME
C
      INFILE=FILENAME//'.INP'
      OUTFILE=FILENAME//'.OUT'
C
C OPEN INDIVIDUAL CYCLE PLOT FILE
C
      OPEN(UNIT=2,FILE=infile,ACCESS='SEQUENTIAL',FORM=

```

```

        1 'FORMATTED', STATUS='OLD')
        REWIND 2
C
C OPEN CONVERTED_FILENAME.OUT FILE FOR STORING RESULTS
C
        OPEN (UNIT=3, FILE=OUTFILE, ACCESS='SEQUENTIAL', FORM=
        1 'FORMATTED', STATUS='NEW')
        REWIND 3
C
C GET DATA FROM CYCLE PLOT FILE "TITLE"
C
        READ(2,2) TITLE
    2   FORMAT(A80)
C
C WRITE THE TITLE IN THE 'CONVERTED_FILENAME.OUT'
C
        WRITE(3,6) TITLE
    6   FORMAT(X,A80)
C
C GET MAX AND MIN VALUES AND THE NUMBER OF POINTS
C
        READ(2,3) XMIN, XMAX, YMIN, YMAX, NPTS
    3   FORMAT(4(E12.5, 3X), I5)
C
C GET THE DATA POINTS
C
        DO 100 I=1, NPTS
        READ(2,4) X(I), Y(I)
100   CONTINUE
    4   FORMAT(2(E12.5, 3X))
C
        CLOSE (UNIT=2)
C
C SCALE THE DATA
C
        XRANGE=MAX (ABS (XMAX) , ABS (XMIN) )
        YRANGE=MAX (ABS (YMAX) , ABS (YMIN) )
C
        XFACTOR=XSIZE/(2.*XRANGE)
        YFACTOR=YSIZE/(2.*YRANGE)
C
C LOAD DATA PAIRS INTO THE INTEGER*2 VECTORS: VERTS(I,J)
C [NOTE: THIS IS A RASTER TECH ONE/80 SPECIFIC DIRECTIVE
C USED IN A HARDWARE POLYGON PLOT COMMAND] AND SCALE
C THESE TO SCREEN COORDINATES
C
        DO 200 I=1, NPTS
        VERTS(1,I)=IFIX(X(I)*XFACTOR)
        VERTS(2,I)=IFIX(Y(I)*YFACTOR)
200   CONTINUE
C
C FLOOD THE BACKGROUND
C
        CALL VAL8(0)          ! ORANGE
        CALL FLOOD

```

```

C
C DRAW AXES
C
C     CALL VAL8(6)           ! WHITE
C     CALL MOVABS(-XSIZE/2,0)
C     CALL DRWABS(XSIZE/2,0)
C
C     CALL MOVABS(0,-YSIZE/2)
C     CALL DRWABS(0,YSIZE/2)
C
C DRAW THE CURVE
C
C THE PRMFIL SUBROUTINE FILLS THE ENCLOSED CURVE WITH
C COLOR VALUE 1
C
C     CALL PRMFIL(1)
C
C ASSIGN THE COLOR VALUE 1 TO THE PIXELS INSIDE THE
C POLYGON ALL OTHERS ARE ORANGE
C
C     CALL VAL8(1)           ! BLUE
C     CALL MOVABS(0,0)
C
C PLOT THE POLYGON (LOAD CYCLE) ON THE SCREEN
C
C     NVERTS(1)=NPTS
C     CALL POLYGN(1,NVERTS,VERTS)
C
C INTEGRATE BY 'COUNTING THE DOTS'
C
C     TYPE *, 'HERE WE GO!'
C     IX=(-XSIZE/2)
C     IY=(YSIZE/2)
C     TYPE *, 'YSIZE=', YSIZE, ' XSIZE=', XSIZE
C     TYPE *, 'MOVING TO: IX=', IX, ', IY=', IY
C
C MOVE TO UPPER LEFT CORNER OF THE WINDOW. WINDOW ORIGIN
C AT SCREEN CENTER
C
C     CALL MOVABS(IX,IY)
C
C     TYPE *, 'READING WINDOW'
C
C BLANK THE DISPLAY SCREEN TO SPEED UP CALCULATION
C PROCESS (REFRESH OF SCREEN IMAGE REQUIRES CPU TIME.
C BY TURNING THIS OFF, THE TIME TO CONDUCT PIXEL READ
C OPERATIONS ARE CONSIDERABLY REDUCED)
C
C     CALL BLANK(1)
C     TYPE *, 'WINDOW SIZE: ', XSIZE+1, ' BY ', YSIZE+1
C
C READ THE VALUE OF THE PIXELS (RED, GREEN, BLUE) IN
C THE WINDOW BY SCANNING FROM LEFT TO RIGHT AND TOP
C TO BOTTOM
C

```

```

        CALL READW(YSIZE+1,XSIZE+1,IVAL)
        CALL BLANK(0)
C
        TYPE *, 'INTEGRATING'
C
C NOTE THAT XSIZE4 = XSIZE AND YSIZE4 = YSIZE
C TOTAL IS EQUAL TO THE TOTAL NUMBER OF PIXELS IN THE
C THE WINDOW. IT IS USED AS A COUNTER IN THE DO LOOP
C TO EXTRACT FROM THE TOTAL NUMBER OF PIXELS ONLY THOSE
C WHICH HAVE THE COLOR VALUE OF 1.
C
        TOTAL=(XSIZE4+1)*(YSIZE4+1)
C
C INITILIZE THE COUNTER
C
        ICOUNT=0
C
C BYTE VECTOR 'IVAL' CONTAINS THE COLOR LOOK-UP DEFINITION
C FOR EACH PIXEL IN THE WINDOW. COMPARE THE COLOR OF EACH
C PIXEL TO SEE IF IT MATCHES THAT ASSIGNED TO THE
C HYSTERSIS LOOP (COLOR VALUE = 1). IF IT DOES, ADD ONE
C TO THE COUNTER, ICOUNT, WHICH REPRESENTS THE SUM OF ALL
C PIXELS OF THAT COLOR
C
        DO 300 I=1,TOTAL
        IF(IVAL(I).EQ.1) ICOUNT=ICOUNT+1
300    CONTINUE
        TYPE *, 'INTEGRATION COMPLETE'
        TYPE *, 'ICOUNT=', ICOUNT
C
C CONVERT THE NUMBER OF PIXELS TO ENERGY UNITS AND STORE
C THE VALUE IN "AREA"
C
        AREA=FLOAT(ICOUNT)/(XFACTOR*YFACTOR)
        TYPE *, 'AREA=', AREA
C
C WRITE THE VALUES OF ICOUNT AND AREA INTO FILE CALLED
C 'CONVERTED_FILENAME.OUT'
C
        WRITE(3,FMT=7) ICOUNT,AREA
7      FORMAT(X, 'ICOUNT=', I10, ' AREA=', F10.5)
        CLOSE(3)
C
C LOOP BACK TO THE READ STATEMENT AND GET ANOTHER FILENAME
C
        GOTO 500
C
1000  CONTINUE
        CLOSE(1)
C
        CALL QUIT
        CALL EXIT
C
        STOP
        END

```

APPENDIX B: PROGRAM "GRAPH"

A FORTRAN program listing of "Graph" is presented in the following section. This was implemented on a VAX 11/750 computer system with a DMA driven Raster Technologies One/80 color raster display device.

Graph is an interactive program which permits the user to graphically display the results from a cyclic load test on a raster device. The user is presented with a menu from which the following may be chosen:

1. A plot of the lateral load vs. column displacement history simultaneously with an animation showing the deflected position of the column. The user has the choice of plotting either the total energy dissipated by the column during the test or plotting the energy dissipated per cycle. Each plot occupies one screen quadrant.
2. A comparison of the energy dissipated per cycle for a maximum of three tests. This subroutine also allows interactive scaling of individual test data so that a scale factor between tests can be determined.
3. A plot of the total energy dissipated during a test. Up to six tests may be displayed simultaneously.
4. A plot of the lateral load vs. column displacement using the entire screen. This enlarged display allows the user to determine if anything unusual occurred during a certain portion of the test; for example, a drop in load due to the fracturing of spiral or longitudinal reinforcement.

C *****

C PROGRAM GRAPH

C PURPOSE:

C TO PRESENT THE DATA FROM CYCLIC TESTS ON A
C GRAPHICS DEVICE.

C GRAPHICS:

C THE PROGRAM MAKES USE OF A RASTER MODEL ONE/80
C COLOR GRAPHICS DEVICE FOR OUTPUT DISPLAY. CONSULT
C THE RASTER TECHNOLOGIES HANDBOOK FOR EXPLANATIONS
C OF CALLS TO THE "ONELIB" LIBRARY.

C FILE STRUCTURE:

C PROGRAM GRAPH IS ACTUALLY A COLLECTION OF GRAPHICS
C ORIENTED PROGRAMS WHICH SERVE AS AIDS FOR THE INTERPRETATION
C OF CYCLIC LOAD DATA FROM DYNAMIC OR PSUEDO-DYNAMIC TESTS.
C SPECIFICALLY, A MENU OPTION PERMITS ACCESS TO THE FOLLOWING
C SUBPROGRAMS:

- C o ANIMATED PLOTTING OF THE LOAD DISPLACEMENT CURVE WITH
C A VISUAL QUEUE IN THE FORM OF A DEFLECTING COLUMN SPECIMEN.
C THIS PROGRAM ALSO PLOTS (ON THE SAME SCREEN) EITHER THE
C TOTAL ENERGY DISSIPATED DURING THE COURSE OF A SPECIFIC TEST
C OR THE ENERGY DISSIPATED DURING EACH CYCLE (AS A BAR TYPE
C HISTOGRAM).

C Subroutines involved: [MAIN, CYCLE, COLPLOT, ENERGY,
C INDIVENE]

- C o COMPARISON OF ENERGY ABSORBED PER CYCLE FOR UP TO THREE
C COMPLETE TESTS. PLOTTED AS A BAR TYPE HISTOGRAM.
C INTERACTIVE SCALING OF THE VALUES ALLOWS FOR EASY
C DETERMINATION OF THE SCALE BETWEEN TESTS.

C Subroutines involved: [COMPARE, REDRAW]

- C o COMPARISON OF TOTAL ENERGY ABSORBED DURING A COMPLETE
C TEST WITH UP TO SIX DIFFERENT TESTS BEING COMPARED.
C CURRENT OPTIONS PERMIT NON-DIMENSIONALIZATION OF ENERGY WITH
C RESPECT TO DIFFERING VALUES OF f'_c AND $\Delta-y$. THE PROGRAM
C SUMS ENERGY DISSIPATED UP TO THE ULTIMATE STATE OF THE
C STRUCTURE. THE ULTIMATE STATE BEING DEFINED AS 0.8 TIMES
C THE MOMENT AT $u = 2$ (AS DISCUSSED IN THE MAIN PAPER).

C Subroutines involved: [COMTOTAL]

- C o LOAD-DISPLACEMENT LINE PLOT ONLY. USES FULL SCREEN
C DIMENSIONS FOR GREATER DETAIL IN ANALYSIS OF BEHAVIOR.

TO BE CONTRASTED WITH THE FIRST OPTION IN WHICH THE LOAD DISPLACEMENT PLOT APPEARS IN THE LOWER LEFT HAND QUADRANT OF THE SCREEN.

Subroutines involved: [LINEPLOT]

EACH OF THESE PROGRAMS REQUIRES DATA ENTRY IN A SPECIFIC FORMAT. THE AVAILABLE DATA WILL BE IN ONE OF TWO POSSIBLE FORMS:

- a) A FILE CONTAINING (X,Y) COORDINATE PAIRS WHICH CAN BE USED TO GENERATE, FOR EXAMPLE, LOAD-DISPLACEMENT HYSTERESIS PLOTS FOR A SPECIFIC TEST. AS DESCRIBED BELOW, THIS DATA MUST BE IN A SPECIFIC FORM WHICH INCLUDES A TITLE FOR THE DATA, THE DATA MAXIMA AND MINIMA, THE NUMBER OF (X,Y) PAIRS, AND (X,Y) DATA.
- b) AS FILE CONTAINING A DATA TITLE, AND THE INTEGRATED AREA INSIDE ONE HYSTERESIS LOOP FOR A SPECIFIED TEST. THESE CAN BE GENERATED AUTOMATICALLY USING THE PROGRAM TURBO_LOOP DESCRIBED IN APPENDIX A.

Example:

A TEST CONTAINS FIVE COMPLETE LOAD CYCLES. THE FOLLOWING FILES MUST BE GENERATED:

LOAD-DISPLACEMENT FILES (GENERATED AT NBS USING POLYCONV. THESE CAN BE GENERATED EXTERNALLY USING ANY PROGRAM WHICH PRODUCES A FILE HAVING OUTPUT IN THE FORMAT SPECIFIED BELOW:

- 1) CYCLE1.INP
- 2) CYCLE2.INP
- 3) CYCLE3.INP
- 4) CYCLE4.INP
- 5) CYCLE5.INP

Total Energy per Cycle Files (Output from TURBO-LOOP)

- 6) CYCLE1.OUT
- 7) CYCLE2.OUT
- 8) CYCLE3.OUT
- 9) CYCLE4.OUT
- 10) CYCLE5.OUT

TO AID IN AUTOMATING THE PROGRAM, A NUMBER OF ADDITIONAL FILES ARE NECESSARY. THESE ARE AS FOLLOWS:

- a) LIST.LIS: ONLY USED IN TURBO_LOOP. CONTAINS THE LOAD DISPLACEMENT FILES TO BE ANALYZED (INTEGRATED). IN THE ABOVE EXAMPLE, FILES 1-5 WOULD BE IN LIST.LIS. WITH ONE FILENAME PER LINE, WITHOUT THE EXTENSION ".INP" -- THE PROGRAM AUTOMATICALLY ADDS THOSE DURING EXECUTION. UPON

C EXECUTION WITH INPUT AS LIST.LIS, THE OUTPUT FROM TURBO_
C LOOP WILL BE FILES 6-11 AS LISTED ABOVE, WITH THE
C EXTENSION ".OUT" APPENDED.
C
C b) FILENAME.LIS: ANY FILENAME SUPPLIED BY THE USER CONTAINING
C A LIST OF ".INP" FILES AS DESCRIBED ABOVE (A LIST OF
C SPECIFIED LOAD CYCLE FILES FOR A GIVEN TEST) WITH THE
C FILE EXTENSION ".LIS". USED IN PROGRAM GRAPH FOR PROCESSING
C OF ONE SPECIFIC SET OF TEST DATA. IN THE ABOVE EXAMPLE,
C FILENAME.LIS WOULD INCLUDE FILES 1-5 AND FOR THIS EXAMPLE
C IS THE SAME AS LIST.LIS. NOTE THAT FILENAME.LIS, LIKE
C LIST.LIS, CONTAINS THE FILE TTILES, ONE PER LINE, WITH NO
C EXTENSION ".INP".
C
C c) SEEFIL.LIS: A FILE CONTAINING A DATABASE CONSISTING OF ALL
C FILENAME.LIS FILES IN THE USER'S DIRECTORY. USED FOR DATA
C MANAGEMENT (AND TO JOG THE USER'S MEMORY OF JUST WHAT
C HE/SHE HAS AVAILABLE)
C
C d) REFTITLE.LIS: USED ONLY IN SUBROUTINE COMPARE, WHICH
C DISPLAYS INDIVIDUAL CYCLE ENERGIES FOR ONE TO THREE
C DIFFERENT TESTS. THE FILE REFTITLE.LIS CONTAINS A LIST
C (ONE PER LINE) OF ALL POSSIBLE DESCRIPTORS FOR EXISTING
C LOAD CYCLES. THE TITLES IN THE FILES WITH THE ".OUT"
C EXTENSION MUST HAVE THE **EXACT** SAME FORMAT. FOR THIS
C SET OF TESTS, THE TITLES MUST BE IN FORMAT:
C
C DISPLACEMENT-DUCTILITY "DEL",CYCLE-NUMBER-AT-GIVEN-DUCTILITY
C
C WHERE
C
C DISPLACEMENT DUCTILITY IS AN INTEGER BEGINNING IN COLUMN 2
C CYCLE-NUMBER-AT-GIVEN-DUCTILITY IS AN INTEGER VALUE EQUAL
C TO THE CYCLE NUMBER AT A GIVEN DUCTILITY LEVEL.
C
C NOTE: THE FORMAT MAY BE CHANGED BUT IF SO, IT MUST BE
C CHANGED IN BOTH THE REFTITLE.LIS AND IN EACH OF THE FILES
C WITH THE ".OUT" EXTENSIONS.
C
C FOR EXAMPLE, SUPPOSE TEST1 HAS THE FOLLOWING CYCLE DESCRIPTORS:
C
C 1 DEL, 1
C 2 DEL, 1
C 2 DEL, 2
C 4 DEL, 1
C 4 DEL, 2
C
C and TEST2 has
C
C 1 DEL, 1
C 2 DEL, 1
C 2 DEL, 2
C 3 DEL, 1
C 3 DEL, 2

C 3 DEL, 3

C THE FILE REFTITLE.LIS TO BE USED WHEN COMPARING THESE TWO TESTS
C SHOULD APPEAR AS FOLLOWS:

C REFTITLE.LIS

C 1 DEL, 1
C 2 DEL, 1
C 2 DEL, 2
C 3 DEL, 1
C 3 DEL, 2
C 3 DEL, 3
C 4 DEL, 1
C 4 DEL, 2

C IF ADDITIONAL TESTS ARE TO BE COMPARED, THEN REFTITLE.LIS SHOULD
C INCLUDE ALL UNIQUE CYCLE DESCRIPTORS FOR THE SET OF TESTS IN
C ASCENDING ORDER (DUCTILITY FIRST, CYCLE NUMBER AT A PARTICULAR
C DUCTITLITY SECOND)

C DATA FORMAT:

C THE FOLLOWING PROCEDURE IS USED TO GENERATE THE DATA

- C 1) GENERATE PLOT FILES CONSISTING OF ONE COLUMN
C EACH OF THE Y-COORDINATES (TYPICALLY LOAD) AND
C THE X-COORDINATES (TYPICALLY DISPLACEMENT).
C THESE PLOT FILES ARE AUTOMATICALLY GENERATED
C USING PROGRAM UT:\$DDP FROM ANY SET OF TEST
C DATA OBTAINED EITHER BY THE TTF FACILITY OR BY
C THE LARGE SCALE TEST FACILITY IN BUILDING 202.
C EACH PLOT FILE SHOULD ONLY REPRESENT ONE CYCLE.
- C 2) STRIP KEY DATA FROM THE PLOT FILES NEEDED BY
C GRAPH. THIS CAN BE DONE AUTOMATICALLY BY
C RUNNING THE CONVERSION PROGRAM "POLYCONV" OR
C "JLG" AND ENTERING THE NAMES OF THE TWO PLOT
C FILES, THE FILENAME OF THE CONVERTED DATA
C (MUST INCLUDE ".INP" EXTENSION) AND THE
C IDENTIFYING TITLE TO BE PLOTTED ON THE RASTER
C TECH MODEL ONE/80. THE CONVERTED FORMAT AFTER
C RUNNING "POLYCONV" OR "JLG" IS AS FOLLOWS:
 - C A) TITLE (A80 FORMAT)
 - C B) XMIN, XMAX, YMIN, YMAX, NPTS

C WHERE

C XMIN - MINIMUM VALUE OF THE X-COORDINATE IN
C E12.5 FORMAT

C XMAX - MAXIMUM VALUE OF THE X-COORDINATE IN


```

C *****
C
C GRAPHICS SUBROUTINES FOR THE RASTER TECH MODEL ONE/80
C
C NOTE THAT THE PARAMETERS IN THE CALL STATEMENTS MUST
C BE IN INTEGER*2 FORMAT
C
C RTSET(1,180) IDENTIFIES THE GRAPHICS MODEL
C RTINIT('GDA0:',5) INITIALIZES THE SYSTEM; ACTIVATES DMA
C I/O PORT
C ENTGRA ENTER GRAPHICS MODE
C LUT8(I,R,G,B) CHANGES THE COLOR ENTRIES IN "I" OF
C COLOR LOOK-UP TABLE TO THE SPECIFIED
C R, G, B VALUES
C VAL8(I) SETS THE CURRENT PIXEL COLOR VALUE TO
C THE VALUE "I"
C FLOOD CHANGES ALL DISPLAYED PIXELS TO THE
C CURRENT PIXEL COLOR VALUE
C PRMFIL(I) SETS FLAG TO INDICATE WHETHER THE
C GRAPHIC PRIMITIVES ARE DRAWN FILLED
C OR UNFILLED WITH THE CURRENT PIXEL
C VALUE.
C I = 1 FILLED
C I = 0 UNFILLED
C TEXTN(X,Y,K,L) SETS TEXT SIZE TO X & Y VALUES AND THE
C ANGLE OF THE TEXT TO THE K & L VALUES
C TEXT1(I,J) DRAWS HORIZONTAL TEXT STRING, J, WHICH
C CONSISTS OF I CHARACTERS
C TEXTC(I,J) SETS TEXT SIZE TO I AND THE ANGLE, J,
C AT WHICH THE TEXT IS TO BE DRAWN
C MOVREL(IX,IY) MOVES CURRENT POINT BY RELATIVE AMOUNT
C SPECIFIED BY IX & IY
C MOVABS(IX,IY) CHANGES CURRENT POINT TO POINT SPECI-
C FIED BY IX & IY
C POLYGN(I,J,K) DRAWS "I" NUMBER OF POLYGON WHICH HAS
C "J" NUMBER OF VERTICES WHICH HAVE "K"
C COORDINATES.
C RECTAN(IX,IY) DRAWS RECTANGLE WITH ONE CORNER AT THE
C CURRENT POINT AND THE OPPOSITE CORNER
C SPECIFIED BY (IX,IY)
C DRWABS(IX,IY) DRAWS A LINE FROM CURRENT POINT TO
C POINT SPECIFIED BY (IX,IY)
C EMPTYB EMPTIES THE BUFFER CONTENTS TO THE
C GRAPHICS DEVICE
C QUIT EXITS GRAPHICS MODE AND RETURNS TO
C ALPHA MODE
C
C *****
C
C CHARACTER*80 TITLE
C CHARACTER FILENAME*10,INFILE*14,OUTFILE*14,NAME*10,
C 1 XNAME*14, XNOMBRE*14,YLIST*9,ZLIST*14,ANAME*80
C
C DIMENSION X(400),Y(400)

```

```

      INTEGER*2 TITLE(40),IDX(16),IDY(16),
      1          OVERTIT(15)
      INTEGER*2 IX,IY,NCOUNT,DISPMT,ENERABS
C
C INPUT IDX AND IDY VALUES TO USED FOR BOLD TEXT
C
      DATA IDX/0,1,0,-1,0,1,1,0,0,1,0,0,0,-1,-1,-1/,
      1      IDY/0,0,1,0,1,0,0,-1,-1,0,1,1,1,0,0,0/
      REAL MAXX,MINX,MAXY,MINY
C
C ASK USER FOR TYPE OF PLOTS
C
1104  TYPE *, 'DO YOU WANT'
      TYPE *, ' '
      TYPE *, ' 1 = LOAD-DISPLACEMENT AND ENERGY PLOT'
      TYPE *, ' 2 = COMPARISON OF ENERGY ABSORBED/CYCLE'
      TYPE *, ' 3 = COMPARISON OF TOTAL ENERGY ABSORBED'
      TYPE *, ' 4 = SEE AVAILABLE LIST OF TESTS FOR'
      TYPE *, ' 5 = LOAD-DISPLACEMENT LINE PLOT ONLY'
      TYPE *, ' 6 = EXIT'
      READ(5,311) IANS1
311   FORMAT(I2)
      IF(IANS1.EQ.1) GOTO 1002
      IF(IANS1.EQ.2) GOTO 1102
      IF(IANS1.EQ.3) GOTO 1101
      IF(IANS1.EQ.4) GOTO 1108
      IF(IANS1.EQ.5) GOTO 1109
      IF(IANS1.EQ.6) GOTO 1003
C
C
C IF OPTION #4 IS CHOSEN, SHOW AVAILABLE TESTS FOR PLOTTING
C
C
1108  TYPE *, ' '
      TYPE *, ' AVAILABLE LIST OF TEST FILE NAMES FOR PLOTTING'
      TYPE *, ' '
      OPEN(10,FILE='SEEFIL.LIS',ACCESS='SEQUENTIAL',
      1 FORM='FORMATTED',STATUS='OLD')
      TYPE *, ' '
1007  READ(10,FMT=1004,END=1005) ANAME
1004  FORMAT(A80)
      TYPE 1004,ANAME
      GOTO 1007
1005  CONTINUE
      GOTO 1104
C
C
C IF OPTION # 2 IS CHOSEN, CALL SUBROUTINE TO COMPARE THE
C ENERGY ABSORBED/CYCLE
C
C
1102  CALL COMPARE(IDX,IDY)
      GOTO 1104
C
C

```

```

C IF OPTION # 3 IS CHOSEN, CALL SUBROUTINE TO COMPARE THE
C TOTAL ENERGY ABSORBED
C
C
1101 CALL COMTOTAL(IDX, IDY)
      GOTO 1104
C
C
C IF OPTION # 5 IS CHOSEN, CALL SUBROUTINE TO FOR LOAD-
C DISPLACEMENT LINE PLOT
C
C
1109 CALL LINEPLOT(IDX, IDY)
      GOTO 1104
C
C *****
C
C IF OPTION # 1 IS CHOSEN, BEGIN ROUTINE
C
C A) TO PLOT THE LOAD-DISPLACEMENT CYCLES
C B) TO PLOT THE INDIVIDUAL OR CUMULATIVE ENERGY PLOT
C C) TO SHOW THE ANIMATED COLUMN MOVEMENT
C
C ALL ON THE SAME SCREEN
C
C VARIABLE DEFINITIONS:
C
C MAXX          MAXIMUM X-COORDINATE (DISPLACEMENT) VALUE
C                AMONG ALL THE CYCLES IN A TEST
C MINX          MINIMUM X-COORDINATE (DISPLACEMENT) VALUE
C                AMONG ALL THE CYCLES IN A TEST
C MAXY          MAXIMUM Y-COORDINATE (FORCE) VALUE
C MINY          MINIMUM Y-COORDINATE (FORCE) VALUE
C YLIST         FILE WHICH CONTAINS THE LISTING OF FILES
C                (XNAME) IN WHICH THE PAIRS OF DATA POINTS ARE
C                STORED.
C ZLIST         EQUIVALENT TP YLIST WITH '.LIS' EXTENSION
C XNAME.INP     FILE WHICH CONTAINS THE PAIRS OF DATA POINTS
C                FOR ONE CYCLE TO BE PLOTTED. SEE DOCUMENTA-
C                TION IN TURBO_LOOP FOR CONVERTING THE TEST
C                DATA FROM THE PDP 11/34 TO THE VAX 11/750.
C XNOMBRE.OUT   FILE WHICH CONTAINS THE TITLE OF THE CYCLE
C                AND THE ENERGY ABSORBED FOR THAT CYCLE
C DISPMT        INDEX TO LOCATE THE X-COORDINATE OF THE
C                POLYGON WHICH SHOWS THE CUMULATIVE ENERGY PLOT
C                IN SUBROUTINE ENERGY
C ENERABS       INDEX TO LOCATE THE Y-COORDINATE OF THE
C                POLYGON WHICH SHOWS THE CUMULATIVE ENERGY PLOT
C                IN SUBROUTINE ENERGY
C TOTDISP       MAXIMUM TOTAL DISPLACEMENT THAT THE STRUCTURE
C                TRAVELS
C TOTENERGY     MAXIMUM TOTAL ENERGY THAT THE STRUCTURE
C                ABSORBED
C IDX, IDY      VARIABLES USED IN A DO-LOOP WHICH RESULTS IN

```

```

C          BOLD TYPE PRINT ON THE GRAPHICS DEVICE.
C          BASICALLY, THE PIXELS ARE REDRAWN ONE PIXEL
C          UP OR DOWN OR "SMEARED" TO PRODUCE THIS
C          BOLD EFFECT
C X(I)     VECTOR WHICH CONTAINS THE X-COORDINATES OF THE
C          HYSTERESIS CURVE ( TYPICALLY DISPLACEMENT)
C Y(I)     VECTOR WHICH CONTAINS THE Y-COORDINATE OF THE
C          HYSTERESIS CURVE (TYPICALLY LOAD)
C NCOUNT  INDEX USED TO CHANGE THE PLOT COLORS
C INFILE.INP  SAME AS XNAME.INP
C OUTFILE.INP  SAME AS XNOMBRE.OUT
C OVERTIT   OVERALL TITLE OF THE PLOT
C
C SUBROUTINES CALLED:
C
C 1)  CYCLE
C 2)  COLPLOT
C 3)  ENERGY OR INDIVENE
C
C *****
C DETERMINE THE MAXIMUM AND MINIMUM VALUES FOR THE TEST.
C THESE VALUES WILL BE USED TO SCALE THE PLOTS
C
C Initialize variables into which the max. and min. values
C will be stored.
C
C
1002  MAXX = 0.0
      MINX = 0.0
      MAXY = 0.0
      MINY = 0.0
      TOTDISP = 0.0
      TOTENERGY = 0.0
      DISPMT = 0
      ENERABS = 0
      AREAMAX = 0.0
C
      CLOSE(10)
      TYPE *, ' '
      TYPE *, 'BEGIN LOAD-DISPLACEMENT PLOT'
      TYPE *, 'ENTER NAME OF LIST FILE (9 CHARACTERS) '
      READ (5,518) YLIST
518   FORMAT(A9)
      ZLIST = YLIST//'.LIS'
C
C Open the file where all the test names have been stored
C
      OPEN(1,FILE=ZLIST,STATUS='OLD',ACCESS='SEQUENTIAL',
      1 FORM='FORMATTED')
1130  CONTINUE
C
C LOOP ON THIS READ STATEMENT UNTIL ALL THE FILES HAVE

```

```

C   BEEN READ
C
C       READ(1,FMT=1,END=1100) NAME
C
C   PUT EXTENSION ON THE FILENAME.
C   All files to be used have to have the extension ".INP"
C   or ".OUT"
C
C       XNAME=NAME//'.INP'
C       XNOMBRE = NAME//'.OUT'
C
C   OPEN FILE CONTAINING THE DATA POINTS
C
C       OPEN(4,FILE=XNAME,ACCESS='SEQUENTIAL',FORM='FORMATTED',
C           1 STATUS='OLD')
C       REWIND 4
C
C   OPEN FILE CONTAINING THE RESULTS OF THE ENERGY
C   CALCULATION FROM TURBO_LOOP
C
C       OPEN(11,FILE=XNOMBRE,ACCESS='SEQUENTIAL',FORM='FORMATTED',
C           1 STATUS='OLD')
C       REWIND 11
C
C   TITLE HAS TO BE READ BECAUSE THE FILE IS SEQUENTIAL I.E.
C   ITEMS LOCATED BEFORE THE DESIRED ITEM HAVE TO BE READ
C   BEFORE THE DESIRED ITEM CAN BE READ
C
C       READ(11,46) TITLE
46      FORMAT(40A2)
C
C   READ THE VALUE OF THE ENERGY ABSORBED PER CYCLE FROM THE
C   '.OUT' FILE
C
C       READ(11,50) ICOUNT,AREA
50      FORMAT(8X,I10,7X,F10.5)
C       CLOSE(UNIT=11)
C
C   READ THE TITLE FROM THE FILE CONTAINING THE DATA POINTS
C
C       READ(4,45) TITLE
45      FORMAT(40A2)
C
C   Open the test file and extract from it the max. and min.
C   values
C
C       READ(4,40) XMIN,XMAX,YMIN,YMAX
40      FORMAT(4(E12.5,3X))
C       CLOSE(UNIT=4)
C
C   DETERMINE THE MAX AND MIN VALUES OF X AND Y FROM ALL THE
C   TESTS TO BE INTEGRATED.
C
C       TOTDISP = TOTDISP + ABS(XMAX) + ABS(XMIN)
C       TOTENERGY = TOTENERGY + AREA

```

```

IF(XMAX.GT.MAXX) MAXX = XMAX
IF(XMIN.LT.MINX) MINX = XMIN
IF(YMAX.GT.MAXY) MAXY = YMAX
IF(YMIN.LT.MINY) MINY = YMIN
IF(AREA.GT.AREAMAX) AREAMAX = AREA
GO TO 1130

```

```

C
1100 CONTINUE
REWIND 1

```

```

C
C
C
NCOUNT=0

```

```

C
C INITIALIZE THE GRAPHICS DEVICE
C

```

```

CALL RTSET(1,180)
CALL RTINIT('GDA0:',5)
CALL ENTGRA

```

```

C
C LOAD THE COLOR MAP
C

```

```

CALL LUT8(0,255,200,255) ! VERY LIGHT PURPLE
CALL LUT8(1,255,150,255) ! LIGHT PURPLE
CALL LUT8(2,255,0,255) ! RED PURPLE
CALL LUT8(3,188,150,234) ! PURPLE
CALL LUT8(4,0,0,190) ! BLUE PURPLE
CALL LUT8(5,75,75,255) ! BRIGHT BLUE
CALL LUT8(6,0,255,255) ! BRIGHT LIGHT BLUE
CALL LUT8(7,175,255,255) ! LIGHT BLUE
CALL LUT8(8,0,200,200) ! BLUE GREEN
CALL LUT8(9,0,175,0) ! OLIVE GREEN
CALL LUT8(10,130,230,130) ! LIGHT OLIVE GREEN
CALL LUT8(11,0,255,0) ! BRIGHT GREEN
CALL LUT8(12,165,255,165) ! LIGHT GREEN
CALL LUT8(13,255,255,175) ! LIGHT YELLOW
CALL LUT8(14,255,255,100) ! LIGHT YELLOW
CALL LUT8(15,255,175,50) ! YELLOW-ORANGE
CALL LUT8(16,255,120,0) ! ORANGE
CALL LUT8(17,255,0,0) ! RED
CALL LUT8(18,255,130,130) ! DUSKY PINK
CALL LUT8(19,255,175,175) ! LIGHT PINK
CALL LUT8(20,255,200,200) ! PALE PINK
CALL LUT8(21,200,200,200) ! LIGHT GRAY
CALL LUT8(22,150,150,150) ! GRAY
CALL LUT8(23,75,75,75) ! DARK GRAY
CALL LUT8(24,30,30,30) ! GRAY-BLACK
CALL LUT8(30,255,255,255) ! WHITE
CALL LUT8(31,0,0,0) ! BLACK
CALL LUT8(32,255,246,0) ! CHROMIUM YELLOW

```

```

C
C ENTER THE OVERALL TEST TITLE
C

```

```

TYPE *, ' '
TYPE *, ' ENTER TEST TITLE (15 CHARACTERS) '

```

```

      READ(5,461) OVERTIT
461   FORMAT(15A2)
      TYPE *, ' '
      TYPE *, 'PROCESSING MODE'
      TYPE *, '1 = AUTO'
      TYPE *, '0 = MANUAL'
      READ (5,5001) NAUTO
5001  FORMAT(I2)
C
C   FLOOD THE BACKGROUND
C
      CALL VAL8(31)           ! BLACK
      CALL FLOOD
C
C   PLACE THE OVERALL TITLE IN THE UPPER LEFT CORNER OF THE
C   SCREEN
C
      CALL VAL8(32)
      CALL TEXTN(90,90,0,0)
      CALL MOVABS(-580,450)
      DO 470 I=1,16
      CALL MOVREL(IDX(I),IDY(I))
      CALL TEXT1(15,OVERTIT)
470   CONTINUE
C
C   ASK USER FOR TYPE OF ENERGY PLOT
C
      TYPE *, ' '
      TYPE *, ' CUMULATIVE ENERGY OR INDIVIDUAL ENERGY '
      TYPE *, ' 1 = CUMULATIVE ENERGY PLOT '
      TYPE *, ' 2 = INDIVIDUAL ENERGY PLOT '
      READ *, ANW
C
C
      OPEN(1,file=ZLIST,status='old',access='sequential',
1       form='formatted')
C
500   CONTINUE
C
      READ(1,fmt=1,end=1000) filename
1     FORMAT(A20)
      TYPE *, 'working on file ',filename
C
C   PUT EXTENSION ON FILENAME
C
      infile=filename//'.inp'
      outfile=filename//'.out'
C
C
C   OPEN 'FILENAME.INP' TO READ THE DATA POINTS NECESSARY TO
C   PLOT THE HYSTERESIS LOOPS
C
      OPEN(UNIT=2,FILE=infile,ACCESS='SEQUENTIAL',FORM='FORMATTED',
1 STATUS='OLD')
      REWIND 2

```

```

C
C OPEN 'FILENAME.OUT' TO OBTAIN THE ENERGY CALCULATED BY
C PROGRAM 'TURBO_LOOP'
C
      OPEN(UNIT=3,FILE=OUTFILE,ACCESS='SEQUENTIAL',FORM='FORMATTED',
1      STATUS='OLD')
      REWIND 3
C
      READ(2,2) TITLE
2      FORMAT(40A2)
      READ(3,60) TITLE
60      FORMAT(40A2)
      READ(3,55) ICOUNT, AREA
55      FORMAT(8X,I10,7X,F10.5)
C
      READ(2,3) XMIN,XMAX,YMIN,YMAX,NPTS
3      FORMAT(4(E12.5,3X),I5)
C
C READ DATA POINTS AND STORE IN X(I) AND Y(I) VECTORS
C
      DO 100 I=1,NPTS
      READ(2,4) X(I),Y(I)
100     CONTINUE
4      FORMAT(2(E12.5,3X))
C
      CLOSE(UNIT=2)
C
      CLOSE(3)
C
C COLPLOT PLOTS THE ANIMATED MOVEMENT OF THE COLUMN IN THE UPPER
C LEFT QUADRANT OF THE SCREEN AS DATA POINTS ON THE HYSTERESIS
C CURVE ARE PLOTTED IN THE LOWER LEFT QUADRANT OF THE SCREEN
C
      CALL COLPLOT(NPTS,X,Y,IDX,IDY,NCOUNT,MAXX,MAXY,
1      MINX,MINY,XMAX,XMIN)
C
C CYCLE REPLOTS THE HYSTERESIS CURVE SHOWN IN COLPLOT
C EXCEPT THIS ROUTINE FILLS THE AREA WITHIN THE CURVE WITH
C A COLOR DETERMINED BY 'NCOUNT'
C
      CALL CYCLE(NPTS,NCOUNT,IDX,IDY,TITLE,MAXX,MAXY,MINX,
1      MINY,X,Y)
C
C USER HAS THE OPTION TO CHOOSE EITHER 'ENERGY' OR
C 'INDIVENE' SUBROUTINE
C
C ENERGY PLOTS THE TOTAL ENERGY ABSORBED BY THE STRUCTURE
C IN THE UPPER RIGHT QUADRANT OF THE SCREEN
C
      IF(ANW.EQ.1)CALL ENERGY(XMAX,XMIN,NCOUNT,TOTDISP,
1      TOTENERGY,AREA,DISPMT,ENERABS,IDX,IDY)
C
C INDIVENE PLOTS THE INDIVIDUAL CYCLE ENERGY BAR GRAPH
C HISTOGRAM IN THE UPPER RIGHT CORNER OF THE SCREEN
C

```

```

IF (ANW.EQ.2) CALL INDIVENE (AREA, NCOUNT, XMAX, XMIN,
1 AREAMAX, TOTDISP, IDX, IDY)
C
NCOUNT=NCOUNT+1
IF (NAUTO .EQ. 1) GOTO 500
TYPE *, ' '
TYPE *, 'ANOTHER CYCLE ? 1=YES, 0=NO'
READ *, ANS
IF (ANS.EQ.0) GOTO 1000
GOTO 500
C
1000 CONTINUE
CLOSE(1)
C
C
GOTO 1104
C
1003 TYPE *, '***** BYE *****'
CALL QUIT
CALL EXIT
C
STOP
END
C
C

```

```

C *****
C
C SUBROUTINE CYCLE
C
C PURPOSE: TO PLOT THE HYSTERESIS CURVES OBTAINED FOR A
C          STRUCTURE FROM A CYCLIC TEST
C
C CALLED FROM: MAIN
C
C USAGE: CALL CYCLE(NPTS, NCOUNT, IDX, IDY, TITLE, MAXX, MAXY,
C          MINX, MINY, X, Y)
C
C PARAMETERS:
C
C NPTS      NUMBER OF POINTS USED TO PLOT THE HYSTERESIS
C           CURVE
C NCOUNT   INDEX USED TO CHANGE THE COLOR OF THE PLOT
C IDX       SEE MAIN PROGRAM
C IDY       " " "
C TITLE     TITLE OF THE PARTICULAR CYCLE TO BE PLOTTED
C           E.G . 2 DEL, 2
C MAXX     SEE MAIN PROGRAM
C MAXY     " " "
C MINX     " " "
C MINY     " " "
C
C OTHER SUBROUTINES CALLED: NONE (OTHER THAN THE RASTER
C TECH 'ONELIB' ROUTINES: SEE PROGRAM 'MAIN')
C
C SUBROUTINE SPECIFIC PARAMETERS:
C
C XSIZE     LENGTH OF X-AXIS
C YSIZE     LENGTH OF Y-AXIS
C OFFSETX   USED TO OFFSET THE X-COORDINATE OF THE AXES
C           ORIGIN BY A SPECIFIED AMOUNT
C OFFSETY   USED TO OFFSET THE Y-COORDINATE OF THE AXES
C           ORIGIN BY A SPECIFIED AMOUNT
C X RANGE   MAX DISTANCE IN THE FORWARD DIRECTION OR THE
C           MAX DISTANCE IN THE REVERSE DIRECTION THAT THE
C           COLUMN WAS DISPLACED. USED TO SCALE THE X-AXIS
C Y RANGE   MAX LATERAL LOAD REQUIRED TO DISPLACE THE
C           STRUCTURE IN THE FORWARD DIRECTION OR THE MAX
C           LATERAL LOAD TO DISPLACE THE STRUCTURE IN THE
C           REVERSE DIRECTION. USED TO SCALE THE Y-AXIS
C XFACTOR   UNIT: PIXELS/UNIT LENGTH. USED TO CONVERT
C           UNITS OF LENGTH TO NUMBER OF PIXELS
C YFACTOR   UNIT: PIXELS/UNIT FORCE. USED TO CONVERT UNITS
C           OF FORCE TO NUMBER OF PIXELS
C LEY       DEFINES THE Y-COORDINATE OF THE UPPER LEFT
C           CORNER OF THE RECTANGLES USED IN THE LEGEND
C REY       DEFINES THE Y-COORDINATE OF THE LOWER RIGHT
C           CORNER OF THE RECTANGLES USED IN THE LEGEND

```

```

C OFFX1 X-COORDINATE OF THE LEFT (NEGATIVE) END OF THE
C X-AXIS
C OFFX2 X-COORDINATE OF THE RIGHT (POSITIVE) END OF THE
C X-AXIS
C OFFY1 Y-COORDINATE OF THE BOTTOM (NEGATIVE) END OF THE
C Y-AXIS
C OFFY2 Y-COORDINATE OF THE TOP (POSITIVE) END OF THE
C Y-AXIS
C TITLE NAME OF THE CYCLE IN FILES WITH THE '.OUT '
C CYCLES

```

```

C *****

```

```

C SUBROUTINE CYCLE(NPTS, NCOUNT, IDX, IDY, TITLE, MAXX,
C 1 MAXY, MINX, MINY, X, Y)

```

```

C DIMENSION X(400), Y(400)

```

```

C INTEGER*2 NCOUNT, LEY, REY, OFFSETY, OFFSETX, OFFX1,
C 1 OFFX2, OFFY1, OFFY2, XSIZE, YSIZE

```

```

C INTEGER*2 IDX(16), IDY(16), NVERT(1), VERTS(2, 400),
C 1 TITLE(40)

```

```

C REAL MAXX, MINX, MAXY, MINY

```

```

C SET PROGRAM VARIABLES

```

```

C XSIZE = 640
C YSIZE = 512

```

```

C SET OFFSET VALUES SO THAT THE PLOT IS DRAWN IN
C THE THIRD QUADRANT

```

```

C OFFSETX = -300
C OFFSETY = -250

```

```

C NCOUNT = ZERO FOR THE FIRST CYCLE PLOT. THE RANGE
C ONLY NEEDS TO BE SET ONCE AND THEREFORE THE PROGRAM
C WILL SKIP THE NEXT STATEMENTS FOR CYCLES GREATER THAN
C ONE

```

```

C IF (NCOUNT.GT.0) GOTO 3010

```

```

C DETERMINE THE XRANGE AND YRANGE

```

```

C XRANGE=MAX(ABS(MAXX), ABS(MINX))
C YRANGE=MAX(ABS(MAXY), ABS(MINY))

```

```

C DETERMINE THE XFACTOR AND YFACTOR

```

```

C XFACTOR=XSIZE/(2.*XRANGE)

```

```
YFACTOR=YSIZE/(2.*YRANGE)
```

```
C  
C  
C DRAW THE CURVE  
C  
C  
C
```

```
C The outer DO loop is used so that when J=1, the polygon  
C is filled and when J=2, the polygon is outlined  
C  
C
```

```
3010 DO 210 J=1,2
```

```
C CONVERT THE DATA POINTS INTO INTEGER*2 FORMAT AND ALSO  
C TO NUMBER OF PIXELS  
C
```

```
DO 200 I=1,NPTS  
VERTS(1,I)=IFIX(X(I)*XFACTOR)  
VERTS(2,I)=IFIX(Y(I)*YFACTOR)  
200 CONTINUE
```

```
C  
C DRAW AXES  
C
```

```
CALL VAL8(30) ! WHITE
```

```
C  
C DEFINE THE ENDS OF THE X & Y AXES  
C
```

```
OFFX1 = ( -XSIZE/2 + OFFSETX)  
OFFY1 = ( -YSIZE/2 + OFFSETY)  
OFFX2 = ( XSIZE/2 + OFFSETX)  
OFFY2 = ( YSIZE/2 + OFFSETY)
```

```
C  
C MOVE CURRENT POINT TO THE LEFT END OF THE X-AXIS  
C
```

```
CALL MOVABS(OFFX1,OFFSETY)
```

```
C  
C DRAW LINE TO THE RIGHT END OF THE X-AXIS  
C
```

```
CALL DRWABS(OFFX2,OFFSETY)
```

```
C  
C MOVE CURRENT POINT TO THE BOTTOM OF THE Y-AXIS  
C
```

```
CALL MOVABS(OFFSETX,OFFY1)
```

```
C  
C DRAW A LINE TO THE TOP END OF THE Y-AXIS  
C
```

```
CALL DRWABS(OFFSETX,OFFY2)
```

```
C  
C DETERMINE WHETHER TO FILL THE POLYGON OR NOT USING THE  
C DO LOOP INDEX  
C
```

```
IF(J.EQ.1) CALL PRMFIL(1)  
IF(J.EQ.2) CALL PRMFIL(0)
```

```
C  
C DETERMINE THE CURRENT PIXEL COLOR USING THE DO LOOP  
C INDEX, NCOUNT
```

```

C
    IF(J.EQ.1) CALL VAL8(NCOUNT) ! VARIED COLORS
    IF(J.EQ.2) CALL VAL8(30)      ! WHITE
    CALL MOVABS(OFFSETX,OFFSETY)
C
C DRAW POLYGON
C
    NVERT(1)=NPTS
    CALL POLYGN(1,NVERT,VERTS)
C
C DRAW LEGEND TO ASSOCIATE THE COLOR OF THE LOOPS WITH A
C CYCLE NUMBER. THE LEGEND IS A SERIES OF RECTANGLES
C FILLED WITH THE APPROPRIATE COLORS
C
    LEY = -50 - 20*NCOUNT
    REY = LEY - 25
C
C MOVE TO THE UPPER LEFT CORNER OF THE RECTANGLE
C
    CALL MOVABS(275,LEY)
    CALL RECTAN(300,REY)
C
C PLACE THE TEXT 20 PIXELS TO THE RIGHT OF THE RECTANGLE
C
    CALL MOVABS(320,REY)
C
C CALL RASTER TECH ROUTINE TO SET SIZE OF TEXT
C
    CALL TEXTN(30,30,0,0)
C
C SET CURRENT PIXEL VALUE TO WHITE
C
    CALL VAL8(30)
C
C IN BOLD TYPE, PLACE THE TITLE OF THE CYCLE NEXT TO THE
C COLORED RECTANGLE
C
    DO 400 I = 1,4
    CALL MOVREL(IDX(I),IDY(I))
    CALL TEXT1(40,TITLE)
400 CONTINUE
C
C EMPTY CONTENTS OF BUFFER ONTO THE SCREEN
C
    CALL EMPTYB
210 CONTINUE
C
    RETURN
    END
C
C
C

```

```

C *****
C
C SUBROUTINE ENERGY
C
C PURPOSE: PLOTS THE CUMULATIVE ENERGY ABSORBED BY THE
C          STRUCTURE SUBJECTED TO CYCLIC LOADING
C
C CALLED FROM: MAIN PROGRAM
C
C USAGE:
C
C CALL ENERGY(XMAX,XMIN,NCOUNT,TOTDISP,TOTENERGY,AREA,
C             DISPMT,ENERABS,IDX,IDY)
C
C PARAMETERS:
C
C XMAX      MAXIMUM VALUE OF THE X-COORDINATE (TYPICALLY
C           DISPLACEMENT)
C XMIN      MINIMUM VALUE OF THE Y-COORDINATE (TYPICALLY
C           FORCE)
C NCOUNT    SEE MAIN PROGRAM
C TOTDISP   "   "   "
C TOTENERGY "   "   "
C AREA      ENERGY ABSORBED BY THE STRUCTURE FOR ONE CYCLE
C DISPMT    SEE MAIN PROGRAM
C ENERABS   "   "   "
C IDX       "   "   "
C IDY       "   "   "
C
C
C OTHER SUBROUTINES CALLED: NONE ( OTHER THAN THAN THE
C RASTER TECH 'ONELIB' ROUTINES.  SEE PROGRAM 'MAIN'.)
C
C
C SUBROUTINE SPECIFIC PARAMETERS:
C
C XTIC      DISPLACEMENT EQUAL TO 100 PIXELS IN UNITS OF
C           LENGTH
C YTIC      LOAD EQUAL TO 100 PIXELS IN UNITS OF FORCE
C XDIV      EQUIVALENT TO XTIC IN CHARACTER FORMAT
C YDIV      EQUIVALENT TO YTIC IN CHARACTER FORMAT
C INTXDIV   EQUIVALENT TO XTIC IN INTEGER*2 FORMAT
C INTYDIV   EQUIVALENT TO YTIC IN INTEGER*2 FORMAT
C XSCALE    UNITS: PIXELS/UNIT LENGTH.  USED TO CONVERT
C           LENGTH TO NUMBER OF PIXELS
C YSCALE    UNITS: PIXELS/UNIT FORCE.  USED TO CONVERT
C           FORCE TO NUMBER OF PIXELS
C TOTX      TOTAL DISTANCE THAT A STRUCTURE WAS
C           DISPLACED IN A GIVEN CYCLE
C X0        DEFINES THE X-COORDINATE OF THE LOWER LEFT
C           CORNER OF THE POLYGON USED IN THE HISTOGRAM
C Y0        DEFINES THE Y-COORDINATE OF THE LOWER LEFT
C           CORNER OF THE POLYGON USED IN THE HISTOGRAM
C X1        DEFINES THE X-COORDINATE OF THE UPPER RIGHT

```

```

C          CORNER OF THE POLYGON.  EQUAL TO THE TOTX
C Y1      DEFINES THE Y-COORDINATE OF THE UPPER RIGHT
C          CORNER OF THE POLYGON.  EQUAL TO THE TOTAL
C          ENERGY ABSORBED IN A GIVEN CYCLE
C X2      SUMMATION OF THE TOTAL DISPLACEMENT OF THE
C          STRUCTURE IN A GIVEN CYCLE FOR ALL THE CYCLES
C Y2      SUMMATION OF THE ENERGY ABSORBED PER CYCLE FOR
C          ALL THE CYCLES

```

```

C *****

```

```

C          SUBROUTINE ENERGY(XMAX,XMIN,NCOUNT,TOTDISP,
C          1 TOTENERGY,AREA,DISPMT,ENERABS,IDX,IDY)
C
C          INTEGER*2 NCOUNT,X0,Y0,DISPMT,ENERABS,JX,
C          1 X1,Y1,X2,Y2,JL
C
C          INTEGER*2 NVERT(1),VERT(2,5),IDX(16),IDY(16)
C
C          CHARACTER*2 XDIV(3),YDIV(3)
C          INTEGER*2 INTXDIV(3),INTYDIV(3)
C          EQUIVALENCE (XDIV,INTXDIV)
C          EQUIVALENCE (YDIV,INTYDIV)
C
C          IF NCOUNT IS GREATER THAN ZERO, THE TITLES AND THE AXES
C          WILL ALREADY HAVE BEEN DRAWN AND DO NOT NEED TO BE
C          REDRAWN
C
C          IF(NCOUNT.GT.0) GOTO 300
C
C          DRAW THE AXES WITH THE ORIGIN AT (50,50)
C
C          MOVE TO ORIGIN
C
C          CALL MOVABS(50,50)
C
C          DRAW THE X-AXIS, 550 PIXELS IN LENGTH
C
C          CALL DRWABS(600,50)
C
C          MOVE TO THE ORIGIN
C
C          CALL MOVABS(50,50)
C
C          DRAW THE Y-AXIS, 450 PIXELS IN LENGTH
C
C          CALL DRWABS(50,500)
C
C          INSERT TITLE FOR THE HISTOGRAM
C
C          CALL TEXTN(40,40,0,0)
C          CALL MOVABS(200,-30)

```

```

C
C USE DO LOOP FOR BOLD TEXT
C
      DO 420 I=1,9
      CALL MOVREL(IDX(I),IDY(I))
      CALL TEXT1(23,'TOTAL ENERGY ABSORPTION')
420  CONTINUE
C
C LABEL X-AXIS
C
      CALL MOVABS(350,5)
      CALL TEXTN(35,35,0,0)
      DO 450 I=1,9
      CALL MOVREL(IDX(I),IDY(I))
      CALL TEXT1(14,'DISP. (INCHES)')
450  CONTINUE
C
C LABEL Y-AXIS
C
      CALL MOVABS(0,150)
      CALL TEXTC(30,90)
      DO 460 I=1,9
      CALL MOVREL(IDX(I),IDY(I))
      CALL TEXT1(15,'ENERGY (KIP-IN)')
460  CONTINUE
C
C
C FIND THE SCALE OF THE AXES:  X-AXIS = 500 PIX,
C Y-AXIS = 400 PIX
C
      XSCALE = 500.0/TOTDISP
      YSCALE = 400.0/TOTENERGY
C
C DRAW THE TIC MARKS ON THE AXES
C
C X-AXIS, DIVIDED INTO 5 SEGMENTS WITH EACH SEGMENT EQUAL
C TO 100 PIXELS
C
      CALL TEXTN(17,17,0,0)
      DO 350 L=1,5
      JX = (50 + L*100)
      CALL MOVABS(JX,46)
      CALL DRWABS(JX,54)
      XL = L
C
C ASSIGN SCALE VALUES TO THE AXIS
C
C TRANSLATE DATA, XTIC, FROM INTERNAL STORAGE TO CHARACTER
C FORMAT USING "ENCODE" STATEMENT
C
C USE EQUIVALENCE STATEMENT TO PUT THAT DATA (WHICH IS NOW
C IN CHARACTER FORMAT) TO INTEGER*2 FORMAT
C
      XTIC = (1.0/XSCALE*100.0)*XL

```

```

        ENCODE(6,351,XDIV) XTIC
351    FORMAT(F6.2)
        JL = 35 + L*100
        CALL MOVABS(JL,35)
C
C    USE DO LOOP TO OBTAIN BOLD NUMBERS
C
        DO 353 N=1,4
        CALL MOVREL(IDX(N),IDY(N))
        CALL TEXT1(6,INTXDIV)
353    CONTINUE
C
350    CONTINUE
C
C    Y-AXIS, DIVIDED INTO 4 SEGMENTS WITH EACH SEGMENT EQUAL
C    TO 100 PIXELS
C
        CALL TEXTC(15,90)
        DO 360 L=1,4
        JX = (50 + L*100)
        CALL MOVABS(46,JX)
        CALL DRWABS(54,JX)
C
C    ASSIGN SCALE VALUES TO THE AXIS
C
        XL = L
        YTIC = (1.0/YSCALE*100.0)*XL
        ENCODE(6,352,YDIV) YTIC
352    FORMAT(F6.2)
        JL = 35 + L*100
        CALL MOVABS(40,JL)
C
C    USE DO LOOP TO OBTAIN BOLD NUMBERS
C
        DO 354 N=1,4
        CALL MOVREL(IDX(N),IDY(N))
        CALL TEXT1(6,INTYDIV)
354    CONTINUE
C
360    CONTINUE
C
C    THE PLOT IS PRESENTED AS A SIDEWAYS BAR GRAPH WITH THE
C    WIDTH OF EACH BAR EQUAL TO THE ENERGY ABSORBED FOR A
C    GIVEN CYCLE
C
C    SET NO. OF VERTICES IN POLYGON
C
        NVERT(1) = 4
C
C    DEFINE THE POSITION OF THE VERTICES
C
300    X0 = DISPMT + 50
        Y0 = ENERABS + 50
        CALL MOVABS(X0,Y0)
C

```

```

C  DEFINE LOWER LEFT CORNER OF THE POLYGON
C
      VERT(1,1) = 0
      VERT(2,1) = 0
C
C  DEFINE THE LOWER RIGHT CORNER OF THE POLYGON
C
      VERT(1,2) = 600-X0
      VERT(2,2) = 0
C
C  SUM TOTAL DISPLACEMENT AND ENERGY
C
      TOTX = ABS(XMAX) + ABS(XMIN)
      X2 = DISPMT
      Y2 = ENERABS
      DISPMT = DISPMT + IFIX(TOTX*XSCALE)
      ENERABS = IFIX(AREA)*YSCALE + ENERABS
      X1 = DISPMT - X2
      Y1 = ENERABS - Y2
C
C  DEFINE THE UPPER LEFT CORNER OF THE POLYGON
C
      VERT(1,4) = X1
      VERT(2,4) = Y1
C
C  DEFINE THE UPPER RIGHT CORNER OF THE POLYGON
C
      VERT(1,3) = 600 - X0
      VERT(2,3) = Y1
C
C  DRAW FILLED POLYGON
C
      CALL VAL8(NCOUNT)
      CALL PRMFIL(1)
      CALL POLYGN(1,NVERT,VERT)
C
C  OUTLINE THE POLYGON IN WHITE
C
      CALL VAL8(30)
      CALL PRMFIL(0)
      CALL POLYGN(1,NVERT,VERT)
C
C
      CALL EMPTYB
      RETURN
      END
C
C
C
C

```

```

C *****
C
C SUBROUTINE INDIVENE
C
C PURPOSE: TO PLOT THE ENERGY ABSORBED IN EACH CYCLE BY
C A STRUCTURE AS A BAR CHART TYPE HISTOGRAM.
C THE WIDTH OF EACH BAR REPRESENTS THE DISPLACEMENT
C DUCTILITY AT THAT CYCLE WHILE THE HEIGHT
C REPRESENTS THE ENERGY DISSIPATED DURING THAT
C CYCLE ( THE AREA INSIDE THE HYSTERESIS CURVE)
C
C CALLED FROM: PROGRAM MAIN
C
C USAGE: CALL INDIVENE (AREA, NCOUNT, XMAX, XMIN, AREAMAX,
C TOTDISP, IDX, IDY)
C
C PARAMETERS:
C
C AREA ENERGY ABSORBED BY STRUCTURE IN A PARTICULAR
C CYCLE
C NCOUNT INDEX USED CHANGE THE COLOR OF THE PLOT
C XMAX MAXIMUM X-COORDINATE
C XMIN MINIMUM Y-COORDINATE
C AREAMAX TOTAL ENERGY ABSORBED BY THE STRUCTURE, USED TO
C SET THE ON THE Y-AXIS
C TOTDISP SEE MAIN PROGRAM
C IDX " " "
C IDY " " "
C
C OTHER SUBROUTINES CALLED: NONE (OTHER THAN THE RASTER
C TECH 'ONELIB' SUBROUTINES. SEE PROGRAM MAIN)
C
C SUBROUTINE SPECIFIC PARAMETERS:
C
C SCALEX UNITS: PIXELS/UNIT LENGTH. CONVERTS UNITS
C OF LENGTH TO NUMBER OF PIXELS
C SCALEY UNITS: PIXELS/UNIT ENERGY. CONVERTS UNITS OF
C ENERGY TO NUMBER OF PIXELS
C TICY AMOUNT OF ENERGY EQUAL TO 100 PIXELS IN UNITS
C OF ENERGY
C DIVY EQUIVALENT TO TICY IN CHARACTER FORMAT
C INTDIVY EQUIVALENT TO TICY IN INTEGER*2 FORMAT
C DELY2 LENGTH EQUIVALENT TO 2 TIMES DELTA Y IN NUMBER
C OF PIXELS. USED TO SHOW THE SCALE FOR THE BAR
C WIDTHS
C XTOT TOTAL DISTANCE THAT A STRUCTURE WAS DISPLACED
C IS A GIVEN CYCLE
C X0 VARIABLE USED IN LOCATING THE UPPER RIGHT
C CORNER OF THE BAR IN THE HISTOGRAM
C XDISP SUMMATION OF THE TOTAL DISPLACEMENT OF A
C STRUCTURE IN A GIVEN CYCLE OVER ALL THE CYCLES
C YENER ENERGY ABSORBED IN A GIVEN CYCLE IN NUMBER OF
C PIXELS

```



```

        DO 620 I=1,4
        JX = 50 + I*100
        CALL MOVABS(46,JX)
        CALL DRWABS(54,JX)
        XL = I
        TICY = (1.0/SCALEY*100.0)*XL
C
C CONVERT TICY TO CHARACTER FORMAT AND THEN TO INTEGER*2
C FORMAT USING THE ENCODE STATEMENT
C
        ENCODE(6,621,DIVY) TICY
621     FORMAT(F6.0)
C
C MOVE TO LOCATION TO PLACE THE VALUE OF THE TICK MARKS
C
        JL = 25 + I*100
        CALL MOVABS(40,JL)
C
C USE DO LOOP TO OBTAIN BOLD NUMBERS
C
        DO 622 N=1,4
        CALL MOVREL(IDX(N),IDY(N))
        CALL TEXT1(6,INTDIVY)
622     CONTINUE
620     CONTINUE
C
C PLACE THE TITLE, 'SCALE', IN THE UPPER RIGHT CORNER OF
C THE SCREEN
C
        CALL VAL8(30)                ! WHITE
        CALL MOVABS(380,450)
        CALL TEXTN(30,30,0,0)
        DO 610 I = 1,4
        CALL MOVREL(IDX(I),IDY(I))
        CALL TEXT1(5,'SCALE')
610     CONTINUE
C
C PLOT A SCALE FOR DUCTILITY FACTOR USING 2 TIMES DELTA Y
C
C FIND THE LENGTH OF 2 DELTA Y. DELTA Y IS DEFINED AS THE
C AVERAGE OF THE DISPLACEMENT TO YIELD LOAD IN THE FIRST
C CYCLE IN THE FORWARD DIRECTION PLUS THE DISPLACEMENT IN THE
C REVERSE DIRECTION DIVIDED BY 0.75.
C
C THE FACTOR OF 2 IS APPLIED BECAUSE THE STRUCTURE
C WAS DISPLACED 2 DELTA Y IN ONE DIRECTION AND 2 DELTA Y
C IN THE REVERSE DIRECTION RESULTING IN A TOTAL DISPLACEMENT
C OF 4 TIMES DELTA Y. THEREFORE, DEL2 IS NOT ACTUALLY 2 TIMES
C DELTA Y BUT IS HOWEVER, REPRESENTATIVE OF THE TOTAL
C DISPLACEMENT AT 2 TIMES DELTA Y.
C
C THE CONSTANT 375 IS ADDED TO MOVE THE LOCATION
C OF THE SCALE TO 375 PIXELS RIGHT OF THE SCREEN ORIGIN
C
        DELY2 = IFIX((ABS(XMAX)+ABS(XMIN))*4.0/3.0)*2.0*

```

```

1 SCALEX)+375
C
C DRAW THE SCALE WHICH IS A LINE REPRESENTING THE WIDTH OF
C THE BAR FOR 2 DELTA Y
C
CALL MOVABS(375,415)
CALL DRWABS(375,425)
CALL MOVABS(DELY2,415)
CALL DRWABS(DELY2,425)
DO 660 I=1,4
IY = 418 + I
CALL MOVABS(375,IY)
CALL DRWABS(DELY2,IY)
660 CONTINUE
C
C LABEL SCALE REPRESENTING DISPLACEMENT DUCTILITY. PLACE THE
C LABEL 25 PIXELS TO RIGHT OF THE SCALE
C
DELY2 = DELY2 + 25
CALL MOVABS(DELY2,415)
CALL TEXTN(25,25,0,0)
DO 670 I=1,4
CALL MOVREL(IDX(I),IDY(I))
CALL TEXT1(9,'2 DELTA Y')
670 CONTINUE
C
C INSERT TITLE OF THE HISTOGRAM
C
CALL TEXTN(40,40,0,0)
CALL MOVABS(175,-30)
DO 630 I=1,9
CALL MOVREL(IDX(I),IDY(I))
CALL TEXT1(23,'ENERGY ABSORPTION/CYCLE')
630 CONTINUE
C
C LABEL X-AXIS
C
CALL MOVABS(125,5)
CALL TEXTN(35,35,0,0)
DO 640 I=1,9
CALL MOVREL(IDX(I),IDY(I))
CALL TEXT1(33,'WIDTH OF BARS = TOTAL CYCLE DISP.')
640 CONTINUE
C
C LABEL Y-AXIS
C
CALL MOVABS(0,150)
CALL TEXTC(30,90)
DO 650 I=1,9
CALL MOVREL(IDX(I),IDY(I))
CALL TEXT1(15,'ENERGY (KIP-IN)')
650 CONTINUE
C
C SET NO. OF VERTICES IN POLYGON USED TO REPRESENT A BAR
C ON THE HISTOGRAM

```

```

C
C      NVERT(1) = 4
C
C  DEFINE VERTICES
C
C  INITIALIZE VALUES
C
C      XDISP = 0
C      XTOT = 0
C
C  THIS PART OF THE SUBROUTINE PLOTS THE INDIVIDUAL CYCLE
C  ENERGY AS A BAR ON THE HISTOGRAM
C
C 600      XO = XDISP + 50
C
C  MOVE TO THE LOWER RIGHT CORNER OF THE LAST BAR DRAWN OR
C  IN THE CASE OF THE FIRST BAR, MOVE TO THE ORIGIN OF THE
C  AXES
C
C      CALL MOVABS(XO,50)
C
C  FIND THE TOTAL DISPLACEMENT OF THE COLUMN FOR THE CYCLE,
C  XTOT
C
C      XTOT = IFIX((ABS(XMAX) + ABS(XMIN)) *
C      1 SCALEX)
C      XDISP = XDISP + XTOT
C
C  NOTE:  THE POINTS DEFINED BY VERT(I,J) ARE RELATIVE TO THE
C  CURRENT POINT AS DEFINED BY THE MOVABS CALL
C
C  DEFINE THE LOWER LEFT CORNER OF THE BAR
C
C      VERT(1,1) = 0
C      VERT(2,1) = 0
C
C  DEFINE THE LOWER RIGHT CORNER OF THE BAR BY MOVING OVER
C  TO THE RIGHT BY AN AMOUNT EQUAL TO THE DISPLACEMENT TRANSVERSED
C  IN A GIVEN CYCLE
C
C      VERT(1,2) = XTOT
C      VERT(2,2) = 0
C
C  SCALE THE HEIGHT OF THE BAR
C
C      YENER = IFIX(AREA*SCALEY)
C
C  DEFINE THE UPPER RIGHT CORNER OF THE BAR BY MOVING UP AN
C  AMOUNT EQUAL TO THE ENERGY DISSIPATED IN A GIVEN CYCLE
C
C      VERT(1,3) = XTOT
C      VERT(2,3) = YENER
C
C  DEFINE THE UPPER LEFT CORNER OF THE BAR
C

```

```
VERT(1,4) = 0
VERT(2,4) = YENER
```

```
C
C DRAW BAR FILLED WITH COLOR VALUE = NCOUNT
C
```

```
CALL VAL8(NCOUNT)
CALL PRMFIL(1)
CALL POLYGN(1,NVERT,VERT)
```

```
C
C OUTLINE THE BAR IN WHITE
C
```

```
CALL VAL8(30)
CALL PRMFIL(0)
CALL POLYGN(1,NVERT,VERT)
```

```
C
CALL EMPTYB
RETURN
END
```

```

C *****
C
C
C SUBROUTINE COLPLOT
C
C PURPOSE: TO ANIMATE THE COLUMN MOVEMENT AS THE THE
C          HYSTERESIS CURVE IS BEING PLOTTED
C
C CALLED FROM: PROGRAM MAIN
C
C USAGE: CALL COLPLOT(NPTS,X,Y,IDX,IDY,NCOUNT,MAXX,MAXY,
C          MINX,MINY,XMAX,XMIN)
C
C PARAMETERS:
C
C NPTS      NUMBER OF DATA POINTS IN A GIVEN CYCLE
C X(I)      X-COORDINATE OF THE DATA POINT TYPICALLY THE
C           DISPLACEMENT
C Y(I)      Y-COORDINATE OF THE DATA POINT
C IDX       SEE MAIN PROGRAM
C IDY       " " "
C NCOUNT    " " "
C MAXX     " " "
C MAXY     " " "
C MINX     " " "
C MINY     " " "
C XMAX     MAXIMUM X VALUE FOR A PARTICULAR CYCLE
C XMIN     MINIMUM X VALUE FOR A PARTICULAR CYCLE
C
C
C OTHER SUBROUTINES CALLED: NONE (OTHER THAN THE RASTER
C TECH 'ONELIB' SUBROUTINE CALLS. SEE PROGRAM MAIN)
C
C SUBROUTINE SPECIFIC PARAMETERS:
C
C SCALE     UNITS: PIXELS/UNIT LENGTH. ARBITRARY VALUE
C           CHOSEN TO MAGNIFY THE ANIMATED COLUMN DISPLACEMENT
C COLX      DISPLACEMENT OF COLUMN IN NUMBER OF PIXELS
C OFFSETX   USED TO RELOCATE THE X-COORDINATE OF THE
C           ORIGIN OF THE AXES FROM THE SCREEN ZERO
C OFFSETY   USED TO RELOCATE THE Y-COORDINATE OF THE
C           ORIGIN OF THE AXES FROM THE SCREEN ZERO
C XSIZE     LENGTH OF X-AXIS IN PIXELS
C YSIZE     LENGTH OF Y-AXIS IN PIXELS
C XRANGE    MAXIMUM DISTANCE THAT THE STRUCTURE WAS
C           DISPLACED IN EITHER THE FORWARD OR REVERSE
C           DIRECTION FROM ALL THE CYCLES IN A TEST
C YRANGE    MAXIMUM LOAD REQUIRED TO DISPLACE THE STRUCTURE
C           IN EITHER THE FORWARD OR REVERSE DIRECTION
C           FROM ALL THE CYCLES IN A TEST
C XFACTOR   UNITS: PIXELS/UNIT OF LENGTH. USED TO CONVERT
C           COLUMN DISPLACEMENT TO NUMBER OF PIXELS
C YFACTOR   UNITS: PIXEL/UNIT OF FORCE. USED TO CONVERT
C           THE LATERAL LOAD TO NUMBER OF PIXELS
C IA,IB     VARIABLES USED TO DETERMINE THE LOCATION OF

```

```

C      THE ARROW HEAD
C  ARROW  LEFT END OF THE ARROW WHICH SHOWS THE
C          DIRECTION OF THE LATERAL LOAD.  THIS POINT IS
C          LOCATED 70 PIXELS TO THE RIGHT OF THE COLUMN.
C  ENDARR LOCATES WHICH END, LEFT OR RIGHT, OF THE
C          ARROW SHAFT THE ARROW HEAD SHOULD GO
C  IEND   LOCATES THE END OF THE ARROW HEAD
C  X0     USED TO IDENTIFY THE DATA POINT PLOTTED PRIOR
C          TO THE CURRENT DATA POINT
C  X1     X-COORDINATE OF THE DATA POINT PLOTTED PRIOR
C          TO THE CURRENT DATA POINT
C  X2     X-COORDINATE OF THE CURRENT DATA POINT TO BE
C          PLOTTED
C  Y1     Y-COORDINATE OF THE DATA POINT PLOTTED PRIOR
C          TO THE CURRENT DATA POINT
C  Y2     Y-COORDINATE OF THE CURRENT DATA POINT
C  OFFX1  X-COORDINATE OF THE LEFT (NEGATIVE) END OF
C          THE X-AXIS
C  OFFX2  X-COORDINATE OF THE RIGHT (POSITIVE) END OF
C          THE X-AXIS
C  OFFY1  Y-COORDINATE OF THE BOTTOM (NEGATIVE) END OF THE
C          Y-AXIS
C  OFFY2  Y-COORDINATE OF THE TOP (POSITIVE) END OF THE
C          Y-AXIS
C  XC * YC  DEFINES A POINT ALONG THE DEFLECTED LENGTH OF
C          THE COLUMN IN REAL NUMBER FORMAT
C  XC1 & YC1  DEFINES THE LAST POINT ALONG THE DEFLECTED
C          COLUMN LENGTH TO BE PLOTTED IN INTEGER*2
C          FORMAT
C  XC2 & YC2  DEFINES THE CURRENT POINT ALONG THE DEFLECTED
C          COLUMN LENGHT TO BE PLOTTED IN INTEGER*2
C          FORMAT

```

```

C *****

```

```

C
C  SUBROUTINE COLPLOT(NPTS,X,Y,IDX,IDY,NCOUNT,MAXX,
C  1 MAXY, MINX,MINY,XMAX,XMIN)
C
C  DIMENSION X(400),Y(400),XC(20),YC(20)
C
C  INTEGER*2 COLX,NEWX,NEWY,OFFSETX,OFFSETY,X0,X1,Y1,
C  1 X2,Y2,OFFX1,OFFX2,OFFY1,OFFY2,XSIZE,YSIZE,ARROW,
C  2 ENDARR,IEND
C
C  INTEGER*2 IDX(16),IDY(16),VERTS(2,400),NVERTS(1),
C  1 YC1,YC2,XC1,XC2,XC10,YC10
C
C  REAL MAXX,MINX,MINY,MAXY
C
C  CALL PRMFIL(0)
C  CALL VAL8(30)

```

```

C SET SCALE EQUAL TO 20 PIX/INCH SO THAT THE MOVEMENT OF
C THE COLUMN IS MAGNIFIED
C
      IF(MAXX.GT.5) SCALE = 4.0
      IF(MAXX.LE.5) SCALE = 20.0
C
C
C SET PROGRAM VARIABLES
C
      XSIZE = 640
      YSIZE = 512
      XC(1) = 0.0
      YC(1) = 0.0
C
C SET OFFSET VALUES SO THAT THE PLOT IS DRAWN IN
C THE THIRD QUADRANT
C
      OFFSETX = -300
      OFFSETY = -250
C
C IF NCOUNT > 0, THE AXES AND TITLES HAVE ALREADY BEEN
C PLOTTED AND DO NOT NEED TO BE REPLOTTED AND THE NEXT
C PART OF THE ROUTINE IS OMITTED
C
      IF (NCOUNT.GT.0) GOTO 3001
C
C DETERMINE THE XRANGE AND YRANGE WHICH ARE USED TO SCALE
C THE X & Y AXES RESPECTIVELY
C
      XRANGE=MAX(ABS(MAXX),ABS(MINX))
      YRANGE=MAX(ABS(MAXY),ABS(MINY))
C
C DETERMINE THE SCALE FOR THE X-AXIS, XFACTOR
C
      XFACTOR=XSIZE/(2.*XRANGE)
C
C DETERMINE THE SCALE FOR THE Y-AXIS, YFACTOR
C
      YFACTOR=YSIZE/(2.*YRANGE)
C
C
C DRAW AXES USED FOR THE HYSTERESIS CURVE PLOTS
C
      CALL VAL8(30)                                ! WHITE
C
C DETERMINE THE ENDS OF THE X AND Y AXES
C
      OFFX1 = ( -XSIZE/2 + OFFSETX)
      OFFY1 = ( -YSIZE/2 + OFFSETY)
      OFFX2 = ( XSIZE/2 + OFFSETX)
      OFFY2 = ( YSIZE/2 + OFFSETY)
C
C DRAW THE X-AXIS
C
      CALL MOVABS(OFFX1,OFFSETY)

```

```
CALL DRWABS(OFFX2,OFFSETY)
```

```
C  
C DRAW THE Y-AXIS  
C
```

```
CALL MOVABS(OFFSETX,OFFY1)  
CALL DRWABS(OFFSETX,OFFY2)
```

```
C  
C INSERT TITLES  
C  
C
```

```
CALL VAL8(30) ! WHITE  
CALL MOVABS(-315,20)
```

```
C  
C CALL RASTER TECH ROUTINE TO SET TEXT SIZE AND FOR  
C HORIZONTAL TEXT  
C
```

```
CALL TEXTN(35,35,0,0)
```

```
C  
C LABEL Y-AXIS  
C
```

```
DO 410 I=1,9  
CALL MOVREL(IDX(I),IDY(I))  
CALL TEXT1(4,'LOAD')  
410 CONTINUE
```

```
C  
C LABEL THE X-AXIS  
C
```

```
CALL MOVABS(-10,-280)  
DO 430 I=1,9  
CALL MOVREL(IDX(I),IDY(I))  
CALL TEXT1(12,'DISPLACEMENT')  
430 CONTINUE
```

```
C  
C DISPLAY OVERALL TITLE OF PLOT  
C
```

```
CALL MOVABS(-250,-450)  
CALL TEXTN(40,40,0,0)  
DO 440 I=1,9  
CALL MOVREL(IDX(I),IDY(I))  
CALL TEXT1(24,'LOAD-DISPLACEMENT CYCLES')
```

```
440 CONTINUE  
3001 CONTINUE
```

```
C  
C THE ANIMATED COLUMN WILL BE SHOWN IN THE UPPER LEFT  
C CORNER OF THE SCREEN  
C
```

```
C DRAW BASE OF THE COLUMN  
C
```

```
CALL MOVABS(-500,225)  
CALL RECTAN(-100,100)
```

```
C  
C READ IN THE DATA POINTS AND CONVERT TO INTEGER*2 FORMAT AND  
C TO NUMBER OF PIXELS  
C
```

```
DO 220 I=1,NPTS
```

```

      VERTS(1,I) = IFIX(X(I)*XFACTOR)
      VERTS(2,I) = IFIX(Y(I)*YFACTOR)
C
C   DETERMINE IA AND  IB
C
      IF(X(I).EQ.XMAX) IA = I
      IF(X(I).EQ.XMIN) IB = I
220   CONTINUE
C
C   DRAW THE MOVEMENT OF THE COLUMN
C
      DO 240 I=1,NPTS
C
C   THIS LOOP IS USED TO ERASE THE COLUMN IN ITS PREVIOUS
C   POSITION
C
      DO 230 J=1,2
      IF(J.EQ.1) CALL VAL8(30)      ! WHITE
      IF(J.EQ.2) CALL VAL8(31)      ! BACKGROUND COLOR,BLACK
C
C   IF I > 1, THE COLUMN AT ZERO POSITION SHOULD NOT BE
C   DRAWN
C
      IF(I.GT.1) GOTO 245
C
C   DRAW COLUMN AT ZERO POSITION
C
      CALL MOVABS(-330,225)
      CALL RECTAN(-270,425)
C
C   CALCULATE COLX
C
245   COLX = IFIX(X(I)*SCALE-330.0)
C
C   DEFINE LOAD ARROW DEFLECTION.  ARROW IS USED TO INDICATE THE
C   DIRECTION OF THE LATERAL LOAD
C
      ARROW = COLX + 70
C
C   IF I < IA, THE COLUMN IS DEFLECTING TO THE RIGHT AND THE
C   ARROW HEAD IS LOCATED AT THE RIGHT END OF THE ARROW
C   SHAFT
C
      IF(I.LE.IA) ENDARR = ARROW + 75
C
C   IF I > IA, THE COLUMN IS DEFLECTING TO THE LEFT AND THE
C   ARROW HEAD IS LOCATED AT THE LEFT END OF THE ARROW
C   SHAFT
C
      IF(I.GT.IA.AND.IB.LE.IB) ENDARR = ARROW
C
C   IF IA < I < IB, THE COLUMN IS DEFLECTING TO THE RIGHT AND THE
C   ARROW HEAD IS LOCATED AT THE RIGHT END OF THE ARROW
C   SHAFT
C

```

```
IF(I.GT.IB) ENDARR = ARROW + 75
```

```
C  
C DRAW ARROW USING DO LOOP TO CREATE BOLD EFFECT  
C
```

```
DO 235 N=1,5
```

```
C  
C DRAW THE ARROW SHAFT, LENGTH = 75 PIXELS  
C
```

```
CALL MOVABS(ARROW,417+N)  
CALL DRWABS(ARROW+75,417+N)
```

```
C  
C DRAW ARROW HEAD  
C
```

```
CALL MOVABS(ENDARR,417+N)  
IF(I.LE.IA) IEND = -20  
IF(I.GT.IA.AND.I.LE.IB) IEND = 20  
IF(I.GT.IB) IEND = -20  
CALL DRWABS(ENDARR+IEND,437+N)  
CALL MOVABS(ENDARR,417+N)  
CALL DRWABS(ENDARR+IEND,398+N)
```

```
235 CONTINUE
```

```
C  
C DRAW COLUMN MOVING  
C
```

```
C THE COLUMN HEIGHT IS DIVIDED INTO 10 DISCRETE SEGMENTS  
C OR 10 POINTS WITH EACH POINT EQUAL TO 20 PIXELS ABOVE  
C THE PREVIOUS POINT  
C
```

```
DO 231 M = 1,10  
IM = M+1  
XN =M
```

```
C  
C DEFINE THE COORDINATES OF THE (N+1) DATA POINT. RECALL  
C THAT XC(1) AND YC(1) HAVE ALREADY BEEN DEFINED  
C PREVIOUSLY  
C
```

```
XC(IM) = 20.0*XN
```

```
C  
C GIVEN A VALUE OF X, THE VALUE OF Y IS FOUND BY THE EQUATION  
C FROM MCGUIRE AND GALLAGHER, "MATRIX STRUCTURAL  
C ANALYSIS", 1979, PG. 87  
C
```

```
Y = [X**2 (3*L - X)]/6*EI
```

```
YC(IM) = (X(I)*SCALE)*(XC(IM)**2)*(600.0-XC(IM))/  
1 16000000.0
```

```
C  
C CHANGE THESE VALUES TO INTEGER*2 FORMAT  
C
```

```
C XC1 & YC1 DEFINE THE LAST POINT (N-1) TO BE PLOTTED  
C
```

```
C XC2 AND YC2 DEFINE THE CURRENT POINT (N) TO BE PLOTTED  
C
```

```
YC1 = IFIX(YC(M))
```

```

        YC2 = IFIX(YC(IM))
        XC1 = IFIX(XC(M))
        XC2 = IFIX(XC(IM))
C
C   DRAW THE DEFLECTED LEFT LINE OF THE COLUMN
C
C   MOVE THE LAST POINT TO BE PLOTTED
C
C       CALL MOVABS(-330+YC1,225+XC1)
C
C   DRAW A LINE FROM THE LAST POINT (N-1) TO THE CURRENT
C   POINT (N)
C
C       CALL DRWABS(-330+YC2,225+XC2)
C
C   DRAW THE DEFLECTED RIGHT LINE OF THE COLUMN
C
C       CALL MOVABS(-270+YC1,225+XC1)
C       CALL DRWABS(-270+YC2,225+XC2)
231  CONTINUE
C
C   DRAW A LINE AT THE TOP OF THE COLUMN CONNECTING THE LEFT
C   AND RIGHT VERTICAL COLUMN LINES
C
C       YC10 = IFIX(YC(11))
C       XC10 = IFIX(XC(11))
C       CALL MOVABS(-330+YC10,225+XC10)
C       CALL DRWABS(-270+YC10,225+XC10)
C
C   SHOW THE LOAD-DISPLACEMENT CORRESPONDING TO THE COLUMN
C   MOVEMENT
C
C   WHEN J = 2, THE COLUMN IN ITS PREVIOUS POSITION IS
C   'ERASED' OR STATED MORE ACCURATELY, REDRAWN IN
C   BACKGROUND COLOR. THE HYSTERESIS PLOT IS
C   HOWEVER, NOT ERASED. THE GOTO 230 WILL ENSURE THIS.
C
C       IF(J.EQ.2) GOTO 230
C
C   IF I = 1, THIS IS THE FIRST DATA POINT TO BE PLOTTED.
C   MOVE TO THE ORIGIN OF THE AXES AND THE 'GOTO 260'
C   STATEMENT DIRECTS THE PROGRAM TO DRAW A LINE FROM THE
C   AXES ORIGIN TO THE FIRST DATA POINT
C
C   IF I > N FOR N > 1, DEFINE THE (N-1) POINT AS (X1,Y1)
C   AND THE CURRENT POINT AS (X2,Y2).
C
C       IF(I.GT.1) GOTO 250
C       CALL MOVABS(OFFSETX,OFFSETY)
C       GOTO 260
250  X0 = I-1
C       X1 = OFFSETX + VERTS(1,X0)
C       Y1 = OFFSETY + VERTS(2,X0)
C
C   MOVE TO THE (N-1) POINT PLOTTED

```

```

C
    CALL MOVABS(X1,Y1)
260  X2 = OFFSETX + VERTS(1,I)
    Y2 = OFFSETY + VERTS(2,I)
C
C  DRAW A LINE FROM THE (N-1) POINT TO THE N th POINT
C
    CALL DRWABS(X2,Y2)
    CALL EMPTYB
230  CONTINUE
240  CONTINUE
C
C  DRAW COLUMN AT ZERO POSITION
C
    CALL VAL8(30)
    CALL MOVABS(-330,225)
    CALL RECTAN(-270,425)
C
C  ERASE THE CYCLE
C
C
C  CALL VAL8(18)
C  NVERTS(1) = NPTS
C  CALL MOVABS(OFFSETX,OFFSETY)
C  CALL POLYGN(1,NVERTS,VERTS)
C  CALL EMPTYB
    RETURN
    END
C
C
C

```

```

C *****
C
C SUBROUTINE COMPARE
C
C PURPOSE: TO COMPARE ENERGY ABSORBED PER CYCLE BETWEEN A
C          MAXIMUM OF 3 TESTS. THIS COMPARISON IS
C          PRESENTED IN A BAR GRAPH TYPE HISTOGRAM. SCALING
C          OF VALUES PERMITS THE EASY DETERMINATION OF THE
C          SCALE BETWEEN TESTS.
C
C          THESE ENERGIES HAVE BEEN NORMALIZED BY THE
C          YIELD DISPLACEMENT AND THE CONCRETE
C          COMPRESSIVE STRENGTH. THE USER MAY CHOOSE
C          NOT TO DO SO BY ENTERING ONES FOR THE YIELD
C          DISPLACEMENTS AND CONCRETE COMPRESSIVE STRENGTHS.
C
C CALLED FROM: PROGRAM MAIN
C
C USAGE: CALL COMPARE(IDX, IDY)
C
C PARAMETERS:
C
C IDY     SEE MAIN PROGRAM
C IDX     SEE MAIN PROGRAM
C
C OTHER SUBROUTINES CALLED: REDRAW AND RASTER TECH 'ONELIB'
C ROUTINES. SEE PROGRAM MAIN.
C
C SUBROUTINE SPECIFIC PARAMETERS:
C
C ISIZE   SETS THE SIZE OF THE CYCLE TITLES TO BE
C          PLOTTED
C LENX    LENGTH OF X-AXIS
C LENY    LENGTH OF Y-AXIS
C ORIGINX X-COORDINATE OF THE ORIGIN OF THE AXES
C ORIGINY Y-COORDINATE OF THE ORIGIN OF THE AXES
C ALIST(I) I th FILENAME OF TEST TO BE COMPARED. THIS
C          FILE CONTAINS THE NAMES OF ALL THE CYCLES,
C          ONE PER LINE, IN A GIVEN TEST. THESE NAMES
C          ARE THE CONVERTED FILENAMES. SEE
C          DOCUMENTATION IN PROGRAM MAIN FOR MORE
C          INFORMATION
C ATITLE  NAME OF A CYCLE CONTAINED IN ALIST
C BLIST   EQUIVALENT OF ALIST BUT WITH '.LIS' EXTENSION
C          ATTACHED
C BTITLE  EQUIVALENT OF ATITLE BUT WITH '.OUT' EXTENSION
C          ATTACHED
C CTICK   THE AMOUNT OF ENERGY EQUAL TO 100*I PIXELS
C          WHERE I = 1, 2, ... TO THE NUMBER OF DIVISIONS
C          OF THE Y-AXIS IN UNITS OF ENERGY
C TICK    EQUIVALENT TO CTICK IN CHARACTER FORMAT
C INTTICK EQUIVALENT TO CTICK IN INTEGER*2 FORMAT
C NUMCYCLE(I) THE TOTAL NUMBER OF CYCLES IN THE I th TEST

```

```

C  INUMCYC      TOTAL NUMBER OF CYCLES FOR ALL THE TESTS
C              USED TO SCALE THE X-AXIS
C  XCYC        EQUIVALENT OF INUMCYC IN REAL NUMBER FORMAT
C  ENERGMAYX   MAXIMUM ENERGY ABSORBED PER CYCLE FORM ALL
C              THE TESTS TO BE COMPARED.  USED TO SCALE THE
C              Y-AXIS
C  YIELD(I)    YIELD DISPLACEMENT OF THE I th TEST
C  CONC_COMP(I) CONCRETE COMPRESSIVE STRESS OF THE I th TEST
C  ATIT(I,J)   J th TITLE OF CYCLE IN THE I th TEST
C  INTITLE     EQUIVALENT TO ATIT IN INTEGER*2 FORMAT
C  ENERGY(I,J) ENERGY ABSORBED IN CYCLE J OF THE I th TEST
C  ZTIT(I)     I th TITLE CONTAINED IN FILE 'REFTITLE.LIS'
C  NUMTEST     NUMBER OF TESTS TO BE COMPARED
C  CSCALEY     UNITS:  PIXEL/UNIT OF ENERGY.  CONVERTS THE
C              ENERGY ABSORBED TO NUMBER OF PIXELS
C  NTEST       VARIABLE USED TO TRANSFER OUT OF THE LOOP TO
C              PLOT THE BAR GRAPH WHEN ALL THE CYCLES HAVE
C              BEEN PLOTTED
C  NDONE(I)    VARIABLE USED TO ENSURE THAT NTEST IS
C              INCREMENTED ONLY ONCE BY THE I th TEST TO BE
C              COMPARED
C  X0          X-COORDINATE OF THE LOWER LEFT OF THE BAR
C  Y0          Y-COORDINATE OF THE LOWER LEFT OF THE BAR
C  X1          X-COORDINATE OF THE UPPER RIGHT OF THE BAR
C  Y1          Y-COORDINATE OF THE UPPER RIGHT OF THE BAR
C  X2          X-COORDINATE USED TO POSITION THE TITLE OF
C              THE CYCLE ABOVE THE BAR
C  Y2          Y-COORDINATE USED TO POSITION THE TITLE OF
C              THE CYCLE ABOVE THE BAR
C  LY1        Y-COORDINATE OF THE LOWER LEFT OF THE RECTANGLES
C              USED IN THE LEGEND
C  LY2        Y-COORDINATE OF THE UPPER RIGHT OF THE
C              RECTANGLES USED IN LEGEND
C  PRE_SCALE  VARIABLE PASSED BACK FROM SUBROUTINE REDRAW. IT IS AN
C              ARRAY WHICH STORES THE SCALE FACTOR FOR EACH TEST.  THE
C              SCALING IS CUMULATIVE.  I.E.  IF A TEST HAS BEEN SCALED
C              BY A FACTOR OF "a" AND SCALING OF THE SAME TEST IS
C              ASKED FOR AGAIN, THIS TIME BY A FACTOR OF "b", THE
C              RESULTING ENERGY THAT IS PLOTTED IS SCALED BY ab.

```

```

C *****
C
C

```

```

C      SUBROUTINE COMPARE(IDX, IDY)

```

```

C      INTEGER*2  IDX(16), IDY(16), INTTICK(4), INTITLE(7, 50, 50),
C      1  LTITLE(7, 50), TEST(3, 100), REPEAT(3)

```

```

C      INTEGER*2  X0, Y0, X1, Y1, X2, Y2, LY1, LY2, LY3, ISIZE,
C      1  ORIGINX, ORIGINY, LENX, LENY, TESTNO

```

```

C      CHARACTER*14  ALIST(50), ATIT(50, 50), ZTIT(50)
C      CHARACTER*9   ATITLE
C      CHARACTER*18  BLIST, BTITLE

```

```

C      CHARACTER*2 TICK(4)
C
C      DIMENSION ENERGY(50,50),NUMCYCLE(100),TOTAREA(10),
1 NDONE(10),YIELD(5),CONC_COMP(5),PRE_SCALE(3)
C
C      EQUIVALENCE(TICK,INTTICK)
C      EQUIVALENCE(ALIST,LTITLE)
C      EQUIVALENCE(ATIT,INTITLE)
C
C      INITIALIZE GRAPHICS DEVICE
C
C      CALL RTSET(1,180)
C      CALL RTINIT('GDA0:',5)
C      CALL ENTGRA
C
C      TYPE *,' '
C      TYPE *,' BEGIN COMPARISON OF ENERGY ABSORBED/CYCLE'
C      TYPE *,' '
C      TYPE *,' HOW MANY TESTS WOULD YOU LIKE TO COMPARE?
1 (3 MAX)'
700  READ(5,700) NUMTEST
C      FORMAT(I2)
C      IF(NUMTEST.GT.3) NUMTEST=3
C      ENERGYMAX = 0.0
C      TYPE *,' '
C
C      READ TEST NAMES TO BE COMPARED
C
C      DO 701 I=1,NUMTEST
C      TYPE 795,I
795  FORMAT(' ENTER LIST FILE NAME',I2,' TO BE COMPARED')
C      READ(5,703) ALIST(I)
703  FORMAT(A14)
C      TYPE 748,ALIST(I)
C
C      NOTE FOR PROPER COMPARISON, FC AND DELTA Y SHOULD BE
C      FACTORED INTO THE RESPONSE
C
C      748  FORMAT(' YIELD DISPLACEMENT FOR ',A14,'= ?')
C      READ(5,*) YIELD(I)
C      TYPE 749,ALIST(I)
749  FORMAT(' CONCRETE COMPRESSIVE STRENGTH IN KSI
1 FOR ',A14,'= ?')
C      READ(5,*) CONC_COMP(I)
C      BLIST = ALIST(I)//'.LIS'
C
C      J IS USED TO DETERMINE THE NUMBER OF CYCLES IN A GIVEN
C      TEST. IT IS INITIALIZED AT THIS POINT.
C
C      J = 1
C
C      INITIALIZE TOTAREA(I)
C

```

```

      TOTAREA (I) = 0.0
C
C OPEN FILE CONTAINING THE LIST OF CYCLES
C
      OPEN(12,FILE=BLIST,ACCESS='SEQUENTIAL',FORM='FORMATTED',
      1 STATUS='OLD')
      REWIND 12
C
C READ THE NAME OF THE FIRST FILE TO BE PLOTTED
C LOOP ON THIS READ STATEMENT UNTIL ALL THE FILES HAVE
C BEEN READ
C
798      READ(12,FMT=703,END=799) ATITLE
C
C ATTACH '.OUT' EXTENSION TO THE NAME JUST READ
C
      BTITLE = ATITLE//'.OUT'
C
C OPEN THE '.OUT' FILE
C
      OPEN(7,FILE=BTITLE,ACCESS='SEQUENTIAL',FORM='FORMATTED',
      1 STATUS='OLD')
      REWIND 7
C
C READ THE TITLE OF THE CYCLE AND STORE IT IN ATIT (I,J)
C
      READ(7,704) ATIT(I,J)
704      FORMAT(A14)
C
C READ THE ENERGY ABSORBED IN THAT CYCLE AND STORE IT IN
C ENERGY (I,J)
C
      READ(7,705) ICOUNT,ENERGY(I,J)
705      FORMAT(8X,I10,7X,F10.5)
C
C NORMALIZE THE ENERGY ABSORBED BY THE YIELD DISPLACEMENT
C AND THE CONCRETE COMPRESSIVE STRENGTH
C
      ENERGY(I,J) = ENERGY(I,J)/(YIELD(I)*CONC_COMP(I))
C
C DETERMINE THE MAXIMUM ENERGY ABSORBED PER CYCLE FROM ALL
C THE TESTS TO BE COMPARED
C
      IF(ENERGY(I,J).GT.ENERGYMAX) ENERGYMAX = ENERGY(I,J)
C
C FIND THE NUMBER OF CYCLES IN TEST(I) AND STORE IT
C IN NUMCYCLE(I)
C
730      NUMCYCLE(I) = J
      J = J + 1
      GOTO 798
799      CONTINUE
C
C FIND THE MAX. ENERGY ABSORBED FROM AMONG THE MODELS
C

```

```

C      IF(TOTAREA(I).GT.TOTENERGY) TOTENERGY = TOTAREA(I)
      CLOSE(12)
      CLOSE(7)
701    CONTINUE
C
C      LOAD COLOR MAP
C
      CALL LUT8(48,150,150,150)      ! GRAY
      CALL LUT8(50,255,0,0)         ! RED
      CALL LUT8(51,0,0,0)           ! BLACK
      CALL LUT8(52,0,0,255)        ! BLUE
      CALL LUT8(53,255,255,200)    ! YELLOW
      CALL LUT8(54,0,255,0)        ! GREEN
C
C      FLOOD BACKGROUND
C
      CALL VAL8(48)                 ! GRAY
      CALL FLOOD
C
C      DEFINE THE ORIGIN AT (-450,-460)
C
      ORIGINX = -450
      ORIGINY = -460
C
C      SET THE LENGTH OF THE AXES
C      X-AXIS = 900 PIXELS
C      Y-AXIS = 900 PIXELS
C
      LENX = 900
      LENY = 900
      CALL VAL8(51)                 ! BLACK
C
C      DRAW THE AXES USING DO LOOP TO THICKEN THE LINES
C
      DO 706 I=1,5
C
C      DRAW THE X-AXIS
C
      CALL MOVABS(ORIGINX,ORIGINY-3+I)
      CALL DRWABS(ORIGINX+LENX,ORIGINY-3+I)
C
C      DRAW THE Y-AXIS
C
      CALL MOVABS(ORIGINX-3+I,ORIGINY)
      CALL DRWABS(ORIGINX-3+I,ORIGINY+LENY)
706    CONTINUE
C
C      SET SCALE FOR Y-AXIS
C
      CSCALEY = 800.0/ENERGYMAX
C
C      DRAW TICK MARKS AND THE VALUES FOR EACH TICK MARK
C
C      CALL SUBROUTINE FOR VERTICAL TEXT
C

```

```

        CALL TEXTC(35,90)
C
C   DIVIDE THE Y-AXIS INTO 8 SEGMENTS
C
        DO 707 I = 1,8
        IX = ORIGINY-2 + I*100
        DO 708 J = 1,3
        CALL MOVABS(ORIGINX-5,IX+J)
        CALL DRWABS(ORIGINX+5,IX+J)
708    CONTINUE
C
C   CALCULATE CTICK WHICH IS THE AMOUNT OF ENERGY EQUAL TO
C   I*100 PIXELS IN UNITS OF ENERGY
C
        XI = I
        CTICK = (1.0/CSCALEY*100.0)*XI
C
C   CONVERT CTICK INTO CHARACTER FORMAT AND STORE IT IN TICK
C   USING THE ENCODE STATEMENT
C
C   ENCODE (I,J,K)
C   I = NUMBER OF CHARACTERS IN TO BE TRANSLATED TO
C   CHARACTER FORMAT
C   J = REFERS TO THE FORMAT STATEMENT
C   K = ARRAY NAME REFERENCE
C
        ENCODE(8,709,TICK)CTICK
709    FORMAT(F8.2)
C
C   II IS USED IN POSITIONING THE VALUES NEXT TO THE TICK
C   MARKS
C
        II = ORIGINY-55 + I*100
        CALL MOVABS(ORIGINX-20,II)
        DO 710 J =1,4
        CALL MOVREL(IDX(J),IDY(J))
        CALL TEXT1(8,INTTICK)
710    CONTINUE
707    CONTINUE
C
C   LABEL Y-AXIS
C
        CALL VAL8(51)                                ! BLACK
C
C   CALL RASTER TECH ROUTINE TO SET SIZE OF TEXT AND FOR
C   VERTICAL TEXT
C
        CALL TEXTC(70,90)
        CALL MOVABS(ORIGINX-100,ORIGINY+200)
C
C   DISPLAY TITLE OF Y-AXIS
C
        DO 712 I=1,9
        CALL MOVREL (IDX(I),IDY(I))
        CALL TEXT1(29,'ENERGY/(DELTA Y * FC) (IN**2)')

```

```

712     CONTINUE
C
C     DISPLAY TITLE FOR PLOT
C
C         CALL VAL8(51)
C
C     CALL RASTER TECH SUBROUTINE TO SET SIZE OF TEXT AND FOR
C     HORIZONTAL TEXT
C
C         CALL TEXTN(60,60,0,0)
C
C     BEGIN WRITING THE TITLE IN THE LOWER LEFT CORNER OF THE
C     SCREEN
C
C         CALL MOVABS(-375,-500)
C
C     DISPLAY TEXT ON SCREEN
C
C         DO 750 IK=1,16
C         CALL MOVREL(IDX(IK),IDY(IK))
C         CALL TEXT1(26,'COMPARISON OF CYCLE ENERGY')
750     CONTINUE
C
C     FIND THE TOTAL NUMBER OF CYCLES FROM ALL THE TESTS TO
C     DETERMINE THE WIDTH OF BAR IN THE BAR GRAPHS
C
C         INUMCYC = 0
C         DO 711 I=1,NUMTEST
C         INUMCYC = NUMCYCLE(I) + INUMCYC
711     CONTINUE
C         XCYC = INUMCYC
C
C     FIND THE MAXIMUM WIDTH OF THE BAR SO THAT ALL THE BARS
C     WILL FIT ON THE X-AXIS
C
C         CSCALEX = 900.0/XCYC
C
C     INITIALIZE NTEST
C
C         NTEST = 0
C
C     ISCALEX IS THE INTEGER FORM OF CSCALEX
C
C         ISCALEX = CSCALEX
C
C     K IS USED AS AN INDEX TO LOCATE XO
C
C         K = 0
C
C     OPEN FILE 'REFTITLE.LIS'
C
C         OPEN(9,FILE='REFTITLE.LIS',ACCESS='SEQUENTIAL',
C         1 FORM='FORMATTED',STATUS='OLD')
C         REWIND 9
C

```

```

C READ THE TITLES OF THE CYCLES CONTAINED IN REFTITLE.LIS
C AND STORE THE TITLE IN ZTIT(I). NOTE THAT THE COUNTER
C IS SET AT 39 BECAUSE THERE ARE 39 TITLES IN REFTITLE.LIS.
C IF THE NUMBER OF TITLES IN REFTITLE.LIS IS CHANGED THE
C COUNTER MUST BE CHANGED TO EQUAL THIS NEW NUMBER.
C
      DO 726 IP = 1,39
      READ(9,727) ZTIT(IP)
726   CONTINUE
727   FORMAT(A14)
      CLOSE(9)
C
C INITIALIZE NDONE WHICH CAN BE SET EQUAL TO ANY NUMBER
C OTHER THAN ZERO
C
      DO 745 I = 1,NUMTEST
      NDONE(I) = I
745   CONTINUE
C
C INITIALIZE THE VARIABLES USED TO STORE THE LOCATION OF THE
C BARS
C
      I1 = 0
      I2 = 0
      I3 = 0
C
C CALL SUBROUTINE TO FILL IN BAR GRAPH
C
      CALL PRMFIL(1)
C
C BEGIN LOOP TO COMPARE THE TITLE OF A CYCLE FROM A TEST
C TO A TITLE IN THE REFERENCE LIST OF TITLES, ZTIT.
C REFTITLE.LIS CONTAINS 39 TITLES AND AS A RESULT THE OUTER
C LOOP, DO 713, IS LOOPED 39 TIMES.
C
      DO 713 J = 1,39
      DO 714 I = 1,NUMTEST
C
C IF J IS GREATER THAN THE NO. OF CYCLES IN TEST(I), THEN
C ALL CYCLES IN THAT TEST HAS BEEN PLOTTED. CONTROL IS
C THEN TRANSFERRED TO STATEMENT 715 WHERE NTEST IS
C INCREASED BY ONE. WHEN NTEST EQUALS THE NUMBER OF
C TESTS, NUMTEST, THEN ALL THE TESTS HAVE BEEN PLOTTED AND
C CONTROL IS TRANSFERRED OUT OF THE LOOP AND THE PROGRAM
C CONTINUES
C
      IF(J.GT.NUMCYCLE(I)) GOTO 715
C
C IF THE J th TITLE IN THE I th TEST, ATIT(I,J), MATCHES
C THE J th TITLE, ZTIT(J), IN REFTITLE.LIS THEN THAT CYCLE
C ENERGY IS PLOTTED
C
C IF NOT, TRANSFER TO STATEMENT 716 WHERE ATIT(I,J+1) IS
C SET EQUAL TO ATIT(I,J) SO THAT IT MAY BE COMPARED TO
C ZTIT(J+1) UNTIL A MATCH IS FOUND

```

```

C
      IF(ATIT(I,J).NE.ZTIT(J)) GOTO 716
C
C   M IS USED AS AN INDEX SO THAT BAR GRAPHS FROM THE SAME
C   TEST ARE PLOTTED IN THE SAME COLOR
C
      M = 49 + I
      CALL VAL8(M)
      K = K + 1
C
C   STORE THE "PLACEMENT" OF THE BAR IN TEST(I,J)
C   I.E. THE N th BAR TO BE PLOTTED
C
      IF(I.EQ.1) THEN
          I1 = I1 + 1
          II = I1
      ENDIF
      IF(I.EQ.2) THEN
          I2 = I2 + 1
          II = I2
      ENDIF
      IF(I.EQ.3) THEN
          I3 = I3 + 1
          II = I3
      ENDIF
      TEST(I,II) = K
C
C   X0 AND Y0 ARE THE X & Y COORDINATES OF THE LOWER LEFT
C   CORNER OF THE BAR GRAPH
C
      X0 = ORIGINX+3+(K-1)*ISCALEX
      Y0 = ORIGINY+3
C
C   X1 AND Y1 ARE THE X & Y COORDINATES OF THE UPPER RIGHT
C   CORNER OF THE BAR GRAPH
C
      X1 = ISCALEX + X0
      Y1 = IFIX(ENERGY(I,J)*CSCALEY)+ORIGINY
C
C   DRAW THE BAR TO REPRESENT THE ENERGY ABSORBED IN THAT
C   CYCLE
C
      CALL MOVABS(X0,Y0)
      CALL RECTAN(X1,Y1)
C
C   X2 & Y2 LOCATE THE POSITION TO WRITE THE TITLES
C
      X2 = X1 - 7
      Y2 = Y1 + 5
C
C   ISIZE IS THE SIZE OF THE TEXT
C
      ISIZE = ISCALEX + 7
C
C   LABEL BARS WITH THEIR APPROPRIATE TITLES

```

```

C
CALL VAL8(51)                                ! BLACK
CALL TEXTC(ISIZE,90)
CALL MOVABS(X2,Y2)
DO 717 IJ = 1,4
CALL MOVREL(IDX(IJ),IDY(IJ))
CALL TEXT1(14,INTITLE(1,I,J))
717 CONTINUE

C
C AFTER THE BAR HAS BEEN PLOTTED AND LABELED, CONTINUE WITH
C THE NEXT CYCLE
C
C GOTO 714

C
C INCREMENT J IN ATIT(I,J) TO ATIT(I,J+1) AND
C ENERGY(I,J) TO ENERGY(I,J+1)
C
C EXAMPLE:
C
C GIVEN:  ATIT(I,1) = B,  ENERGY(I,1) = 5
C         ATIT(I,2) = D,  ENERGY(I,2) = 3
C
C AND
C         ZTIT(1) = A
C         ZTIT(2) = B
C         ZTIT(3) = C
C         ZTIT(4) = D
C
C FOR J = 1
C
C ATIT(I,1) = B DOES NOT MATCH ZTIT(1) = A AND
C THE PROGRAM TRANSFERS TO STATEMENT 716 WHERE
C
C ATIT(I,3) IS "CREATED" AND SET EQUAL TO ATIT(I,2) = D
C AND ATIT(I,2) IS SET EQUAL TO ATIT(I,1) = B AND
C ENERGY(I,3) IS ALSO "CREATED" AND SET EQUAL TO
C ENERGY(I,2) = 3 AND ENERGY(I,2) IS SET EQUAL TO
C ENERGY(I,1) = 5. THE NUMBER OF CYCLES IS INCREASED
C BY ONE TO ACCOUNT FOR THIS "NEW" ADDITION.
C
C FOR J = 2,
C
C ATIT(I,2), NOW EQUAL TO B, IS COMPARED WITH ZTIT(2) = B.
C SINCE THESE TWO TITLES MATCH, THE CYCLE ENERGY IS PLOTTED
C IF NOT, TRANSFER TO STATEMENT 716 WILL OCCUR AGAIN.
C
C FOR J = 3,
C
C ATIT(I,3) = D IS COMPARED WITH ZTIT(3) = C. THESE
C TITLES DO NOT MATCH AND THE PROGRAM TRANSFERS TO
C STATEMENT 716 WHERE
C
C ATIT(I,4) IS "CREATED" AND SET EQUAL TO ATIT(I,3) = D
C ENERGY(I,4) IS "CREATED" AND SET EQUAL TO ENERGY(I,3)
C EQUAL TO 3 AND NUMCYCLE IS INCREASED BY ONE TO ACCOUNT FOR
C THIS 'NEW' ADDITION.

```

```

C
C   FOR J=4,
C
C   ATIT(I,4) NOW EQUAL TO D IS COMPARED WITH ZTIT(4) = D
C   AND A MATCH IS FOUND.  THE CYCLE IS THEN PLOTTED.
C
C
716   DO 718 II=NUMCYCLE(I),J,-1
      ATIT(I,II+1) = ATIT(I,II)
      ENERGY(I,II+1) = ENERGY(I,II)
718   CONTINUE
      NUMCYCLE(I) = NUMCYCLE(I) + 1
      GOTO 714
C
C   NDONE(I) IS EQUAL TO ZERO ONLY WHEN ALL THE CYCLES IN
C   TEST(I) HAVE BEEN PLOTTED.  NDONE(I) IS SET EQUAL TO
C   ZERO WHEN THIS COMPLETION IS FIRST NOTED.  THE 'IF'
C   STATEMENT ENSURES THAT NTEST IS ONLY INCREMENTED ONCE
C   FOR EACH TEST.
C
715   IF(NDONE(I).EQ.0) GOTO 714
      NDONE(I) = 0
C
C   INCREMENT NTEST BY ONE ONLY WHEN ALL THE CYCLES IN A
C   GIVEN TEST HAS BEEN PLOTTED.
C
      NTEST = NTEST + 1
      IF(NTEST.EQ.NUMTEST) GOTO 719
C
714   CONTINUE
713   CONTINUE
C
C   DRAW THE LEGEND IN THE UPPER RIGHT CORNER OF THE SCREEN
C   TO SHOW COLORS AND CORRESPONDING TESTS NAMES
C
719   DO 720 IM = 1,NUMTEST
      DO 721 IN = 1,2
      M = 49 + IM
C
C   FOR IN = 1, COLOR THE RECTANGLE WITH COLOR VALUE M
C
      IF(IN.EQ.1)CALL PRMFIL(1)
      IF(IN.EQ.2)CALL PRMFIL(0)
C
C   FOR IN = 2, OUTLINE THE RECTANGLE WITH BLACK
C
      IF(IN.EQ.1)CALL VAL8(M)
      IF(IN.EQ.2)CALL VAL8(51)
C
C   DEFINE THE Y-COORDINATE OF THE UPPER LEFT CORNER OF THE
C   RECTANGLE
C
      LY1 = 375-30*(IM-1)
C

```

```

C  DEFINE THE Y-COORDINATE OF THE LOWER RIGHT CORNER OF THE
C  RECTANGLE
C
C      LY2 = 375-30*IM
C
C  MOVE TO THE UPPER LEFT CORNER OF THE RECTANGLE
C
C      CALL MOVABS(450,LY1)
C
C  DRAW THE RECTANGLE
C
C      CALL RECTAN(490,LY2)
C
C  INSERT THE TITLES 5 PIXELS TO THE RIGHT OF THE RECTANGLES TO
C  ASSOCIATE A COLOR WITH A TEST
C
C      LY3 = LY2 + 5
C
C  CALL RASTER TECH SUBROUTINE TO SET THE SIZE OF THE TEXT AND
C  FOR HORIZONTAL TEXT
C
C      CALL TEXTN(37,37,0,0)
C      CALL MOVABS(505,LY3)
C
C  DISPLAY TITLES ON THE SCREEN
C
C      DO 722 IO=1,9
C      CALL MOVREL(IDX(IO),IDY(IO))
C      CALL TEXT1(14,LTITLE(1,IM))
722  CONTINUE
721  CONTINUE
720  CONTINUE
C
C      CALL EMPTYB
C
C  INITIALIZE REPEAT
C
C      DO 780 I = 1,NUMTEST
C      REPEAT(I) = 0
780  CONTINUE
C
C  PROMPT USER FOR SCALING OF ENERGIES BETWEEN MODEL AND PROTOTYPE
C
725  TYPE *, ' DO YOU WANT TO SCALE THE ENERGY?  1 = YES, 0 = NO'
      READ(5,770) IANS2
770  FORMAT(I2)
      TYPE *, ' '
      IF(IANS2.EQ.0) GOTO 900
C
C  WARN USER TO SCALE THE TEST(S) WITH THE SMALLER VALUES
C  AS THE SCALE FOR THE Y-AXIS WHICH IS SET FOR THE LARGER
C  VALUES WILL NOT BE CHANGED
C
C      TYPE *, ' *** NOTE ***'
C      TYPE *, ' CHANGE SCALE(S) FOR THE TEST(S) WITH SMALLER VALUES

```

```

        1 ONLY'
        TYPE *, ' '
C
C INITIALIZE SCALE FOR THE TESTS
C
        DO 790 II = 1, NUMTEST
        PRE_SCALE(II) = 1.0
790    CONTINUE
C
C SHOW USER THE LIST OF TESTS AND PROMPT FOR THE NUMBER OF THE
C TEST TO BE SCALED
C
901    DO 735 I = 1, NUMTEST
        TYPE 740, I, ALIST(I)
735    CONTINUE
740    FORMAT(4X, I1, ' = ', A14)
        TYPE *, ' '
        TYPE *, ' ENTER THE NUMBER OF THE TEST TO BE SCALED'
        READ (5, 770) TESTNO
        BLIST = ALIST(TESTNO) // '.LIS'
        TYPE *, ' '
        TYPE *, ' ENTER SCALE FOR ', ALIST(TESTNO)
        READ(5, *) SCALE
        CALL REDRAW_BARS (BLIST, TESTNO, SCALE, TEST, ORIGINX, ORIGINY,
            1 CSCALEY, ISIZE, ISCALEX, YIELD, CONC_COMP, REPEAT, PRE_SCALE)
C
C SHOW THE CURRENT SCALES FOR THE TESTS
C
        TYPE *, ' '
        DO 800 II = 1, NUMTEST
        TYPE *, ' SCALE FOR ', ALIST(II), '= ', PRE_SCALE(II)
800    CONTINUE
C
C PROMPT USER FOR SCALING ANOTHER TEST
C
        TYPE *, ' '
        TYPE *, ' SCALE ANOTHER TEST? 1 = YES, 0 = NO'
        READ(5, 770) IANS3
        IF(IANS3.EQ.1) GOTO 901
C
900    RETURN
        END
C
C
C

```

```

C *****
C
C SUBROUTINE COMTOTAL
C
C PURPOSE: TO SHOW THE COMPARISON OF THE ENERGY UP TO
C
C           ABSORBED BY A STRUCTURE SUBJECTED TO CYCLIC
C           LOAD. THE COMPARISON IS SHOWN IN A BAR TYPE
C           HISTOGRAM. A MAXIMUM OF 6 COMPARISONS CAN BE
C           MADE
C
C CALLED FROM: PROGRAM MAIN
C
C USAGE: CALL COMTOTAL(IDX, IDY)
C
C PARAMETERS:
C
C   IDX  SEE MAIN PROGRAM
C   IDY  "   "   "
C
C OTHER SUBROUTINES CALLED: NONE ( OTHER THAN RASTER
C TECH 'ONELIB' ROUTINES. SEE PROGRAM MAIN)
C
C SUBROUTINE SPECIFIC PARAMETERS:
C
C NUMTEST  NUMBER OF TESTS TO BE COMPARED
C ALIST    TEST FILE NAME WHICH CONTAINS ALL CYCLE NAMES
C BLIST    EQUIVALENT TO ALIST BUT WITH '.LIS' EXTENSION
C ATITLE   CYCLE NAME CONTAINED IN BLIST
C BTITLE   EQUIVALENT TO ATITLE BUT WITH '.OUT'
C          EXTENSION
C ATIT(I,J) J th TITLE IN THE I th TEST CONTAINED IN BTITLE
C TOTAREA(I) TOTAL ENERGY ABSORBED IN THE I th TEST
C TOTENERGY MAXIMUM TOTAL ENERGY ABSORBED BY THE STRUCTURE FROM
C           AMONG ALL THE TESTS TO BE COMPARED
C ORIGINX  X-COORDINATE OF THE ORIGIN OF THE AXES
C ORIGINY  Y-COORDINATE OF THE ORIGIN OF THE AXES
C LENX     LENGTH OF THE X-AXIS
C LENY     LENGHT OF THE Y-AXIS
C CSCALEY  UNITS: PIXELS/UNIT OF ENERGY. USED TO
C          CONVERT UNITS OF ENERGY TO NUMBER OF PIXELS
C CSCALEX  UNITS: PIXELS/NO. OF TESTS COMPARED. USED TO
C          FIT THE TOTAL NUMBER OF TESTS TO BE COMPARED ON THE
C          X-AXIS
C CTICK    AMOUNT OF ENERGY EQUAL TO I*100 PIXELS IN
C          UNITS OF ENERGY WHERE I = 1, 2, ... TO THE NUMBER
C          OF DIVISIONS OF THE Y AXIS
C TICK     EQUIVALENT TO CTICK IN CHARACTER FORMAT
C INTTICK  EQUIVALENT TO CTICK IN INTEGER*2 FORMAT
C X0       X-COORDINATE OF THE LOWER LEFT CORNER OF A
C          BAR IN THE HISTORGRAM
C Y0       Y-COORDINATE OF THE LOWER LEFT CORNER OF A
C          BAR IN THE HISTORGRAM
C X1       X-COORDINATE OF THE UPPER RIGHT CORNER OF A
C          BAR IN THE HISTOGRAM

```

```

C   Y1           Y-COORDINATE OF THE UPPER RIGHT CORNER OF A
C               BAR IN THE HISTOGRAM
C   LY1          Y-COORDINATE OF THE UPPER LEFT CORNER OF THE
C               RECTANGLE USED IN THE LEGEND
C   LY2          Y-COORDINATE OF THE LOWER RIGHT CORNER OF THE
C               RECTANGLE USED IN THE LEGEND
C   LY3          Y-COORDINATE USED TO PLACE THE TITLE ASSOCIATING
C               A COLOR WITH A CYCLE NEXT TO THE RECTANGLE IN
C               THE LEGEND

```

```

C *****

```

```

C               SUBROUTINE COMTOTAL(IDX, IDY)
C
C               INTEGER*2  IDX(16), IDY(16), INTTICK(4), LTITLE(7, 50)
C
C               INTEGER*2  X0, Y0, X1, Y1, LY1, LY2, LY3,
C               1  ORIGINX, ORIGINY, LENY, LENX
C
C               CHARACTER*9  ATITLE
C
C               CHARACTER*14  ALIST(50), ATIT(50, 50)
C
C               CHARACTER*18  BLIST, BTITLE, CTITLE
C
C               CHARACTER*80  TITLE
C
C               CHARACTER*2  TICK(4)
C
C               DIMENSION  TOTAREA(10), ENERGY(50, 50)
C
C               EQUIVALENCE(TICK, INTTICK)
C               EQUIVALENCE(ALIST, LTITLE)
C
C               TYPE *, ' '
C               TYPE *, ' BEGIN COMPARISON OF TOTAL ENERGY ABSORBED '
C               TYPE *, ' '
C               TYPE *, 'HOW MANY TESTS WOULD YOU LIKE TO COMPARE?
C               1 (6 MAX) '
C               READ(5, 700) NUMTEST
700          FORMAT(I2)
C               IF(NUMTEST.GT.6) NUMTEST=6
C
C               INITIALIZE TOTENERGY
C
C               TOTENERGY = 0.0
C
C               READ TEST NAMES
C
C               TYPE *, ' '
C               DO 701 I=1, NUMTEST
C               TYPE 795, I
795          FORMAT(' ENTER LIST FILE NAME', I2, ' TO BE COMPARED')

```

```

      READ(5,703) ALIST(I)
703   FORMAT(A14)
      BLIST = ALIST(I)//'.LIS'
C
C   J IS USED TO DIFFERENTIATE THE ENERGY FOR A CYCLE IN A
C   GIVEN TEST AND IS INITIALIZED AT THIS POINT
C
      J = 1
C
C   OPEN LIST FILE CONTAINING THE NAMES OF ALL THE CYCLES
C
      OPEN(6,FILE=BLIST,ACCESS='SEQUENTIAL',FORM='FORMATTED',
          1 STATUS='OLD')
      REWIND 6
C
C   TOTAREA = TOTAL ENERGY ABSORBED IN THE TEST
C
      TOTAREA(I) = 0.0
C
C   READ THE CYCLE NAME IN THE LIST. LOOPING ON THE READ
C   STATEMENT UNTIL ALL THE NAMES HAVE BEEN READ
C
798   READ(6,FMT=703,END=799) ATITLE
      BTITLE = ATITLE//'.OUT'
C
C   OPEN THE CYCLE FILE
C
      OPEN(7,FILE=BTITLE,ACCESS='SEQUENTIAL',FORM='FORMATTED',
          1 STATUS='OLD')
      REWIND 7
C
C   READ THE TITLE OF THE CYCLE
C
      READ(7,704) ATIT(I,J)
704   FORMAT(A14)
C
C   READ THE PIXEL COUNT FROM THE NUMERICAL INTEGRATION AND THE
C   ENERGY FOR THAT CYCLE
C
      READ(7,705) ICOUNT,ENERGY(I,J)
705   FORMAT(8X,I10,7X,F10.5)
C
C   SUM ENERGY FOR TEST(I) AND STORE IN TOTAREA(I)
C
      TOTAREA(I) = TOTAREA(I) + ENERGY(I,J)
C
C   SUM THE ENERGY ONLY UP TO THE ULTIMATE STATE. ULTIMATE STATE
C   IS DEFINED AS WHEN THE HORIZONTAL LOAD IS LESS THAN 0.8 TIMES
C   THE HORIZONTAL LATERAL LOAD OBTAINED DURING THE FIRST CYCLE
C   AT 2 TIMES DELTA Y. (SEE ZAHN, F. A., REFERENCE [30])
C
      IF(J.LT.2) GOTO 730
      CTITLE = ATITLE//'.INP'
C
C   OPEN THE FILE WHICH CONTAINS THE DATA POINTS AND THE MAX.

```

```

C AND MIN. VALUES
C
      OPEN(20,FILE=CTITLE,ACCESS='SEQUENTIAL',FORM='FORMATTED',
      1 STATUS='OLD')
      REWIND 20
C
C READ THE TITLE
C
      READ(20,10) TITLE
10     FORMAT(40A2)
C
C READ THE MAX AND MIN DISPLACEMENTS AND LOADS
C
      READ(20,30) XMIN,XMAX,YMIN,YMAX,NPTS
30     FORMAT(4(E12.5,3X),I5)
C
C CALCULATE THE ULTIMATE LOAD AS 0.8 TIMES THE PEAK LATERAL
C LOAD AT 2 TIMES THE YIELD DISPLACEMENT
C
      IF(J.GT.2) GOTO 40
      ULTLOAD = 0.80 * YMAX
      GOTO 730
C
C COMPARE THE PEAK LATERAL LOAD FOR EACH CYCLE TO THE ULTIMATE
C LOAD. IF THE LOAD FOR THAT CYCLE IS LESS THAN THE ULTIMATE
C LOAD, THE TOTAL ENERGY WILL ONLY BE SUMMED UP TO AND INCLUDING
C THIS CYCLE
C
40     IF(YMAX.LT.ULTLOAD) GOTO 799
C
730    J = J + 1
      GOTO 798
799    CONTINUE
C
C FIND THE MAXIMUM ENERGY ABSORBED FOR A GIVEN TEST FROM
C AMONG ALL THE TESTS TO BE COMPARED AND STORE IT IN
C TOTENERGY
C
      IF(TOTAREA(I).GT.TOTENERGY) TOTENERGY = TOTAREA(I)
      CLOSE(6)
      CLOSE(7)
      CLOSE(20)
701    CONTINUE
C
C INITIALIZE GRAPHICS DEVICE
C
      CALL RTSET(1,180)
      CALL RTINIT('GDA0:',5)
      CALL ENTGRA
C
C LOAD COLOR MAP
C
      CALL LUT8(48,150,150,150)      ! GRAY
      CALL LUT8(50,255,0,0)         ! RED
      CALL LUT8(51,255,255,100)     ! YELLOW

```

```

      CALL LUT8(52,0,0,255)      ! BLUE
      CALL LUT8(53,0,0,0)       ! BLACK
      CALL LUT8(54,0,255,0)    ! GREEN
      CALL LUT8(55,255,0,255)  ! PURPLE
C
C FLOOD BACKGROUND
C
      CALL VAL8(48)             ! GRAY
      CALL FLOOD
C
C DEFINE ORIGIN OF AXES AT (-450,-460)
C
      ORIGINX = -400
      ORIGINY = -450
C
C SET LENGTHS OF X-AXIS AND Y-AXIS
C
      X-AXIS = 900 PIXELS
      Y-AXIS = 900 PIXELS
C
      LENX = 800
      LENY = 800
C
C DRAW AXES
C
      CALL VAL8(53)
      DO 706 I=1,5
      CALL MOVABS(ORIGINX,ORIGINY-3+I)
      CALL DRWABS(ORIGINX+LENX,ORIGINY-3+I)
      CALL MOVABS(ORIGINX-3+I,ORIGINY)
      CALL DRWABS(ORIGINX-3+I,ORIGINY+LENY)
706 CONTINUE
C
C SET SCALE FOR THE Y-AXIS, YLENY IS EQUAL TO LENY IN REAL
C NUMBER FORMAT
C
      YLENY = LENY
      CSCALEY = (YLENY-100.0)/TOTENERGY
C
C CALL RASTER TECH ONE/80 ROUTINE FOR VERTICAL TEXT
C
      CALL TEXTC(30,90)
C
C DIVIDE THE Y-AXIS INTO 7 SEGMENTS
C
      DO 707 I = 1,7
      IX = ORIGINY-2 + I*100
C
C DRAW TICK MARKS AND THE VALUES FOR EACH TICK MARK
C
      DO 708 J = 1,3
      CALL MOVABS(ORIGINX-5,IX+J)
      CALL DRWABS(ORIGINX+5,IX+J)
708 CONTINUE
C

```

```

C  CALCULATE CTICK
C
      XI = I
      CTICK = (1.0/CSCALEY*100.0)*XI
C
C  CONVERT CTICK INTO CHARACTER FORMAT AND STORE IT IN TICK
C  USING THE ENCODE STATEMENT
C
C  ENCODE (I,J,K)
C  I = NUMBER OF CHARACTERS TO BE TRANSLATED TO CHARACTER
C  FORMAT
C  J = REFERS TO THE FORMAT STATEMENT
C  K = ARRAY NAME REFERENCE
C
      ENCODE(8,709,TICK) CTICK
709  FORMAT(F8.0)
C
C  II IS USED IN POSITIONING THE VALUES NEXT TO THE TICK
C  MARKS
C
      II = ORIGINY-55 + I*100
      CALL MOVABS(ORIGINX-20,II)
      DO 710 J1 =1,4
      CALL MOVREL(IDX(J1),IDY(J1))
      CALL TEXT1(8,INTTICK)
710  CONTINUE
707  CONTINUE
C
C  LABEL Y-AXIS
C
      CALL VAL8(53)
      CALL TEXTC(70,90)
      CALL MOVABS(ORIGINX-100,ORIGINY+200)
      DO 712 I=1,9
      CALL MOVREL (IDX(I),IDY(I))
      CALL TEXT1(15,'ENERGY (KIP-IN)')
712  CONTINUE
C
C  FIND THE SCALE FOR THE X-AXIS.  THIS IS ACTUALLY THE WIDTH OF
C  THE BARS
C
      XLENX = LENX
      CSCALEX = (XLENX-75.0)/NUMTEST
C
C  ISCALEX IS THE INTEGER FORM OF CSCALEX
C
      ISCALEX = CSCALEX
C
C  K IS USED AS AN INDEX TO LOCATE X0
C
      K = 0
C
C  SET THE SIZE OF THE TITLE OF THE HISTOGRAM TO 70 X 70
C  PIXELS
C

```

```

CALL TEXTN(70,70,0,0)
CALL VAL8(53)                                ! BLACK
C
C BEGIN THE TITLE IN THE UPPER LEFT CORNER OF THE SCREEN
C
CALL MOVABS(-400,425)
C
C WRITE THE TITLE ON THE SCREEN
C
DO 740 IK = 1,16
CALL MOVREL(IDX(IK),IDY(IK))
CALL TEXT1(32,'TOTAL ENERGY ABSORBED BY COLUMN')
740 CONTINUE
C
C CALL SUBROUTINE TO FILL IN BAR GRAPH
C
CALL PRMFIL(1)
C
C BEGIN LOOP TO PLOT BAR GRAPH
C
DO 714 I = 1,NUMTEST
C
M IS USED TO CHANGE THE COLOR OF THE BAR GRAPHS
C
M = 49 + I
CALL VAL8(M)
K = K + 1
C
C X0 & Y0 ARE THE X & Y COORDINATES OF THE LOWER CORNER OF
C THE BAR GRAPH
C
X0 = ORIGINX+3+(K-1)*ISCALEX
Y0 = ORIGINY+3
C
C X1 AND Y1 ARE THE X & Y COORDINATES OF THE UPPER RIGHT
C CORNER OF THE BAR GRAPH
C
X1 = ISCALEX + X0
Y1 = IFIX(TOTAREA(I)*CSCALEY)+ORIGINY
C
C DRAW THE BAR (RECTANGLE)
C
CALL MOVABS(X0,Y0)
CALL RECTAN(X1,Y1)
C
714 CONTINUE
C
C DRAW THE LEGEND IN THE UPPER RIGHT CORNER OF THE SCREEN
C TO SHOW THE BAR COLORS AND CORRESPONDING TEST NAMES
C
DO 720 IM = 1,NUMTEST
DO 721 IN = 1,2
M = 49 + IM
C
C FOR I = 2, THE RECTANGLE IS FILLED WITH THE APPROPRIATE

```

```

C BAR COLOR
C
C     IF(IN.EQ.1)CALL PRMFIL(1)
C
C FOR IN = 2, THE RECTANGLE IS OUTLINED IN BLACK
C
C     IF(IN.EQ.2)CALL PRMFIL(0)
C
C SET THE CURRENT PIXEL COLOR VALUE. THIS IS A FUNCTION OF
C THE VALUE OF 'IN'
C
C     IF(IN.EQ.1)CALL VAL8(M)
C     IF(IN.EQ.2)CALL VAL8(53)
C
C DEFINE THE UPPER LEFT CORNER OF THE RECTANGLE
C
C     LY1 = 325-30*(IM-1)
C
C DEFINE THE LOWER RIGHT CORNER OF THE RECTANGLE
C
C     LY2 = 325-30*IM
C
C DRAW THE RECTANGLE
C
C     CALL MOVABS(420,LY1)
C     CALL RECTAN(460,LY2)
C
C INSERT TITLES NEXT TO THE RECTANGLES 5 PIXELS TO THE
C RIGHT OF THE RECTANGLE
C
C     LY3 = LY2 + 5
C
C CALL RASTER TECH SUBROUTINE FOR SIZE OF TEXT AND FOR
C HORIZONTAL TEXT
C
C     CALL TEXTN(37,37,0,0)
C     CALL MOVABS(485,LY3)
C
C DISPLAY TITLES ON THE SCREEN
C
C     DO 722 IO=1,9
C     CALL MOVREL(IDX(IO),IDY(IO))
C     CALL TEXT1(14,LTITLE(1,IM))
722 CONTINUE
721 CONTINUE
720 CONTINUE
C
C     CALL EMPTYB
C
C     RETURN
C     END
C
C

```

```

C *****
C
C SUBROUTINE LINEPLOT
C
C PURPOSE: STAND-ALONE PACKAGE TO PLOT THE HYSTERESIS
C CURVE OF A STRUCTURE SUBJECTED TO CYCLIC
C LOADS. USES FULL SCREEN (IN CONTRAST) TO
C SUBROUTINE CYCLE WHICH USED 1/4 OF THE SCREEN)
C
C CALLED FROM: PROGRAM MAIN
C
C USAGE: CALL LINEPLOT(IDX, IDY)
C
C PARAMETERS:
C
C IDX SEE MAIN PROGRAM
C IDY " " "
C
C OTHER SUBROUTINES CALLED: NONE ( OTHER THAN RASTER
C TECH 'ONELIB' ROUTINES. SEE PROGRAM MAIN)
C
C SUBROUTINE SPECIFIC PARAMETERS:
C
C NAUTO VARIABLE USED TO DETERMINE 'AUTOMATIC' (I.E.
C NO INPUT REQUIRED BY USER) PLOTTING OF
C HYSTERESIS CURVES OR MANUAL PLOTTING
C NAUTO = 1 AUTOMATIC
C NAUTO = 0 MANUAL
C
C NCOUNT VARIABLE USED TO CHANGE THE COLOR OF THE
C HYSTERESIS PLOT
C
C X(I) X-COORDINATE OF THE I th DATA POINT
C Y(I) Y-COORDINATE OF THE I th DATA POINT
C YLIST NAME OF THE TEST FILE WHICH CONTAINS ALL THE
C NAMES OF THE CYCLES IN THAT TEST
C ZLIST EQUIVALENT TO YLIST BUT WITH '.LIS' EXTENSION
C NAME NAME OF FILE OF A GIVEN CYCLE. THIS FILE
C CONTAINS THE DATA POINTS AND TITLE OF THE
C CYCLE
C XNAME EQUIVALENT TO NAME BUT WITH '.INP' EXTENSION
C TITLE TITLE OF THE CYCLE IN XNAME FILE
C XSIZE LENGTH OF X-AXIS IN PIXELS
C YSIZE LENGTH OF Y-AXIS IN PIXELS
C XRANGE THE MAXIMUM DISTANCE THE STRUCTURE WAS DISPLACED
C IN EITHER THE FORWARD OR REVERSE DIRECTIONS
C YRANGE THE MAXIMUM FORCE TO DISPLACE THE STRUCTURE IN
C EITHER THE FORWARD OR REVERSE DIRECTIONS
C XFACTOR UNITS: PIXELS/UNIT LENGTH. USED TO CONVERT
C LENGTH TO NUMBER OF PIXELS
C YFACTOR UNITS: PIXELS/UNIT FORCE. USED TO CONVERT
C FORCE TO NUMBER OF PIXELS
C OFFX1 X-COORDINATE OF THE LEFT (NEGATIVE) END OF
C THE X-AXIS
C OFFX2 X-COORDINATE OF THE RIGHT (POSITIVE) END OF
C THE X-AXIS
C OFFY1 Y-COORDINATE OF THE BOTTOM (NEGATIVE) END OF

```

```

C          THE Y-AXIS
C OFFY2    Y-COORDINATE OF THE TOP (POSITIVE) END OF
C          THE Y-AXIS
C OFFSETX  AMOUNT BY WHICH THE X-COORDINATE OF THE AXES
C          ORIGIN IS MOVED FROM THE SCREEN ZERO
C OFFSETY  AMOUNT BY WHICH THE Y-COORDINATE OF THE AXIS
C          ORIGIN IS MOVED FROM THE SCREEN ZERO
C IRED,    DETERMINES THE AMOUNT OF RED TO BE USED
C JRED     IN COLOR(X) WITH 0 = NO RED USED, AND 255 =
C          MAXIMUM AMOUNT OF RED USED
C IGREEN,  DETERMINES THE AMOUNT OF GREEN TO BE USED
C JGREEN   IN COLOR(X) WITH 0 = NO GREEN USED, AND 255 =
C          MAXIMUM AMOUNT OF GREEN USED
C IBLUE,   DETERMINES THE AMOUNT OF BLUE TO BE USED
C JBLUE    IN COLOR(X) WITH 0 = NO BLUE USED, AND 255 =
C          MAXIMUM AMOUNT USED

```

```

C *****

```

```

C          SUBROUTINE LINEPLOT(IDX, IDY)
C          CHARACTER filename*10, infile*14, outfile*14, NAME*10,
C          1 XNAME*14, XNOMBRE*14, YLIST*9, ZLIST*14, ANAME*80

```

```

C          DIMENSION X(400), Y(400)
C          INTEGER*2 TITLE(40), IDX(16), IDY(16),
C          1 OVERTIT(20), X1(400), Y1(400)
C          INTEGER*2 IX, IY, NCOUNT, LEY, REY, OFFSETX, OFFSETY,
C          1 OFFX1, OFFX2, OFFY1, OFFY2, IRED, IGREEN, IBLUE,
C          2 JRED, JGREEN, JBLUE

```

```

C          INPUT IDX AND IDY VALUES TO USED FOR BOLD TEXT

```

```

C          REAL MAXX, MINX, MAXY, MINY

```

```

C          DETERMINE THE MAX AND MIN VALUES OF X AND Y FROM ALL
C          THE TESTS TO BE INTEGRATED.

```

```

C          Initialize variables into which the max. and min.
C          values will be stored.

```

```

C          1002    MAXX = 0.0
C                 MINX = 0.0
C                 MAXY = 0.0
C                 MINY = 0.0
C                 TOTDISP = 0.0

```

```

C          TYPE *, ' '
C          TYPE *, 'BEGIN LOAD-DISPLACEMENT LINE PLOT'
C          TYPE *, 'ENTER NAME OF LIST FILE (9 CHARACTERS)'
C          518    READ (5, 518) YLIST
C                 FORMAT(A20)

```

```

        ZLIST = YLIST//'.LIS'
C
C   Open the file where all the cycle names have been stored
C
        OPEN(1,FILE=ZLIST,STATUS='OLD',ACCESS='SEQUENTIAL',
          1 FORM='FORMATTED')
1130  CONTINUE
C
C   READ THE CYCLE NAME
C
        READ(1,FMT=1,END=1100) NAME
C
C   PUT EXTENSION ON THE FILENAME.
C   All files to be used have to have the extension ".INP"
C   or ".OUT"
C
        XNAME=NAME//'.INP'
C
C   Open the test file and extract from it the max. and min.
C   values
C
        OPEN(4,FILE=XNAME,ACCESS='SEQUENTIAL',FORM='FORMATTED',
          1 STATUS='OLD')
        REWIND 4
C
C   TITLE HAS TO BE READ BECAUSE THE FILE IS SEQUENTIAL I.E.
C   ITEMS LOCATED BEFORE THE DESIRED ITEM HAVE TO BE READ
C   BEFORE THE DESIRED ITEM CAN BE READ
C
C
        READ(4,45) TITLE
45    FORMAT(40A2)
C
C   READ THE MAX AND MIN VALUES FROM THE FILES
C
        READ(4,40) XMIN,XMAX,YMIN,YMAX
40    FORMAT(4(E12.5,3X))
        CLOSE(UNIT=4)
C
C   DETERMINE THE SCREEN BOUNDS BASED ON MAX AND MIN X & Y
C   VALUES
C
        TOTDISP = TOTDISP + ABS(XMAX) + ABS(XMIN)
        IF(XMAX.GT.MAXX) MAXX = XMAX
        IF(XMIN.LT.MINX) MINX = XMIN
        IF(YMAX.GT.MAXY) MAXY = YMAX
        IF(YMIN.LT.MINY) MINY = YMIN
        GO TO 1130
C
1100  CONTINUE
        REWIND 1
C
C   NCOUNT TO PLOT THE CURVES IN DIFFERENT COLORS
C
        NCOUNT=0

```

```

C
C INITIALIZE THE GRAPHICS DEVICE
C
      CALL RTSET(1,180)
      CALL RTINIT('GDA0:',5)
      CALL ENTGRA
C
C LOAD THE COLOR MAP
C
      CALL LUT8(0,255,200,255) ! VERY LIGHT PURPLE
      CALL LUT8(1,255,150,255) ! LIGHT PURPLE
      CALL LUT8(2,255,0,255) ! RED PURPLE
      CALL LUT8(3,188,150,234) ! PURPLE
      CALL LUT8(4,0,0,190) ! BLUE PURPLE
      CALL LUT8(5,75,75,255) ! BRIGHT BLUE
      CALL LUT8(6,0,255,255) ! BRIGHT LIGHT BLUE
      CALL LUT8(7,175,255,255) ! LIGHT BLUE
      CALL LUT8(8,0,200,200) ! BLUE GREEN
      CALL LUT8(9,0,175,0) ! OLIVE GREEN
      CALL LUT8(10,130,230,130) ! LIGHT OLIVE GREEN
      CALL LUT8(11,0,255,0) ! BRIGHT GREEN
      CALL LUT8(12,165,255,165) ! LIGHT GREEN
      CALL LUT8(13,255,255,175) ! LIGHT YELLOW
      CALL LUT8(14,255,255,100) ! LIGHT YELLOW
      CALL LUT8(15,255,175,50) ! YELLOW-ORANGE
      CALL LUT8(16,255,120,0) ! ORANGE
      CALL LUT8(17,255,0,0) ! RED
      CALL LUT8(18,255,130,130) ! DUSKY PINK
      CALL LUT8(19,255,175,175) ! LIGHT PINK
      CALL LUT8(20,255,200,200) ! PALE PINK
      CALL LUT8(21,200,200,200) ! LIGHT GRAY
      CALL LUT8(22,150,150,150) ! GRAY
      CALL LUT8(23,75,75,75) ! DARK GRAY
      CALL LUT8(24,30,30,30) ! GRAY-BLACK
      CALL LUT8(30,255,255,255) ! WHITE
      CALL LUT8(31,0,0,0) ! BLACK
      CALL LUT8(32,255,246,0) ! CHROMIUM YELLOW
C
      TYPE *, ' '
      TYPE *, ' ENTER TEST TITLE (20 CHARACTERS) '
      READ(5,461) OVERTIT
461  FORMAT(20A2)
      TYPE *, ' '
      TYPE *, 'PROCESSING MODE'
      TYPE *, '1 = AUTO'
      TYPE *, '0 = MANUAL'
      READ (5,5001) NAUTO
5001  FORMAT(I2)
C
C FLOOD THE BACKGROUND
C
      CALL VAL8(31) ! BLACK
      CALL FLOOD
C

```

```

C PLACE OVERALL TITLE IN TOP CENTER OF SCREEN
C
C CALL VAL8(32) ! CHROMIUM YELLOW
C
C CALL RASTER TECH SUBROUTINE TO SET SIZE OF TEXT AND FOR
C HORIZONTAL TEXT
C
C CALL TEXTN(90,90,0,0)
C CALL MOVABS(-175,450)
C
C BEGIN 'WRITING' TITLE ON SCREEN
C
C DO 470 I=1,16
C CALL MOVREL(IDX(I),IDY(I))
C CALL TEXT1(15,OVERTIT)
470 CONTINUE
C
C OPEN THE TEST FILE CONTAINING THE CYCLE NAMES AGAIN IN
C PREPARATION FOR PLOTTING
C
C open(1,file=ZLIST,status='old',access='sequential',
C 1 form='formatted')
C
C 500 continue
C
C read(1,fmt=1,end=1000) filename
C 1 format(a20)
C type *,'working on file ',filename
C
C PUT EXTENSION ON FILENAME
C
C infile=filename//'.inp'
C
C READ INDIVIDUAL CYCLE DATA
C
C OPEN(UNIT=2,FILE=infile,ACCESS='SEQUENTIAL',FORM='FORMATTED',
C 1 STATUS='OLD')
C REWIND 2
C
C
C READ(2,2) TITLE
C 2 FORMAT(40A2)
C
C READ(2,3) XMIN,XMAX,YMIN,YMAX,NPTS
C 3 FORMAT(4(E12.5,3X),I5)
C
C READ THE DATA POINTS
C
C DO 100 I=1,NPTS
C READ(2,4) X(I),Y(I)
C 100 CONTINUE
C 4 FORMAT(2(E12.5,3X))
C
C CLOSE(UNIT=2)

```

```

C
C
C SET LENGTHS OF THE X & Y AXES
C
      XSIZE = 1000
      YSIZE = 850
C
C SET OFFSET VALUES TO PLACE ORIGIN AT -20,0
C
      OFFSETX = -20
      OFFSETY = 0
C
C IF NCOUNT > 1, THE X & Y SCALE FACTORS AND RANGES WILL
C ALREADY HAVE BEEN DEFINED AND DO NOT NEED TO BE REDEFINED
C
      IF (NCOUNT.GT.0) GOTO 3010
C
C FIND THE MAXIMUM DISPLACEMENT AND LOAD FROM AMONG ALL THE
C CYCLES
C
      XRANGE=MAX(ABS(MAXX),ABS(MINX))
      YRANGE=MAX(ABS(MAXY),ABS(MINY))
C
C FIND THE SCALES FOR THE X AND Y AXES
C
      XFACTOR=XSIZE/(2.*XRANGE)
      YFACTOR=YSIZE/(2.*YRANGE)
C
C
C DRAW THE CURVE
C
C THE OUTER LOOP IS USED TO THICKEN THE LINES IN THE PLOT
C
3010 DO 210 J=1,4
C
C SCALE THE DATA AND LOAD IT INTO INTEGER*2 VECTORS
C
      DO 200 I=1,NPTS
      X1(I)=IFIX(X(I)*XFACTOR) + J - 2 + OFFSETX
      Y1(I)=IFIX(Y(I)*YFACTOR) + J - 2 + OFFSETY
200 CONTINUE
C
C AGAIN IF NCOUNT > 0, THE AXES WILL ALREADY HAVE BEEN
C DRAWN AND DO NOT NEED TO BE REDRAWN
C
      IF(NCOUNT.GT.0) GOTO 211
      CALL VAL8(30) ! WHITE
C
C DEFINE THE ENDS OF THE X & Y AXES
C
      OFFX1 = ( -XSIZE/2 + OFFSETX)
      OFFY1 = ( -YSIZE/2 + OFFSETY)
      OFFX2 = ( XSIZE/2 + OFFSETX)
      OFFY2 = ( YSIZE/2 + OFFSETY)

```

```

C
C DRAW THE X-AXIS
C
      DO 213 IM = 1,3
      CALL MOVABS(OFFX1,OFFSETY+IM-2)
      CALL DRWABS(OFFX2,OFFSETY+IM-2)
C
C DRAW THE Y-AXIS
C
      CALL MOVABS(OFFSETX+IM-2,OFFY1)
      CALL DRWABS(OFFSETX+IM-2,OFFY2)
213 CONTINUE
C
C DRAW POLYGON
C
211 CALL VAL8(NCOUNT)
C
      CALL PRMFIL(0)
      CALL MOVABS(X1(1),Y1(1))
      DO 215 II = 2,NPTS
      CALL DRWABS(X1(II),Y1(II))
215 CONTINUE
C
C DRAW LEGEND
C
C IF J = 1, FILL THE RECTANGLE WITH COLOR VALUE = NCOUNT
C
      IF(J.EQ.1) CALL PRMFIL(1)
      IF(J.EQ.1) CALL VAL8(NCOUNT)
C
C IF J = 2, OUTLINE THE RECTANGLE IN WHITE
C
      IF(J.EQ.2) CALL PRMFIL(0)
      IF(J.EQ.2) CALL VAL8(30)
C
C IF J > 2, THE LEGEND DOES NOT NEED TO REDRAWN AND THE
C PROGRAM SKIPS THE NEXT SECTION
C
      IF(J.GT.2) GOTO 212
C
C DEFINE THE UPPER LEFT CORNER OF THE RECTANGLE
C
      LEY = -25 - 22*NCOUNT
C
C DEFINE THE LOWER RIGHT CORNER OF THE RECTANGLE
C
      REY = LEY - 25
C
C DRAW THE RECTANGLE
C
      CALL MOVABS(385,LEY)
      CALL RECTAN(410,REY)
C
C LABEL LEGEND
C

```

```

        CALL MOVABS(430,REY)
        CALL TEXTN(30,30,0,0)
        CALL VAL8(30)
C
C   USE DO LOOP TO CREATE BOLD EFFECT
C
        DO 400 I = 1,4
        CALL MOVREL(IDX(I),IDY(I))
        CALL TEXT1(40,TITLE)
400    CONTINUE
212    CONTINUE
        CALL EMPTYB
210    CONTINUE
C
        NCOUNT=NCOUNT+1
        IF (NAUTO .EQ. 1) GOTO 500
        TYPE *,' '
        TYPE *,'ANOTHER CYCLE ? 1 = YES, 0 = NO'
        READ *,ANS
        IF (ANS.EQ.0) GOTO 1000
        goto 500
C
1000   CLOSE (1)
C
C   PROMPT USER FOR COLOR CHANGE
C
10005  TYPE *,' CHANGE COLORS ? 1 = YES, 0 = NO'
        READ *,ICANS
C
C   IF NO COLOR CHANGE IS NEEDED, GO TO THE END OF THE
C   SUBROUTINE
C
        IF(ICANS.EQ.0) GOTO 10001
C
C   DETERMINE IF THE BACKGROUND COLOR IS TO BE CHANGED
C
        TYPE *,' BACKGROUND COLOR, CHANGE ? 1 = YES, 0 = NO'
        READ *, IBACK
C
C   IF NO CHANGE TO THE BACKGROUND COLOR IS NEEDED, ASK USER
C   FOR THE NEXT COLOR CHANGE
C
        IF(IBACK.EQ.0) GOTO 10002
C
C   IF SO, PROMPT USER FOR COLOR VALUES
C
        TYPE *,' ENTER VALUES FOR RED, GREEN BLUE'
        READ *, IRED, IBLUE, IGREEN
C
C   CHANGE THE COLOR VALUES FOR THE BACKGROUND IN THE
C   LOOK-UP TABLE TO THE ONE ASKED FOR BY THE USER
C
        CALL LUT8(31,IRED,IBLUE,IGREEN)
        CALL EMPTYB
C

```

```

10002  TYPE *, 'AXES AND TITLE COLORS, CHANGE ? 1 = YES, 0 = NO'
        READ *, IAXIS
C
C  IF NO COLOR CHANGE TO THE AXES OR TITLES IS NEEDED, LOOP
C  BACK AND PROMPT USER FOR COLOR CHANGE AGAIN
C
        IF(IAXIS.EQ.0) GOTO 10005
        TYPE *, ' ENTER VALUES FOR RED, GREEN, BLUE '
        READ *, JRED, JGREEN, JBLUE
C
C  CHANGE THE COLOR VALUES FOR THE AXES AND TITLES IN THE
C  COLOR LOOK-UP TABLE TO THE ONE ASKED FOR BY THE USER
C
        CALL LUT8(30, JRED, JGREEN, JBLUE)
        CALL EMPTYB
C
C  LOOP BACK AND PROMPT USER FOR COLOR CHANGE
C
        GOTO 10005
10001  CONTINUE
C
        RETURN
        END
C

```

```

C *****
C
C SUBROUTINE REDRAW_BARS
C
C PURPOSE:  USED TO ERASE AND REDRAW THE BARS REPRESENTING THE
C           INDIVIDUAL ENERGY SO THAT THE USER MAY INTERACTIVELY
C           SCALE THE ENERGY VALUES
C
C CALLED FROM SUBROUTINE COMPARE
C
C USAGE:  CALL REDRAW_BARS(BLIST,TESTNO,SCALE,TEST,ORIGINX,
C           ORIGINY,CSCALEY,ISIZE,ISCALEX,YIELD,CONC_COMP,
C           REPEAT)
C
C PARAMETERS:
C
C TRANSFERRED INTO THE SUBROUTINE:
C
C BLIST      THE NAME TO THE TEST TO BE REDRAWN
C TESTNO     THE NUMBER OF THE TEST TO BE REDRAWN
C SCALE      SCALE USED TO MODIFY THE ENERGY
C ORIGINX    X-COORDINATE OF THE ORIGIN OF THE AXES
C ORIGINY    Y-COORDINATE OF THE ORIGIN OF THE AXES
C ISIZE      SIZE OF THE TEXT
C CSCALEY    SCALE FOR THE Y-AXIS, USED TO CONVERT FROM UNITS
C           OF ENERGY TO NUMBER OF PIXELS
C ISCALEX    SCALE FOR THE X-AXIS, USED TO DEFINE THE WIDTH OF
C           THE BARS
C YIELD      YIELD DISPLACEMENT OF A PARTICULAR TEST
C CONC_COMP  CONCRETE COMPRESSIVE STRENGTH
C
C TRANSFERRED OUT TO SUBROUTINE COMPARE:
C
C PRE_SCALE  ARRAY WHICH STORES THE SCALE FACTOR FOR EACH TEST.
C           SCALING IS CUMULATIVE.  I.E.  IF A TEST HAS BEEN
C           SCALED BY A FACTOR OF "a" AND SCALING OF THE SAME
C           TEST IS ASKED FOR AGAIN, THIS TIME BY A FACTOR OF
C           "b" THE RESULTING ENERGY THAT IS PLOTTED IS
C           SCALED BY ab.
C
C SUBROUTINE SPECIFIC PARAMETERS:
C
C ENERGY(I) ENERGY FOR CYCLE I
C SCALED_ENER(I) THE SCALED ENERGY I.E. ENERGY*SCALE
C ATITLE      TITLE OF THE FILE FOR A CYCLE.  THIS FILE CONTAINS
C           THE TITLE OF THE CYCLE, ATIT AND THE DATA POINTS
C           OF THAT CYCLE.
C BTITLE      EQUAL TO ATITLE WITH ".OUT" EXTENSION
C ATIT        TITLE OF A CYCLE IN FILE ATITLE
C REPEAT      VARIABLE USED TO DETERMINE IF A TEST HAS BEEN
C           SCALED PREVIOUSLY
C NOCYCLE     ARRAY WHICH STORES THE NUMBER OF CYCLES FOR EACH
C           TEST
C
C *****

```

```

C
C
SUBROUTINE REDRAW_BARS(BLIST,TESTNO,SCALE,TEST,ORIGINX,
1 ORIGINY,CSCALEY,ISIZE,ISCALEX,YIELD,CONC_COMP,REPEAT,
2 PRE_SCALE)
C
INTEGER*2 TESTNO,TEST(3,100),IDX(16),IDY(16),
1 INTITLE(7,50,50),ORIGINX,ORIGINY,X0,Y0,X1,Y1,X2,Y2,
2 REPEAT(3),ISIZE
C
CHARACTER*18 BLIST,BTITLE
C
CHARACTER*14 ATIT(50,50),ATITLE
C
DIMENSION ENERGY(50,50),SCALED_ENER(50,50),YIELD(3),
1 CONC_COMP(3),NOCYCLE(50),PRE_SCALE(3)
C
EQUIVALENCE (ATIT,INTITLE)
C
DATA IDX/0,1,0,-1,0,1,1,0,0,1,0,0,0,-1,-1,-1/,
1 IDY/0,0,1,0,1,0,0,-1,-1,0,1,1,1,0,0,0/
C
C CHECK IF THE TEST HAS BEEN SCALED BEFORE, IF IT HAS THE
C ENERGY PER CYCLE WILL NOT BE INITIALIZED BUT REMAIN AS IT
C PREVIOUSLY WAS
C
IF(REPEAT(TESTNO).GT.0) GOTO 140
C
OPEN THE FILE WHICH CONTAINS THE LIST OF THE TITLE OF EACH CYCLE
C
OPEN(1,FILE=BLIST,ACCESS='SEQUENTIAL',FORM='FORMATTED',
1 STATUS='OLD')
REWIND 1
C
INITIALIZE VARIABLE USED AS A COUNTER OF THE NUMBER OF CYCLES
C
JJ = 1
C
READ THE TITLE OF THE CYCLE
C
10 READ(1,FMT=20,END=100)ATITLE
20 FORMAT(A14)
BTITLE = ATITLE//'.OUT'
C
OPEN THE FILE WHICH CONTAINS THE ENERGY ABSORBED FOR A CYCLE
C
OPEN(2,FILE=BTITLE,ACCESS='SEQUENTIAL',FORM='FORMATTED',
1 STATUS='OLD')
REWIND 2
C
READ THE TITLE OF THE CYCLE AND THE ENERGY
C
READ(2,20) ATIT(TESTNO,JJ)
READ(2,30) ICOUNT,ENERGY(TESTNO,JJ)
30 FORMAT(8X,I10,7X,F10.5)

```

```

C
C NORMALIZE THE ENERGY BY THE YIELD DISPLACEMENT AND CONCRETE
C COMPRESSIVE STRENGTH
C
      ENERGY(TESTNO,JJ) = ENERGY(TESTNO,JJ)/(YIELD(TESTNO)*
      1 CONC_COMP(TESTNO))
      JJ = JJ + 1
      CLOSE(2)
      GOTO 10
100    CONTINUE
      CLOSE(1)
C
C SCALE THE ENERGY
C
      NOCYCLE(TESTNO) = JJ
      140    DO 50 M = 1,NOCYCLE(TESTNO)
      SCALED_ENER(TESTNO,M) = ENERGY(TESTNO,M)*SCALE
      50    CONTINUE
C
      CALL PRMFIL(1)
C
C BEGIN LOOP TO ERASE THEN DRAW THE BARS
C
      DO 110 I = 1,NOCYCLE(TESTNO)
C
C FOR K = 1, ERASE THE OLD BAR
C FOR K = 2, DRAW THE NEW BAR
C
      DO 120 K = 1,2
      IF(K.EQ.1) CALL VAL8(48)           ! BACKGROUND, GRAY
      IF(K.EQ.2) CALL VAL8(49+TESTNO)
C
C DEFINE THE LOWER LEFT COORDINATES OF THE BAR
C
      X0 = ORIGINX + 3 +(TEST(TESTNO,I)-1)*ISCALEX
      Y0 = ORIGINY + 3
C
C DEFINE THE UPPER RIGHT CORNER OF THE BAR
C
      X1 = ISCALEX + X0
      IF(K.EQ.1) Y = ENERGY(TESTNO,I)
      IF(K.EQ.2) Y = SCALED_ENER(TESTNO,I)
      Y1 = IFIX(Y*CSCALEY) + ORIGINY
C
C ERASE/DRAW THE BAR
C
      CALL MOVABS(X0,Y0)
      CALL RECTAN(X1,Y1)
C
C DEFINE THE COORDINATES TO PLACE/ERASE THE TITLE OF THE CYCLE
C
      X2 = X1 - 7
      Y2 = Y1 + 5
C
C SET COLOR VALUE TO GRAY TO ERASE AND BLACK TO REDRAW

```

```

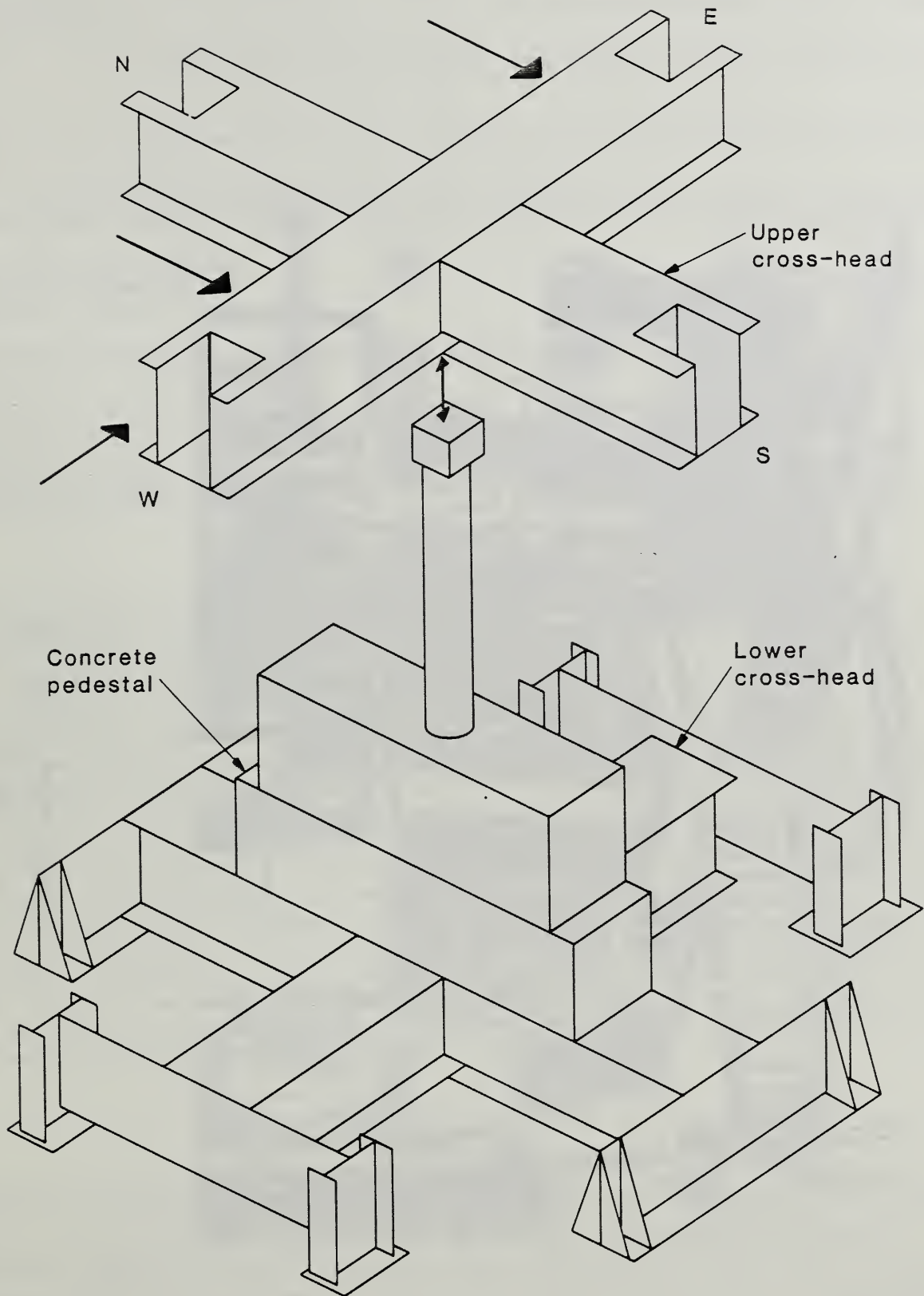
C
      IF(K.EQ.1) CALL VAL8(48)           ! GRAY
      IF(K.EQ.2) CALL VAL8(51)         ! BLACK
C
C SET THE TEXT SIZE AND ORIENTATION
C
      CALL TEXTC(ISIZE,90)
C
C MOVE TO THE COORDINATES TO PLACE THE TITLE
C
      CALL MOVABS(X2,Y2)
      DO 130 L = 1,4
      CALL MOVREL(IDX(L),IDY(L))
      CALL TEXT1(14,INTITLE(1,TESTNO,I))
130   CONTINUE
120   CONTINUE
110   CONTINUE
C
C SET REPEAT = TESTNO
C
      REPEAT(TESTNO) = TESTNO
C
C SET ENERGY TO SCALED ENERGY
C
      DO 150 I = 1,NOCYCLE(TESTNO)
      ENERGY(TESTNO,I) = SCALED_ENER(TESTNO,I)
150   CONTINUE
C
C MULTIPLE THE PREVIOUS SCALE BY THE NEW SCALE AND STORE IT IN
C PRE_SCALE TO KEEP TRACK OF THE SCALE FOR EACH TEST
C
      PRE_SCALE(TESTNO) = SCALE*PRE_SCALE(TESTNO)
C
      CALL EMPTYB
      RETURN
      END

```

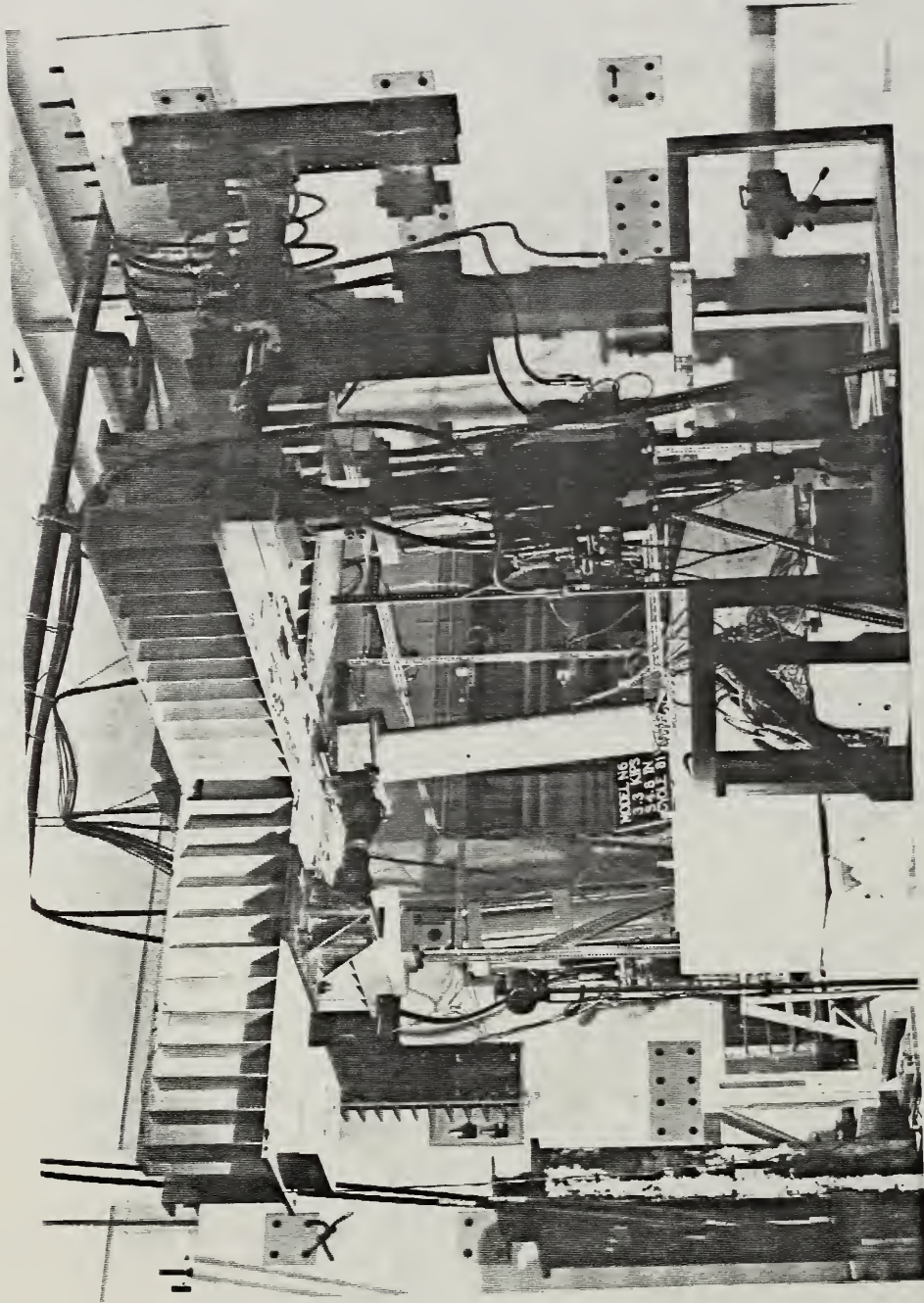
APPENDIX C: TRI-DIRECTIONAL TESTING FACILITY (TTF)

The installation of the TTF at NBS began in 1981 and was completed in 1984. Its capabilities include application of controlled displacements and/or forces in three orthogonal directions simultaneously as well as moments about each axis. One of the uses of the TTF is for "quasi-static" testing. Specimens approximately 10 ft. (3.05 m) in length, 10 ft. (3.05 m) wide and 12 ft. (3.66 m) high or smaller could be tested in the TTF.

The loading surface of the TTF consists of two crossheads. The lower crosshead is attached to a structural tie-down floor. The upper crosshead is attached to the lower one by means of three double-ended hydraulic actuators which are part of a general closed-loop, servo-controlled hydraulic system. Each of the vertical hydraulic actuators has a total stroke of 12 in. (300 mm) and a load capacity of 150 kips (670 kN) in tension and compression. The horizontal actuators, parallel to the north-south axis of the TTF, have a stroke of 12 in. (300 mm) and a load capacity of 85 kips (380 kN) in tension and compression each. The horizontal actuator parallel to the east-west axis of the TTF has a stroke of 6 in. (150 mm) and a load capacity of 220 kips (975 kN) in tension and compression. The horizontal actuators are attached by swivel end fittings to the crossheads and vertical post-tensioned concrete buttresses which serve as relatively stiff reaction walls. The vertical actuators also have swivel end fittings which are used to attach the bottom crosshead to the upper crosshead. These swivel fittings allow the actuators to have an unrestrained rotation of 270° in the plane of the swivel and about 10° in the other planes. The hydraulic actuators, data acquisition and data manipulation are controlled by a DEC PDP 11/34 computer. A schematic of the TTF is shown in Fig. C.1 with a model column installed and a photograph of a model being tested in the TTF is shown in Fig. C.2.



Schematic of TTF
FIGURE C1



Flexure Model in the TTF

Fig. C2

U.S. DEPT. OF COMM. BIBLIOGRAPHIC DATA SHEET (See Instructions)		1. PUBLICATION OR REPORT NO. NBSIR 86-3494	2. Performing Organ. Report No.	3. Publication Date JANUARY 1987
4. TITLE AND SUBTITLE BEHAVIOR OF 1/6-SCALE MODEL BRIDGE COLUMNS SUBJECTED TO CYCLIC INELASTIC LOADING				
5. AUTHOR(S) Geraldine S. Cheek and William C. Stone				
6. PERFORMING ORGANIZATION (If joint or other than NBS, see instructions) NATIONAL BUREAU OF STANDARDS DEPARTMENT OF COMMERCE WASHINGTON, D.C. 20234			7. Contract/Grant No.	8. Type of Report & Period Covered
9. SPONSORING ORGANIZATION NAME AND COMPLETE ADDRESS (Street, City, State, ZIP) 1. National Science Foundation (NSF) 2. National Bureau of Standards (NBS) 3. Federal Highway Administration (FHWA) 4. California Department of Transportation (CALTRANS)				
10. SUPPLEMENTARY NOTES <input type="checkbox"/> Document describes a computer program; SF-185, FIPS Software Summary, is attached.				
11. ABSTRACT (A 200-word or less factual summary of most significant information. If document includes a significant bibliography or literature survey, mention it here) Circular, spirally reinforced concrete bridge columns were subjected to cyclic inelastic loading in the laboratory. The bridge columns were one-sixth scale models of prototype columns designed in accordance with current California Department of Transportation specifications. A total of six models were tested. Three of the models were constructed with microconcrete, and three were constructed with ready-mix concrete using pea gravel. Variables included the aspect ratio, magnitude of axial load, and the use of microconcrete versus ready-mix. The models were subjected to slow reversed cyclic loading with the axial load held constant. Results from the tests are presented in the form of energy absorption, load-displacement curves, longitudinal steel strains, and displacement profiles. Comparisons of the ultimate moment capacities, measured displacement ductilities, plastic hinge lengths, and the failure mode for the six models are discussed. Comparisons with previous studies are presented along with a discussion of design codes in the U.S., New Zealand, and Japan. A series of graphics-based computer programs, developed to speed the analysis and interpretation of the experimental data, are discussed. Source code is provided.				
12. KEY WORDS (Six to twelve entries; alphabetical order; capitalize only proper names; and separate key words by semicolons) Behavior; Bridge Columns; computer graphics; concrete; ductility; energy absorption capacity; failure; lateral load; microconcrete; modelling; plastic hinge				
13. AVAILABILITY <input checked="" type="checkbox"/> Unlimited <input type="checkbox"/> For Official Distribution. Do Not Release to NTIS <input type="checkbox"/> Order From Superintendent of Documents, U.S. Government Printing Office, Washington, D.C. 20402. <input checked="" type="checkbox"/> Order From National Technical Information Service (NTIS), Springfield, VA. 22161			14. NO. OF PRINTED PAGES 291	
			15. Price \$24.95	

